# MINERALOGY AND GEOCHEMISTRY OF DETRITAL RUTILE FROM THE SIBAYA FORMATION, KWAZULU-NATAL.

by

## SIKSHA BRAMDEO

**Submitted in fulfilment of the requirements for the Master's degree in Science in the Discipline of Geology at the University of Durban-Westville**

**January 2002**

**Supervisor: Professor J.N. Dunlevey**

# DECLARATION

I declare this is my original work, both in conception and in execution, except where specific acknowledgement is made to work of others.

S. Bramdeo

Date:January 2002

Place: Durban

# TABLE OF CONTENTS

## CHAPTER FOUR: RUTILE MINERAL CHEMISTRY

## CHAPTER FIVE: DATA ANALYSIS

# LIST OF FIGURES

# LIST OF TABLES

# Abstract

Rutile, although not a major component of detrital heavy mineral deposits, is a valuable source of titanium oxide. Theoretically rutile is pure titanium dioxide ($TiO_2$) and should form white or colourless tetragonal crystals with a density of 4.25gm/ml. However, natural rutile although tetragonal, displays a variety of colours ranging from red through brown to black, yellow or blue, variable density between 4.23 to 5.50g/ml as well as a range in the magnetic susceptibility and electrical conductivity. In addition to these variations exhibited by natural rutile, samples from detrital heavy mineral deposits normally contain, in addition to homogenous grains, composite grains, in which rutile is intergrown with one or more mineral species, commonly quartz, feldspar and ilmenite.

The Sibaya Formation, like most detrital heavy mineral deposits, has a polymictic source, and as such contains rutile grains formed in many different chemical environments. Homogenous rutile grains display a chemical variation with a preference for the select few elements, which are compatible with the rutile cyrstallographic structure. The ions that substitute for titanium ($Ti^{4+}$) in the crystal lattice are a reflection of chemical environment in which the crystal formed. The size and charge of the $Ti^{4+}$ ion greatly restricts the species that may enter the rutile crystal lattice, with $Sb^{3+}$, $V^{3+}$, $Fe^{3+}$, $Cr^{3+}$, $Sn^{4+}$, $Mo^{4+}$, $W^{4+}$, $Mn^{4+}$, $Bi^{5+}$, $Nb^{5+}$, $Ta^{5+}$, $Sb^{5+}$, $V^{5+}$, being theoretically compatible with the size and charge of the $Ti^{4+}$ ion. Electron microprobe analysis of detrital rutile grains from the Sibaya Formation, KwaZulu-Natal show that elements, $Nb^{5+}$, $Ta^{5+}$, $Al^{3+}$, $Zr^{4+}$, $Si^{4+}$, $Fe^{3+}$, $Cr^{3+}$, and $V^{5+}$, commonly substitute for the $Ti^{4+}$ ion. However, $Sb^{3+}$, $Sn^{4+}$, $Mo^{4+}$, $W^{4+}$ and $Bi^{5+}$ were not present at detectable levels implying that the provenance area is not enriched in these elements. Although the high $Fe^{3+}$ values were expected in the rutile grains, as $Fe^{3+}$ is common in many rocks, the high $Si^{4+}$ values encountered were not expected, as $Si^{4+}$ is not normally compatible with $Ti^{4+}$ ion, as noted by their distinct separation in rutilated quartz. The anomalous $Si^{4+}$ content of certain grains suggests that within the provenance area rutile

bearing rocks formed under unusual conditions, such as high pressure, temperature and silicon activity where the high charge density of the $Si^{4+}$ ion would favour the inclusion of $Si^{4+}$ into the rutile lattice.

The chemical variation of the rutile grains causes significant variation in the magnetic susceptibility and electrical conductivity, and thus has marked effects on mineral processing, which relies heavily on magnetic and electrostatic separation techniques. The data presented indicates that individual homogenous rutile grains displays significant range of chemical composition, commonly containing other oxides from a fraction of a weight percent to well over 10wt%.

Data plots of $TiO_2$, FeO and 'other' oxides ($Nb_2O_5$, $Ta_2O_5$, $Al_2O_3$, $ZrO_2$, $SiO_2$, $Cr_2O_3$ and $V_2O_3$), showed that many of the more magnetic rutile grains appeared to be FeO enriched and contained a higher proportion of 'other' oxides. However, some grains that just had higher proportions of 'other' oxides and a lower FeO content were also magnetic. Thus magnetic susceptibility although strongly influenced by the presence of FeO, can also be enhanced by the substitutions of other oxides.

The vast majority of rutile grains from the electrostatic fractions were relatively $TiO_2$ pure, and contained low concentrations of 'other' oxides. However, some grains did have slightly enhanced $SiO_2$ and $V_2O_3$ concentrations, which appear to enhance the conductivity of the grains.

Four main colour groups were differentiated from the population of rutile grains from the Sibaya Formation, these being, reddish brown, black, blue and yellow. No single oxide seemed solely responsible for the colour of rutile grains. However, the red rutile grains had a slightly but significantly higher $Cr_2O_3$ and $Nb_2O_5$ content, whereas black rutile grains appeared to be $V_2O_3$ and $Nb_2O_5$ enriched. The blue colour of rutile grains appears to be influenced by a combination of $SiO_2$, $Al_2O_3$ and $Nb_2O_5$ substitutions. The yellow rutile grains had

slightly enhanced FeO and $Nb_2O_5$ concentrations. Although these differences are very small, trace quantities of certain elements and different combinations of elements can have a strong effect on colour.

Apart from $Fe^{3+}$, no single element; appears to be solely responsible for variations noted in the physical characteristics (magnetic susceptibility, electrostatic conductivity and colour) of homogenous rutile grains from the Sibaya Formation. However a combination of substituting elements appears to influence magnetic susceptibility and electrical conductivity. An enhanced $Fe^{3+}$ content normally increases the magnetic susceptibility although combinations of other elements may have the same effect on $Fe^{3+}$ poor grains. In general terms, the purer the rutile grain, the more likely it is, to be non-magnetic and conductive. Substitutions of 'other' oxides appear to decrease the conductivity of rutile grains. The relationship between grain colour and chemistry is also not very clear, verifying the widely held view that grain colour is often the result of more than just mineral chemistry.

# Acknowledgements

# 1. Introduction

Titanium is the ninth most abundant, as well as an economically important element within the earth's crust. Titanium does not occur as a native metal, but is found in a series of oxides and silicate minerals (Gribble, 1988). The two main industrial products from titanium minerals are:

1. titanium dioxide pigments
2. titanium metal

Currently most of the world's titanium production is used to satisfy the demand for pigment production, with only 5% used in the manufacture of titanium metal and alloys (Wipplinger, 1998).

The pigment industry consumes almost 95% of all titanium minerals mined (Force, 1991). Titanium dioxide, in the form of rutile has a very high refractive index (2.6 - 2.9) and this coupled with non-toxicity and relative abundance makes it a chief opacifying pigment. The main uses of titanium pigments are in the production of paints, lacquers, enamels (57%) plastics (17%), paper (15%), with the rubber, coated fabrics and textiles, printing ink, ceramics and cosmetics industries accounting for virtually all the remainder (Wipplinger, 1998). As $TiO_2$ is non-toxic, it has replaced virtually all the lead-based compounds and pigments used in the early twentieth century. Titanium dioxide is also able to absorb ultraviolet light, and thus when present in paint slows down the degradation by sunlight. Being non-toxic and biologically inert titanium dioxide is also used as a whitening agent in food preparation (Wipplinger, 1998). Currently there are no known cost-effective alternatives for titanium dioxide pigments (Wipplinger, 1998).

Compared to steel; titanium metal is 45% lighter but virtually as strong. In addition, titanium metal has twice the strength of aluminium while it is only 60% heavier. At normal atmospheric conditions, and even at elevated temperatures and pressures, titanium is resistant to corrosion and is unaffected by sea-water. Titanium metal does

1

not react with organic compounds, strong alkalis, sulphur and sulphur compounds, chlorinated solvents, chlorides and hydrochloric acid (Wipplinger, 1998). The inertness of titanium metal in these environments together with its resistance to corrosion make it ideal for use in electric utilities, chemical processing, off shore oil recovery, oil refining, water desalination, medical prosthetics and implants as well as in marine applications. Furthermore, as titanium metal is stable at high temperature it is widely used in the 'hot zones' of aircraft. To date no suitable substitutes have been found for titanium in these applications (Wipplinger, 1998).

## 1.1 Titanium Deposits

In titanium mineral mining emphasis is placed on the concentration of titanium within minerals as well as the phase in which titanium is present. Only minerals having titanium present in the oxide phase and in concentrations greater than 25% (Table 1.1) are considered to have economic value (Force, 1991).

Common titanium bearing minerals that are mined are the three polymorphs of $TiO_2$ (rutile, anatase, brookite), ilmenite ($FeTiO_3$), and perovskite ($CaTiO_3$) (Table 1.1).

Titanium minerals are mined from hard crystalline rocks, weathered rocks and unconsolidated sediments (Force, 1991). However, the unconsolidated sediments shoreline placer deposits are much more important than any other deposit type. At present shoreline placer deposits supply more than half the titanium minerals mined (Force, 1991) and contain reserves of many tens of million of tonnes of titanium oxide minerals. In placer shoreline deposits titanium oxides have been concentrated with other heavy minerals by wave action.

| Mineral | Theoretical Formula | $TiO_2$ Content % |
|---|---|---|
| **OXIDES** | | |
| Rutile | $TiO_2$ | >95 |
| Anatase | $TiO_2$ | >95 |
| Brookite | $TiO_2$ | >95 |
| Ilmenite | $FeTiO_3$ | ~52 |
| Perovskite | $CaTiO_3$ | ~59 |
| Magnetite (titaniferous) | $Fe_3O_4$ | 0-15 |
| **SILICATES** | | |
| Titanite | $CaTiSiO_5$ | ~41 |
| Melanitic garnet | $Ca_3Fe_2Si_3O_{12}$ | 0-17 |
| Biotite | $K_2(Mg,Fe)_4(Fe,Al,Ti)_2 Si_6Al_2O_{20}(OH,F)_4$ | 0-6 |
| Calcic amphiboles | $(Na,K)Ca_2(Mg,Fe,Al)_5 Si_6Al_2O_{22}(OH,F)_2$ | 0-10 |
| Augite (titanaugite) | $Ca(Mg,Fe,Ti)(Si,Al)_2O_6$ | 0-9 |

Table 1.1    Composition of some common titanium minerals

The value of shoreline placer deposits is further enhanced by the presence of several other economically important accessory minerals such as zircon and monazite. Weathering within placer deposits further enhances the titanium dioxide content as ilmenite loses iron to produce a titanium rich ilmenite, which can be refined using the chloride process. The chloride process converts $TiO_2$ to $TiCl_4$ that can be used either for the production of titanium pigments or titanium metal. The chloride process requires a high $TiO_2$ feedstock as it can be poisoned by some trace elements. The combination of having rutile, ilmenite, and enriched ilmenite together with a range of other economically important accessory minerals all in loose, well sorted sediments makes mining shoreline

3

placer deposits easier and more economically attractive than almost any other type of titanium deposit.

## 1.2 South Africa and the World Titanium Market

Information on titanium reserves, production and exports in the world is summarised in Table 1.2.1. Although South Africa has the world's largest reserve base, it is ranked second in terms of production and is the third largest exporter of titanium. The South African titanium mineral reserves account for 21% of the world's reserve base even though Australia is the world's largest producer and exporter of titanium.

Table 1.2.1   World reserves, production and export of titanium, 1998 (Joseph 2000)

| Country | Reserve Base | | | Production | | | Exports | | |
|---------|------|------|------|------|------|------|------|------|------|
| | *Mt | % | Rank | *kt | % | Rank | kt | % | Rank |
| Austrailia | 131 | 18.9 | 2 | 1 560 | 33.8 | 1 | 1 350 | 37.2 | 1 |
| South Africa | 146 | 21.0 | 1 | 1 043 | 22.6 | 2 | 526 | 14.5 | 3 |
| Canada | 36 | 5.2 | 8 | 890 | 19.3 | 3 | 800 | 22.0 | 2 |
| Norway | 40 | 5.8 | 7 | 264 | 5.7 | 4 | #401 | 11.0 | 4 |
| India | 46 | 6.6 | 5 | 214 | 4.6 | 5 | #50 | 1.4 | 7 |
| Ukraine | 16 | 2.3 | 10 | 150 | 3.2 | 6 | 212 | 5.8 | 5 |
| USA | 77 | 11.1 | 4 | 140 | 3.0 | 7 | 24 | 0.7 | 9 |
| Malaysia | 1 | 0.4 | 11 | 125 | 2.7 | 8 | #115 | 3.2 | 6 |
| China | 41 | 5.9 | 6 | 75 | 1.6 | 9 | 19 | 0.5 | 10 |
| Brazil | 103 | 14.9 | 3 | 60 | 1.4 | 10 | - | - | - |
| Sri Lanka | 18 | 2.6 | 9 | 20 | 0.4 | 11 | 30 | 0.8 | 8 |
| Other | 37 | 5.3 | - | 80 | 1.7 | - | 106 | 2.9 | - |
| Total | 692 | 100.0 | | 4 621 | 100.0 | | 3 633 | 100.0 | |

Notes:     * Metal content          # 1996 figures          - No data

kt:thousand tons          Mt: million tons

Reviews in 1999, of the titanium feedstock market predicted a supply deficit early in the year 2000 (Murphy and Taylor, 1999). The market for titanium is driven by the demand for titanium dioxide pigments, which accounts for about 93% of total titanium mineral consumption. In a study undertaken by TZ Minerals International (Murphy and Taylor,

4

1999) it was predicted that pigment consumption would increase by as much as 4% in 2000.

In the non-pigment sector (titanium metal and alloys) production declined substantially in 1999 due to a reduced demand, caused by a lower consumption in the commercial aircraft industry (Murphy and Taylor, 1999). The overall demand for titanium mineral can therefore be attributed to strong growth in the pigment industry (Murphy and Taylor, 1999).

In terms of titanium mineral production, Australia remained the largest supplier of titanium, accounting for 33.8% of supply in 1998, followed by South Africa at 22.6% and Canada at 19.3% (Murphy and Taylor, 1999).

## 1.3 South African Titanium Deposits

Heavy mineral placer deposits occur along both the east and west coasts of South Africa (Fig. 1.3.1). The importance of heavy mineral deposits along the east coast was first established by an extensive prospecting and drilling programme undertaken between 1968 and 1972 (Fockema, 1986). Based on the data obtained Richards Bay Minerals was established in 1975 and following a two year construction period, mining commenced in 1977.

The west coast of Southern Africa has for a long time been exploited for alluvial diamonds (Wipplinger, 1998). Heavy mineral deposits along the west coast were investigated in the 1950's by the Geological Survey of South Africa. However, these mineral deposits have only recently been mined, with mining in this area only commencing in 1994 (Wipplinger, 1998).
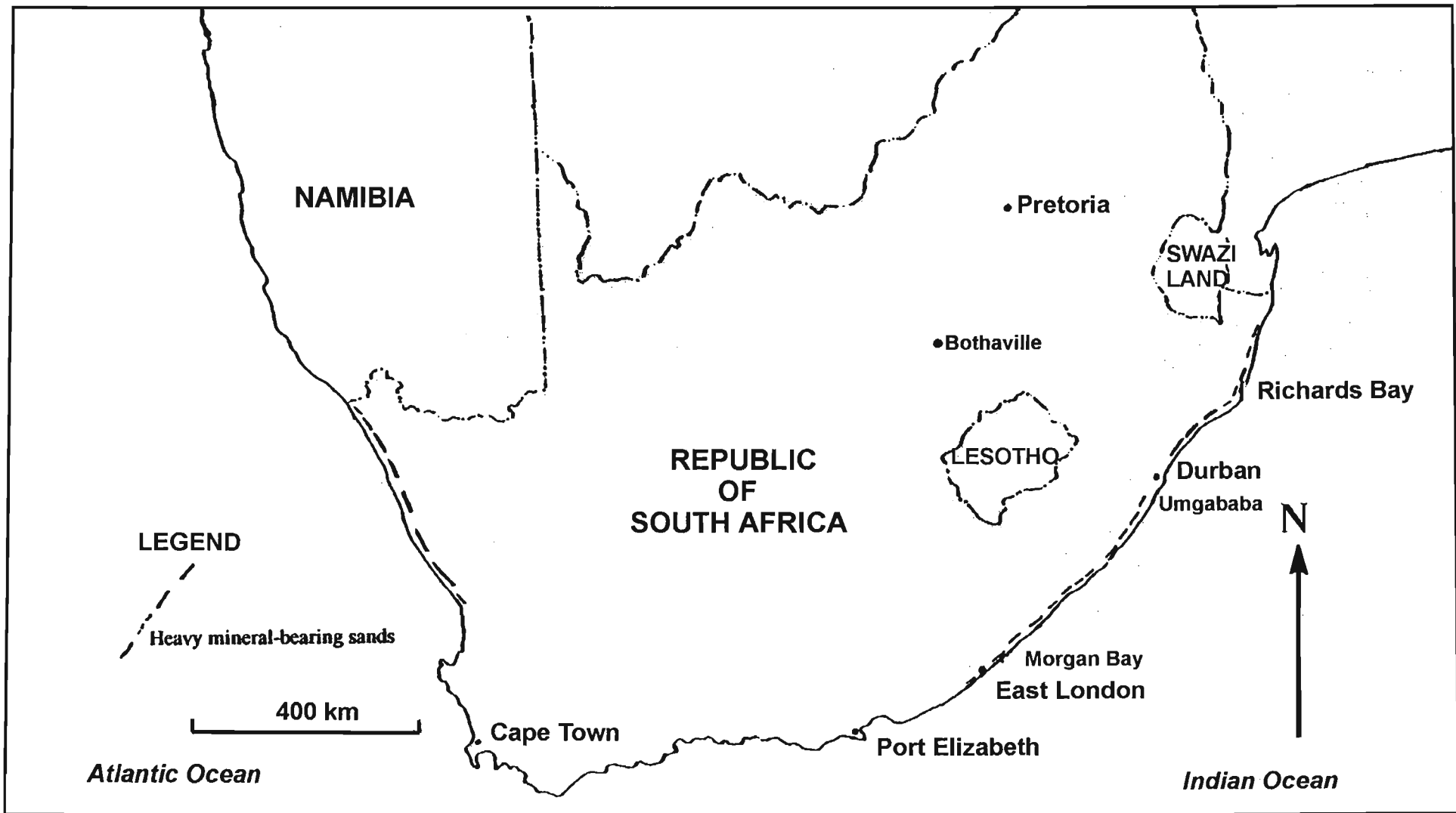
Fig. 1.3.1 Map showing the distribution of 'heavy mineral' deposits along east and west coast of South Africa.

The heavy mineral deposits along the west coast of South Africa extend from Strandfontein in the south to the mouth of the Orange River in the north. Economically viable heavy mineral deposits approximately 40km north of the Olifants River mouth led to the establishment of an open cast mining operation known as Namakwa Sands in 1994 (Rozendaal, *et al.*, 1999). These deposits have been described as Cainozoic to Recent sediments overlying a Pre-Cambrian Mokolian basement. The heavy minerals are concentrated in semi consolidated to unconsolidated sands of Palaeo and Recent strandlines, as well as in overlying aeolian dunes (Rozendaal, *et al.*, 1999).

## 1.4 Titanium Mineral Recovery from Placer Deposits

Unconsolidated heavy mineral placer deposits are commonly mined using a suction dredge technique. Artificial ponds are created within the dune fields to carry the suction-cutting dredges and floating gravity concentrators. The loose sand is mined by the dredger, which undercuts the ore-body causing the sand to slump into the pond forming a slurry. The slurry is pumped to the floating concentrator where it is first screened to remove oversize material, roots and other debris. The sand is then passed onto a gravity circuit where a series of Humphries Spirals separate the heavy from the light minerals. The light minerals are discarded as tailings and the heavy minerals undergo further processing (Fig. 1.4.1) in the main mineral separating plant. However, before the heavy minerals leave the floating concentrator magnetite is removed and rejected to tailings using low intensity wet magnets. The tailings from the floating concentrator are used to resculpture dunes prior to revegitation. The heavy mineral fraction known as the heavy mineral concentrate (HMC) is transported to stockpiles and then the Mineral Separation Plant (MSP) where the concentrate is further processed.

7
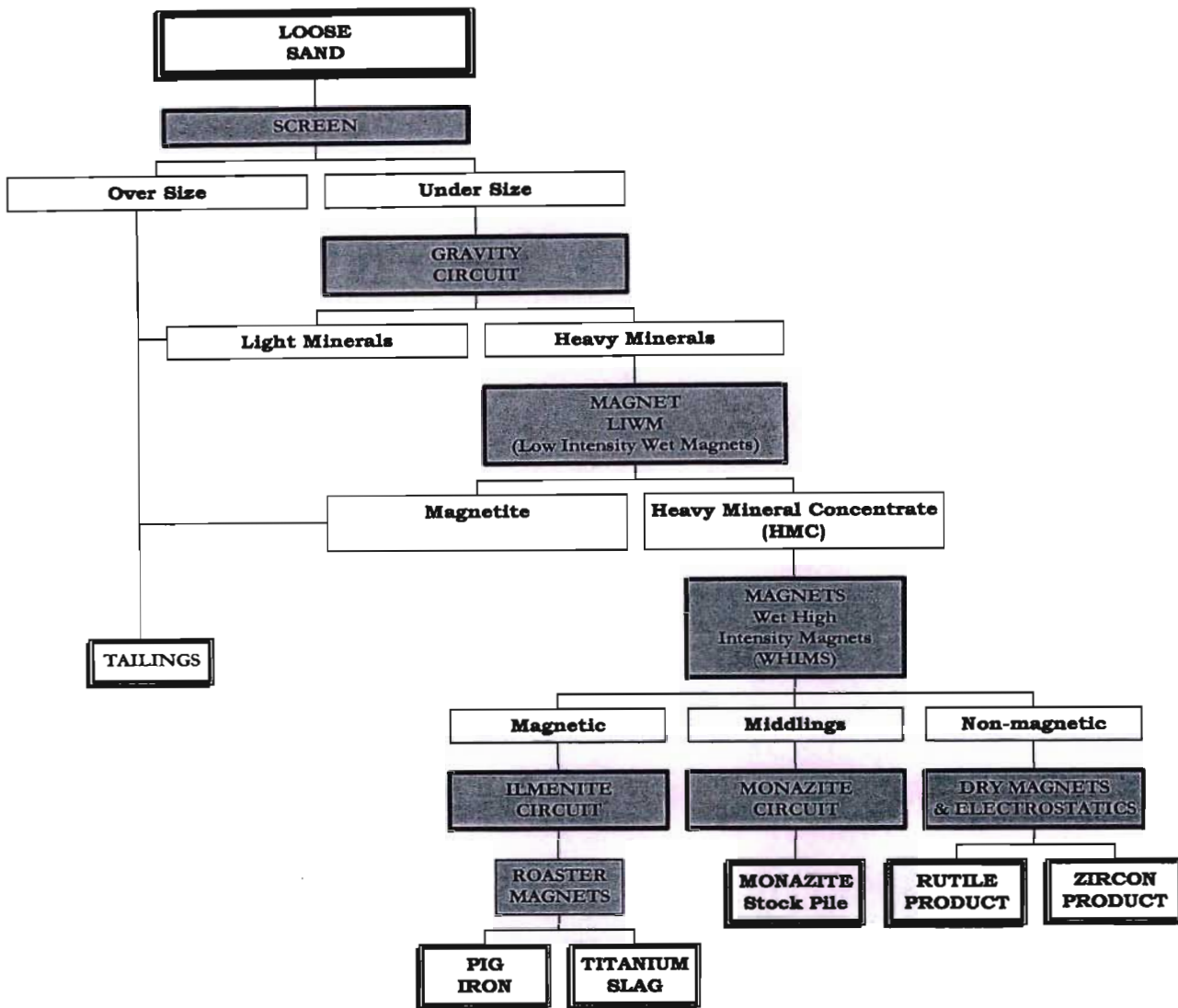
Fig. 1.4.1 Flow chart illustrating mineral processing at Richards Bay Minerals

At the MSP, wet high intensity magnets are used to separate the HMC into magnetic, non-magnetic and middling streams (Fig. 1.4.1). The middlings are sent to the monazite stockpile. The magnetic stream is treated by the ilmenite circuit using a roasting process to form two products, titanium slag and pig iron. The non-magnetic stream is processed using a series of dry magnets and electrostatic separators to form a non-magnetic and non-conductive zircon product and a non-magnetic and conductive rutile product. The major uses of the product from the ilmenite, conductive rutile and nonconductive zircon circuits are outlined in Table 1.4.1.

8

Table 1.4.1: Ilmenite, rutile and zircon: some products and uses (Coastal and Environmental Services, 1982).

| ILMENITE ($FeTiO_3$) | RUTILE ($TiO_2$) | ZIRCON ($ZrSiO_4$) |
|---|---|---|
| **High quality pig iron** <br><br>• Used in the ductile iron foundry industry and the automotive industry (eg. brake callipers, crankshafts and steering knuckles). <br><br>**Titania slag** <br><br>• Used as a basic pigment for paint manufacture. <br><br>• Used in high-quality paper, plastics, textiles, cosmetics, colouring of foodstuffs, white baked enamel finishes on domestic appliances. | **Rutile sand** <br><br>• A raw material used in the production of pigments for paints, plastics, rubber and textiles. <br><br>• Renders a high-quality titanium metal used in aeronautics industry. <br><br>• Used as flux for welding electrodes. <br><br>**Titanium metal** <br><br>• Used in air and spacecraft manufacture, surgical, instruments, prosthetics and sporting equipment. | **Zircon** <br><br>• Used in ceramic glazes for tiles and sanitary ware. <br><br>• Used in the production of steel and glass and as a moulding sand in foundries. Coats television screens to protect viewers from x-rays. <br><br>• Used in control rods in nuclear reactors. <br><br>• Used in antiperspirants - the powdery white substance. |

## 1.5 Rutile recovery problems

The recovery of valuable rutile involves several technical problems. In contrast to ilmenite, which contains over 40% of iron and can easily be extracted, using magnets; rutile may behave anomalously during mineral processing in the mineral separation plant.

There are two major reasons for the anomalous behaviour of rutile and subsequent losses during mineral separation i.e.:

1. the presence of composite grains (grains containing more that one mineral) and,

2. the anomalous chemistry of homogenous grains.

Previous studies have revealed that composite rutile grains influence the behaviour of rutile during mineral processing (Mdludlu, 1997). Apparently homogenous grains can sometimes contain up to 15wt% of other elements and this is believed to influence the physical properties, and adversely affect the efficiency of mineral processing (Mdludlu, 1997).

Theoretically rutile is composed of pure titanium dioxide ($TiO_2$) with predictable physical properties. However, natural rutile is composed of 85-99% titanium dioxide, with a density ranging from 4.23-5.5 g/cm$^3$ (Deer *et al.*, 1985). There is also great diversity in the colour of natural rutile from reddish brown to black, violet, yellow and green.

The large variance in both colour and density shown by rutile can be attributed to the <1 to 15% of the other elements that are compatible with the rutile crystallographic structure (Deer *et al.* 1985). These elements within the rutile structure are also thought to influence the behaviour of rutile during mineral processing. Specifically the magnetic susceptibility and electrical conductivity of the rutile grains appear to be affected by small variations in chemical composition (K. Pietersen, *pers. comm.* 2000).

10

# 2. Regional Geology

## 2.1 Overview

Heavy mineral placer deposits occur intermittently along the west and east coast of Southern Africa (Fig. 1.3.1). At present, the South African titanium mineral industry has two major contributors, Richards Bay Minerals (RBM) and Namakwa Sands. This study involves samples extracted from the Richards Bay placer deposit in KwaZulu-Natal on the eastern coast.

## 2.2 Study Area

The economically important heavy minerals of the Sibaya Formation studied were obtained from Ponds A, B, and C in the ore body (a shoreline placer deposit) mined by Richards Bay Minerals. The ore body, which is situated in the late Pleistocene to Holocene coastal dune field at the southern end of the Zululand Plain, is approximately 125km in length and on average 5km wide, extends from some 25km south of the town of Richards Bay to 25km north of the St. Lucia Estuary (Fig. 2.2.1).

In the study area the Sibaya Formation rests unconformably upon the underlying Kwambonambi Formation. The heavy mineral suite within these young deposits has been concentrated due to coastal aeolian separation processes. The Kwambonambi and Sibaya Formations were formed by a complex series of marine transgressions and regressions associated with the last ice age (Hobday and Orme, 1974; Hobday and Jackson, 1979). Shallow marine and aeolian environments dominate both the Kwambonambi and Sibaya stratigraphic units, and the sediments were interpreted by Fockema (1986) as comprising of long seif dunes and large 'whale-back' dunes. The seif dunes of the Kwambonambi Formation are parallel to the modern day south-south westerly wind direction, while the 'whale back' dunes formed as seif dunes that migrated

11
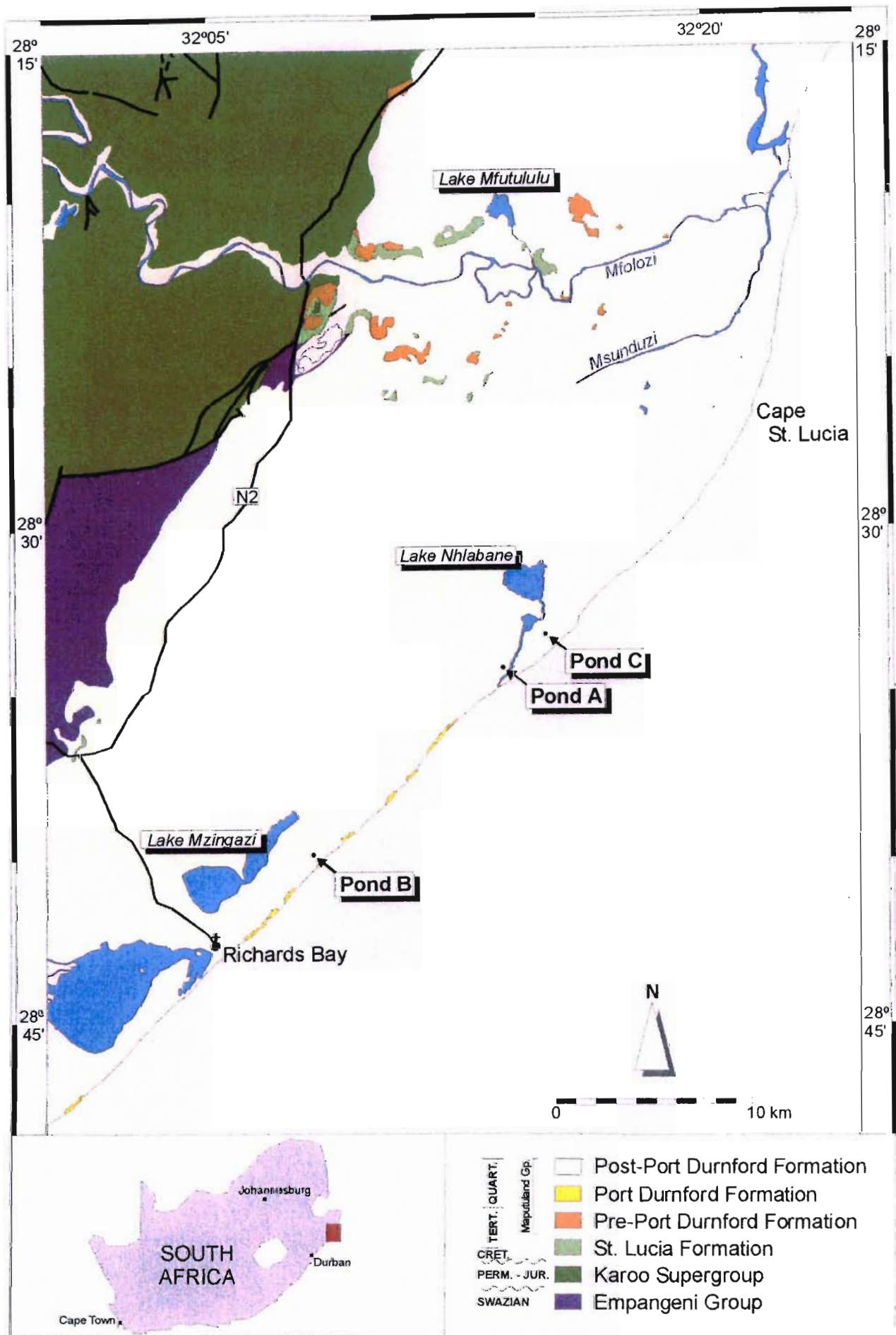
Fig. 2.2.1 Geologic map of the study area indicating sampling points.

inland at an angle to the coast. As this study focuses on the titanium bearing heavy mineral of this shoreline placer deposit, in particular rutile, samples were collected from three currently worked mining ponds, within the RBM mining lease area (Fig. 2.2.1).

The samples collected consisted of the heavy mineral concentrate (HMC) produced by the mining Ponds A, B, and C. The samples were then separated under controlled laboratory conditions and are considered to be the equivalent of RBM's rutile, zircon and ilmenite products.

## 2.3 Stratigraphy of KwaZulu-Natal

The stratigraphy of KwaZulu-Natal (Fig. 2.3.1) ranges from the highly metamorphosed Archean Kaapvaal Craton of Swazian Age to the unconsolidated sediments of the Maputuland Group (Hugo 1993). The Natal Group rests unconformably on the older rocks of the Natal Structural and Metamorphic Province with a hiatus of approximately 500Ma. The Natal Group is a predominantly sedimentary sequence consisting of feldspathic and micaceous sandstone with subordinate quartz arenite, mudrock and conglomerate (Johnson, 1994). This succession is approximately 600m thick and contains cross-bedding and ripple marks that are preserved within the sandstones (Uken, 1999). Overlying the Natal Group unconformably is the Carboniferous to Lower Jurassic Karoo Supergroup. It forms a sedimentary-volcanic sequence up to 10 000m in thickness. The glacial diamictites, sandstones and shale of Dwyka Group were deposited throughout much of the Karoo Basin and forms the basal unit of the Karoo Supergroup (Smith, *et al.* 1993). The Dwyka Group is conformably overlain by marine sandstones and shales of the Permian Ecca Group (Johnson, 1994). The Ecca Group marks the environmental transition from glacial (deposits dominated by melt water flooding) to low energy fluvial systems (Smith, 1990). The succeeding Beaufort Group consists of 3000m of fluvial deposits accumulated over a period of 20Ma, was deposited

| GROUPS AND FORMATIONS | | AGE | LITHOLOGY |
|---|---|---|---|
| MAPUTULAND GROUP | Sibaya Formation<br>Kwambonambi Formation<br>Kosi Bay Formation<br>Port Durnford Formation<br>Umkwelane Formation<br>Uloa Formation | Miocene - Recent | sand<br>sand<br>sand, clay<br>sand, silt, clay, shale<br>sandstones<br>calcarenites, conglomerates, coquinas |
| ZULULAND GROUP | | Cretaceous | Siltstones, sandstones |
| KAROO SUPERGROUP | Drakensberg Group<br>Stormberg Group<br>Beaufort Group<br>Ecca Group<br>Dwyka Group | Carboniferous-Jurassic | basalt<br>sandstones, mudstones<br>sandstones, mudstones<br>shales, mudstones<br>diamictites |
| NATAL GROUP | | Ordovician – Silurian | Sandstones, arkose, quartz-arenites, mudrocks, conglomerates |
| PONGOLA SUPERGROUP | Mozaan Group<br><br>Nsuze Group | Namibian | sandstone, conglomerate, banded ironstone, shale<br><br>basalt, pyroclastics, limestones |
| NATAL METAMORPHIC PROVINCE | | Mokolian | Amphibolites, gneisses, schists, granite, charnokite |

Fig. 2.3.1 Schematic representation of the stratigraphy of KwaZulu-Natal.

in a swamp-like environment, giving rise to mudstones containing a rich fossil assemblage (Smith, *et al.* 1993). Immediately overlying the Beaufort Group are the sandstones of the Stormberg Group, which were deposited as large dunes in a desert environment (Smith, *et al.* 1993). Overlying the Stormberg Group is the Drakensberg Group, which consists of a 1.5km thick basalt accumulation. This violent episode of Jurassic volcanism terminated the infilling of the Karoo basin, and signalled the onset of the breakup of Gondwana (Smith, 1990).

The Zululand Group rests unconformably on the Karoo Sequence; the Cretaceous sediments of the Zululand Group are 10 to 733m thick and comprise siltstones and minor sandstones with concretions and shelly layers. Cainozoic sediments of the Maputoland Group accumulated unconformably upon the Zululand Group (SACS, 1980).

## 2.4 Cainozoic Sediments

Much controversy surrounds the post-Mesozoic stratigraphy of the Zululand coastal plain. Both Hobday and Orme, (1974); and Hobday and Jackson (1979) described the stratigraphy of the Zululand coastal plain, "as units of Recent/Holocene aeolian sediments; overlying a Cainozoic Port Durnford Formation; that has a base comprising of Cretaceous sediments". However, this nomenclature ignored the marked unconformities within the Port Durnford Formation as well as the unconformity between the Port Durnford Formation and the overlying aeolian sediments. The South African Council on Stratigraphy (SACS) Cainozoic Working Group has proposed that the term Port Durnford Formation should be restricted to the lagoonal sediments that were previously termed the Lower Argillaceous Member. The term Kosi Bay Formation was introduced for the red, brown and white sands previously termed the Upper Argillaceous Member of the Port Durnford Formation (Singh 1995; G. Botha *pers. comm.* 1999).

Hobday and Orme (1974) referred to all the Holocene sediments as 'cover-sands', which they considered to have been deposited during a marine transgression. Within these

15

beds, large scale cross-bedding was identified by Hobday and Jackson (1979) who re-interpreted the sands as aeolian coastal dunes formed during a marine regression. Fockema (1986) suggested that the aeolian sediments be divided into older Inland Aeolianites and younger Coastal Aeolianites. SACS (1980) renamed the Inland Aeolianites of Fockema (1986) as the Kwambonambi Formation and the Coastal Aeolianites; as the Sibaya Formation.

## 2.5 Revised Stratigraphy

The latest informal stratigraphic subdivision (Botha, 1987, Botha *pers. comm.* 1999) of the Zululand coastal plain deposits emphasizes a Maputoland Group subdivided into, Uloa, Umkwelane, Port Durnford, Kosi Bay, Kwambonambi and Sibaya Formations (Fig. 2.5.1 and Table 2.5.1)

Table 2.5.1 Summary of the revised stratigraphy of KwaZulu-Natal (Maud and Botha, 2000)

| Formation | Lithology | Age |
|---|---|---|
| Sibaya Formation | Loose, medium to fine grained sands forming coastal dune cordon. | Present day to Mid Holocene |
| Kwambonambi Formation | Brown to grey fine grained, unconsolidated to semi-consolidated sands forming inland dunes. | Late Pleistocene and Holocene |
| Kosi Bay Formation | Lignite and dune sands. | Late Pleistocene |
| Port Durnford Formation | Mudstones and clayey sand . | Middle to late Pleistocene |
| Umkwelane Formation | Aeolianite and calcarenite. | Pliocene |
| Uloa Formation | Calc-arenites, conglomerates and coquinas | Mio-Pliocene |

| | | high coastal dune cordon of calcareous sand | SIBAYA FORMATION |
| | | inland stablised dunes redistributed sand (non-calcareous and diatomite | KWAMBONAMBI FORMATION |
| | | reddish soil, 'Berea-type' red sand | |
| | | cross-bedded sand, local calcarenite lensiod carbonaceous sand | KOSI BAY FORMATION |
| | | beachrock, coral-bearing coquina (± 120ka) lignite (78ka) fossiliferous mudrock, aeolian calcarenite and red sandstone | PORT DURNFORD FORMATION |
| | | red sandy soil decalcified Unkwelane Fm. | |
| | | aeolian cross-bedded calcarenite | UMKWELANE FORMATION |
| | | coquina and conglomerate | ULOA FORMATION |

Holocene <150m

mid- to late Pleistocene 10m up to 100m ±10m

late Miocene to Pliocene <50m <20m <10m

Palaeocene, Mesozoic, Palaeozioc and Precambrian bedrock

MAPUTALAND GROUP

Fig. 2.5.1    Revised stratigraphy of the Zululand coastal Plain after the Cainozoic Task Group (after Botha, 1987).

## 2.5.1 Uloa Formation

The Uloa Formation is approximately 10m thick and consists of calcarenites, conglomerates and coquinas (Johnson, 1994). The beds contain a rich assemblage of marine invertebrates, including the distinctive Pecten Beds (SACS 1980). This formation has been dated biostratigraphically as late Miocene to early Pliocene (Johnson, 1994). The concentration of shells in beds of this formation suggests deposition in lag deposits, most likely related to a marine regression (Johnson, 1994), indicating an overall littoral deposition environment.

## 2.5.2 Umkwelane Formation

The Umkwelane Formation consists of compact, poorly cemented, medium to coarse grained sandstones, interbedded with free flowing coarse sands (Fockema 1986), with intercalated thin gravel beds formed in slightly incised channel beds. Marine shell fragments occur throughout this formation and are sometimes concentrated in shell beds (Fockema, 1986). The top of the Umkwelane Formation has been re-worked, and forms a red, sandy palaeosoil devoid of fossils (Singh, 1995). Fockema (1986) deduced a biostratigraphically constrained Pliocene Age for these strata. The thin gravel beds are considered to represent fluvially confined deposition and the gravel beds in association with shell bearing layers an indication of a marginal marine or lacustrine depositional environment. The Umkwelane Formation is of Pliocene Age and considered to have been deposited during a marine transgression (Fockema, 1986). Taking into account the marine character of the shells the formation, it is considered to have been deposited during a marine transgression (Fockema, 1986).

## 2.5.3 Port Durnford Formation

The Port Durnford Formation is 4 to 6m thick and, consists of a basal unit of unconsolidated fine-grained sandstones, silts and clays (Johnson, 1994), containing fossil wood and mammal remains as well as fragments of marine invertebrate, and fish (Hobday and Orme, 1974). The Port Durnford Formation is considered to be of mid Pleistocene Age (Singh 1995), and is overlain in places by a lignite bed, up to 0.25m thick and unconsolidated medium-grained sands are characterised by large-scale cross-bedding (Hobday and Orme, 1974). The lignite bed is found in the lower 1.5m of the Kosi Bay Formation.

Grain-size characteristics, the lignite bed and the assemblage of both marine and terrestrial animals together with tree logs suggest a lagoonal or perhaps estuarine depositional environment (Hobday and Orme, 1974) for the Port Durnford Formation.

## 2.5.4 Kosi Bay Formation

There is a marked erosive unconformity between the Port Durnford Formation and the Kosi Bay Formation. The Kosi Bay Formation overlying the Port Durnford Formation has a thickness of up to 100m. Singh (1995), distinguished three distinct units with gradational contacts in the Kosi Bay Formation; a basal unit consisting of a white clay rich sand; an intermediate unit composed of white clay-rich layer with reddish patches that coalesce towards the top of the unit; and an uppermost unit made up of unconsolidated to semi-consolidated red sands.

Singh (1995) interpreted the Kosi Bay Formation as an aeolian deposit and attributed the variation to weathering and interaction with ground water.

19

## 2.5.5 Kwambonambi Formation

The Kwambonambi Formation is composed of brown and grey fine-grained, unconsolidated to semi-consolidated sands with large scale cross-bedding and is approximately 50-80m thick. These sands are characterised by well-rounded, partly frosted grains. Johnson (1994) interpreted the Kwambonambi Formation as coastal seif dunes that have a Holocene Age.

## 2.5.6 Sibaya Formation

The Sibaya Formation consists of loose, medium to fine-grained sands, containing abundant bioclasts and heavy minerals (ilmenite, rutile, zircon and monazite) in high concentrations. The maximum observed dune height in the Sibaya Formation is 100m, containing large-scale, cross-bedding. Abundant low-order truncation surfaces separate the beds into numerous cross-bed sets. The dune sands of the Sibaya Formation are still accumulating as the strong on-shore winds carry beach sands inland.

From the bedding characteristics and relationship to the underlying Kwambonambi Formation Fockema (1986) interpreted the Sibaya Formation as a series of large aeolian dunes resulting from the inland migration of seif dunes.

The depositional environment of the Sibaya Formation is considered to have been very similar to that of the Kwambonambi Formation. Beach sands, enriched in heavy minerals by tidal and wave action, were blown into relatively narrow, parallel series of coastal seif dunes. Westward directed palaeocurrents indicate that the strong on-shore winds were responsible for eventual accumulation of the sands in to prominent high dunes further inland (Force, 1991).

# 3. Mineral Processing

## 3.1 Overview of mineral processing

The heavy mineral deposit at Richards Bay is an unconsolidated sedimentary deposit of aeolian origin with the heavy minerals disseminated throughout coastal dunes of the Sibaya Formation. Extraction of heavy mineral bearing sands involves suction dredge techniques in which artificial ponds are created, to carry the suction-cutting dredges and floating gravity concentrators. The heavy minerals are separated from the light gangue before leaving the mining ponds for further processing at the centralised mineral separation plant. Behind the mining ponds, dunes are re-shaped and rehabilitated, returning the land to its appearance prior to mining. The dune rehabilitation scheme initiates and develops the processes that developed the Coastal Dune Forest Ecosystem. Although the complete rehabilitation sequence takes over 20 years the final product is virtually identical to that found in pristine areas (K. Pietersen pers. comm. 1999).

## 3.2 Heavy Mineral Extraction at Richards Bay

The area to be mined is surveyed and ore reserve drilling is done on a 50 x 50m grid. This provides information of the ore-body, aids in the design of economic mine paths for the dredger to follow and provides data for topographic reconstruction.

Before mining commences, trees and other vegetation are stripped about 100 m ahead of the mining pond, commercial timber species are harvested, stumps uprooted and non-commercial trees are felled and stacked. The area is bulldozed and the tree material (stumps, roots and felled trees) is collected and transported to mined out areas. The top 10-15 cm of the topsoil containing humus and seeds, is removed and either stockpiled or directly transferred to an area undergoing rehabilitation. Stockpiles of organic-rich material are kept for a minimum time period only, in order to avoid the loss of seed viability.

21

A rotating bucket wheel mines the face ahead of the dredger, undercutting the face and causing the loose sand to slump into the pond. Densely compacted sand is mined using high pressure water jets. The ponds can advance up to 12m a week at a rate of 3000 tons/hour mining a 17m long face.

The suction dredger feeds the slurry (water and sand mixture) to the floating concentrator where the sand is screened to remove roots and other debris, which is transported to the mined out areas and used for the re-shaping of the dunes back to their original appearance. In the floating concentrator the heavy valuable minerals are separated from the light minerals. The difference in density between the valuable and valueless minerals allows the use of a gravity separation process. The slurry is passed over a series of Humphries spirals, separating the heavy from the light minerals. At this stage magnetite and chromite are removed from the heavy mineral fraction using magnetic roll separators. The magnetite and chromite together with the light minerals (tailings) are returned to the dunes. The heavy mineral concentrate, HMC as it is now known, leaves the floating concentrator and is pumped ashore, de-watered and temporarily stockpiled for transportation to the mineral separation plant. The heavy mineral concentrate represents about 5% of the total sand mined, thus the bulk of the sand mined (95%) which consists of light minerals and non-valued heavy minerals is used to re-shape the dunes. (Coastal and Environmental Services, 1982)

## 3.3 Dune Rehabilitation

The light minerals and non-valued heavy minerals (tailings) are pumped to a tailings stacker and de-watered. Together with the collected tree material the tailings are used to re-shape the dunes, bringing back the original topography. The topsoil, which was stripped off ahead of mining is spread over the re-shaped dunes, providing a source of humus as well as seeds of indigenous species. Artificial windbreaks are erected at 10m intervals for additional protection against wind. A mixture of babala grass (*Pennisetum*

*americanum*) an annual millet grass, sunnhemp (*Crotalaria sp.*) and sunflower (*Helio annuus*), together with as many indigenous seeds as possible are sown in the topsoil. The cereals germinate quickly and serve to protect the other young seedlings against harsh wind and rain. The cereals die off after 12 to 15 months leaving behind a healthy cover of indigenous species and within a few months the area is covered with *Acacia karoo* pioneer trees. After five to ten years the pioneer species form a canopy under which trees of a mature coastal forest begin to appear. After 15 to 20 years the acacia trees die off, leaving vegetation virtually identical to the indigenous dune forest. At the land owners' request, a desired crop of commercial trees, mostly *Casserina*, is planted (Coastal and Environmental Services, 1982).

## 3.4 Mineral Separation

In this study samples of about 9kg each were collected from the heavy mineral concentrate stockpiles at each of the three different mining ponds A, B and C operated by Richards Bay Minerals in May 1999. These samples were subsequently separated by the author, under controlled laboratory conditions using equipment (roll magnets and high tension electrostatic separators) at the RBM mineral processing laboratories. The separation scheme used (Fig. 3.5.1) replicates, as closely as possible on the laboratory scale, that utilised in the RBM minerals separation plants for bulk processing of HMC from the mining ponds. Three main mineral separation techniques were applied; (1) magnetic separation, (2) electrostatic separation and (3) heavy liquid separation (Appendix A2). Density separation was always the last step after the magnetic separation and electrostatic separation.
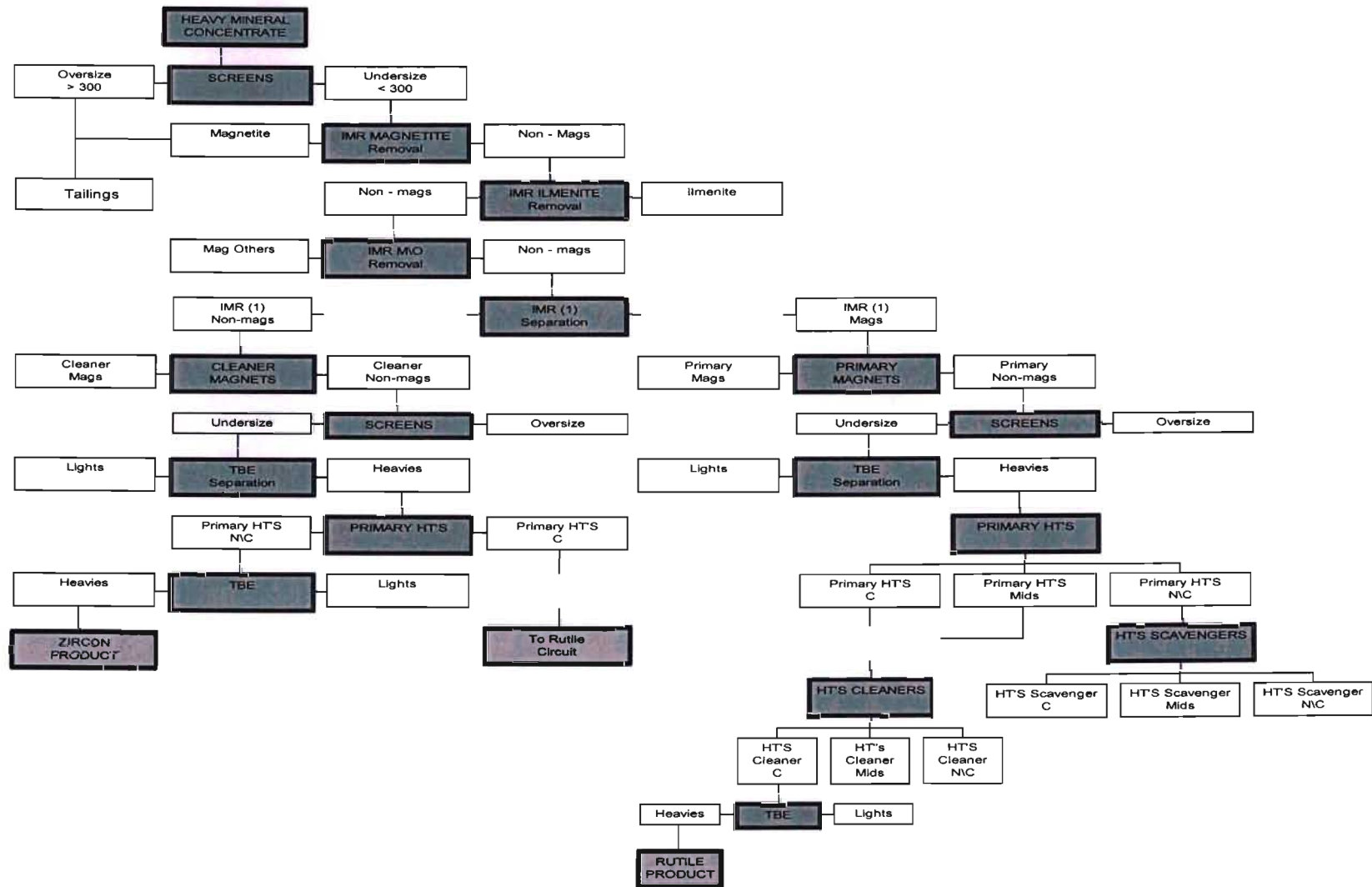
Fig. 3.5.1 Laboratory scheme used for the separation of heavy mineral concentrates to produce rutile and zircon products.

The first step of the separation scheme was to de-slime and dry the three samples in an oven set at 100 °C. In comparison with mining Ponds B and C; Pond A had a high slimes content implying that the ore-body at Pond A had, at the time of sampling, a higher slimes (i.e. clay) content or that the washing process on the barge was significantly less efficient.


## 3.5 Separation Techniques

## 3.5.1 Magnetic Separation

After de-sliming the samples were screened at 710 µm, to remove the oversize particles. The heavy mineral concentrate was then passed through a Carpco Induced Magnetic Roll (IMR) Separator (Appendix A2) at 5, 26, 60 Amp and Max Amp settings respectively. The magnetic fraction was collected at the following stages:

1. after two passes through the Induced Magnetic Roll (IMR) separator set at 5 Amp the 'magnetite' total fraction was removed
2. after two passes at the 26 Amp setting, the 'ilmenite' fraction was removed
3. after one pass at the 60 Amp setting the "mag others" fraction was collected
4. at the max Amp setting, the residual non magnetic sample was split into the 'IMR (1) mags' and the 'IMR (1) non mags' fraction.

The 'IMR (1) non-mags' (NM) followed a circuit that produced a 'zircon product.' Samples were first treated using cleaner magnets; in order to remove the magnetic fraction. The non-magnetic fraction was then screened at 300µm, and the undersize fraction treated with tetra-bromo-ethane (TBE) before commencing with the final stage of electrostatic separation on the heavy fraction (Section 3.5.2).

The 'IMR (1) mags' followed a circuit that produced a 'rutile product'. As with the 'IMR (1) NM'; the 'IMR (1) mags' were first treated with primary magnets, in order to remove the magnetic fraction. The magnetic portion was screened at 300 µm and the undersize

fraction treated with TBE. The 'heavy mineral' fraction was retained for the final stage of electrostatic separation. Table 3.5.1 lists the parameters used for the Induced Magnetic Roll Separator.

| Fraction | Dial Setting | Roll Speed | Vibration Rate | Split setting |
|----------|-------------|------------|----------------|---------------|
| **Magnetite** | 5 Amp | 60 rpm | 4 units | -2 |
| **Ilmenite** | 26 Amp | 60 rpm | 4 units | 3 |
| **Mag Others** | 60 Amp | 60 rpm | 4 units | 0 |
| **IMR (1)** | Max Amp | 40 rpm | 4 units | 2 |
| **Primary Mags** | Max Amp | 40 rpm | 4 units | 2 |
| **Cleaner Mags** | Max Amp | 40 rpm | 4 units | 3 |

Table 3.5.1: Parameters on the Induced Magnetic Roll (IMR) separators for magnetic separation of the samples collected from mining Ponds A, B and C.

## 3.5.2 Electrostatic Separation

A Carpco High Tension Roll Separator was used for the electrostatic separation of the non magnetic samples (Appendix A2). To minimise the effect of atmospheric humidity on the efficiency of the separation, each sample was heated in an oven to 130°C prior to being passed through the High Tension Separators (HT'S). The heavy fraction from the zircon circuit was passed through the Primary HT'S at 18 kV and split into 'conductors' and 'non-conductors' subfractions. The 'non-conductors' were treated with TBE to remove any residual light minerals, and the remaining 'heavies' fraction formed the 'Zircon Product'.

The heavy fraction from the rutile circuit was passed through the Primary HT'S at 20 kV to separate it into 'conductors', 'mids' and 'non-conductors'. The 'non-conductors' were

passed through the HT'S Scavengers at 20 kV. The conductors and mids were combined with the 'conductors' from HT'S Scavengers and used as feed for HT'S Cleaner. After 3 passes on the HT'S Cleaner set at 24 kV, the feed was separated into the three products, HT'S Cleaner Mids, HT'S Cleaner Non-Conductors and HT'S Cleaner Conductors. The HT'S Cleaner 'conductors' were then treated with TBE to remove any residual light minerals. The remaining 'heavies' fraction formed the final 'Rutile Product'. Table 3.5.2 lists the parameters for electrostatic separation.

| Fraction | Setting | Roll Speed | Temperature | Split |
|---|---|---|---|---|
| **Zircon - Primary HT'S** | 18 kV | 220 rpm | 130°C | open |
| **Rutile - Primary HT'S** | 20 kV | 220 rpm | 130°C | -1 & 0 |
| **HT'S Scavengers** | 20 kV | 220 rpm | 130°C | -1 & 0 |
| **HT'S Cleaners** | 20 kV | 220 rpm | 130°C | -1 & 0 |

Table 3.5.2   The parameters on the Carpco High Tension Separators for electrostatic separation of samples collected from ponds A, B and C.

## 3.6 Laboratory Separation Results

The results from the laboratory scale separation are given in Table 3.6.1, and graphical representation of the data is given in Fig. 3.6.1. The dominant fraction from all three mining ponds was the ilmenite fraction (Fig. 3.6.1) as in all cases this constituted almost 80% of the heavy mineral concentrate (HMC). Although Pond C had the highest ilmenite count in the HMC the difference of 0.15% compared to Pond B is of questionable significance, and the difference of 1.52% between Ponds C and A very minor.

27

| FRACTIONS | POND A | POND B | POND C |
|---|---|---|---|
| | % | % | % |
| Oversize (>710μm) | 0.50 | 0.02 | 0.07 |
| Magnetite | 1.38 | 1.14 | 1.66 |
| Ilmenite | 78.12 | 79.49 | 79.64 |
| Cleaner Mags | 4.65 | 3.89 | 4.90 |
| Primary Mags | 3.54 | 6.22 | 4.27 |
| Mag others | 1.90 | 3.16 | 1.47 |
| Oversize - >300μm(Cleaner Mags) | 1.63 | 0.02 | 0.09 |
| Oversize - >300μm (Primary Mags) | 0.01 | 0.00 | 0.00 |
| Zircon product | 4.47 | 3.61 | 3.89 |
| Primary HT'S (C) | 0.99 | 0.92 | 0.83 |
| HT'S Scavengers (M+NC) | 0.05 | 0.26 | 0.16 |
| HT'S Cleaner (M) | 0.08 | 0.16 | 0.13 |
| HT'S Cleaner (NC) | 0.27 | 0.25 | 0.34 |
| Rutlile product | 0.09 | 0.14 | 0.22 |
| Lights | 2.31 | 0.72 | 2.33 |
| TOTAL | 99.99 | 100.00 | 100.00 |

Table 3.6.1  Laboratory separation data for the samples collected RBM Mining Ponds A, B and C.

Fig. 3.6.1 Laboratory separation for samples collected from RBM Mining Ponds, A, B and C.
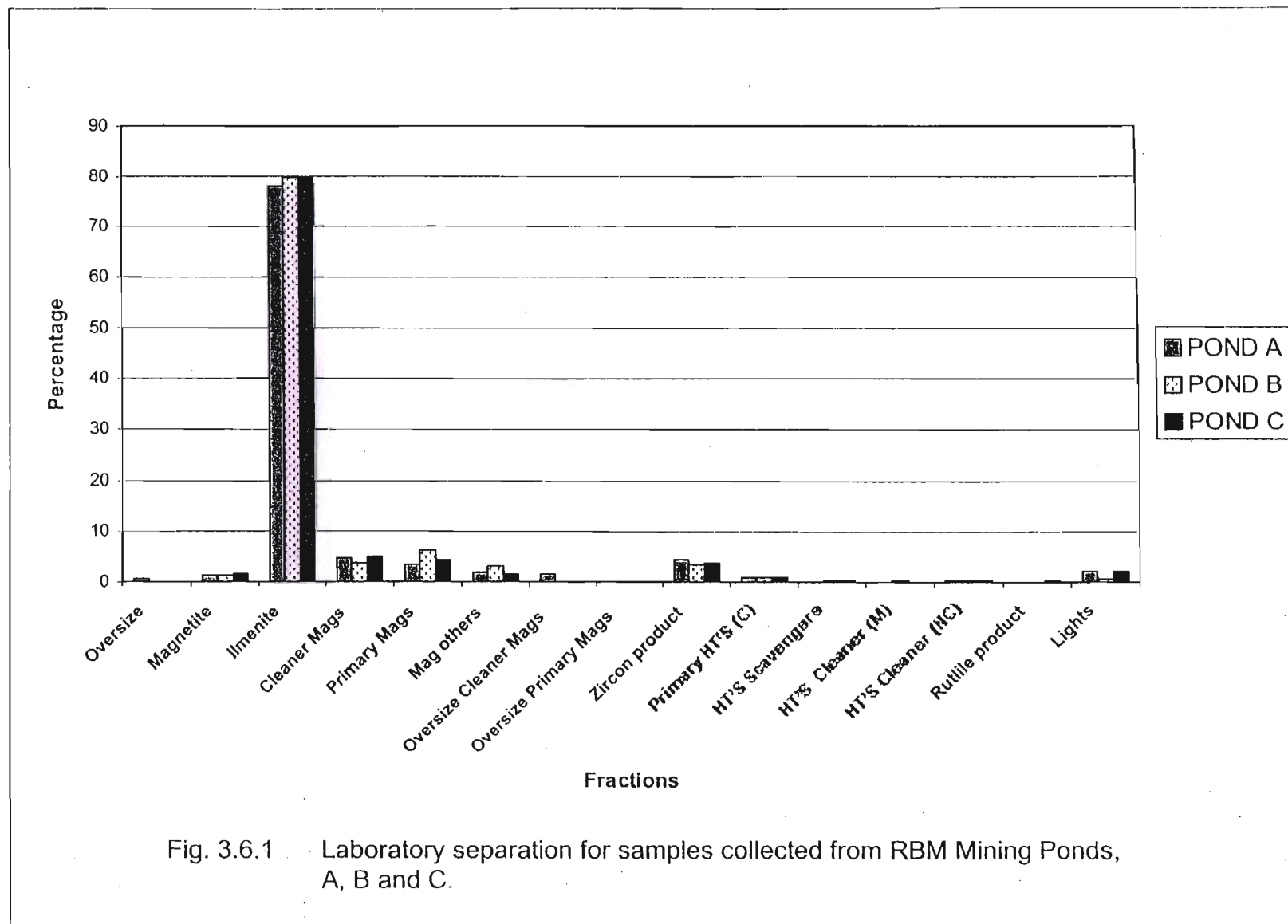
The distribution of the fractions other than ilmenite shown in Fig. 3.6.2 as relationships are somewhat obscured by the very high ilmenite peak in Fig. 3.6.1.

The total 'lights' fraction consists of less than 2½ % of the HMC (Fig. 3.6.2), implying that the density separation at the ponds is effective in removing most of the light minerals from the concentrate. However, the fact that the HMC from Pond B contained less than a third of the light minerals of Ponds A and C suggests that, either the primary separation of the Pond B ore is significantly more efficient, or that the "cut off" conditions could be set too high and maybe causing some loss of valuable heavy minerals.

The magnetite fraction from all three ponds accounted for less than 2% of the total HMC. The initial magnetic separation on the barges therefore appears effective in reducing quantity of magnetite in the HMC.

The screening process on the barges appears relatively efficient in removing the oversize particles from HMC. Pond A however, had a greater percentage of oversize (0.50% >710μm and 1.60% > 300μm) indicating a possible problem in the separation technique on the pond.

Pond A had the lowest ilmenite content (78.12% of HMC) and the lowest rutile product yield (0.09% of HMC), but the highest zircon product yield (4.47% of HMC). This suggests that the ore-body at Pond A is more zircon enriched than the ore bodies mined at Pond B and Pond C.

Pond B had a high ilmenite yield (79.48% of HMC) and a rutile yield of 0.14% of HMC. The zircon yield for Pond B (3.61% of HMC) was lower than that of Ponds A and C. Pond B had a high proportion of 'mag others' fraction compared to Ponds A and C,
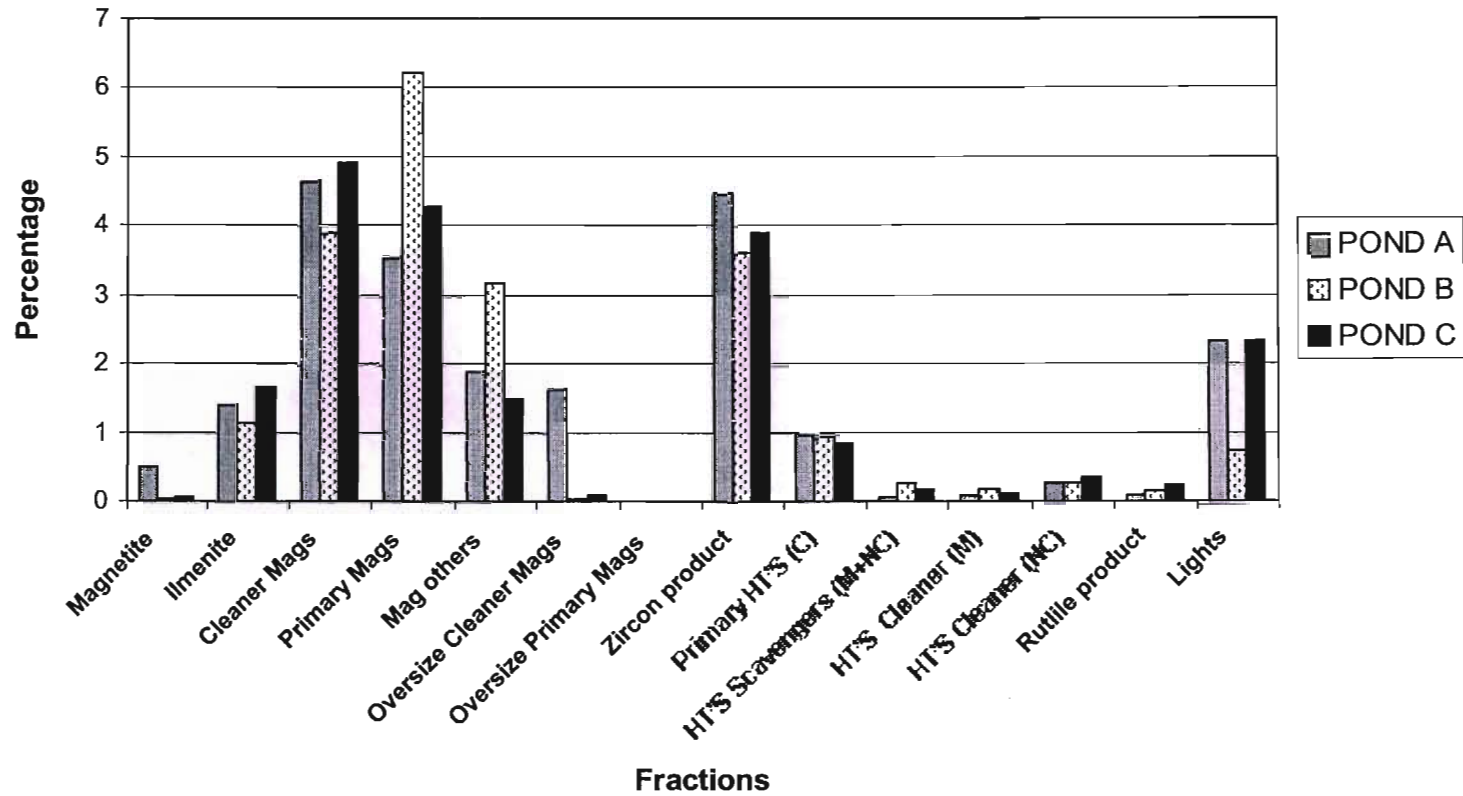
**Fractions**

Fig. 3.6.2 Laboratory separation for samples collected from RBM Mining
Ponds, A, B and C, excluding the dominant ilmenite fraction.

which implies that the ore body at Pond B has a relatively higher proportion of silicate minerals.

Pond C had the highest yield of ilmenite (79.64% of HMC) as well as the highest rutile yield (0.22% of HMC). Pond C had a higher magnetite content then Ponds A and B. The ore body at Pond C was therefore considered to be ilmenite and rutile enriched compared to Ponds A and B.

## 3.7 Rutile Distribution in the Heavy Mineral Concentrate

Optical microscope studies on polished sections prepared from the three mining ponds revealed that rutile occurs in most of the magnetic and electrostatic fractions. The only fractions containing less than 5% rutile were the 'magnetite' fraction, 'oversize' fractions, 'zircon product', the 'HTS scavenger mids' and 'HTS scavenger non-conductors' as well as the 'lights' mineral fractions. Table 3.7.1 shows the fractions containing more than 5% homogenous rutile grains were; 'ilmenite' fraction (6%), 'mag others' (23%), 'cleaner mags' (13%), 'primary mags' (52%) 'primary HT'S conductors' (5%), 'rutile product' (98%), 'HT'S cleaner mids' (78%) and 'HT'S non-conductors' (13%) (Fig. 3.7.1).

| FRACTIONS | % RUTILE |
|---|---|
| Ilmenite | 6 |
| Mag Others | 23 |
| Cleaner Mags | 13 |
| Primary Mags | 52 |
| Primary HT'S (C) | 5 |
| HT'S Cleaner (C) | 98 |
| HT'S Cleaner (M) | 78 |
| HT'S Cleaner (NC) | 13 |

Table 3.7.1 Average rutile content in magnetic and electrostatic fractions.
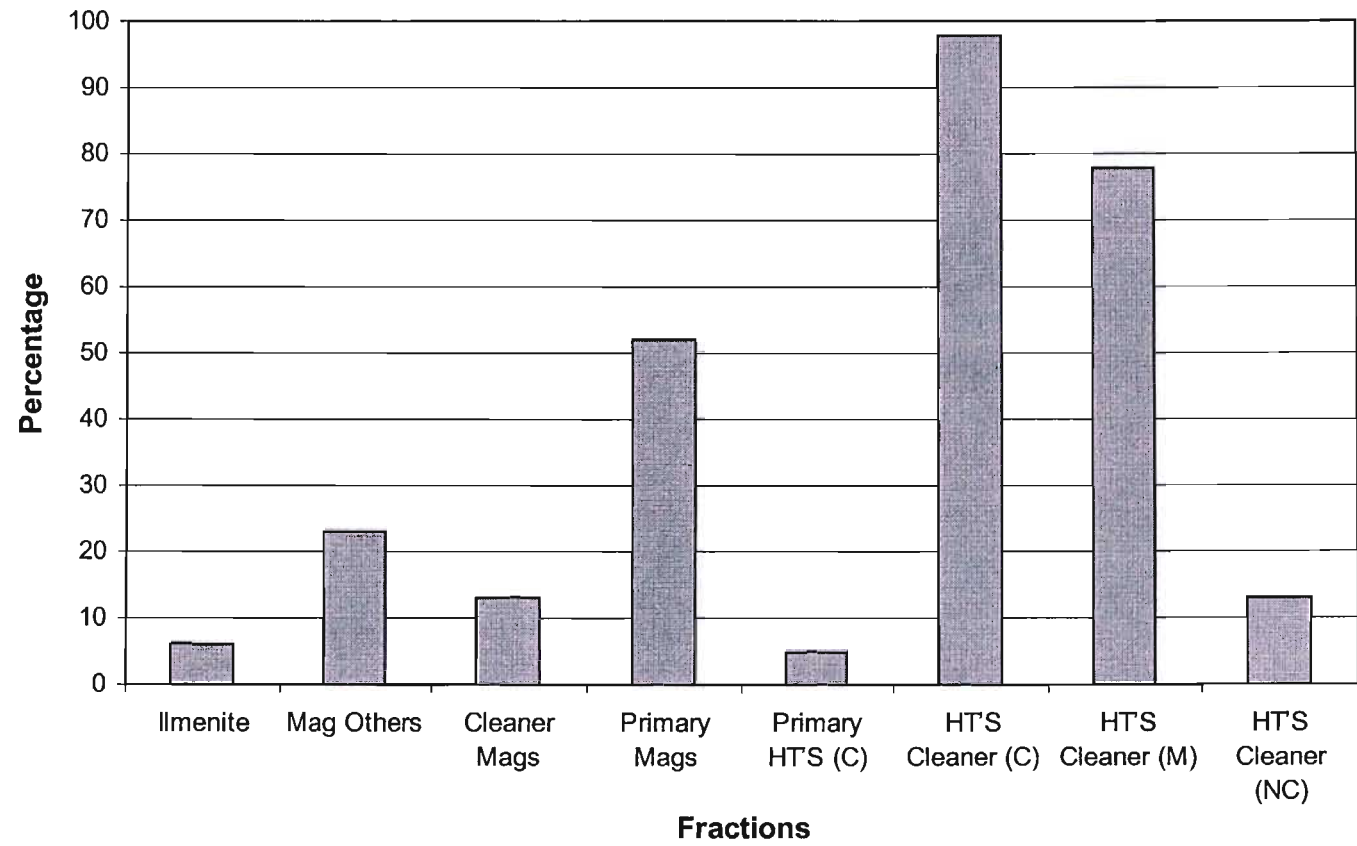
Fig. 3.7.1 The relative content of homogenous rutile grains in each fraction is shown.

The occurrence of rutile grains in most fractions of the heavy mineral concentrates confirms observations (sections 1.5 and 4.4) of the variability of magnetic susceptibility and electrical conductivity of homogenous rutile grains

Representative samples of the 'ilmenite' and 'mag others' fractions were further separated using a Frantz Isodynamic Magnetic Separator (Tables 3.7.2 and 3.7.3). The advantage of using the Frantz Isodynamic Magnetic Separator was that it allowed for the fine adjustment of current, giving better manipulation of the magnetic field than the Carpco Induced Magnetic Roll Separators, and provides an opportunity to separate individual minerals according to their particular properties (Appendix A2). Polished sections of each sub-fraction were studied using optical microscopy and electron probe micro-analysis.

| Current | POND A | | POND B | | POND C | |
|---|---|---|---|---|---|---|
| Settings (A) | g | % | g | % | g | % |
| 0.1 Amp | 0.78 | 7.94 | 0.59 | 5.97 | 0.64 | 6.79 |
| 0.2 Amp | 6.48 | 65.86 | 5.77 | 58.41 | 5.83 | 61.82 |
| 0.3 Amp | 0.87 | 8.85 | 0.56 | 5.67 | 1.36 | 14.42 |
| 0.4 Amp | 0.43 | 4.37 | 1.11 | 11.23 | 0.49 | 5.20 |
| 0.5 Amp | 0.53 | 5.39 | 0.76 | 7.69 | 0.43 | 4.56 |
| 0.6 Amp | 0.20 | 2.03 | 0.52 | 5.26 | 0.16 | 1.70 |
| 0.7 Amp | 0.12 | 1.22 | 0.17 | 1.72 | 0.07 | 0.74 |
| Non mags | 0.43 | 4.34 | 0.40 | 4.05 | 0.45 | 4.77 |
| TOTAL | 9.84 | 100.00 | 9.88 | 100.00 | 9.43 | 100.00 |

Table 3.7.2 : Ilmenite sub-fractions obtained using the Frantz Isodynamic Separator.

| Current | POND A | | POND B | | POND C | |
|---|---|---|---|---|---|---|
| Settings | g | % | g | % | g | % |
| 0.4 Amp | 0.51 | 5.13 | 0.24 | 2.40 | 0.20 | 1.99 |
| 0.5 Amp | 1.94 | 19.50 | 2.05 | 20.46 | 2.33 | 23.16 |
| 0.6 Amp | 2.49 | 25.02 | 2.87 | 28.64 | 1.37 | 13.62 |
| 0.7 Amp | 3.06 | 30.75 | 3.61 | 36.02 | 2.91 | 28.93 |
| 0.8 Amp | 0.42 | 4.22 | 0.23 | 2.30 | 0.63 | 6.26 |
| 0.9 Amp | 0.29 | 2.91 | 0.14 | 1.40 | 0.29 | 2.88 |
| 1.0 Amp | 0.15 | 1.51 | 0.08 | 0.80 | 0.45 | 4.47 |
| 1.1 Amp | 0.10 | 1.01 | 0.08 | 0.80 | 0.29 | 2.88 |
| 1.2 Amp | 0.14 | 1.41 | 0.08 | 0.80 | 0.23 | 2.29 |
| 1.3 Amp | 0.13 | 1.31 | 0.13 | 1.30 | 0.21 | 2.09 |
| 1.4 Amp | 0.08 | 0.80 | 0.07 | 0.70 | 0.17 | 1.69 |
| 1.5 Amp | 0.58 | 5.83 | 0.11 | 1.10 | 0.11 | 1.09 |
| Non mags | 0.06 | 0.60 | 0.33 | 3.29 | 0.87 | 8.65 |
| TOTAL | 9.95 | 100.00 | 10.02 | 100.01 | 10.06 | 100.00 |

Table 3.7.3: Mag others sub-fractions separated using Frantz Isodynamic Separator.

## 3.8 Ilmenite sub-fractions

The ilmenite fractions treated using the Frantz Isodynamic Magnet Separator at a variety of current settings produced a number of ilmenite sub-fractions (Table 3.7.2). All three ponds showed similar trends (Fig. 3.8.1), with the largest fraction (approximately 60%) extracted at 0.2 Amp. The smallest fraction (approximately 3.0%) was removed at 0.7 Amp.
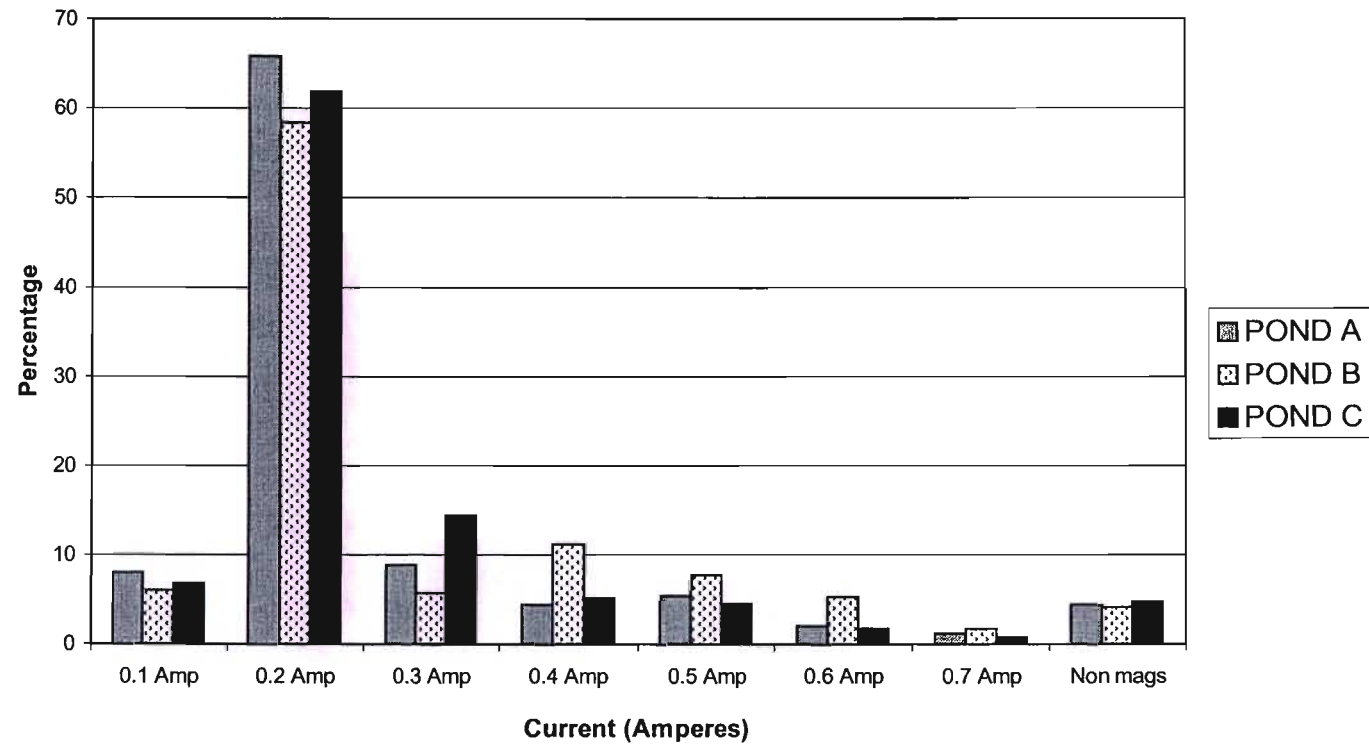
Fig. 3.8.1    Ilmenite sub-fractions separated using the Frantz Isodynamic
Magnetic Separator.

## 3.8.1 Mineralogy

The first three ilmenite sub-fractions (0.1 to 0.3 Amp) consisted of mostly ilmenite, haematite and garnets. Minor minerals include olivine (fayalite variety), amphiboles (actinolite) and pyriboles (Mn enriched silicates, as described by Hugo, 1993).

The 0.4 to 0.5 Amp sub-fraction contained a wider range of minerals, i.e. ilmenite and altered hematite as well as amphiboles, pyroxenes and epidote. Amphiboles were of the hornblende and actinolite variety.

The ilmenites from the 0.6 Amp sub-fraction were titanium enriched; however, most of the fraction consisted of silicates, i.e. garnets, pyroxenes (augite), amphiboles (hornblende, epidote, and actinolite), and olivine (forsterite). Iron-enriched rutile occurred within this magnetic fraction.

The 0.7 Amp sub-fraction was composed of silicates and monazite, with many of the monazite grains having one or more quartz inclusions. Monazite was often found intergrown with rutile, which suggests that a rare earth element enriched environment maybe a possible source area for a significant quantity of the rutile. The rutile grains in this fraction appeared to be iron-enriched (Section 5.2.1.).

Zircon and rutile made up virtually all the non-magnetic fraction. The rutile grains from this fraction appeared to be chemically impure, as they contain silica, iron and aluminium (Section 5.2.2.).

## 3.9 Mag Others sub-fractions

The Mag Others fraction was also separated into sub-fractions using a Frantz Isodynamic Magnetic Separator (Table 3.7.3). As with the ilmenite sub-fractions, all 3 mining ponds showed a similar distribution (Fig. 3.9.1). The bulk of the sample was extracted approximately 75 - 80% within the first four current settings (0.4 - 0.7 Amp).

## 3.9.1 Mineralogy

The first four sub-fractions (0.4 to 0.7 Amp) had the same mineralogy as the corresponding ilmenite sub-fractions

The 0.4 (and 0.7 Amp) sub-fractions(s) contained mostly silicates minerals (garnets, hornblende, epidote, and pyriboles) with some haematite, chromite and ilmenite.

The first occurrence of an iron-enriched rutile was in the 0.6 Amp sub-fraction. The 0.7 Amp sub-fraction contained a range of silicates (garnets, augite and tourmaline), altered ilmenites and rutile. The rutile within this sub-fraction was iron-enriched and also contained traces of silica and alumina (Section 5.3.1.).

Within the 0.8 Amp and 0.9 Amp sub-fractions the dominant minerals extracted were the silicates, with some monazite and zircon. The rutile extracted in this range was iron-enriched, containing impurities of silica and alumina (Section 5.3.1)

At 1.0 Amp the three main minerals extracted were monazite, zircon and silicates. Very few rutile grains were removed at this setting.
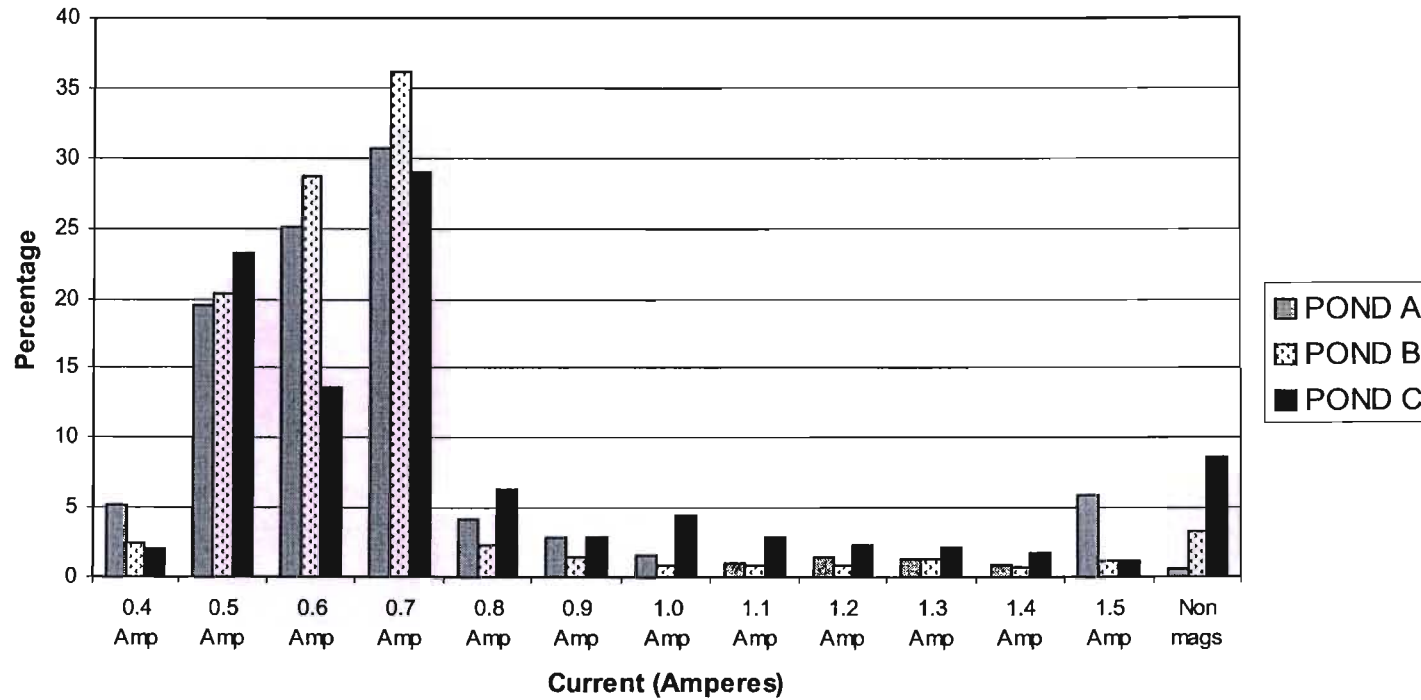
Fig. 3.9.1 Mag others sub-fraction separated using the Frantz
Isodynamic Magnetic Separator.

In the 1.1 to 1.5 Amp range, the quantity of rutile grains increased in relation to the lower currents. Zircons, together with the minerals apatite, titanite and quartz were also extracted. The rutile grains within this range contained only traces of silica and alumina.

The non-magnetic sub-fraction consisted of predominantly rutile and zircon grains, with minor contaminants of iron, silica and alumina.

# 4. Rutile Mineral Chemistry

Titanium dioxide has three polymorphs; rutile, anatase and brookite (Ramdohr 1969) that, although physically different, are almost identical in polished section. Rutile is the high temperature polymorph that is stable at almost all temperatures and pressures. Anatase normally forms at very low temperature and pressure, in part, as a result of weathering (Ramdohr 1980). Anatase is only stable at low temperature and converts to rutile at approximately 600°C, while brookite is metastable and readily transforms to rutile or anatase (Hugo 1993). Table 4.1 gives an outline of the properties of the three polymorphs of titanium dioxide.

## 4.1 Crystal Structure

Each of the three polymorphs of titanium dioxide has a distinctive arrangement of the titanium and oxygen ions and crystal structure. (Fig. 4.1).

In the rutile crystal structure each titanium ion ($Ti^{4+}$) is surrounded by six oxygen ions ($O^{2-}$) at the corners of a slightly distorted octahedron, while each oxygen ion is in turn surrounded by three titanium ions lying in a plane at the apices of an approximately equilateral triangle (Fig. 4.1A) (Lindsley *et al.*, 1976).

Anatase has a similar arrangement of ions to rutile with each titanium ion surrounded by six oxygen ions and every oxygen ion surrounded by three titanium ions. There is, however a structural difference in the mutual arrangement of the oxygen octahedra. In anatase the shared edges at the top and bottom of the octahedra are at right angle (Fig. 4.1B), whilst in rutile the two opposite edges are shared (Lindsley *et al.*, 1976).

In brookite, each titanium ion in the structure is surrounded by three oxygen ions. The structure of brookite (Fig. 4.1C) differs from rutile and anatase in that the mutual

arrangement of the oxygen octahedra lie in zig-zag lines rather than straight lines or rows (Lindsley *et al.*, 1976*)*.

| | Rutile | Brookite | Anatase |
|---|---|---|---|
| **Density (g/cm$^3$)** | 4.23 to 5.50 | 4.08 to 4.18 | 3.82 to 3.97 |
| **Hardness** | 6.0 to 6.5 | 5.5 to 6.0 | 5.5 to 6.0 |
| **Crystal System** | Tetragonal | Orthorhombic | Tetragonal |
| **Optical Character** | Uniaxial (+) | Biaxial (+) | Uniaxial (-) |
| **Conditions of formation** | High temperature and pressure | Medium to low temperature and pressure | Low temperature and pressure |

Table 4.1 Physical properties of the titanium oxide polymorphs (Deer *et al.* 1985).
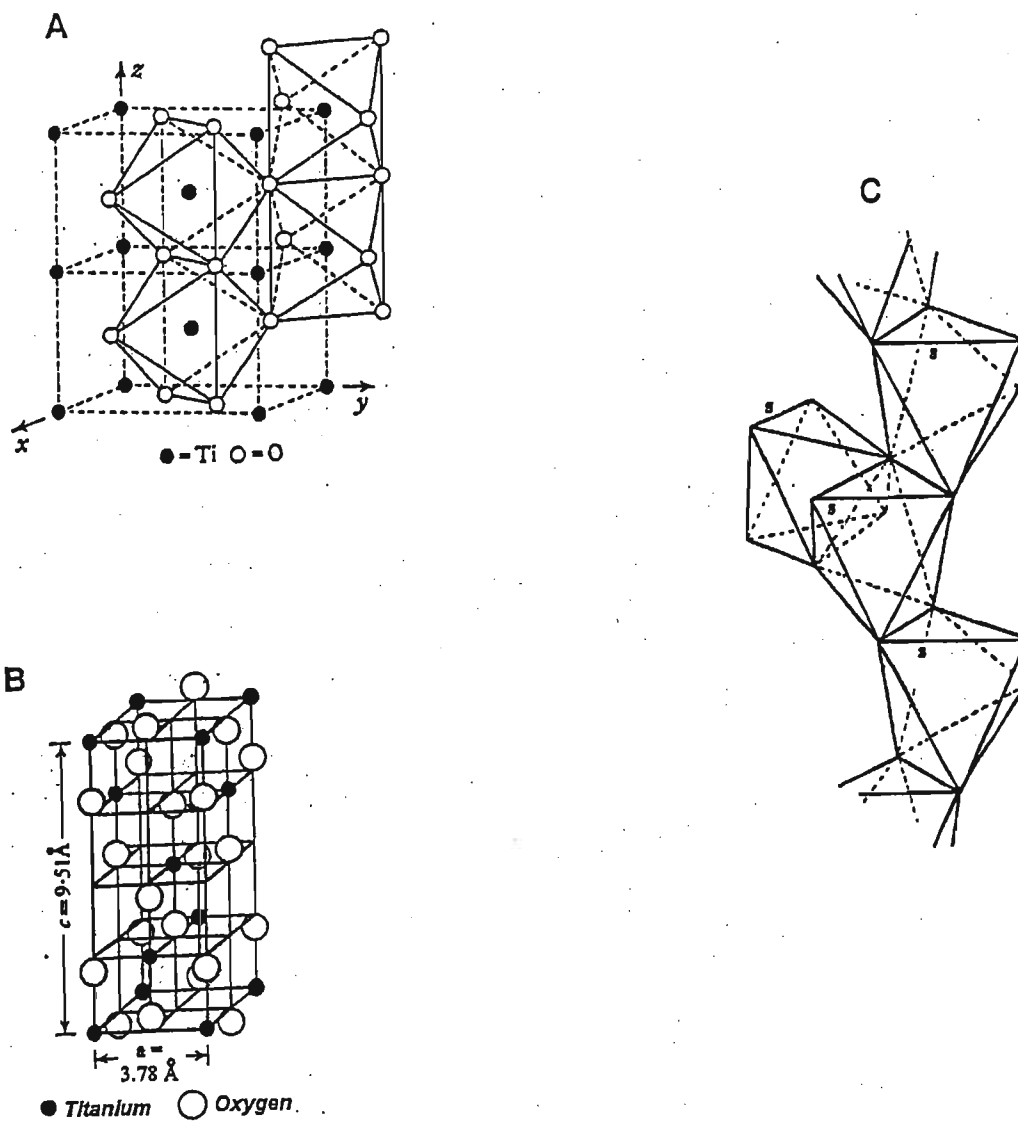
Fig. 4.1 The structures of the TiO$_2$ polymorphs rutile, anatase and brookite (Lindsley, 1976). **A.** Four unit cells of rutile showing the octahedral of oxygen about Ti at the centre of each cell. **B.** Two unit cells of anatase showing the distorted octahedral of oxygen about the Ti (shared edges (s)) are shorter than the unshared edges. **C.** The chain of distorted oxygen octahedral about the Ti ions which make-up the brookite structure.

## 4.2 Rutile Mineralogy

The mineral chemistry of rutile is closely associated with that of iron-titanium oxides due to their complex behaviour at elevated temperatures and pressures (Fig. 4.2). Most iron-titanium oxide minerals can be represented on the $TiO_2$ - $Fe_2O_3$ - $FeO$ system (Fig. 4.2). Although magnetite, ilmenite and haematite are common minerals, their exact chemical composition is difficult to determine due to extensive chemical substitution and problems in establishing the oxidation states of the ions (Force 1991).

The following can be noted for the ternary $TiO_2$ - $Fe_2O_3$ - $FeO$ system (Fig. 4.2):

- the $TiO_2$ polymorphs:
  - rutile –      is tetragonal and stable at most temperatures and pressures,
  - anatase –   Is tetragonal and converts to rutile at above approximately 600°C
  - brookite –   Is orthorhombic; metastable, and will readily transform to anatase and rutile (Hugo 1993)
- ferropseudobrookite ($FeTi_2O_5$) is only stable above 1100°C (Gribble and Hall, 1992) and is an optically homogeneous orthorhombic iron-titanium phase with less than 50mol% $Fe_2TiO_5$ (Hugo 1993)
- pseudobrookite ($Fe_2TiO_5$) is only stable above 585°C (Gribble and Hall, 1992); it is similar to ferropseudobrookite, but with more than 50 mole percent $FeTi_2O_5$ (Hugo 1993)
- ilmenite ($FeTiO_3$) – haematite ($Fe_2O_3$) solid solution series is only complete above 950°C (Gribble and Hall, 1992)

# Mineralogy of the Iron-Titanium Oxides.
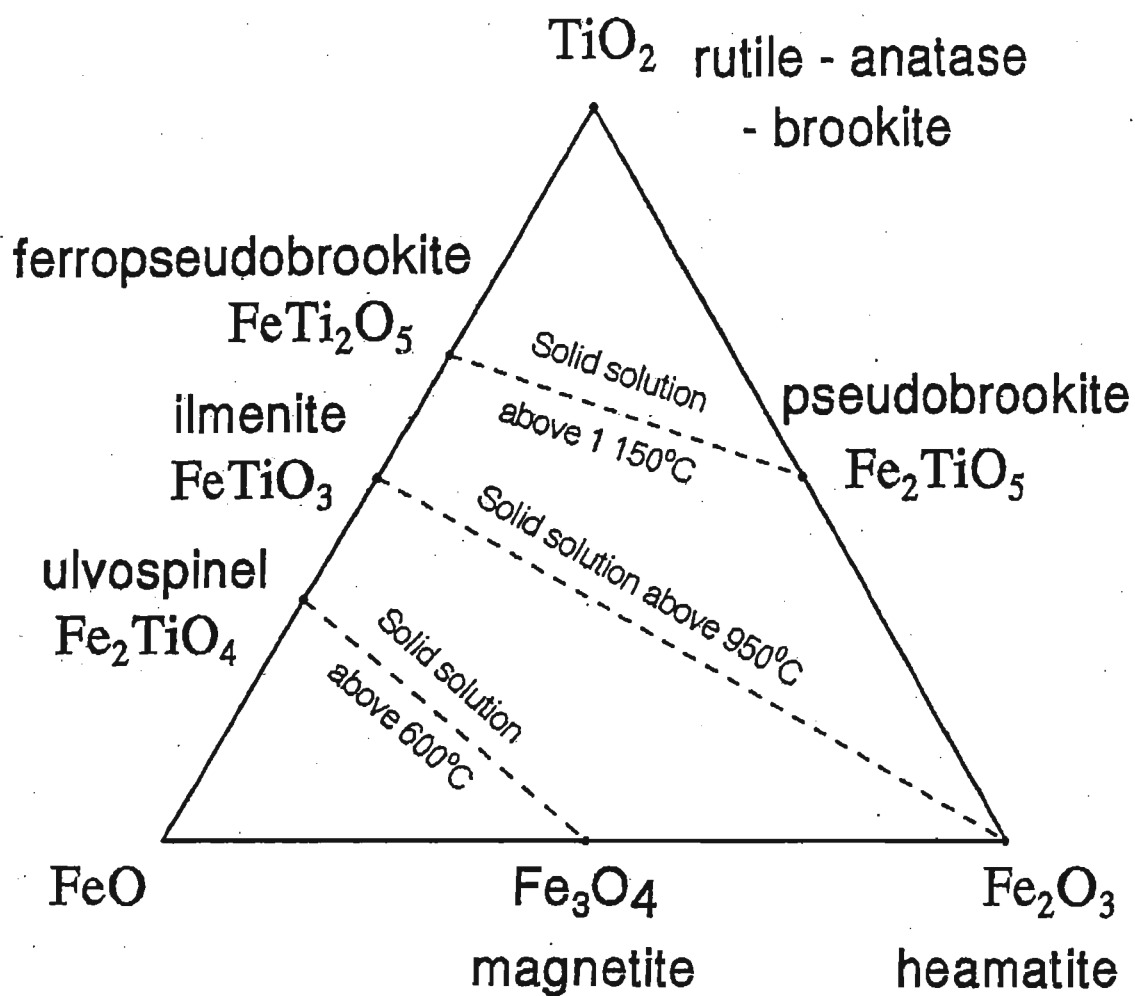


Fig. 4.2     The TiO$_2$ - Fe$_2$O$_3$ - FeO system showing the extent of high temperature solid solution. (After Hugo, 1990 and Mdludlu, 1998)

- ilmenite is a rhombohedral (trigonal) phase consisting of $FeTiO_3$ with up to 6wt% $Fe_2O_3$ in solid solution (Hugo 1993)
- hematite is a trigonal phase with a stoichiometry approaching $Fe_2O_3$ normally with less than 5wt% $TiO_2$ (Hugo 1993)
- bulk composition of hemo-ilmenite and ilmeno-hematite grains depends on the equilibrium temperature (Gribble and Hall, 1992)
- the ulvospinel ($Fe_2TiO_4$) – magnetite ($Fe_3O_4$) solid solution series is only complete above 600°C (Gribble and Hall, 1992);
- magnetite $Fe_3O_4$ is a spinel phase with a stoichiometry approaching $Fe_2O_3$ normally containing less than 5wt% $TiO_2$ (Gribble and Hall, 1992);

## 4.3 Solid Solution

The definition of solid solution is that a single crystalline phase may vary in composition within finite limits without the appearance of an additional phase (Bates and Jackson, 1980). The three mechanisms for solid solution are substitution solid solution, omissional solid solution and interstitial solid solution.

Substitution solid solution is when different atoms may occupy the site if their sizes and charges are such that the geometrical stability and local charge balance is maintained.

Omission solid solution is the removal of atoms from the structure leaving vacancies, in the structure to maintain charge balance during a substitution mechanism.

Interstitial solid solution takes place when mineral interstices which occur between the atomic structural framework of a mineral are used to accommodate cations to balance off substitution solid solution (Putnis and McConnell 1980).

Solid solution is governed by Goldschmidt's Rules, which state (Bloss, 1971):

- ions of similar radii (< 15% size difference) and having a charge difference of no more than one may enter into the same crystal lattice site

- when two ions with the same charge compete for a lattice site the ion of smaller radius will be preferred

- when two ions of the same radius (± 15%) compete for a lattice site the ion with the higher charge will be preferred.

When these ionic substitution rules are applied to the $Ti^{4+}$ ion, only a limited number of ions are found to be compatible. The plot of ionic radius and charge (Fig. 4.3) clearly indicates that $Sb^{3+}$, $V^{3+}$, $Fe^{3+}$, $Cr^{3+}$, $Sn^{4+}$, $Mo^{4+}$, $W^{4+}$, $Mn^{4+}$, $Bi^{5+}$, $Nb^{5+}$, $Ta^{5+}$, $Sb^{5+}$, $V^{5+}$ must be considered as compatible with the $Ti^{4+}$ ion.

The oxidation states of minor components in rutile are governed by the electroneutrality condition (Vlassopoulos et al. 1993).

- Aluminium in rutile is present in the $Al^{3+}$ state and is compensated for by $OH^-$ groups.

- Vanadium in rutile structures may occur in the trivalent or pentavalent state.

- Chromium occurs as a trivalent cation in natural rutile.

- Iron in rutile can be either divalent or trivalent.

- Rutile crystals can be synthesised at 1400°C with up to 25 mol% $Nb_2O_5$ solid solution, but inversion voltammetric studies have shown that above 3 mol% $Nb_2O_5$, the niobium is partly reduced to $Nb^{4+}$. Niobium occupies titanium sites though it can be tetravalent or pentavalent. The niobium content of natural rutile from kimberlite can be up to 20.9 wt%.

- Tantalum is pentavalent and substitutes for titanium
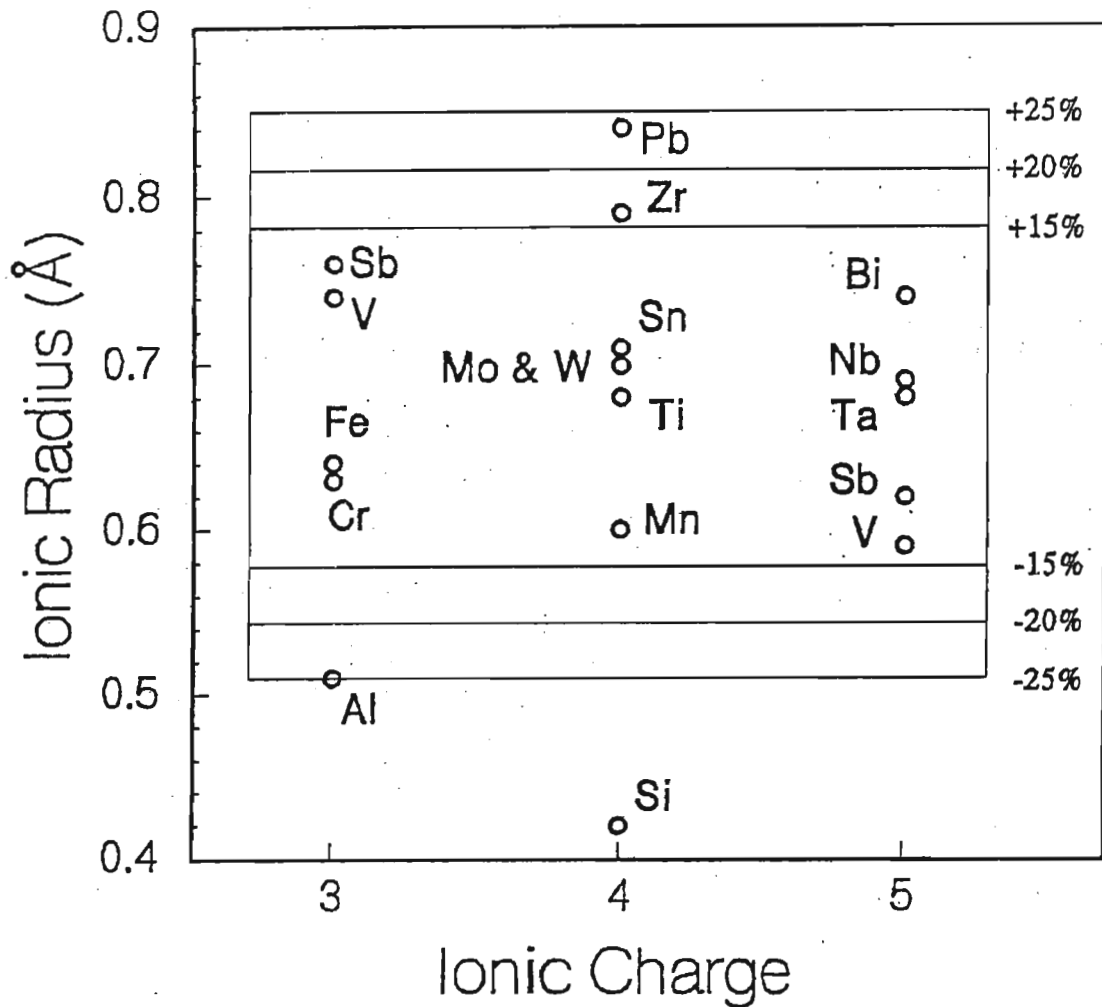
Fig. 4.3 Plot of ionic charge against ionic radius. The ions in the inner portion (i.e.±15% of the titanium ion radius) are considered to be competent for solid solution with titanium, whilst those in the outer portion will only be considered in exceptional circumstances. (After Bramdeo and Dunlevey 1999)

At elevated temperatures and pressures it appears possible that zirconium ions ($Zr^{4+}$) may substitute for titanium ions ($Ti^{4+}$). Under elevated conditions, lead and aluminium may also possibly substitute for titanium. At extremely high temperatures and pressures such as those found in near anatectic metamorphic environments, silicon, which has the same charge and a smaller radius than titanium, may enter solid solution with titanium dioxide from a silicate melt. However as $Ti^{4+}$ ion is approximately 1.7 times larger than the $Si^{4+}$ ion, it cannot enter the quartz lattice; exsolution occurs to form composite mineral grains. This feature is illustrated by rutilated quartz, which has titanium dioxide (rutile) exsolved as needles within quartz (Bramdeo and Dunlevey, 1999, 2000).

Some rutile crystals contain considerable amounts of $Fe^{2+}$ and $Fe^{3+}$, major amounts of niobium and tantalum as well as minor amounts of chromium, aluminium and silicon. The close similarity in the ionic radius between $Ti^{4+}$ and both $Nb^{5+}$ and $Ta^{5+}$ enable the latter ions to enter the titanium lattice site, in these cases the rutile structure is electrostatically balanced either by vacancies in some lattice positions or by the complementary substitution of divalent or trivalent ions such as $Fe^{2+}$, $Fe^{3+}$, $Cr^{3+}$, or $V^{3+}$ (Deer *et al.* 1985).

## 4.4 Rutile Chemistry

## 4.4.1 Hydrogen in Rutile

In general rutile has an affinity for hydrogen. Research done by Vlassopoulos *et al.* (1993) has demonstrated that the $H^+$ content in rutile can be as high as the equivalent of 0.8 wt% $H_2O$. The highest concentration occurs in mantle derived (high pressure) Nb and Cr rich rutile of metasomatic origin. Vlassopoulos *et al.* (1993) considered hydrogen to be present in the crystal structure to compensate for trivalent substitutional cations ($Cr^{3+}$, $Fe^{3+}$, $Al^{3+}$, and $V^{3+}$) that are only partly compensated by pentavalent ions ($Nb^{5+}$, $V^{5+}$ and $Ta^{5+}$).

Coupled substitution of the types:

$$M^{3+} + M^{5+} \leftrightarrow 2Ti^{4+} \text{ and}$$

$$M^{2+} + 2M^{5+} \leftrightarrow 3Ti^{4+}$$
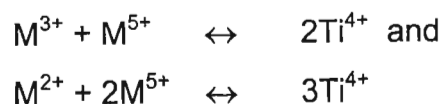
are common in synthetic rutile to maintain electrostatically neutral compounds.

In natural rutile, however, there is normally an overall excess of trivalent over pentavalent impurities per formula unit that is then compensated for by interstitial $H^+$. According to Vlassopoulos et al. (1993), the concentration of $H^+$ per formula unit and the mechanism for substitution is:

$$[H^+] = \Sigma \, [M^{3+}]_{Ti} + 2\Sigma[M^{2+}]_{Ti} - \Sigma \, [M^{5+}]_{Ti}$$

## 4.4.2 TiO$_2$ - NbO$_2$ - TaO$_2$ Relationship

Minerals of the columbite - tantalite group have the general formula $AB_2O_6$ where; A = $Ni^{2+}$ $Fe^{2+}$, $Mn^{2+}$ and B = $Nb^{5+}$, $Ta^{5+}$. When Nb > Ta, the mineral is called columbite and when Ta > Nb, the mineral is called tantalite. Wenger and Armbruster (1993) synthesised a columbite-type compound and a rutile-type compound from a $NiNb_2O_6$ - $TiO_2$ system.

Niobium and tantalum are both pentavalent (for most geologic redox conditions) and have a similar ionic radius. Linnen and Keppler (1997), found that rutile forms an extended solid solution series with columbite due to the structural similarities of the niobium and tantalum ions, and also reported rutile grains with up to 66wt% columbite or tantalite component. Linnen and Keppler (1997), concluded that most of the $Nb^{5+}$ and $Ta^{5+}$ incorporated in rutile is through solid solution with columbite - tantalite end members.

Hassan (1994) demonstrated that homogenous Nb - Ta containing rutiles from Malaysia are magnetic. Furthermore, the study by Hassan (1994) indicates the existence of an isomorphous series between rutile (sensu-stricto) and Ta - Nb enriched rutiles.

## 4.4.3 $Ti^{3+}$ and $Fe^{3+}$ in rutile

In addition to containing $Ti^{4+}$ rutile may also contain $Ti^{3+}$ cations within the crystal lattice (Banfield and Veblen, 1991). These $Ti^{3+}$ ions appear in planes forming potential crystallographic shears within the rutile crystal lattice, and act as a zone of weakness. Furthermore, these zones allow for the substitution of trivalent ($Fe^{3+}$) in the rutile lattice (Banfield and Veblen, 1991). The replacement of $Ti^{3+}$ by $Fe^{3+}$ in the rutile lattice may also form sub microscopic platelets with a hematite structure (Banfield and Veblen, 1991). Bursill *et al.* (1984) proposed a model explaining the formation of pairs of crystallographic shear planes; their model requires that three $Ti^{4+}$ cations replace four $Ti^{3+}$ cations.

$$3Ti^{4+} \leftrightarrow 4Ti^{3+}$$

As much as 16 wt% $Fe_2O_3$ can be accommodated in rutile crystals through crystallographic shear structures and the replacement of $Ti^{3+}$ by $Fe^{3+}$ (Blanchin and Bursill, 1989). According to Banfield and Veblen (1991) the appearance of regularly spaced iron-rich lamellae throughout rutile crystals is due to the exsolution of iron that was originally present in the rutile structure. High temperature and pressure metamorphic conditions would be likely to provide the environment most conducive for iron inclusion by this process.

## 4.4.4 Aluminium in rutile

Bursill et al, 1984 studied aluminium in rutile using synthetic aluminium-doped rutile crystals and proposed that the mechanism whereby $Ti^{4+}$ is replaced by $Ti^{3+}$, allowed for the substitution of trivalent ions ($Al^{3+}$, $Fe^{3+}$, $Cr^{3+}$ etc) for $Ti^{3+}$. Studies conducted by Blanchin and Bursill (1989) revealed that aluminium-doped rutile crystals produced heart-shaped alumina precipitates about 5µm in diameter, after the application of a compressive force at $1000^{0}C$. The results indicated that concentrations of about 0.5wt% $Al_2O_3$ could be accommodated in the $TiO_2$ lattice at temperatures below approximately $1000^{0}C$ by two mechanisms;

1. In crystallographic shear planes developed at low temperature $Al_2O_3$ can be accommodated by the precipitation of small defects that can exist in equilibrium with rutile matrix at higher temperatures. Such defects involve $Al^{3+}$ and $Ti^{3+}$ as substituted and as well as interstitial cations.
2. In the case of $Al_2O_3$ being the predominant solute phase in $TiO_2$, $Al^{3+}$ would substitute for $Ti^{3+}$

The heart-shaped alumina precipitates have a complex bisecting twin interface, which contains modulated structures intermediate between rutile and alumina. These structures act as an efficient buffer to accommodate both changes in stoichiometry and finite lattice misfits between rutile and alumina (Bursill and Blanchin 1989).

## 4.4.5 Niobium and Tungsten in rutile

Michailidis (1997) described chemically inhomogenous accessory rutile grains from the Fanos Aplitic Granite North of Greece, which varied in composition, not only with respect to their niobium, iron and tungsten content, but also with minor to substantial quantities of strontium, tantalum, silica, tin and zirconium. Traces of aluminium, molybdenum, manganese, magnesium and calcium were also present in these anomalous rutile

crystals indicating that, in a niobium-tantalum enriched environment such as that of the Fanos Aplitic Granite, rutile can accept significant quantities niobium and tantalum into the structure.

Given the proper physiochemical environment, the following mechanisms facilitate accommodation of $Nb^{5+}$, $Fe^{3+}$, $Fe^{2+}$, $W^{6+}$, $Sr^{2+}$, $Ta^{5+}$, $Si^{4+}$, $Sn^{4+}$, $Al^{3+}$, $Mo^{6+}$, $Ca^{2+}$, $Mn^{2+}$, $Mg^{2+}$ and $Zr^{4+}$ into the rutile structure:

$$Ti^{4+} \leftrightarrow (Si, Sn, Zr)^{4+}$$
$$2Ti^{4+} \leftrightarrow (Nb, Ta)^{5+} + (Al, Fe)^{3+}$$
$$2Ti^{4+} \leftrightarrow (Mo, W)^{6+} + (Fe, Mn, Mg, Sr, Ca)^{2+}$$
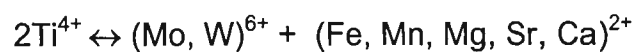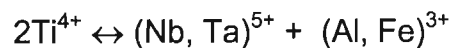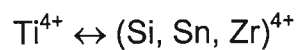
Michailidis (1997) concluded that the concentration and diffusion of Nb and W in aplitic granite melts are important factors controlling the chemical composition of rutile crystals. However, the coexisting fluorine-rich aqueous fluids and the growth dynamics of the rutile crystals were of considerable importance as well.

## 4.4.6 Tungsten in rutile

Tungsten-bearing rutiles are rare (Rice et al., 1998). The first report of a tungsten rich rutile (containing 5.8wt% of $WO_3$) was recorded from Big Bell, Australia, by Graham and Morris, (1973). Other tungsten-rich rutile grains have been reported from the Hemlo Gold Deposits of Ontario, Canada, (Harris, 1986) and the Fanos Aplitic Granite of Northern Greece (Michailidis, 1997). These tungsten-enriched rutile crystals contain 2.3 wt% and 7.5 wt% of $WO_3$ respectively.

Rice et al. (1998) examined tungsten-rich rutile from the Kori Kollo Gold Mine, Bolivia, and found multiple growth and sector zoning. The overall tungsten content ranged from 0.1 to 5.3wt% $WO_3$ with minor amounts of iron, niobium, aluminium and chromium. Although the radii of $W^{6+}$, $Nb^{5+}$, $Ti^{4+}$, $Al^{3+}$, $Cr^{3+}$ and $Fe^{3+}$ are similar, the charge

differences requires additional substitutions to maintain electrical neutrality. The presence of $W^{6+}$ suggests a double substitution mechanism such as

$$2Ti^{4+} \rightarrow Fe^{3+} + W^{6+}.$$

with the excess positive charge being balanced by the vacancies created in the Ti-sites by the loss of oxygen (Rice et al., 1998). There also exists the possibility that iron is present in the reduced state ($Fe^{2+}$) and then the mechanism,

$$2Ti^{4+} \rightarrow Fe^{2+} + W^{6+}$$
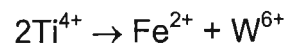
would provide electrical neutrality (Rice et al., 1998).


## 4.4.7. Niobium and chromium in rutile

Nodules of rutile occurring in the Orapa Kimberlite, Botswana, contain lamellar intergrowths of ilmenite (Tollo and Haggerty, 1987). The rutile host is Nb and Cr enriched, whereas the ilmenite intergrowths are Mg and Cr enriched. The mineral chemistry of the rutile host shows a broad range of compositional variation characterised by substitution of niobium (6.5 to 20.9wt% $Nb_2O_5$) and chromium (5.2 to 8.2wt% $Cr_2O_3$) the minor concentrations of iron ($Fe^{2+}$), tantalum ($Ta^{5+}$) and zirconium ($Zr^{4+}$) (Tollo and Haggerty, 1987).

The high pressure Nb and Cr-rutile nodules from the Orapa Kinmberlite are considered to be the result of an exsolution-like process; with a strong partitioning of $Nb^{5+}$ and $Zr^{4+}$ in rutile; and $Mg^{2+}$ in ilmenite, while the $Cr^{3+}$ selectively partitions to a lesser extent in rutile. The equilibrated intergrowths of rutile and ilmenite appear to be related to high-pressure crystallographic shear structures (Tollo and Haggerty, 1987).

## 4.4.8 Chromium in rutile

In view of the constraints based on ionic charge and radii, only chromium ions with charges $Cr^{3+}$ and $Cr^{4+}$ are able to substitute for the $Ti^{4+}$ ion. This substitution is induced industrially for the production of yellow Cr - Ti containing pigments, synthesised by 'firing' oxide mixtures in air at 1 200°C where the stable forms of chromium have oxidation numbers higher than III (Ishida $et$ $al.$, 1990).

Producing Cr-doped $TiO_2$, Ishida $et$ $al.$, (1990) came to the following conclusions:

- Cr-doped rutile has a yellow colour resulting from dissolved $Cr^{3+}$ when the Cr - content was less than 0.1wt% $CrO_3$.
- Cr - doped rutile with a Cr-content equal to 0.2 wt% $CrO_3$ has a maple colour.
- Cr content of up to 1 wt% $CrO_3$; the Cr - doped rutile has a black colour caused from undissolved $CrO_{3-x}$.

## 4.4.9 Zirconium in rutile

During a study of the Khibina Alkaline Complex, NW Russia, Nb - Zr bearing rutile was found to be an accessory mineral (Barkov $et$ $al.$ 1997). This rutile occurred as anhedral grains ranging in size from about 20$\mu$m to 0.5mm. Electron microprobe data showed that the accessory rutile contained up to 2.5 wt% $Nb_2O_5$ and up to 1.2 wt% $ZrO_2$ (Barkov, pers. comm. 1999). The high alkali and Zr content of the igneous melt was considered to have contributed to formation of this unusual substitution. However, $Zr^{4+}$ is rarely analysed for in rutile grains, the true distribution of $Zr^{4+}$ is not known in any detail.

## 4.5 Rutile in geological environments

Rutile is formed in both igneous and metamorphic environments, but in the sedimentary environment the other polymorphs (anatase and brookite) are generated. In the igneous environment rutile precipitates from a fluid phase, but in a metamorphic environment rutile is produced by both solid state metamorphic reactions and crystallisation from a fluid phase. The chemical environment governs the ions available for substitution, with rutile acting as a sink for the tetravalent and pentavalent ions that are not readily compatible with silicate mineral structures.

# 5. Data Analysis

Rutile was found in most of the fifteen sub-fractions of the HMC (Section 4.7, Fig. 4.7.1). The relationship between the geochemistry and the anomalous behaviour of rutile was investigated by means of Electron Probe Micro-Analysis (EPMA).

All fifteen fractions from mining Ponds A, B and C were sub-divided using a sample splitter. Representative samples were taken from each and polished resin ore mounts prepared. Each sample was carbon-coated to approximately 300 Å. Homogenous rutile grains were identified using electron backscatter imagery and then analysed on a JEOL JX8800 RL Superprobe at the University of Durban-Westville. (Appendix A1)

All elements (oxide phase), which according to theory (Section 4.3), could substitute with ease for the $Ti^{4+}$ ion into the rutile crystal lattice were analysed. The suite of elements expressed as oxides; FeO, $SiO_2$, $TiO_2$, $ZrO_2$, $V_2O_3$, $Cr_2O_3$, $Al_2O_3$, $Ta_2O_5$ and $Nb_2O_5$; were analysed by Electron Probe Micro Analysis. Initial analytical schemes also included PbO, $MoO_3$, $WO_3$, $UO_2$, $BiO_2$, and $Sb_2O_5$. However, after completing scans over a number of rutile grains these elements were found to be below the detection limit (Appendix A1) and hence excluded from subsequent analyses. The most common oxide phases found to be substituting for $Ti^{4+}$ ($TiO_2$) in rutile were FeO, $SiO_2$, $ZrO_2$, $V_2O_3$, $Al_2O_3$, and $Nb_2O_5$.

## 5.1 Oversize and Magnetite Fractions

The oversize fraction from all ponds accounted for less than 0.5 wt% of the total HMC. The composition of this fraction included remnants of sea-shells, roots and plant debris, and well-rounded quartz grains. Back-scattered electron imaging was used to detect rutile grains. X-ray maps showing the distribution of titanium were also compiled for these probe sections. No homogenous rutile grains were found to be present in the oversize fraction.

The magnetite fraction from all three ponds, separated during the laboratory separation constituted less than 2.00wt% of the total HMC. Virtually all of the magnetite had been removed on the dredgers and sent to the tailings. The remaining magnetite was probably the result of entrainment during the initial magnetic separation. Back-scattered electron imaging and x-ray maps for titanium did not reveal the presence of any homogenous rutile in the magnetic fraction.

## 5.2 Ilmenite

A representative ilmenite sample was chosen from each of the Ponds and separated magnetically using a Frantz Isodynamic Magnetic Separator (Hutchison, 1974). The magnetic field created can be manipulated by fine adjustments to the current. The ilmenite fraction was split using currents of 0.1 Amp to 0.7 Amp (Table 4.7.2). The magnetic fraction was collected at each stage and the non magnetic fraction formed the feed for the next stage. The residual fraction, which could not be split further, was referred to as the 'non-magnetic ilmenite'. The ilmenite fractions separated at 0.1Amp to 0.7Amp, was referred to as the magnetic ilmenite.

## 5.2.1 Magnetic Ilmenite

## 5.2.1.1 Pond A

Fig. 5.2.1.1 and Table 5.2.1.1 show the distribution of FeO, $SiO_2$, $ZrO_2$, $V_2O_3$, $Al_2O_3$, $Nb_2O_5$, against $TiO_2$ in the magnetic ilmenite fraction of Pond A. The six rutile grains analysed in this fraction had a $TiO_2$ content of 93.292wt% to 98.514wt%, however most grains had $TiO_2$ values of approximately 98.119wt%. The $SiO_2$ values range from 0.331 to 1.167wt% (Fig. 5.2.1.1) with most values clustered around a mean of 0.402wt%.

Fig. 5.2.1.1 Geochemistry of homogenous rutile grains in the magnetic ilmenite fraction of Pond A.
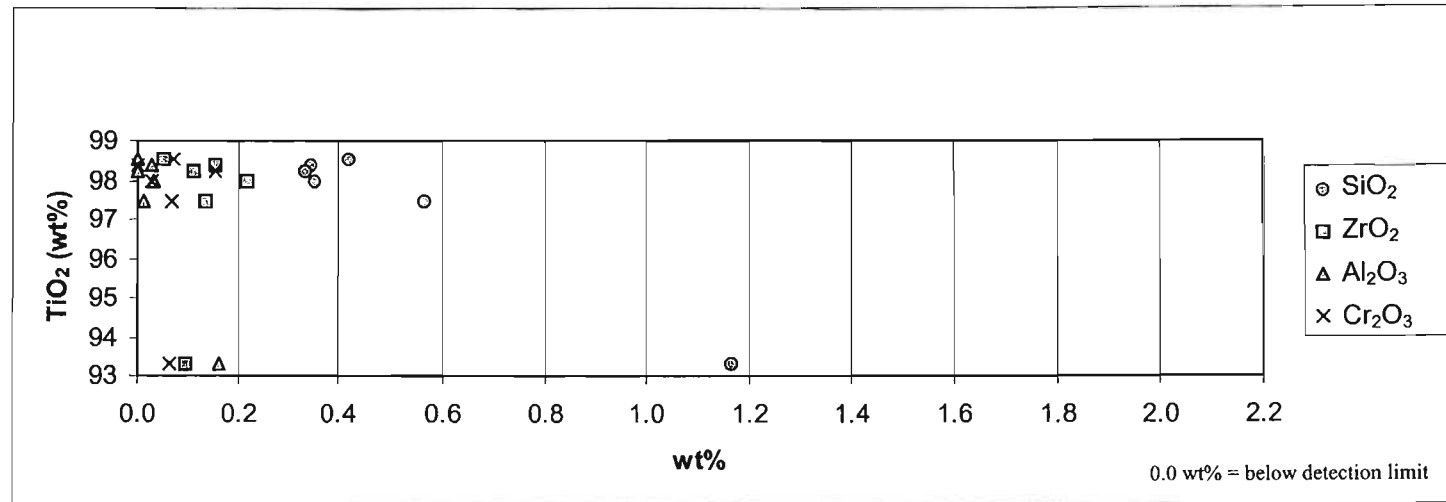
One grain appeared to be $SiO_2$ enriched and containing 1.167wt%. $ZrO_2$ values were all between 0.053 and 0.219wt%, with a mean value of 0.128 wt%. There was a wide range in $V_2O_3$ values from 0.227 to 0.892wt%. The $Nb_2O_5$ values were from 0.106 to 0.416wt%, most rutile grains had an average $Nb_2O_5$ of 0.158wt%, with the exception of one grain, which contained 0.416wt% $Nb_2O_5$. The rutile grains had very little $Al_2O_3$ with values between 0.011 and 0.162wt% (Fig. 5.2.1.1). The mean $Al_2O_3$ content was 0.059wt%. The FeO content of this population had a range of values from 0.126 to 2.079wt%. Although one grain had an extremely high FeO content (2.079wt%), all the others were below 0.600wt% with an average FeO content is 0.251wt%. $Cr_2O_3$ occurred at very low concentrations in these rutile grains with values from below the detection limit of 0.021 up to 0.154wt%. The average $Cr_2O_3$ value was 0.064wt%. $Ta_2O_5$ was below the detection limit of 0.036wt% in all but one grain, which contained 0.052wt% $Ta_2O_5$ (Table 5.2.1.1).

| Oxides | Minimum (wt%) | Maximum (wt%) | *Mean (wt%) |
|---|---|---|---|
| $TiO_2$ | 93.292 | 98.514 | 98.119 |
| $SiO_2$ | 0.331 | 1.167 | 0.402 |
| $ZrO_2$ | 0.053 | 0.219 | 0.128 |
| $V_2O_3$ | 0.227 | 0.892 | 0.501 |
| $Nb_2O_5$ | 0.106 | 0.416 | 0.158 |
| FeO | 0.126 | 2.079 | 0.251 |
| $Al_2O_3$ | # | 0.162 | 0.059 |

Table 5.2.1.1 A summary of electron microprobe results from 'magnetic ilmenite' fraction of Pond A.

*Mean:      Mean values exclude values that are below the detection limit and very high values (see details in text)

#           Lowest values are below the lld

Predictably, the grain in the 'magnetic ilmenite' fraction of Pond A, with the lowest $TiO_2$ content of 93.292 wt%, had relatively high proportions of the other elements, and contained 1.167wt% $SiO_2$, 0.416wt% $V_2O_3$ and 2.079wt% FeO.


## 5.2.1.2 Pond B

Fig. 5.2.1.2 shows the distribution of FeO, $SiO_2$, $ZrO_2$, $V_2O_3$, $Al_2O_3$, $Nb_2O_5$, against $TiO_2$ in the magnetic ilmenite fraction of Pond B and Table 5.2.1.2 presents the analytical data. Eight rutile grains were found and analysed in this fraction. The titanium content of rutile grains from Pond B, 'magnetic ilmenite' fraction (Fig. 5.2.1.2) was from 80.424 to 99.985wt%. All but one of the grains had titanium values in the 95.306 to 99.985wt%, range with a mean of 98.192wt%. The $SiO_2$ values were between 0.076wt% and 4.061wt%, with most grains in the 0.076 to 0.356wt% range and an average $SiO_2$ value of 0.161wt%. One grain had an uncharacteristically high $SiO_2$ value of 4.016wt%. These rutile grains contained very little $ZrO_2$, with values from below the detection limit of 0.017wt% to 0.160wt%. A similar trend was observed for both $V_2O_3$ and $Nb_2O_5$; with values for $V_2O_3$ extending from 0.133wt% the lower limit of detection (lld), to 0.270wt% and $Nb_2O_5$ from 0.049wt% (lld) to 0.249wt%. The mean $V_2O_3$ and $Nb_2O_5$ values were 0.112 and 0.086wt% respectively. There was a large variation in $Al_2O_3$ content, with values from just above the lld (0.026wt%) to as high as 2.601wt%. All rutile grains, with the exception of one grain, had $Al_2O_3$ values in the range of 0.011wt% (lld) to 0.079wt%, with mean value of 0.045wt%. A single grain had a high $Al_2O_3$ value of 2.601wt%, but two grains contained $Al_2O_3$ below the lld. The FeO content showed the largest variation, with values from 0.065wt% to as high as 11.118wt%. Although most grains had FeO values in the range of 0.065wt% to 0.388wt% (mean of 0.229wt%); two grains had very high FeO content of 4.080wt% and 11.118wt%. The grains from this fraction contained virtually no $Cr_2O_3$ or $Ta_2O_5$. Only three grains were $Ta_2O_5$ and $Cr_2O_3$ bearing and these had means of 0.115wt% and 0.030wt% respectively (Table 5.2.1.2).

Fig. 5.2.1.2 Geochemistry of homogenous rutile grains in the magnetic ilmenite fraction of Pond B.

| Oxides | Minimum (wt%) | Maximum (wt%) | *Mean (wt%) |
|--------|---------------|---------------|-------------|
| $TiO_2$ | 80.424 | 99.985 | 98.192 |
| $SiO_2$ | 0.076 | 4.061 | 0.161 |
| $ZrO_2$ | # | 0.160 | 0.075 |
| $V_2O_3$ | # | 0.270 | 0.112 |
| $Nb_2O_5$ | # | 0.249 | 0.086 |
| $Al_2O_3$ | # | 2.601 | 0.045 |
| FeO | 0.065 | 11.118 | 0.229 |

Table 5.2.1.2 A summary of electron microprobe results from 'magnetic ilmenite' fraction of Pond B.

*Mean:     Mean values exclude values that are below the detection limit and very high or low values (see details in text)

#          Lowest values are below the lld

The rutile grain with the lowest titanium content of 80.424wt% had a $SiO_2$ content of 4.061 wt%, $Al_2O_3$ of 2.601wt% and FeO of 11.118wt%.


## 5.2.1.3 Pond C

Fig. 5.2.1.3 is a plot shows the distribution of FeO, $SiO_2$, $ZrO_2$, $V_2O_3$, $Al_2O_3$, $Nb_2O_5$, against $TiO_2$ in the magnetic ilmenite fraction of Pond C and Table 5.2.1.3 the analytical data. Four rutile grains were found in this fraction of 'magnetic ilmenite' from Pond C (Fig. 5.2.1.3) and had a $TiO_2$ content of 97.854 to 97.243wt%, with a mean of 97.594wt%.
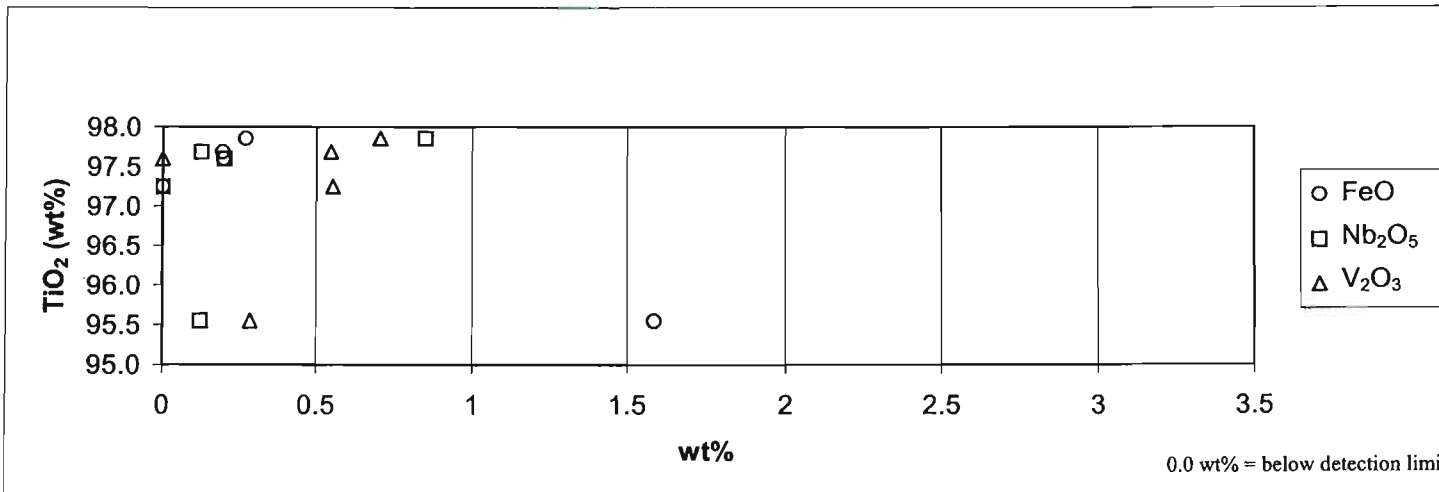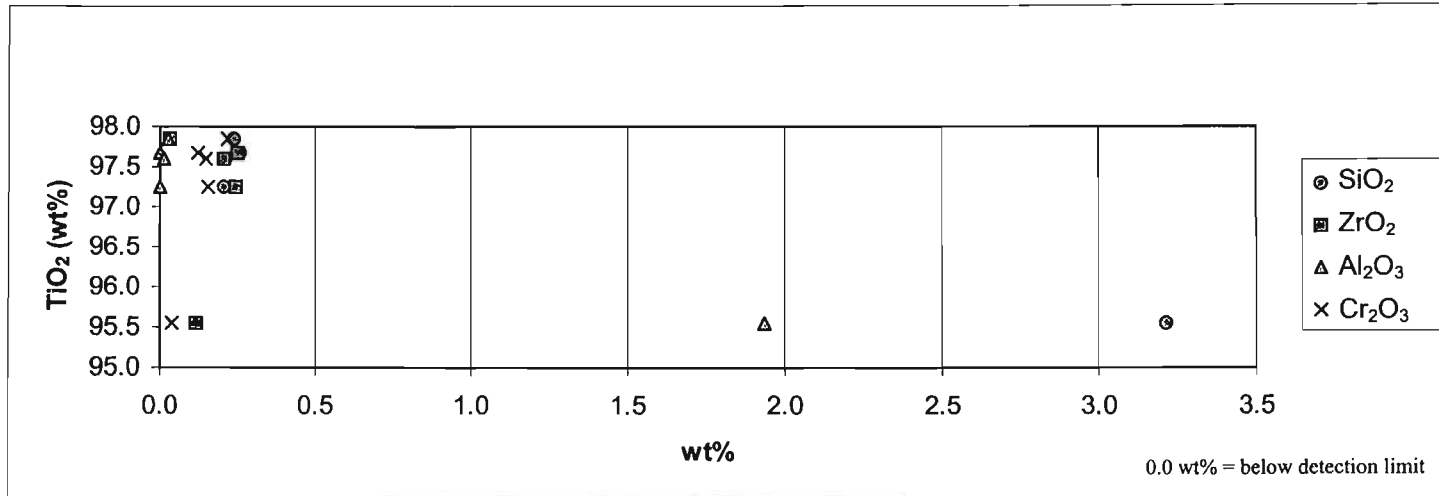
Fig. 5.2.1.3 Geochemistry of homogenous rutile grains in the magnetic ilmenite fraction of Pond C.

The $SiO_2$ values were within a very small range, 0.206 to 0.256wt% and had an average $SiO_2$ content of 0.228wt%. Most of the rutile grains had low $ZrO_2$ values with concentrations of 0.035wt% to 0.249wt%. Apart from the single grain containing 0.035wt% $ZrO_2$, the mean $ZrO_2$ value for this rutile population was 0.233wt%. $V_2O_3$ values were from just above the lld (0.133wt%) to 0.706wt% with a mean $V_2O_3$ content of 0.602wt%. The $Nb_2O_5$ values showed the greatest variation with one grain below the lld, to another with a maximum of 0.849wt%. The mean $Nb_2O_5$ value was 0.391wt%. Only two grains had detectable $Al_2O_3$, of 0.013 and 0.024wt% respectively. The FeO content of the grains varied from 0.027wt% (one grain was below the lld) to 0.267wt%, with a mean of 0.219wt%. $Cr_2O_3$ was present at slightly higher concentrations than in the similar fraction from Pond A and B, with values in the range of 0.120 to 0.218wt%, and a mean $Cr_2O_3$ content of 0.161wt%. $Ta_2O_5$ however was below the detection limit for most grains with only one grain having 0.260wt% (Table 5.2.1.3).

| Oxides | Minimum (wt%) | Maximum (wt%) | *Mean (wt%) |
|---|---|---|---|
| $TiO_2$ | 97.243 | 97.854 | 97.594 |
| $SiO_2$ | 0.206 | 0.256 | 0.228 |
| $ZrO_2$ | 0.035 | 0.249 | 0.233 |
| $V_2O_3$ | # | 0.706 | 0.602 |
| $Nb_2O_5$ | # | 0.849 | 0.391 |
| $Al_2O_3$ | # | 0.024 | 0.019 |
| FeO | # | 0.267 | 0.219 |
| $Cr_2O_3$ | 0.120 | 0.218 | 0.161 |

Table 5.2.1.3 A summary of electron microprobe results from 'magnetic ilmenite' fraction of Pond C.

*Mean:     Mean values exclude values that are below the detection limit and very high or low values (see details in text)

#     Lowest values are below the lld

All grains from the 'magnetic ilmenite' fraction of Pond C had consistent, $SiO_2$ values (0.228wt%) and almost no $Al_2O_3$ (0.019wt%). Rutile grains appeared to be $Cr_2O_3$ (0.161wt%) enriched. Both the $V_2O_3$ and $Nb_2O_3$ content demonstrated the most variability within rutile grains from the 'magnetic ilmenite' fraction of Pond C.


## 5.2.2 Non-Magnetic Ilmenite

## 5.2.2.1 Pond A

The distribution of $TiO_2$, $SiO_2$, $ZrO_2$, $V_2O_3$, $Nb_2O_5$, $Al_2O_3$ and FeO from the 'non-magnetic ilmenite' fraction of Pond A is presented in Fig. 5.2.2.1 and Table 5.2.2.1 the analytical data. Rutile grains in this sub-fraction had $TiO_2$ values in a range from 94.759wt% to 99.993wt%. Of the thirteen grains only two grains had low $TiO_2$ contents (94.759 and 95.650wt%); the others having an average $TiO_2$ content of 99.495wt%. Grains had a maximum $SiO_2$ content of 1.185wt% and a minimum of 0.074 wt%. Three grains had unusually high $SiO_2$ values of 0.928, 0.952 and 1.185wt%; however, most grains, contain less than 0.300wt% $SiO_2$ with a mean of 0.154wt%. $ZrO_2$ ranged from below the lld (0.017wt%) to 0.475wt%, with a mean of 0.226wt%. $V_2O_3$ was distributed in an array from 0.133wt% to 0.834wt%, with a mean of 0.423wt%. The $Nb_2O_5$ contents of the analysed rutile grains were from below the lld (0.049wt%) to 0.167wt%, with an average value of 0.101wt%. $Al_2O_3$ was below the detection limit (0.011wt%) for most of the grains from this fraction. However, the rutile grains with a significant $Al_2O_3$ content contained on average 0.028wt%, with the exception of two very enriched grains containing 0.694 and 0.717wt% $Al_2O_3$. The distribution of FeO in rutile grains was from 0.027 to 1.085wt%. Three grains had high FeO values of 0.811, 1.082, and 1.085 wt%, the rest had a mean of 0.123wt%. $Cr_2O_3$ was present at concentrations of 0.021 to 0.211wt% with the average $Cr_2O_3$ value of 0.099wt% (Table 5.2.2.1).

Fig. 5.2.2.1 Geochemistry of homogenous rutile grains in the non magnetic ilmenite fraction of Pond A.

| Oxides | Minimum (wt%) | Maximum (wt%) | *Mean (wt%) |
|---|---|---|---|
| $TiO_2$ | 94.759 | 99.993 | 99.495 |
| $SiO_2$ | 0.074 | 1.185 | 0.154 |
| $ZrO_2$ | # | 0.475 | 0.226 |
| $V_2O_3$ | # | 0.834 | 0.423 |
| $Nb_2O_5$ | # | 0.167 | 0.101 |
| $Al_2O_3$ | # | 0.717 | 0.028 |
| FeO | # | 1.085 | 0.123 |
| $Cr_2O_3$ | # | 0.211 | 0.099 |

Table 5.2.2.1 A summary of electron microprobe results from 'non magnetic ilmenite' fraction of Pond A.

*Mean:     Mean values exclude values that are below the detection limit and very high or low values (see details in text)

#            Lowest values are below the lld

Rutile grains from the 'non magnetic ilmenite' fraction of Pond A, appeared to be quite chemically pure with most grains having $TiO_2$ contents of less than 98wt%. $SiO_2$, and FeO were present in rutile grains at levels greater than 1.00wt%, while $V_2O_3$ and $Al_2O_3$ were present in some grains at levels greater than 0.500wt%.

## 5.2.2.2 Pond B

The distribution of $TiO_2$, $SiO_2$, $ZrO_2$, $V_2O_3$, $Nb_2O_5$, $Al_2O_3$ and FeO from the 'non-magnetic ilmenite' fraction of Pond B is presented in Fig. 5.2.2.2 and Table 5.2.2.2 the analytical data. Only four grains were identified and analysed from the non-magnetic ilmenite fraction of Pond B. The $TiO_2$ contents varied between 94.343 to 97.489wt%. All four grains had very similar $SiO_2$ values (0.468 to 0.541wt%) with a mean of 0.508wt% $SiO_2$. The rutile grains had $ZrO_2$ values from 0.091 to 0.527wt%. Three of the four analysed grains had an average $ZrO_2$ value of 0.108wt%, with the remaining grain being much higher at 0.527wt% $ZrO_2$. The distribution of $V_2O_3$ in these grains was from 0.479 to 0.964wt%, with a mean value of 0.699wt%. $Nb_2O_5$ had a minimum value of 0.164 and a maximum of 2.185wt%. Apart from the grain having the higher $Nb_2O_5$ content of 2.185wt% the remaining three of the four grains had an average of 0.192wt%. All four grains had very low $Al_2O_3$ values of 0.015 to 0.059wt%, with an average of only 0.034wt%. The FeO content of this rutile fraction was from 0.037 to 0.916wt% with three of the four grains having FeO values with an average of 0.119wt%, and the remaining grain had a higher FeO content of 0.916wt%. $Cr_2O_3$ was present in all the grains analysed, with a minimum of 0.133, a maximum of 0.158wt% and an average value of 0.148wt% (Table 5.2.2.2).

The grains from Pond B had a lower $TiO_2$ content (mean of 96.133wt%) than rutile grains from Pond A (mean of 99.495wt%), for the same fraction. One grain from this fraction appeared to be very $Nb_2O_5$ enriched.

69

Fig. 5.2.2.2 Geochemistry of homogenous rutile grains in the non magnetic ilmenite fraction of Pond B.

| Oxides | Minimum (wt%) | Maximum (wt%) | *Mean (wt%) |
|--------|---------------|---------------|-------------|
| $TiO_2$ | 94.343 | 97.484 | 96.133 |
| $SiO_2$ | 0.468 | 0.541 | 0.508 |
| $ZrO_2$ | 0.091 | 0.527 | 0.108 |
| $V_2O_3$ | 0.479 | 0.964 | 0.699 |
| $Nb_2O_5$ | 0.164 | 2.185 | 0.192 |
| $Al_2O_3$ | 0.015 | 0.059 | 0.034 |
| FeO | 0.037 | 0.916 | 0.119 |
| $Cr_2O_3$ | 0.133 | 0.158 | 0.148 |

Table 5.2.2.2 A summary of electron microprobe results from 'non magnetic ilmenite' fraction of Pond B.

*Mean:     Mean values exclude values that are below the detection limit and very high or low values (see details in text).


## 5.2.2.3 Pond C

The distribution of $TiO_2$, $SiO_2$, $ZrO_2$, $V_2O_3$, $Nb_2O_5$, $Al_2O_3$ and FeO from the 'non-magnetic ilmenite' fraction of Pond C is presented in Fig. 5.2.2.3 and Table 5.2.2.3 the analytical data. Rutile grains from the non-magnetic fraction of Pond C had a minimum $TiO_2$ value of 92.989wt% and a maximum value of 99.202wt%. The mean $TiO_2$ value for this population of rutile grains was 97.463wt%. The $SiO_2$ content of these grains was from 0.120wt% to 1.386wt%, however two of the twelve grains had $SiO_2$ contents in excess of 1.000wt% (1.076 and 1.386wt%). The average $SiO_2$ content for all rutile grains in this set was 0.507wt%. Five of the twelve rutile grains had $ZrO_2$ contents below the detection limit (0.017wt%), while the remaining six grains had $ZrO_2$ values in the range of
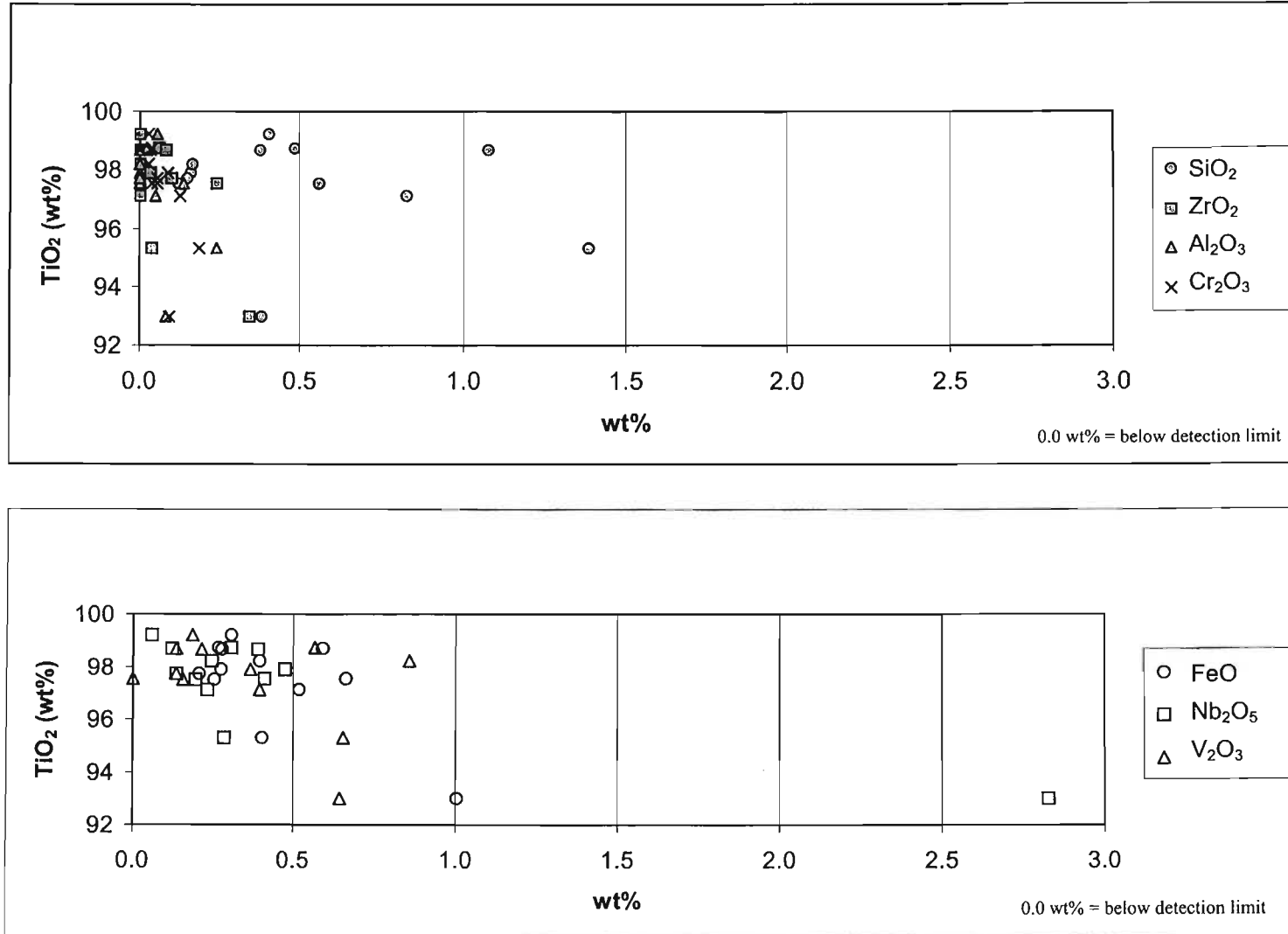
Fig. 5.2.2.3 Geochemistry of homogenous rutile grains in the non magnetic ilmenite fraction of Pond C.

0.017wt% to 0.343wt%. The mean $ZrO_2$ content was 0.126wt%. The $V_2O_3$ content in rutile showed a large distribution of values from below the lld (0.133wt%) to 0.858wt%, with a mean $V_2O_3$ content of 0.392wt%. All the rutile grains contained $Nb_2O_5$ well above the detection limit, with ten grains having $Nb_2O_5$ that was less 0.5wt%; the exception being a single grain that had $Nb_2O_5$ value of 2.825wt%. The mean $Nb_2O_5$ value (excluding the anomalously high $Nb_2O_5$ grain) was 0.259wt%. Five grains had $Al_2O_3$ below the detection limit of 0.011wt%, the rest had concentrations ranging up to 0.240wt%. The mean $Al_2O_3$ content was 0.086wt%. The FeO content of the grains varied from 0.206 to 1.002wt%, with an average at 0.429wt%. $Cr_2O_3$ was also present at low concentrations from below the lld (0.021wt%) to 0.185wt%, with a mean of 0.070wt%. $Ta_2O$ was below the detection limit for most grains; only three grains had a significant $Ta_2O_5$ content, which was on average 0.780wt% (Table 5.2.2.3).

Rutile grains from Pond C had a larger range in $TiO_2$ contents (92.989 to 99.202 wt%), than Ponds A (94.759 to 99.993wt%) and Pond B (94.343 to 97.484wt%). Three grains contain $SiO_2$, $Nb_2O_5$ and FeO at concentrations above 1.000wt%.

| Oxides | Minimum (wt%) | Maximum (wt%) | *Mean (wt%) |
|---|---|---|---|
| $TiO_2$ | 92.989 | 99.202 | 97.463 |
| $SiO_2$ | 0.120 | 1.386 | 0.507 |
| $ZrO_2$ | # | 0.343 | 0.126 |
| $V_2O_3$ | # | 0.858 | 0.392 |
| $Nb_2O_5$ | 0.058 | 2.825 | 0.259 |
| $Al_2O_3$ | # | 0.240 | 0.086 |
| FeO | 0.206 | 1.002 | 0.429 |
| $Cr_2O_3$ | # | 0.185 | 0.070 |

Table 5.2.2.3 A summary of electron microprobe results from 'non magnetic ilmenite' fraction of Pond C.

*Mean:    Mean values excludes values that are below the detection limit and very high or low values (see details in text)

#    Lowest values are below the lld

## 5.3 Mag Others

The mag others fraction contained a large variety of minerals (Section 4.9), and was treated using the same procedure as with the ilmenite fraction (Section 5.2). A representative sub-fraction was taken from each of the Ponds A, B and C and split magnetically using the Frantz Isodynamic Separator (Hutchison, 1974). Separation commenced with a current of 0.4 Amp, which was increased at increments of 0.1 Amp, to 1.5 Amp (Section 4.7). Over 80% of each mag others fraction was removed at current settings between 0.4 to 1.0 Amp (Pond A, 89%; Pond B, 92% and Pond C, 81.31%). The fractions removed between 0.4 to 1.0Amp, were more magnetic than the fractions

removed at 1.1 to 1.5Amp. Thus the fractions removed by the Frantz at current settings of 0.4 to 1.0Amp were referred to as the 'magnetic mag others' and those removed at settings of 1.1 to 1.5Amp referred to as the 'non-magnetic mag others'.

## 5.3.1 Magnetic Mag Others

## 5.3.1.1 Pond A

The distribution of $TiO_2$, $SiO_2$, $ZrO_2$, $V_2O_3$, $Nb_2O_5$, $Al_2O_3$ and FeO from the 'magnetic mag others' fraction of Pond A is presented in Fig. 5.3.1.1 and Table 5.3.1.1 the analytical data. The seven rutile grains analysed from the 'magnetic mag others' fraction and were found to have $TiO_2$ from 94.779wt% to 98.522wt%, and a mean of 97.189wt%. The $SiO_2$ values had a range from 0.135wt% to as high as 4.525wt%. With the exception of the one grain ($SiO_2$, 4.525wt%), the other six grains had an average of 0.465wt%. Only four grains had $ZrO_2$ contents above the detection limit of 0.017wt%. The average $ZrO_2$ values were 0.179wt%. $V_2O_3$ values ranged from below the lld (0.133wt%) to 0.763wt%, with a mean of 0.515wt%. $Nb_2O_5$ displays a trend that was similar to $V_2O_3$, having values from below the lld (0.049wt%) to 0.573wt% and a mean of 0.315wt%. $Al_2O_3$ had a range from below the lld (0.011wt%) to 0.732; however, most grains had a mean of 0.026wt%, with only a single grain reporting a high $Al_2O_3$ value of 0.732wt%. There was a large range in the FeO values, from a minimum of 0.087 to a maximum of 3.540wt%. However, only one grain had a very high FeO (3.54wt%), all other grains from this population had a mean FeO content of 0.370wt%. Only three grains contained $Cr_2O_3$ above the detection limit of 0.021wt% and these had a mean of 0.065wt%. $Ta_2O_5$ was present at concentrations above the lld in all but two of the grains, with a range of 0.036 to 0.110wt% and a mean of 0.061 (Table 5.3.1.1).
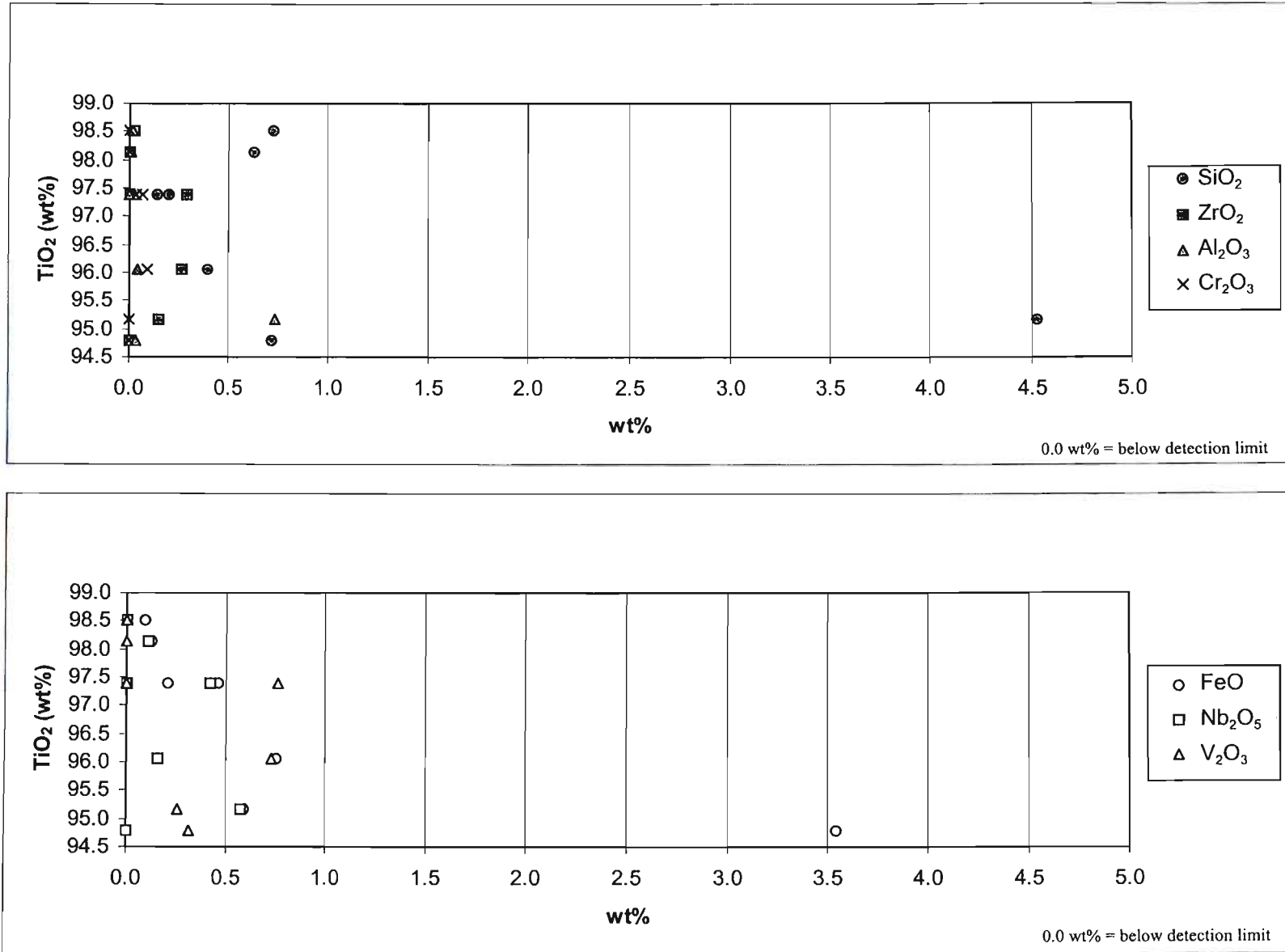
Fig. 5.3.1.1 Geochemistry of homogenous rutile grains in the magnetic mag others fraction of Pond A.

| Oxides | Minimum (wt%) | Maximum (wt%) | *Mean (wt%) |
|--------|--------------|--------------|-------------|
| $TiO_2$ | 94.779 | 98.522 | 97.189 |
| $SiO_2$ | 0.135 | 4.525 | 0.465 |
| $ZrO_2$ | # | 0.283 | 0.179 |
| $V_2O_3$ | # | 0.732 | 0.515 |
| $Nb_2O_5$ | # | 0.573 | 0.315 |
| $Al_2O_3$ | # | 0.732 | 0.026 |
| FeO | 0.087 | 3.540 | 0.370 |
| $Cr_2O_3$ | 0.036 | 0.093 | 0.085 |

Table 5.3.1.1 A summary of electron microprobe results from 'magnetic mag others' fraction of Pond A.

*Mean:     Mean values exclude values that are below the detection limit and very high or low values (see details in text).

#     Lowest values are below the lld

The rutile grain that had the high $SiO_2$ also had a high $Al_2O_3$ content. The FeO enriched grain did not contain a high concentration of any other elements. Grains from the magnetic mag others fraction of Pond A appeared to be $Ta_2O_5$ enriched.

## 5.3.1.2 Pond B

The distribution of $TiO_2$, $SiO_2$, $ZrO_2$, $V_2O_3$, $Nb_2O_5$, $Al_2O_3$ and FeO from the 'magnetic mag others' fraction of Pond B is presented in Fig. 5.3.1.2 and Table 5.3.1.2 the analytical data. There was a great variation in the $TiO_2$ content of rutile with values ranging from

76.844 wt% to 99.138wt% (Fig. 5.3.1.2). However, only two of the thirteen rutile grains had very low $TiO_2$ values of 87.773 and 76.844wt%, the rest had an average $TiO_2$ content of 97.503wt%. $SiO_2$ had a distribution from 0.046 to 1.689wt%, with the mean $SiO_2$ content for this sample being 0.362wt%. Two grains had $ZrO_2$ contents below the detection limit (0.017wt%) whereas other grains had $ZrO_2$ contents up to 0.236wt%. The average $ZrO_2$ value was 0.128wt%. The $V_2O_3$ content in these grains did not exceed 1.000wt%, but values ranged from below the detection limit (0.133wt%) to 0.801wt% with an average of 0.433wt%. Rutile grains showed a great variation in the $Nb_2O_5$ composition, with one grain having a $Nb_2O_5$ content which was below the detection limit (0.049wt%) to another grain that contained 4.567wt% $Nb_2O_5$; however, most grains had an average $Nb_2O_5$ content of 0.233wt%. $Al_2O_3$ was present in the analysed grains at concentrations ranging from a minimum that was below the detection limit of 0.011wt% to a maximum of 2.163wt%. With the exception of the grain with the high $Al_2O_3$ content (2.163wt%), the remaining grains had an average $Al_2O_3$ constituent of 0.328wt%. The FeO content of these grains showed the greatest variability, with grains having as little as 0.069wt% FeO to as much as 21.509wt%. Four of the thirteen grains contained more than 1.000wt% FeO, (5.562wt%, 1.277wt%, 1.012 wt%, and 21.509wt%). Apart from the grain with a FeO content of 21.509wt%, the rest of the grains had an average of 0.780wt% FeO. $Cr_2O_3$ had a range from below the lld (0.021wt%) to 0.166wt%, with an average value of 0.079wt% $Cr_2O_3$. $Ta_2O_5$ was below the detection limits (0.036wt%) for all but one grain that had a value of 0.075wt% (Table 5.3.1.2).

The 'magnetic mag others' fraction contained some grains that were enriched in FeO, (21.509wt%), $Al_2O_3$ (2.163wt%), $Nb_2O_5$ (4.567wt%) and $SiO_2$ (1.689wt%).
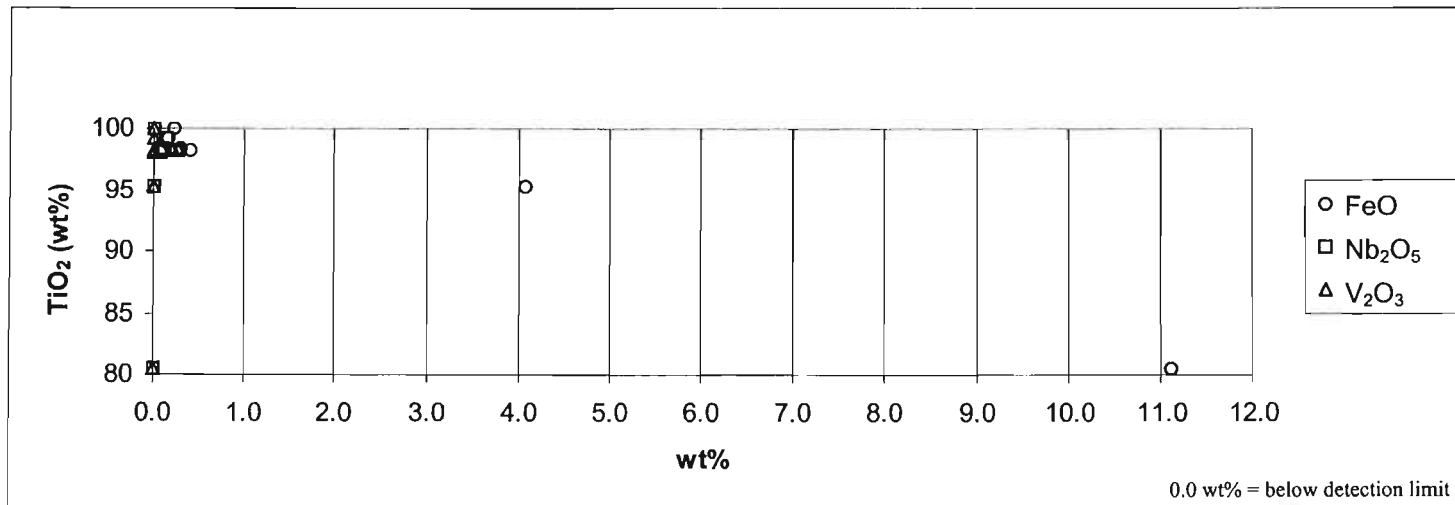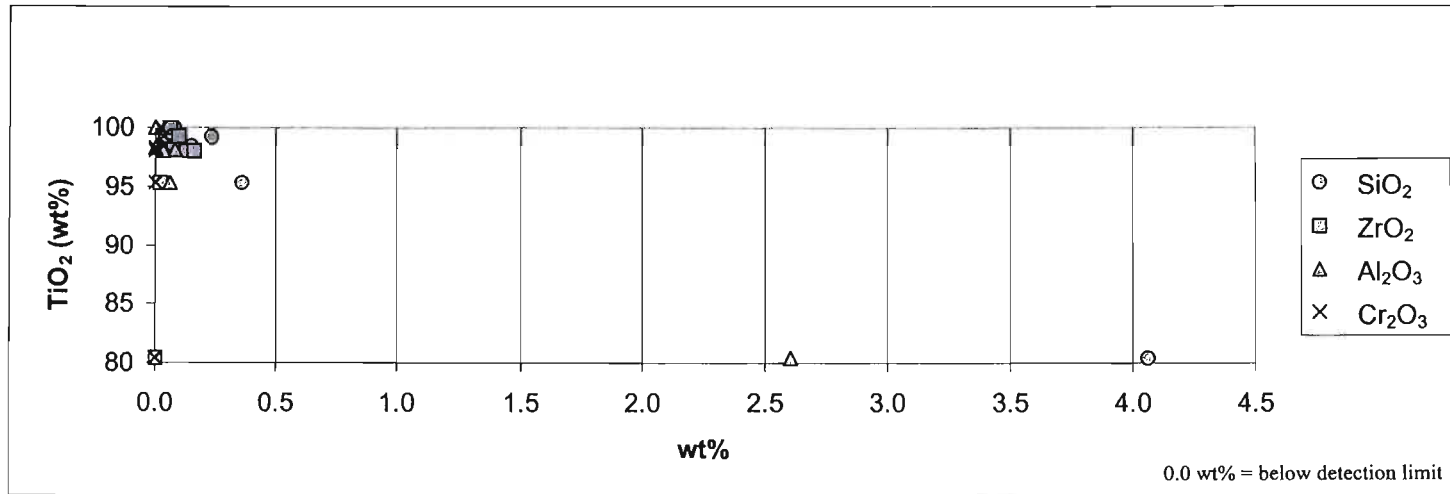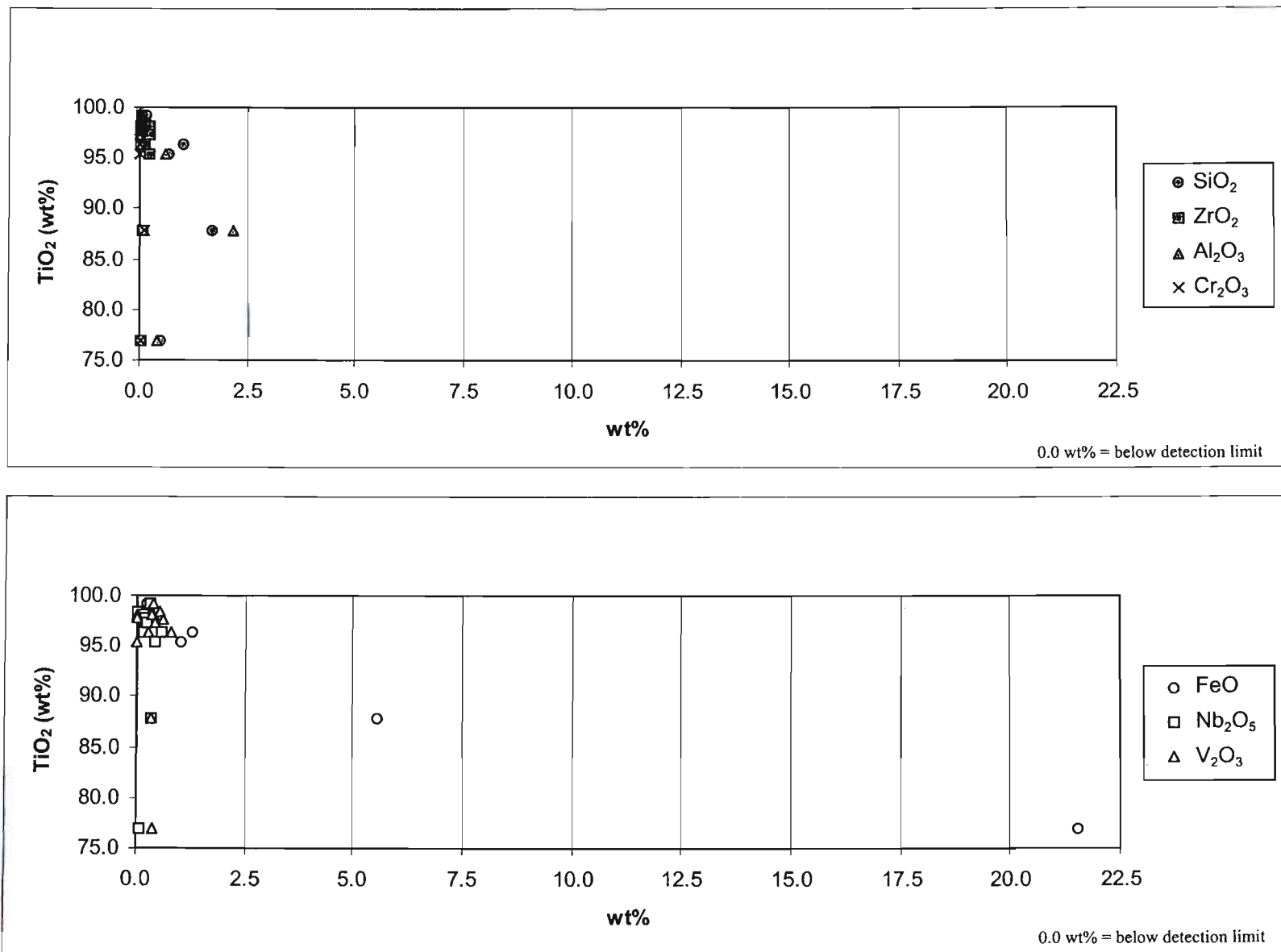
Fig. 5.3.1.2 Geochemistry of homogenous rutile grains in the magnetic mag others fraction of Pond B.

| Oxides | Minimum (wt%) | Maximum (wt%) | *Mean (wt%) |
|---|---|---|---|
| $TiO_2$ | 76.844 | 99.138 | 97.503 |
| $SiO_2$ | 0.046 | 1.689 | 0.362 |
| $ZrO_2$ | # | 0.236 | 0.128 |
| $V_2O_3$ | # | 0.801 | 0.433 |
| $Nb_2O_5$ | # | 4.567 | 0.233 |
| $Al_2O_3$ | # | 2.163 | 0.328 |
| FeO | 0.069 | 21.509 | 0.780 |
| $Cr_2O_3$ | # | 0.166 | 0.079 |

Table 5.3.1.2 A summary of electron microprobe results from 'magnetic mag others' fraction of Pond B.

*Mean:    Mean values exclude values that are below the detection limit and very high or low values (see details in text).

#    Lowest values are below the lld

## 5.3.1.3 Pond C

The distribution of $TiO_2$, $SiO_2$, $ZrO_2$, $V_2O_3$, $Nb_2O_5$, $Al_2O_3$ and FeO from the 'magnetic mag others' fraction of Pond C is presented in Fig. 5.3.1.3 and Table 5.3.1.3 the analytical data. As with Pond B, the $TiO_2$ values display great variation with a minimum value of 82.519wt%, a maximum value of 99.740wt% and a mean $TiO_2$ value of 95.626wt% (Table 5.3.1.3). $SiO_2$ values of the analysed rutile grains were from 0.077wt% to 12.431wt%. However, most of the grains had $SiO_2$ values less than 3.000wt% and a mean 0.551wt%. Only two of the thirty-seven grains had very high $SiO_2$ contents (12.431 and 4.816wt%). $ZrO_2$ forms a minor constituent of the rutile grains, rarely exceeding

Fig. 5.3.1.3 Geochemistry of homogenous rutile grains in the magnetic mag others fraction of Pond C.

| Oxides | Minimum (wt%) | Maximum (wt%) | *Mean (wt%) |
|---|---|---|---|
| $TiO_2$ | 82.519 | 99.740 | 95.626 |
| $SiO_2$ | 0.077 | 12.430 | 0.551 |
| $ZrO_2$ | # | 0.322 | 0.077 |
| $V_2O_3$ | # | 0.734 | 0.470 |
| $Nb_2O_5$ | # | 4.741 | 0.291 |
| $Al_2O_3$ | # | 0.583 | 0.131 |
| FeO | # | 16.482 | 1.175 |
| $Cr_2O_3$ | # | 0.155 | 0.071 |

Table 5.3.1.3 A summary of electron microprobe results from 'magnetic mag others' fraction of Pond C.

*Mean: Mean values exclude values that are below the detection limit and very high or low values (see text for details).

\# Lowest values are below the lld.

0.300wt%, individual values ranged from below the detection limit (0.017wt%) to 0.322wt%, with an average of 0.077wt%. The $V_2O_3$ content of rutile grains did not exceed 1.000wt%; with twenty-two values distributed from below the detection limit (0.133wt%) to 0.734wt%. The average $V_2O_3$ value for the remaining fifteen grains was 0.470wt%. $Nb_2O_5$ values were from the lld (0.049wt%) to 4.741wt%. With the exception of the single grain that had a much higher $Nb_2O_5$ content (4.741wt%), most grains had an average $Nb_2O_5$ content of 0.291wt%. The $Al_2O_3$ values were from below the lld (0.011wt%) to a maximum of 0.583wt%, with a mean $Al_2O_3$ value of 0.131wt%. The FeO content of rutile grains displayed the greatest variation, with values from below the lld (0.027wt%) to as high as 16.482wt%. Although the vast majority of the grains (32 grains) contained less than 5wt% (mean of 1.175wt%), four grains had values of 9.544, 16.482, 6.559 and 7.583wt%. $Cr_2O_3$ values were from below the lld to 0.155wt%, with a mean of

0.071wt%. Majority of the grains (28) had $Ta_2O_5$ values below the detection limit of 0.036wt%. The maximum $Ta_2O_5$ content of a rutile grain from this fraction was 0.193wt% and the average $Ta_2O_5$ content was 0.082wt% (Table 5.3.1.3).


## 5.3.2 Non-Magnetic Mag Others

## 5.3.2.1 Pond A

The distribution of $TiO_2$, $SiO_2$, $ZrO_2$, $V_2O_3$, $Nb_2O_5$, $Al_2O_3$ and FeO from the 'non-magnetic mag others' fraction of Pond A is presented in Fig. 5.3.2.1 and Table 5.3.2.1 the analytical data. The $TiO_2$ content of the analysed grains ranged between 79.873wt% to 99.409wt%. A single grain reported a very low value (79.873wt%) whereas all the others (25 grains) had an average of 97.337wt%. $SiO_2$ had a minimum of 0.078wt% and a maximum of 2.933wt%. Only two grains had $SiO_2$ contents of greater than 1.000wt% (2.933 and 2.109wt%); however, the rest of the grains had a mean of 0.227wt%. All the rutile grains from this fraction contained less than 0.260wt% $ZrO_2$, (below the lld, 0.017 to 0.257wt%) with an average of 0.115wt%. $V_2O_3$ had values in the range from below the lld to 1.225wt%. The overall average $V_2O_3$ content for these grains was 0.693wt%. $Nb_2O_5$ displayed large variations in rutile, with a minimum from below the lld 0.049wt% to a maximum of 2.778wt%. The average $Nb_2O_5$ content was 0.535wt%. $Al_2O_3$ content ranged from below the detection limit (0.011wt%) to as high as 3.456wt%. Apart from the single grain with a very high $Al_2O_3$ (3.456wt%) all the other grains had a mean of 0.100wt%. The FeO content in rutile grains from this fraction showed the most variation, with values in a range from lower than detection limit (0.027wt%) to 11.59wt%. With the exception of a single grain containing 11.59wt% FeO, the rest of the grains had a mean FeO content of 0.827wt%. $Cr_2O_5$ had a range from below the lld, (0.021wt%) to 0.034wt% with a mean of 0.122wt%. $Ta_2O_5$ was below the detection limit in twenty of the analysed grains, and the remaining six grains had a range of 0.036 to 0.044wt% (Table 5.3.2.1).
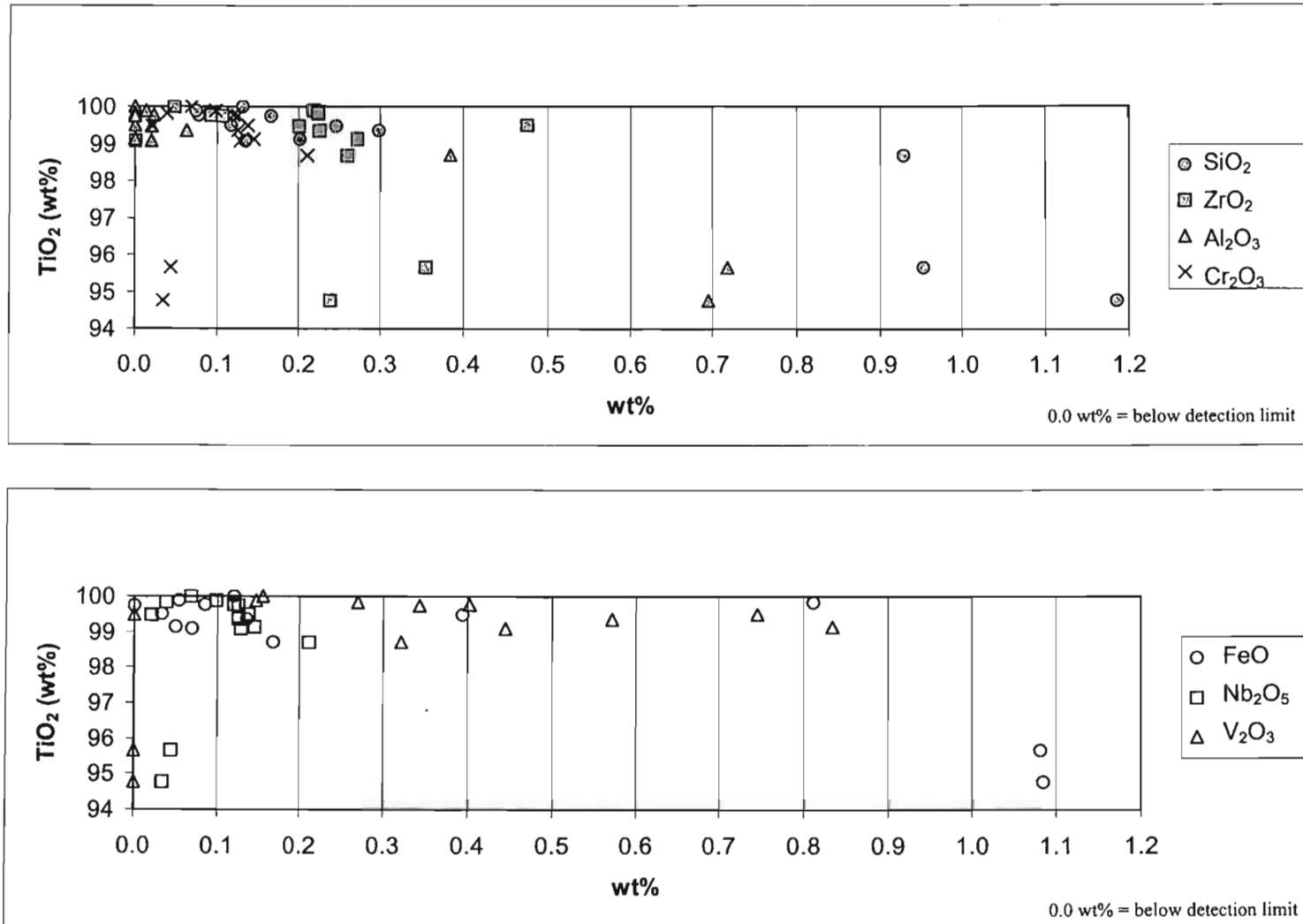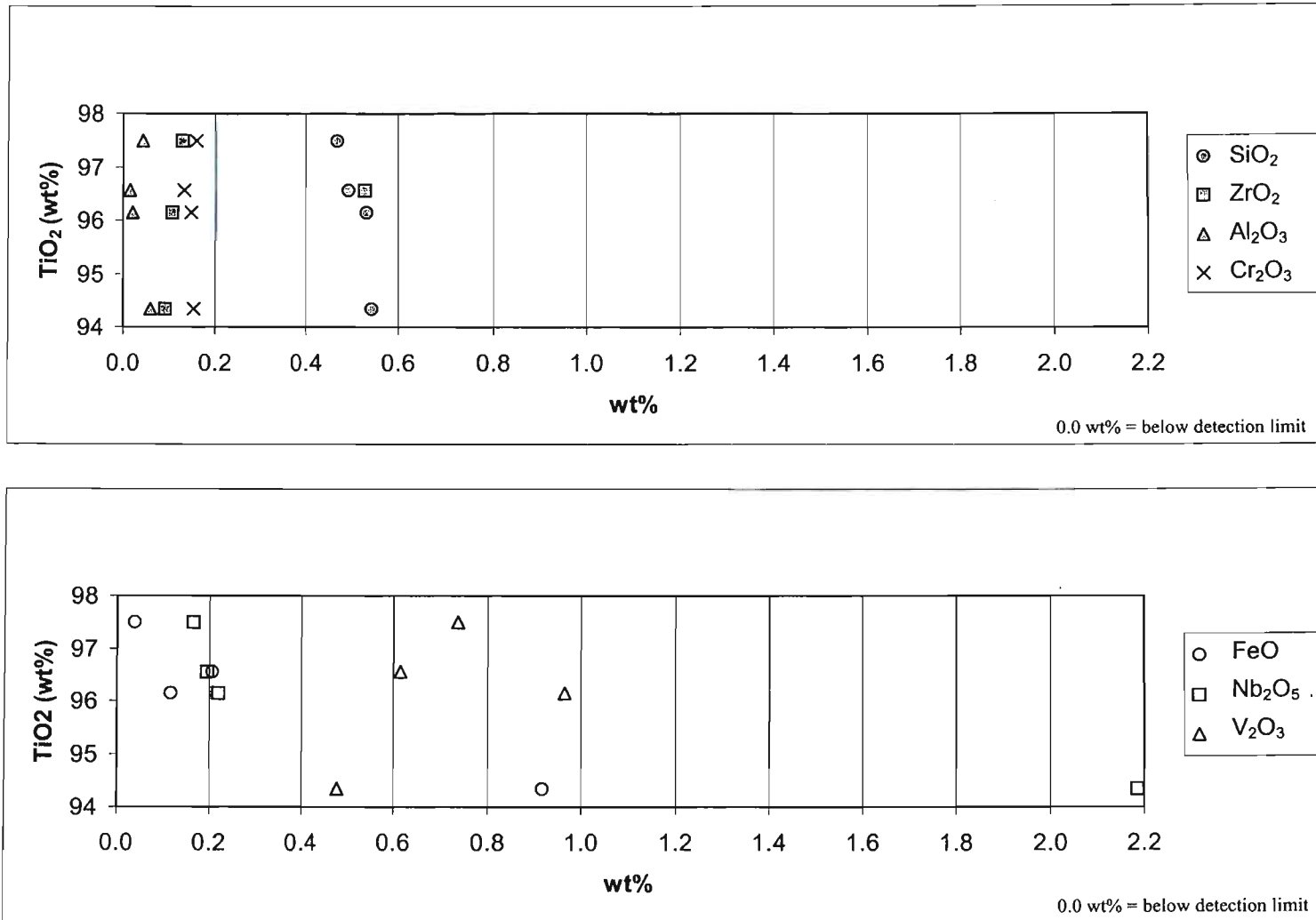
Fig. 5.3.2.1 Geochemistry of homogenous rutile grains in the non magnetic mag others fraction of Pond A.

| Oxides | Minimum (wt%) | Maximum (wt%) | *Mean (wt%) |
|---|---|---|---|
| $TiO_2$ | 79.873 | 99.409 | 97.337 |
| $SiO_2$ | 0.078 | 2.933 | 0.227 |
| $ZrO_2$ | # | 0.257 | 0.115 |
| $V_2O_3$ | # | 1.225 | 0.693 |
| $Nb_2O_5$ | # | 2.778 | 0.535 |
| $Al_2O_3$ | # | 3.456 | 0.100 |
| FeO | # | 11.590 | 0.827 |
| $Cr_2O_3$ | # | 0.034 | 0.122 |

Table 5.3.2.1 A summary of electron microprobe results from 'non - magnetic mag others' fraction of Pond A.

*Mean:   Mean values exclude values that are below the detection limit and very high or low values (see details in text).

#   Lowest values are below the lld

Some of the rutile grains from the 'non-magnetic mag others' fraction appeared to be enriched in FeO (11.590wt%), $Nb_2O_5$ (2.778wt%) and $SiO_2$ (2.933wt%).

## 5.3.2.2 Pond B

The distribution of $TiO_2$, $SiO_2$, $ZrO_2$, $V_2O_3$, $Nb_2O_5$, $Al_2O_3$ and FeO from the 'non-magnetic mag others' fraction of Pond B is presented in Fig. 5.3.2.2 and Table 5.3.2.2 the analytical data. The titanium content of rutile grains found in the 'non-magnetic mag others' fraction from Pond B was between 89.703wt% and 98.843wt%.
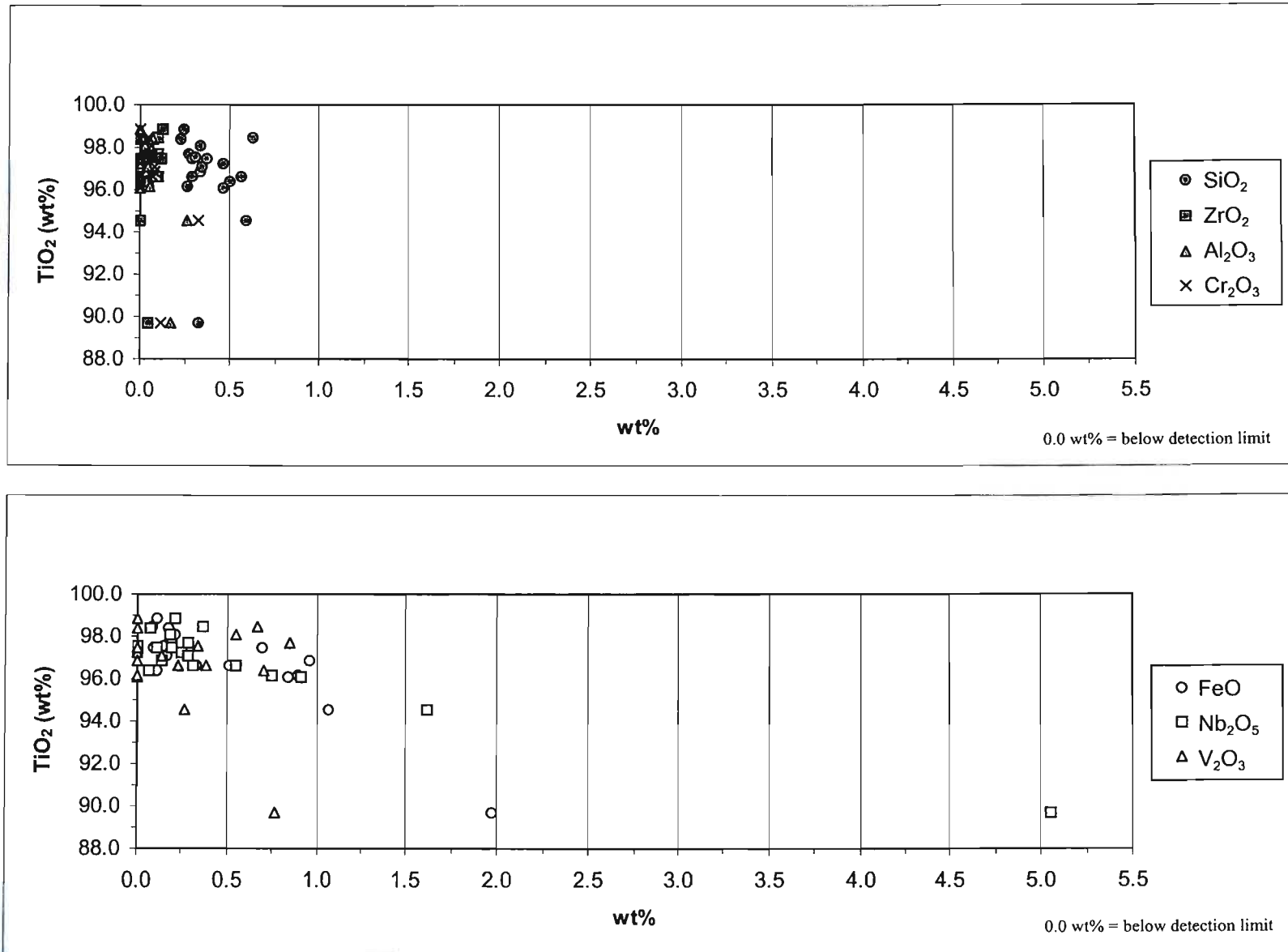
Fig. 5.3.2.2 Geochemistry of homogenous rutile grains in the non magnetic mag others fraction of Pond B.

Only one grain reported a very low $TiO_2$ (89,703wt%), content with the remaining seventeen grains having a mean of 97.149wt%. $SiO_2$ had a distribution from 0.231wt% to 0.629wt%, with an overall average at 0.379wt%. The 'non-magnetic mag others' rutile grains contained less than 0.200wt% $ZrO_2$ having values that ranged from below the lld (0.017wt%) to 0.124wt% with a mean of 0.084wt%. The maximum $V_2O_3$ hosted in a grain was 0.849wt%; although some grains contained less than the detection limit of 0.133wt% $V_2O_3$, the average $V_2O_3$ content of grains was 0.490wt%. The $Nb_2O_5$ content of seventeen of the eighteen analysed rutile grains varied from below the lld to 1.614wt%, with a single enriched grain containing 5.057wt%. The other (seventeen) grains had an average $Nb_2O_5$ content of 0.393wt%. $Al_2O_3$ contents varied from below the detection limit (0.011wt%) to 0.261wt%, with two grains containing slightly higher $Al_2O_3$ contents (0.168 and 0.261wt%). The average $Al_2O_3$ content for the majority of this population was 0.037wt%. The concentration of FeO in rutile grains varied from below the detection limit (0.027wt%) to 1.974wt%. The average FeO content was 0.502wt%. $Cr_2O_3$ content in rutile grains varied from below the detection limit (0.021wt%) to 0.326wt%, with a mean 0.098wt%. $Ta_2O_5$ ranged from 0.098 to 0.800wt% having an average of 0.347wt% (Table 5.3.2.2).

The grains from the 'non-magnetic mag others' fraction contained a grain that was both $Nb_2O_5$ and FeO enriched. Although $Ta_2O_5$ was below the detection limit in ten of the eighteen grains analysed; this fraction had a higher average $Ta_2O_5$ value than any of the other fractions.

| Oxides | Minimum (wt%) | Maximum (wt%) | *Mean (wt%) |
|--------|---------------|---------------|-------------|
| $TiO_2$ | 89.703 | 98.843 | 97.149 |
| $SiO_2$ | 0.231 | 0.624 | 0.379 |
| $ZrO_2$ | # | 0.124 | 0.084 |
| $V_2O_3$ | # | 0.849 | 0.490 |
| $Nb_2O_5$ | # | 5.057 | 0.393 |
| $Al_2O_3$ | # | 0.261 | 0.037 |
| FeO | # | 1.974 | 0.502 |
| $Cr_2O_3$ | # | 0.326 | 0.098 |

Table 5.3.2.2 A summary of electron microprobe results from 'non-magnetic mag others' fraction of Pond B.

*Mean:    Mean values exclude values that are below the detection limit and very high or low values (see details in text).

#    Lowest values are below the lld

## 5.3.2.3 Pond C

The distribution of $TiO_2$, $SiO_2$, $ZrO_2$, $V_2O_3$, $Nb_2O_5$, $Al_2O_3$ and FeO from the 'non-magnetic mag others' fraction of Pond C is presented in Fig. 5.3.2.3 and Table 5.3.2.3 the analytical data. The $TiO_2$ content of the non-magnetic mag others' fraction from Pond C varied between 93.092wt% and 98.826wt%. Apart from one $TiO_2$ poor rutile grain (93.092wt%) the other grains had an average of 97.493wt%. The distribution of $SiO_2$ values in these rutile grains, have ranged from 0.045wt% to 0.361wt% with an average of 0.179wt%. As with Ponds A and B, $ZrO_2$ occurred at low concentrations ranging from the lld (0.017wt%) to 0.298wt%. The average $ZrO_2$ content for this rutile population was 0.109wt%. The $V_2O_3$ distribution in rutile grains ranged from the detection limit
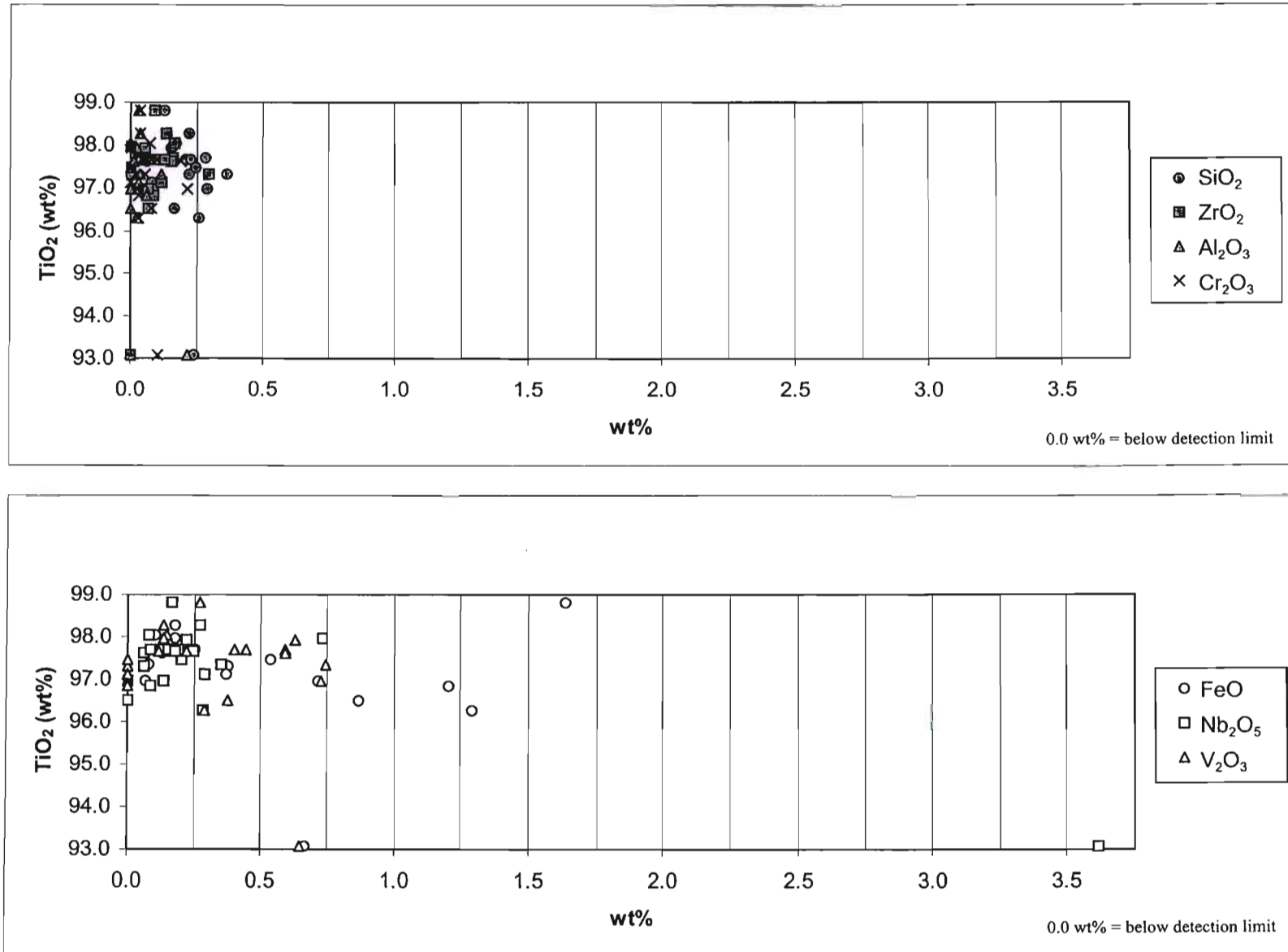
Fig. 5.3.2.3 Geochemistry of homogenous rutile grains in the non magnetic mag others fraction of Pond C.

(0.133wt%) to 0.743wt% with a mean value of 0.422wt%. Majority of the rutile grains (18 grains) had $Nb_2O_5$ values in a range from the detection limit (0.049wt%) to 0.731wt%, with an average of 0.211wt%. A single grain appeared to be $Nb_2O_5$ enriched and had a value of 3.161wt%. $Al_2O_3$ had a relatively narrow range of values from the lld to 0.213wt%, with an average of 0.053wt% $Al_2O_3$ for the rutile grains in this fraction. The FeO content of grains varied from 0.068 to 1.635wt%, with a mean of 0.450wt%. Three rutile grains were FeO enriched having FeO content greater than 1.000wt%. The $Cr_2O_3$ content of rutile grains varied from below the lld (0.021wt%) to 0.213wt%, with a mean of 0.072wt%. $Ta_2O_5$ was below the detection limit in sixteen of twenty-one analysed grains. The rutile grains had a $Ta_2O_5$ range from below the detection limit (0.030wt%) to 0.232wt%, with a mean of 0.108wt% (Table 5.3.2.3).

| Oxides | Minimum (wt%) | Maximum (wt%) | *Mean (wt%) |
|---|---|---|---|
| $TiO_2$ | 96.271 | 98.826 | 97.493 |
| $SiO_2$ | 0.045 | 0.361 | 0.179 |
| $ZrO_2$ | # | 0.298 | 0.109 |
| $V_2O_3$ | # | 0.743 | 0.422 |
| $Nb_2O_5$ | # | 3.161 | 0.211 |
| $Al_2O_3$ | # | 0.213 | 0.053 |
| FeO | 0.068 | 1.635 | 0.450 |
| $Cr_2O_3$ | # | 0.213 | 0.072 |

Table 5.3.2.3 A summary of electron microprobe results from 'non magnetic mag others' fraction of Pond C.

*Mean:     Mean values exclude values that are below the detection limit and very high or low values (see details in text).

#           Lowest values are below the lld

Almost all grains from the 'non-magnetic mag others' fraction contained detectable quantities of $SiO_2$, and FeO. One grain from this fraction was $Nb_2O_5$ enriched, and further three grains were FeO enriched.

## 5.4 Cleaner Mags

### 5.4.1 Pond A

The distribution of $TiO_2$, $SiO_2$, $ZrO_2$, $V_2O_3$, $Nb_2O_5$, $Al_2O_3$ and FeO from the 'cleaner mags' fraction of Pond A is presented in Fig. 5.4.1 and in Table 5.4.1 the analytical data. The $TiO_2$ values of this fraction did not display much variation (98.338 to 99.574wt%), and had a mean $TiO_2$ content of 98.995wt%. As expected, in grains having a high $TiO_2$ content the other elements rarely exceed 1.000wt%. $SiO_2$ occurred at concentrations of 0.065wt% to 0.524wt%, with an average of 0.231wt%. The $ZrO_2$ was content was found to be below 0.200wt% in all of the rutile grains from this fraction. The range of values was from below the lld (0.017wt%) to 0.187wt% with an average for all grains of 0.092wt%. Only three of the fifteen grains contained $V_2O_3$ above the lld, with one of the three grains having 0.283wt%. The average $V_2O_3$ content of these three rutile grains was 0.271wt%. Two grains contained $Nb_2O_5$ below the detection limit (0.049wt%), however, in most grains $Nb_2O_5$ did not exceed 0.3wt%. Values were in a scatter from the lld to 0.264wt%, with an average of 0.189wt%. Rutile grains displayed some variability in the $Al_2O_3$ content with three grains having $Al_2O_3$ content below the lld (0.011wt%), whereas one grain had 0.371wt%. The mean $Al_2O_3$ content (excluding grain with high $Al_2O_3$ and those below the lld) was 0.029wt%. All grains contained FeO, even though in most case it was present at low concentrations. The FeO content ranged from 0.065 to 0.426wt%. Only one grain had a relatively enriched FeO composition of 0.426wt%, whilst the other grains had an average of 0.157wt%. $Cr_2O_3$ had values in the range from below the lld (0.021wt%) to 0.191wt%, with an average of 0.082wt%. Most grains (9 grains) had $Ta_2O_5$ below the lld, the remaining six grains had values ranging from 0.036wt% to 0.335wt%, with an average of 0.1974wt% (Table 5.4.1).

Fig. 5.4.1 Geochemistry of homogenous rutile grains in the cleaner mags fraction of Pond A.

The grains in the 'cleaner mags' fraction had a very high $TiO_2$ contents with very few significant quantities of impurities impurities. With the exception of $SiO_2$, the other elements had concentrations below 0.500wt%.

| Oxides | Minimum (wt%) | Maximum (wt%) | *Mean (wt%) |
|--------|---------------|---------------|-------------|
| $TiO_2$ | 98.337 | 99.574 | 98.995 |
| $SiO_2$ | 0.065 | 0.524 | 0.231 |
| $ZrO_2$ | # | 0.187 | 0.092 |
| $V_2O_3$ | # | 0.283 | 0.271 |
| $Nb_2O_5$ | # | 0.264 | 0.189 |
| $Al_2O_3$ | # | 0.371 | 0.029 |
| FeO | 0.065 | 0.426 | 0.157 |
| $Cr_2O_3$ | # | 0.191 | 0.082 |

Table 5.4.1 A summary of electron microprobe results from 'cleaner mags' fraction of Pond A.

*Mean:       Mean values exclude values that are below the detection limit and very high or low values (see details in text).

#            Lowest values are below the lld

## 5.4.2 Pond B

The distribution of $TiO_2$, $SiO_2$, $ZrO_2$, $V_2O_3$, $Nb_2O_5$, $Al_2O_3$ and FeO from the 'cleaner mags' fraction of Pond B is presented in Fig. 5.4.2 and in Table 5.4.2 the analytical data. The

Fig. 5.4.2 Geochemistry of homogenous rutile grains in the cleaner mags fraction of Pond B.
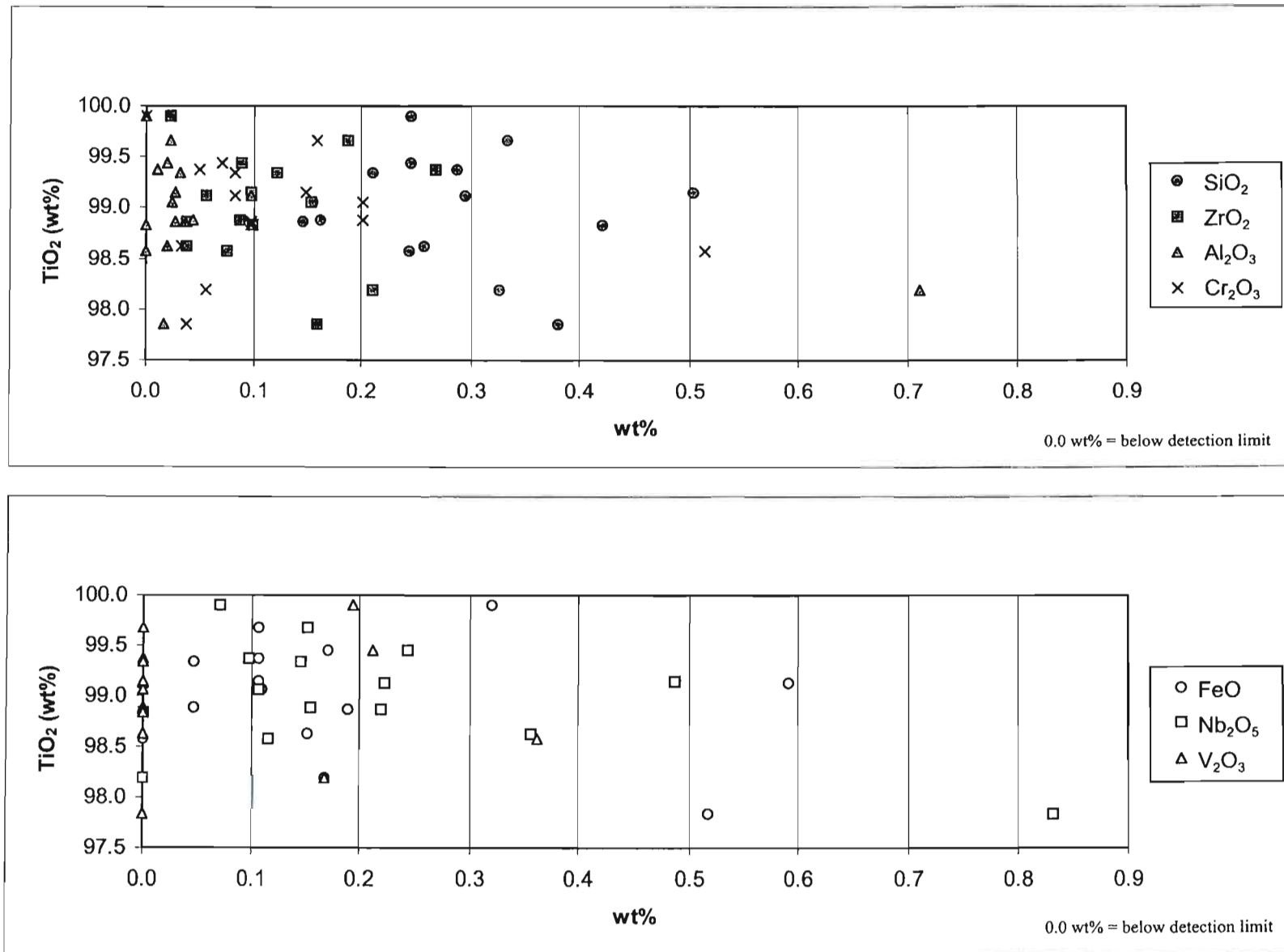
$TiO_2$ values were between 97.845wt% and 99.901wt% with an average of 98.991. All the rutile grains from this fraction had $SiO_2$ present at concentrations between 0.145wt% to 0.504wt% with a mean $SiO_2$ of 0.281wt%. $ZrO_2$ had values in a much smaller range (0.023wt% to 0.267wt%), with a mean of 0.113wt%. Of the fifteen grains, only four had $V_2O_3$ contents above the detection limit (0.133wt%), ranging up to 0.362wt% with a mean of 0.234wt%. The $Nb_2O_3$ content in rutile grains from this fraction had values in the range from below the lld (0.049wt%) to 0.831wt%, with only a single $Nb_2O_5$ enriched (0.831wt%) grain being, the rest of the grains had an average of 0.197wt% of $Nb_2O_5$. $Al_2O_3$ content in the rutile grains were relatively low, (below the $Al_2O_3$ detection limit of 0.011wt% to 0.711wt%) with most grains containing less than 0.100wt% $Al_2O_3$ with a mean of 0.025wt%. the exception was a single grain that contained 0.711wt% $Al_2O_3$. (Table 5.4.2).

| Oxides | Minimum (wt%) | Maximum (wt%) | *Mean (wt%) |
|---|---|---|---|
| $TiO_2$ | 97.845 | 99.901 | 98.991 |
| $SiO_2$ | 0.145 | 0.504 | 0.281 |
| $ZrO_2$ | 0.023 | 0.267 | 0.113 |
| $V_2O_3$ | # | 0.362 | 0.234 |
| $Nb_2O_5$ | # | 0.831 | 0.197 |
| $Al_2O_3$ | # | 0.711 | 0.088 |
| FeO | # | 0.590 | 0.117 |
| $Cr_2O_3$ | # | 0.514 | 0.131 |

Table 5.4.2 A summary of electron microprobe results from 'cleaner mags' fraction of Pond B.

*Mean: Mean values exclude values that are below the detection limit and very high or low values (see details in text).

# Lowest values are below the lld

The FeO content varied from below the lld (0.027wt%) to 0.590wt%, with a mean of 0.177wt%. $Cr_2O_3$ values varied from below the lld (0.021wt%) to 0.514wt%, and had a mean of 0.131wt%. $Ta_2O_5$ was above the detection limit for nine of the fifteen grains, ranging up to 0.292, with an average of 0.146wt% (Table 5.4.2).

All the grains analysed in the 'cleaner mags' fraction were virtually pure $TiO_2$ and contained only small amounts of $SiO_2$, $ZrO_2$ and $Nb_2O_5$.

## 5.4.3 Pond C

The distribution of $TiO_2$, $SiO_2$, $ZrO_2$, $V_2O_3$, $Nb_2O_5$, $Al_2O_3$ and FeO from the 'cleaner mags' fraction of Pond C is presented in Fig. 5.4.3 and in Table 5.4.3 the analytical data. The $TiO_2$ values in these rutile grains from Pond C have a larger spread than Ponds A and B, with values from 96.187 to 98.856wt%, and a mean of 97.903wt%. The $SiO_2$ content varied between 0.224wt% and 1.076wt%, with fifteen of the sixteen grains having a mean $SiO_2$ content of 0.370wt%. Only a single grain had a much higher $SiO_2$ content of 1.076wt%. Almost all grains contained $ZrO_2$, (one grain had $ZrO_2$ below the detection limit) ranging up to 0.299wt%. The average $ZrO_2$ content of these grains was 0.127wt%. Only four grains contained $V_2O_3$ above the detection limit of 0.133wt%, with the maximum $V_2O_3$ content being 0.414wt%. The mean $V_2O_3$ for this fraction was 0.245wt%. All the analysed grains were $Nb_2O_5$ bearing, with values that ranged from the detection limit of 0.049wt% to 0.858wt%, and a mean of 0.284wt%. Seven of the seventeen analysed rutile grains contained $Al_2O_3$ above the detection limit (0.011wt%) to 1.522wt%, with only a single grain containing a high $Al_2O_3$ content (1.522wt%), whereas the other grains contained an average of 0.036wt% $Al_2O_3$. The FeO content in grains ranged from below the detection limit (0.027) to a maximum of 0.593wt%, with an average FeO content for these rutile grains being 0.248wt%. All the grains contained $Cr_2O_3$, varying from 0.033 to 0.197wt%. The average $Cr_2O_3$ content in this fraction was 0.107wt%. Most grains (nine grains) contained $Ta_2O_5$ ranging up to 0.261wt%, with an average 0.137wt% (Table 5.4.3).
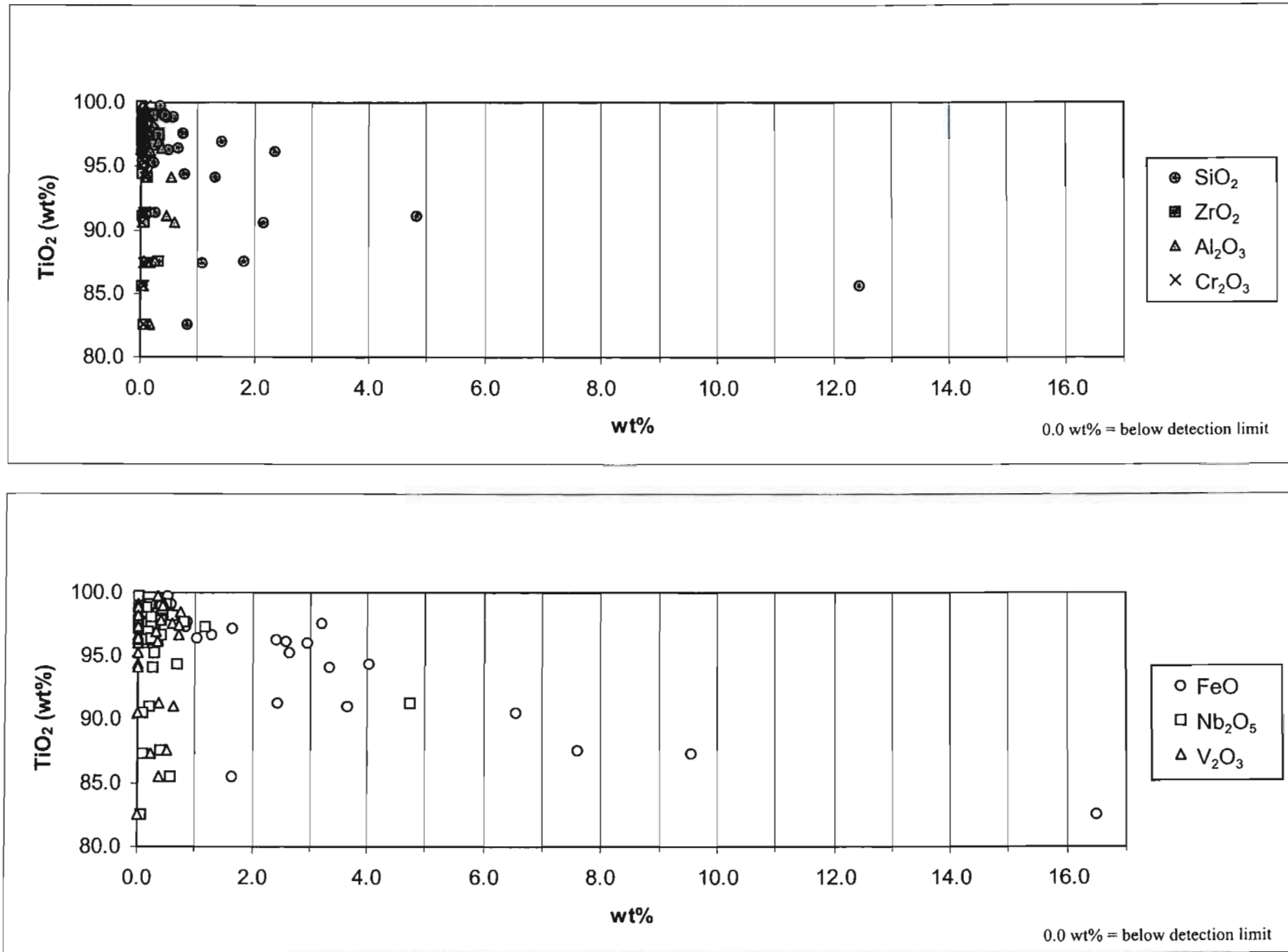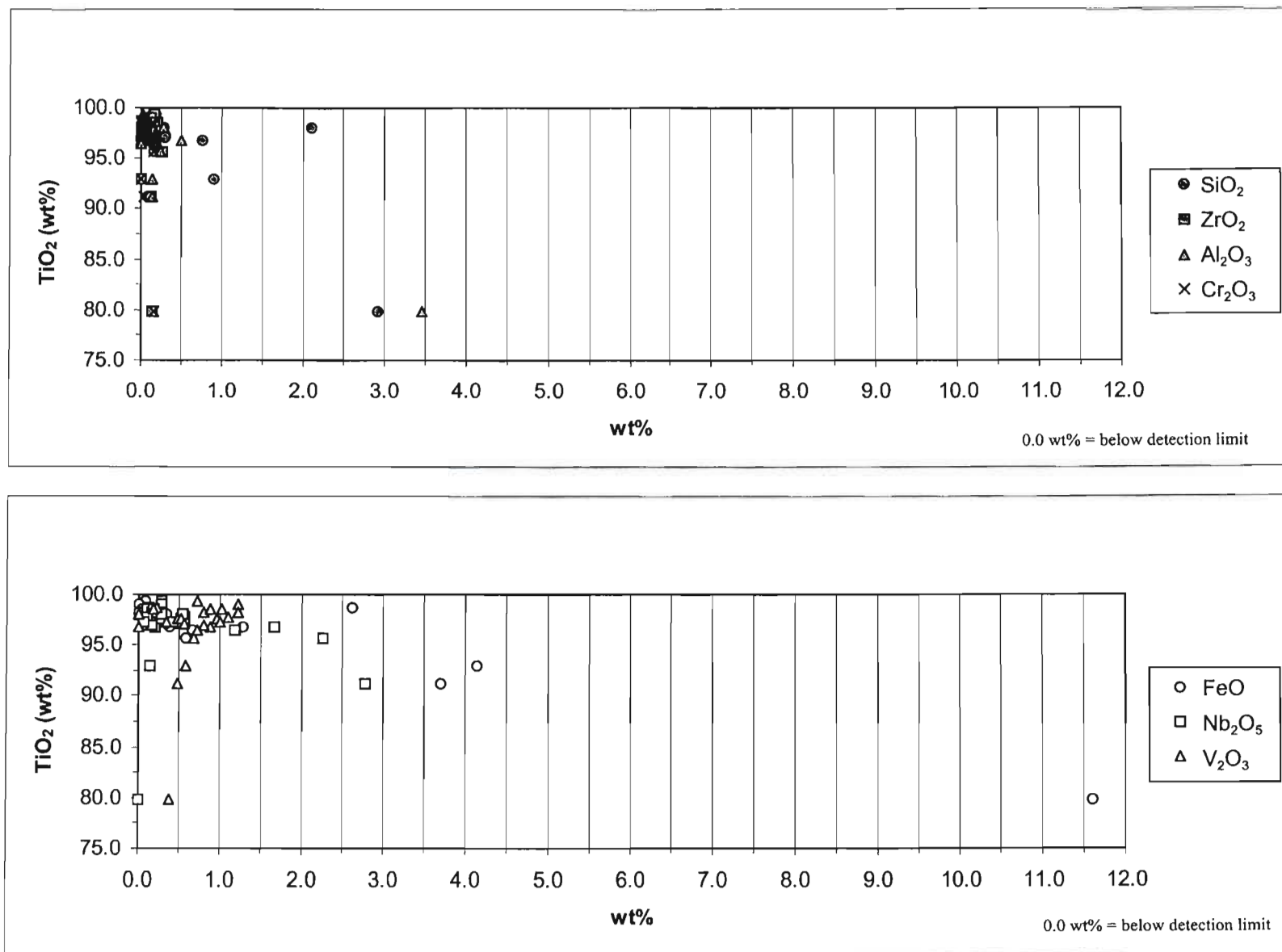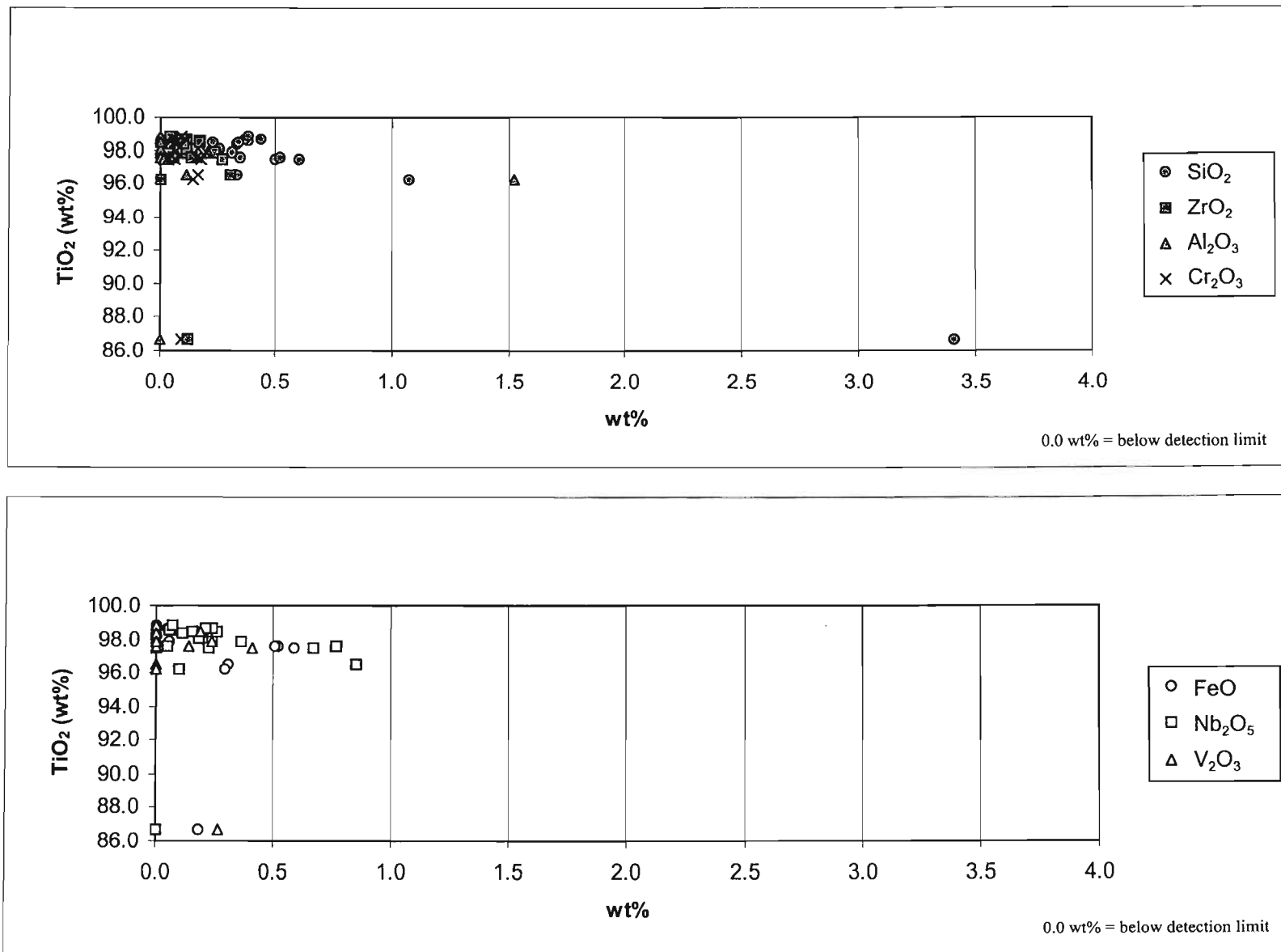
Fig. 5.4.3 Geochemistry of homogenous rutile grains in the cleaner mags fraction of Pond C.

| Oxides | Minimum (wt%) | Maximum (wt%) | *Mean (wt%) |
|---|---|---|---|
| $TiO_2$ | 96.187 | 98.856 | 97.903 |
| $SiO_2$ | 0.224 | 0.601 | 0.370 |
| $ZrO_2$ | 0.038 | 0.299 | 0.135 |
| $V_2O_3$ | # | 0.414 | 0.245 |
| $Nb_2O_5$ | # | 0.858 | 0.284 |
| $Al_2O_3$ | # | 1.522 | 0.058 |
| FeO | # | 0.593 | 0.248 |
| $Cr_2O_3$ | 0.033 | 0.197 | 0.107 |

Table 5.4.3 A summary of electron microprobe results from 'cleaner mags' fraction of Pond C.

*Mean:      Mean values exclude values that are below the detection limit and very high or low values (see details in text).

#           Lowest values are below the lld

All the rutiles from the 'cleaner mags' fraction of Pond C contained $SiO_2$ and $Nb_2O_5$. In comparison to Ponds A and B, rutile grains from Pond C rutile grains had a greater spread in the $Al_2O_3$ content. Only one grain had a slightly higher $Al_2O_3$ content of 1.522wt%.

## 5.5 Primary Mags

## 5.5.1 Pond A

The distribution of $TiO_2$, $SiO_2$, $ZrO_2$, $V_2O_3$, $Nb_2O_5$, $Al_2O_3$ and FeO from the 'primary mags' fraction of Pond A is presented in Fig. 5.5.1 and in Table 5.5.1 the analytical data. The $TiO_2$ content of these grains ranged from 96.526 to 99.658wt%. One grain had a slightly lower $TiO_2$ content of 96.526wt, while the remaining fifteen grains contained on average 99.054wt% $TiO_2$. The $SiO_2$ content of rutile, varied from 0.065wt% to 0.394wt%. The grain that had the very low $TiO_2$ content had a correspondingly high $SiO_2$ content of 0.394wt%. The average $SiO_2$ content for all sixteen grains was 0.166wt%. Even though all grains contained measurable $ZrO_2$ concentrations, these did not exceed 0.500wt%. The values ranged from 0.102wt% to 0.442wt% with a mean $ZrO_2$ content of 0.227wt%. There was a large spread of $V_2O_3$ values; three grains had $V_2O_3$ below the detection limit while others ranged up to a single enriched grain with 1.162wt% $V_2O_3$. Most of the grains (with exception to the enriched grain) had a mean $V_2O_3$ value of 0.276wt%. The $Nb_2O_5$ bearing grains, had values confined to a range from 0.049wt% to 0.259wt%. The average $Nb_2O_5$ composition for the fourteen rutile grains was 0.132wt%. Although most rutile grains (ten grains) contained $Al_2O_3$, above the lld, one grain had a relatively higher $Al_2O_3$ content of 0.159wt%. With the exception of this grain, the rest of the grains had $Al_2O_3$ content of up to 0.072wt%, with an average of 0.035wt%. Fifteen of the sixteen grains contained FeO, with values ranging up to 0.889wt%. One grain had a relatively higher proportion of FeO (0.889wt%) than the other grains, which had an average FeO content of 0.184wt%. $Cr_2O_3$ was above the detection limit for all except one grain, having a maximum of 0.226wt%, and with a mean of 0.113wt%. $Ta_2O_5$ was present at concentration above the detection limit in nine of the sixteen grains ranging from 0.036 to 0.289wt%, with a mean of 0.128wt% (Table 5.5.1).

All the rutile grains analysed in the 'primary mags' fraction contain a proportion of $SiO_2$, $Nb_2O_5$ and FeO. Two grains reported higher $Al_2O_3$ values, and one grain, a high $V_2O_3$ value.
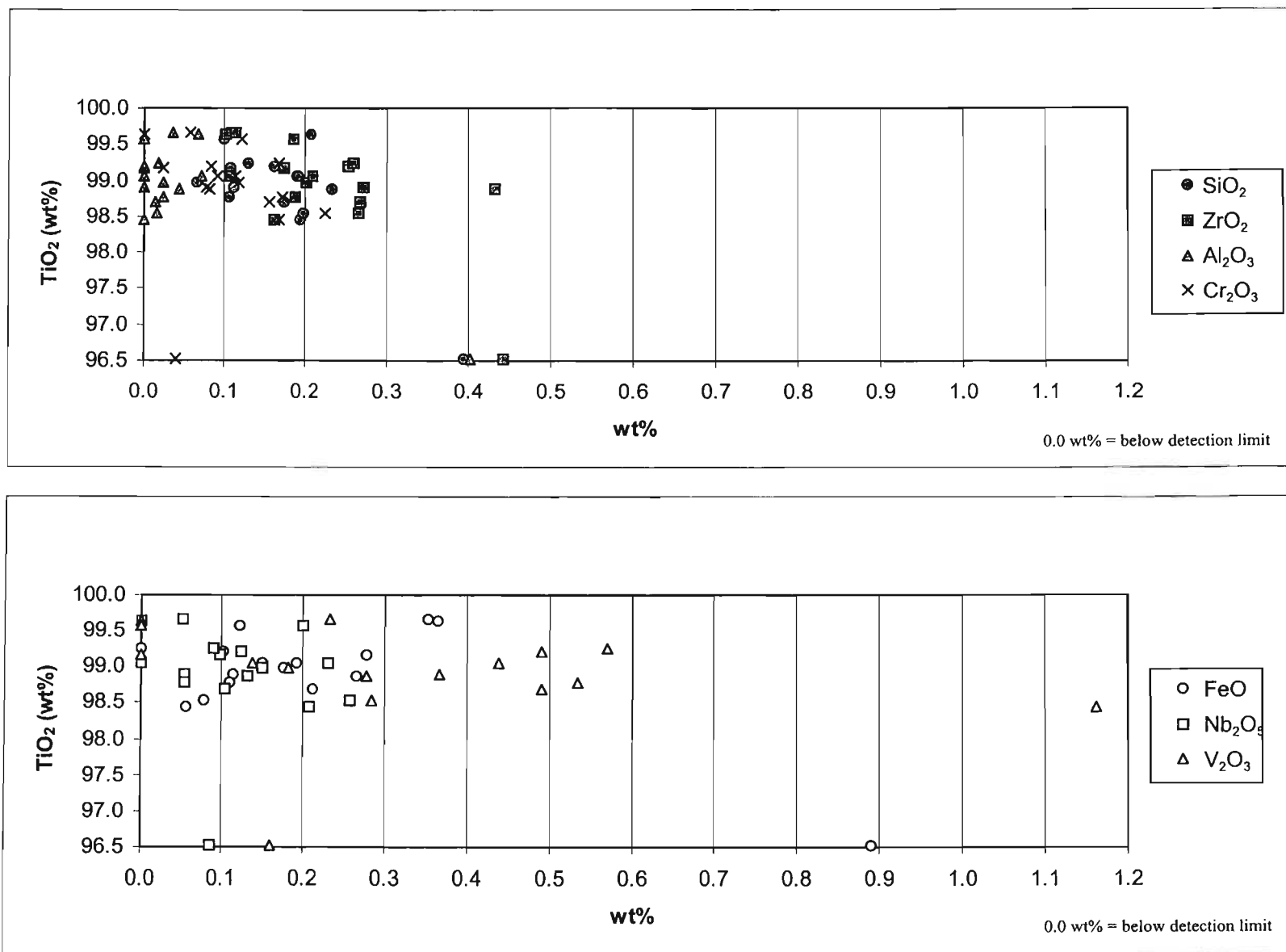
Fig. 5.5.1 Geochemistry of homogenous rutile grains in the primary mags fraction of Pond A.

| Oxides | Minimum (wt%) | Maximum (wt%) | *Mean (wt%) |
|---|---|---|---|
| $TiO_2$ | 96.526 | 99.658 | 99.054 |
| $SiO_2$ | 0.065 | 0.394 | 0.166 |
| $ZrO_2$ | 0.102 | 0.442 | 0.227 |
| $V_2O_3$ | # | 1.162 | 0.347 |
| $Nb_2O_5$ | # | 0.259 | 0.132 |
| $Al_2O_3$ | # | 0.401 | 0.035 |
| FeO | # | 0.889 | 0.184 |
| $Cr_2O_3$ | # | 0.226 | 0.113 |

Table 5.5.1 A summary of electron microprobe results from 'primary mags' fraction of Pond A.

*Mean:     Mean values exclude values that are below the detection limit and very high or low values (see details in text).

#          Lowest values are below the lld

## 5.5.2 Pond B

The distribution of $SiO_2$, $ZrO_2$, $V_2O_3$, $Nb_2O_5$, $Al_2O_3$ and FeO from the 'primary mags' fraction of Pond B is presented in Fig. 5.5.2 and in Table 5.2.2 the analytical data. The $TiO_2$ content of rutile grains from this fraction varied from 96.226wt% to 99.959wt%, having an average $TiO_2$ content of 98.463wt%. All grains contained $SiO_2$ at levels ranging from 0.168wt% up to 2.203wt%. Two grains had much higher $SiO_2$ contents (1.515wt% and 2.203wt%) than the other grains, which had on average 0.254wt% $SiO_2$.
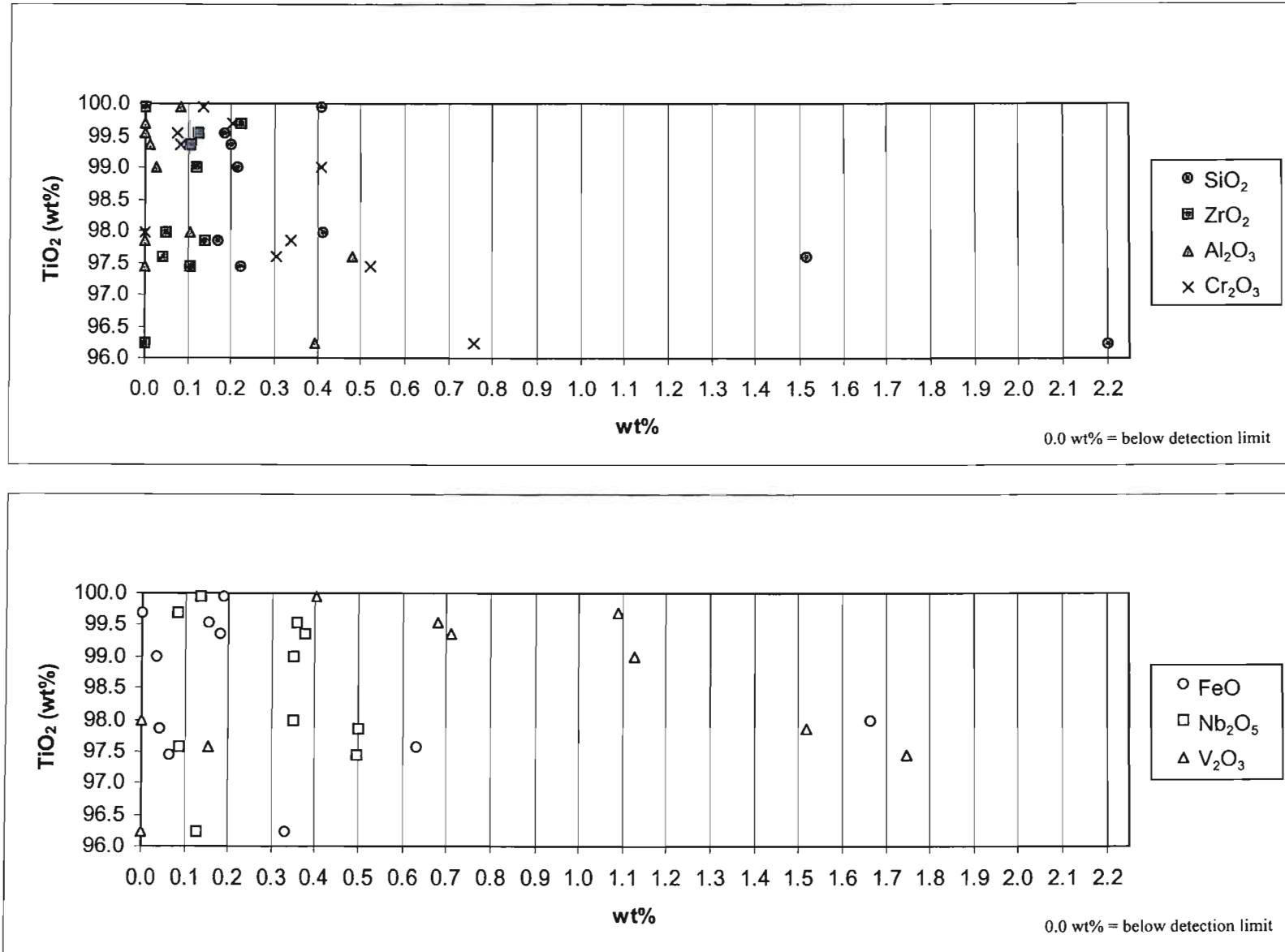
Fig. 5.5.2 Geochemistry of homogenous rutile grains in the primary mags fraction of Pond B.

The $ZrO_2$ composition of rutile grains was up to 0.223wt%, although some grains contained $ZrO_2$ below the lld. The mean $ZrO_2$ content was 0.113wt%. The distribution of $V_2O_3$ in rutile grains had a large spread, two grains had values below the detection limit (0.133wt%) while others contained up to 1.746wt% $V_2O_3$, with a mean $V_2O_3$ content of 0.928wt%. $Nb_2O_5$ was present in all rutile grains, at concentrations from 0.081 to 0.501wt%. The mean $Nb_2O_5$ content for rutile grains was 0.286wt%. The six grains that contained $Al_2O_3$ ranged from just above the lld (0.011wt%) to a single grain with 0.479wt% $Al_2O_3$. The mean $Al_2O_3$ content was 0.183wt%. The FeO composition of rutile grains varied from one grain that had FeO below the lld (0.027wt%) to 1.664wt%. The mean FeO content for the other grains from this fraction (excluding the grain with 1.664wr% FeO) was 0.202wt%. $Cr_2O_3$ had a varied distribution in rutile grains from one grain with a value below the lld (0.021wt%) to a maximum of 0.758wt%, with a mean $Cr_2O_3$ content of 0.314wt%. $Ta_2O_5$ was detected in only four grains and ranged from 0.036 to 0.202wt%, with a mean of 0.164wt% (Table 5.5.2).

| Oxides | Minimum (wt%) | Maximum (wt%) | *Mean (wt%) |
|---|---|---|---|
| $TiO_2$ | 96.226 | 99.959 | 98.463 |
| $SiO_2$ | 0.168 | 2.203 | 0.254 |
| $ZrO_2$ | 0.017 | 0.223 | 0.113 |
| $V_2O_3$ | 0.133 | 1.746 | 0.928 |
| $Nb_2O_5$ | 0.081 | 0.501 | 0.286 |
| $Al_2O_3$ | 0.011 | 0.479 | 0.183 |
| FeO | 0.027 | 1.664 | 0.202 |
| $Cr_2O_3$ | 0.021 | 0.758 | 0.314 |

Table 5.5.2 A summary of electron microprobe results from 'primary mags' fraction of Pond B.

*Mean:      Mean values exclude values that are below the detection limit and very high or low values.
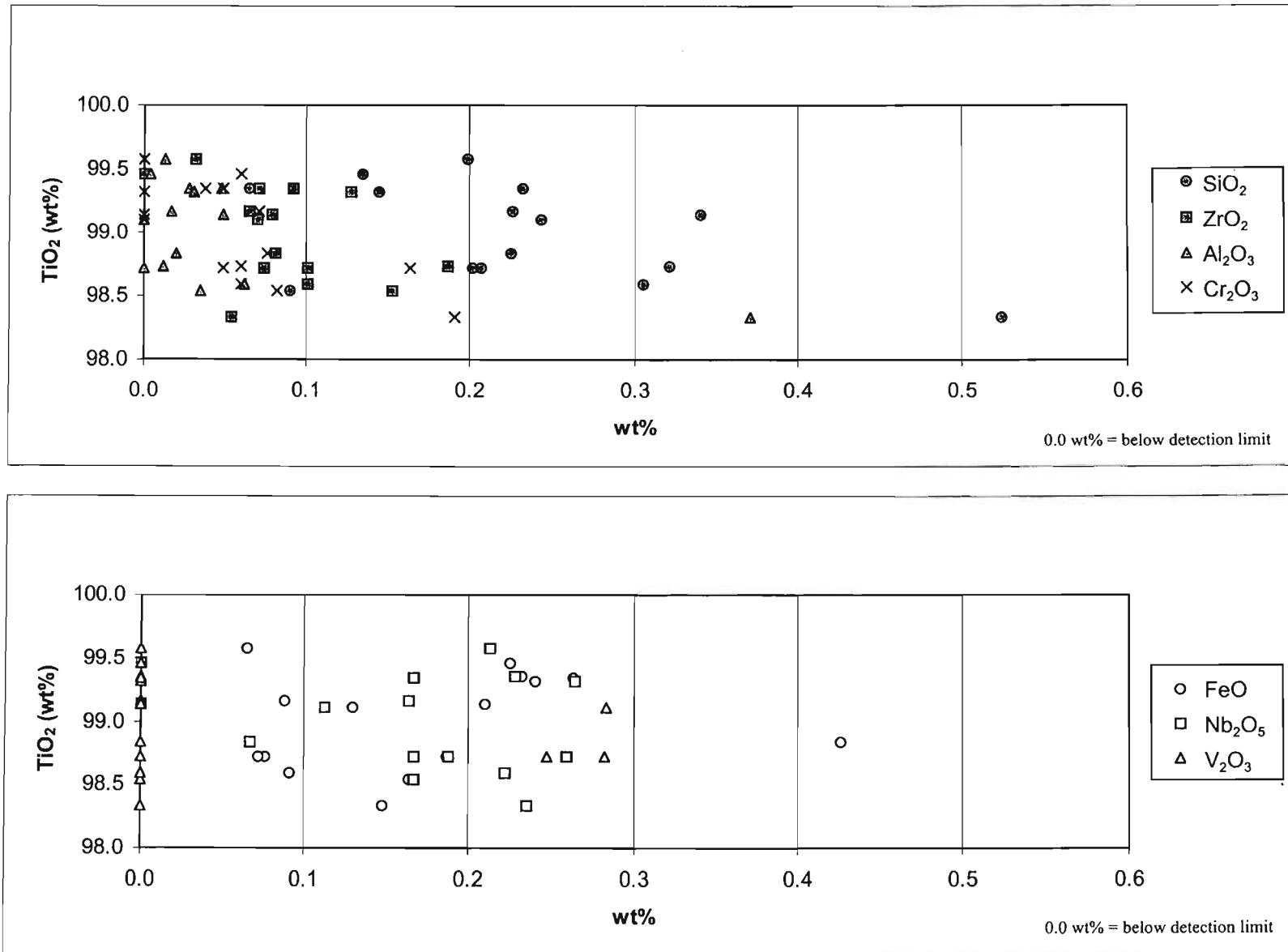
#      Lowest values are below the lld

The rutile grains from 'primary mags' fraction of Pond B, all contain $SiO_2$, and $Nb_2O_5$. Most grains had a very low FeO content, and some grains contained FeO below the lld of 0.027wt%.

## 5.5.3 Pond C

The distribution of $TiO_2$, $SiO_2$, $ZrO_2$, $V_2O_3$, $Nb_2O_5$, $Al_2O_3$ and FeO from the 'primary mags' fraction of Pond C is presented in Fig. 5.5.3 and in Table 5.5.3 the analytical data. All grains had a high $TiO_2$ content, ranging from 96.982wt% to 99.868wt%, with an average of 98.451wt%. All the rutile grains from this fraction contained some $SiO_2$, varying from 0.080wt% to 1.188wt%. With the exception of the grain consisting of 1.188wt% $SiO_2$, the grains had an average of 0.224wt% $SiO_2$. The $ZrO_2$ composition of rutile grains was from one grain below the lld (0.017wt%) to 0.300wt%, with a mean of 0.126wt%. The $V_2O_3$, content ranged from 0.133wt% to 0.893wt% with an average of 0.517wt%. Although two grains contained less than a detectable amount of $Nb_2O_5$, other twelve grains contained up to 0.610wt%, the average $Nb_2O_5$ content was 0.199wt%. Of the fourteen grains, only two grains contained $Al_2O_3$ below the lld; however, most of the twelve rutile grains contained very little $Al_2O_3$ (ranging to 0.488wt%), with three distinct grains having $Al_2O_3$ values of 0.185, 0.221 and 0.488wt%. The overall mean $Al_2O_3$ value for the analysed grains was, 0.093wt%. FeO was present in all the grains at concentrations ranging from 0.037 to 1.028wt%, with the average FeO content being 0.314wt%. $Cr_2O_3$ was present in all but one grain, ranging up to 0.303wt% with a mean of 0.131wt%. Only eight grains contained $Ta_2O_5$, but this was present at very low concentrations of 0.072wt%, and in the other six grains $Ta_2O_5$ was below the detection limit (Table 5.5.3).

All grains from the 'primary mags' fraction of Pond C contained significant amounts of $SiO_2$, $V_2O_3$, FeO and $Cr_2O_3$. A single grain had a $SiO_2$ content of greater than 1wt%. The other elements occurred at concentrations well below 1.000wt%.

104
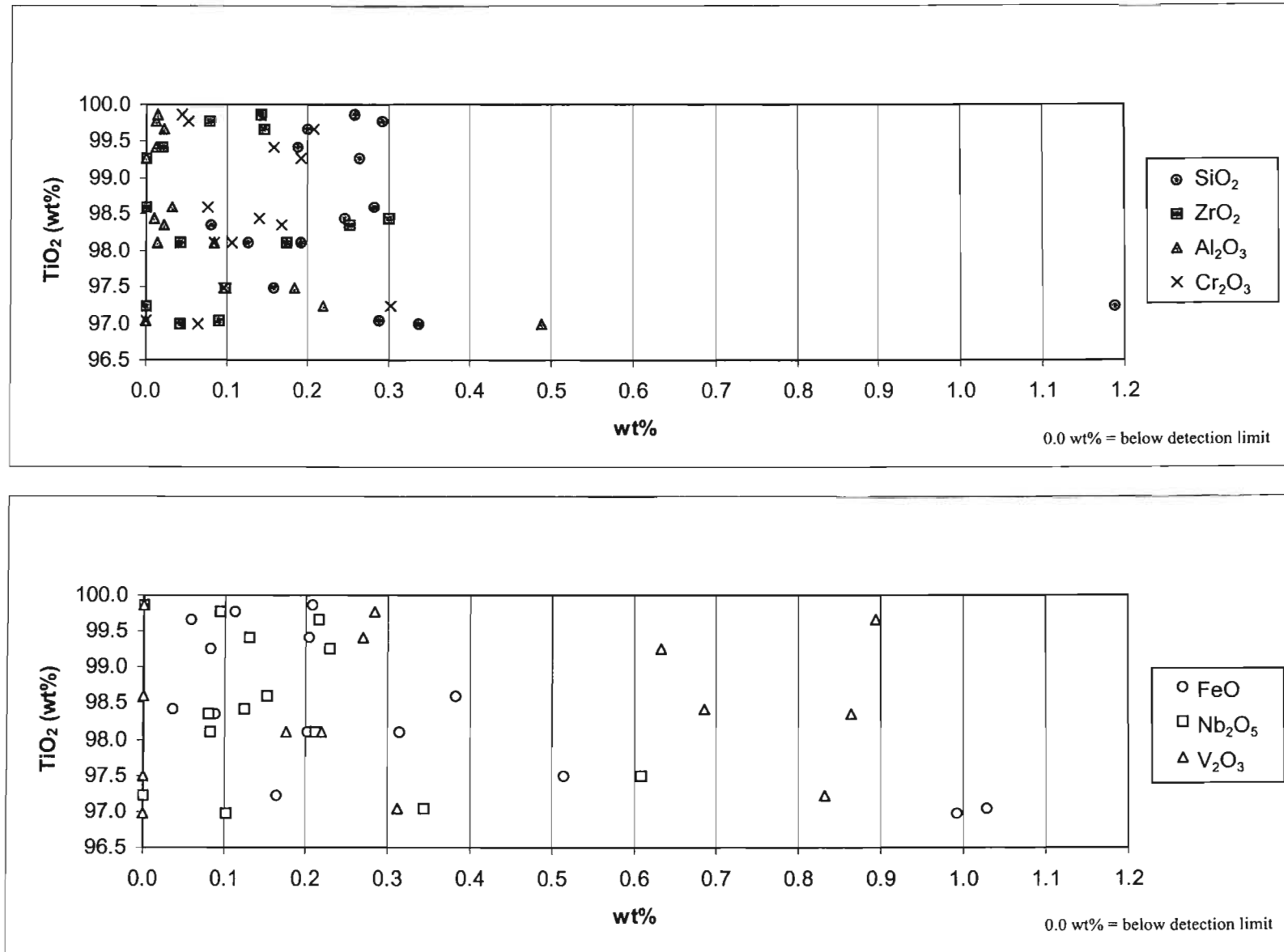
Fig. 5.5.3 Geochemistry of homogenous rutile grains in the primary mags fraction of Pond C.

| Oxides | Minimum (wt%) | Maximum (wt%) | *Mean (wt%) |
|---|---|---|---|
| $TiO_2$ | 96.982 | 99.868 | 98.451 |
| $SiO_2$ | 0.080 | 1.188 | 0.224 |
| $ZrO_2$ | # | 0.300 | 0.126 |
| $V_2O_3$ | # | 0.893 | 0.517 |
| $Nb_2O_5$ | # | 0.610 | 0.199 |
| $Al_2O_3$ | # | 0.488 | 0.093 |
| FeO | # | 1.028 | 0.314 |
| $Cr_2O_3$ | # | 0.303 | 0.131 |

Table 5.5.3 A summary of electron microprobe results from 'primary mags' fraction of Pond C.

*Mean: Mean values exclude values that are below the detection limit and very high or low values.

\# Lowest values are below the lld

# 5.6 Primary HT'S Conductors

## 5.6.1 Pond A

The distribution of $TiO_2$, $SiO_2$, $ZrO_2$, $V_2O_3$, $Nb_2O_5$, $Al_2O_3$ and FeO from the 'primary HT'S conductors' fraction of Pond A is presented in Fig. 5.6.1 and in Table 5.6.1 the analytical data. The $TiO_2$ content of rutile grains from this fraction was restricted to a narrow range between, 98.704wt% to 99.678wt% with a mean of 98.976wt%. All the grains analysed contain traces of $SiO_2$ varying from 0.309wt% to 0.606wt% with an average $SiO_2$ content of 0.406wt%. All grains also contained $ZrO_2$, at concentrations of 0.059wt% to

Fig. 5.6.1 Geochemistry of homogenous rutile grains in the primary HT'S conductors fraction of Pond A.

0.321wt%, and a mean of 0.130wt%. Only three grains of the eight grains contained $V_2O_3$ at levels above the lld, with others containing as much as 0.335wt%. The overall mean for $V_2O_3$ was 0.303wt%. Only one grain contained $Nb_2O_5$ below the detection limit (0.049wt%), the others contained up to 0.234wt%, with an average of 0.159wt%. Only two grains contained $Al_2O_3$ above the detection limit, and these had values of 0.021 and 0.138wt% with the average of the two grains being 0.080wt%. The FeO content of two rutile grains was below the lld, the other seven ranged from 0.027 to 0.175wt%, with a mean of 0.095wt%. $Cr_2O_3$ was present in grains from 0.038wt% to 0.218wt% and had an average of 0.111wt%. $Ta_2O_5$ was below detection in most grains with with only three grains having $Ta_2O_5$ of 0.046, 0.100 and 0.181wt%, giving a mean of 0.109wt% (Table 5.6.1).

| Oxides | Minimum (wt%) | Maximum (wt%) | *Mean (wt%) |
|--------|---------------|---------------|-------------|
| $TiO_2$ | 98.704 | 99.678 | 98.976 |
| $SiO_2$ | 0.309 | 0.606 | 0.406 |
| $ZrO_2$ | 0.059 | 0.321 | 0.130 |
| $V_2O_3$ | # | 0.335 | 0.303 |
| $Nb_2O_5$ | # | 0.234 | 0.159 |
| $Al_2O_3$ | # | 0.138 | 0.080 |
| FeO | # | 0.175 | 0.095 |
| $Cr_2O_3$ | 0.038 | 0.218 | 0.111 |

Table 5.6.1 A summary of electron microprobe results from 'primary mags' fraction of Pond A.

*Mean:      Mean values exclude values that are below the detection limit and very high or low values (see details in text).

#      Lowest values are below the lld

The rutile grains in 'primary mags' fraction of Pond A all had very high $TiO_2$ contents (>98.700wt%). No other element occurred at concentration above 1.00wt%, although all grains contained some $SiO_2$, $ZrO_2$, $Nb_2O_5$, $Cr_2O_3$ and FeO.

## 5.6.2 Pond B

The distribution of $TiO_2$, $SiO_2$, $ZrO_2$, $V_2O_3$, $Nb_2O_5$, $Al_2O_3$ and FeO from the 'primary HT'S conductors' fraction of Pond B is presented in Fig. 5.6.2 and in Table 5.6.2 the analytical data. The analysed rutile grains were very $TiO_2$ pure, with $TiO_2$ contents, in the range of 98.010wt% to 99.872, and a mean of 98.967wt%. All the grains contained between 0.271wt% to 0.468wt% $SiO_2$, with a mean $SiO_2$ content of 0.370wt%. Most of the grains (six of eight analysed grains) contain $ZrO_2$, above the lld (0.017wt%) varying up to 0.314wt%, with a mean of 0.165wt%. Only three grains contained $V_2O_3$ above the detection limit (0.133wt%), ranging to a maximum of 0.352wt%, with a mean of 0.238wt%. The $Nb_2O_5$ content of rutile grains varied from one grain, which was below the lld (0.049) to 0.261wt%; the average $Nb_2O_5$ content being 0.150wt%. The $Al_2O_3$ content in the rutile grains did not exceed 0.100wt%, and was confined to a narrow range, three grains were below the detection limit (0.011wt%) the other five had up to 0.044wt%, with an average of 0.018wt%. Only one grain had FeO content below the lld (0.027wt%), the other grains ranged up to 0.312wt%, having an average FeO content of 0.137wt%. Significant $Cr_2O_3$ measured in six of the eight grains and ranged up to 0.202wt%, with a mean $Cr_2O_3$ content of 0.126wt%. Most grains did not contain $Ta_2O_5$, however three grains had $Ta_2O_5$ contents above the detection limit, ranging from 0.036 to 0.270wt%, with an average of 0.096wt% (Table 5.6.2).

The rutile grains from the 'primary HT'S conductors' fraction of Pond B had a very high $TiO_2$ content, thus restricting the quantity of other ions substituting into the rutile lattice, with no element contributing more than 0.500wt% to the rutile grain. However, all grains contain detectable levels of $SiO_2$.
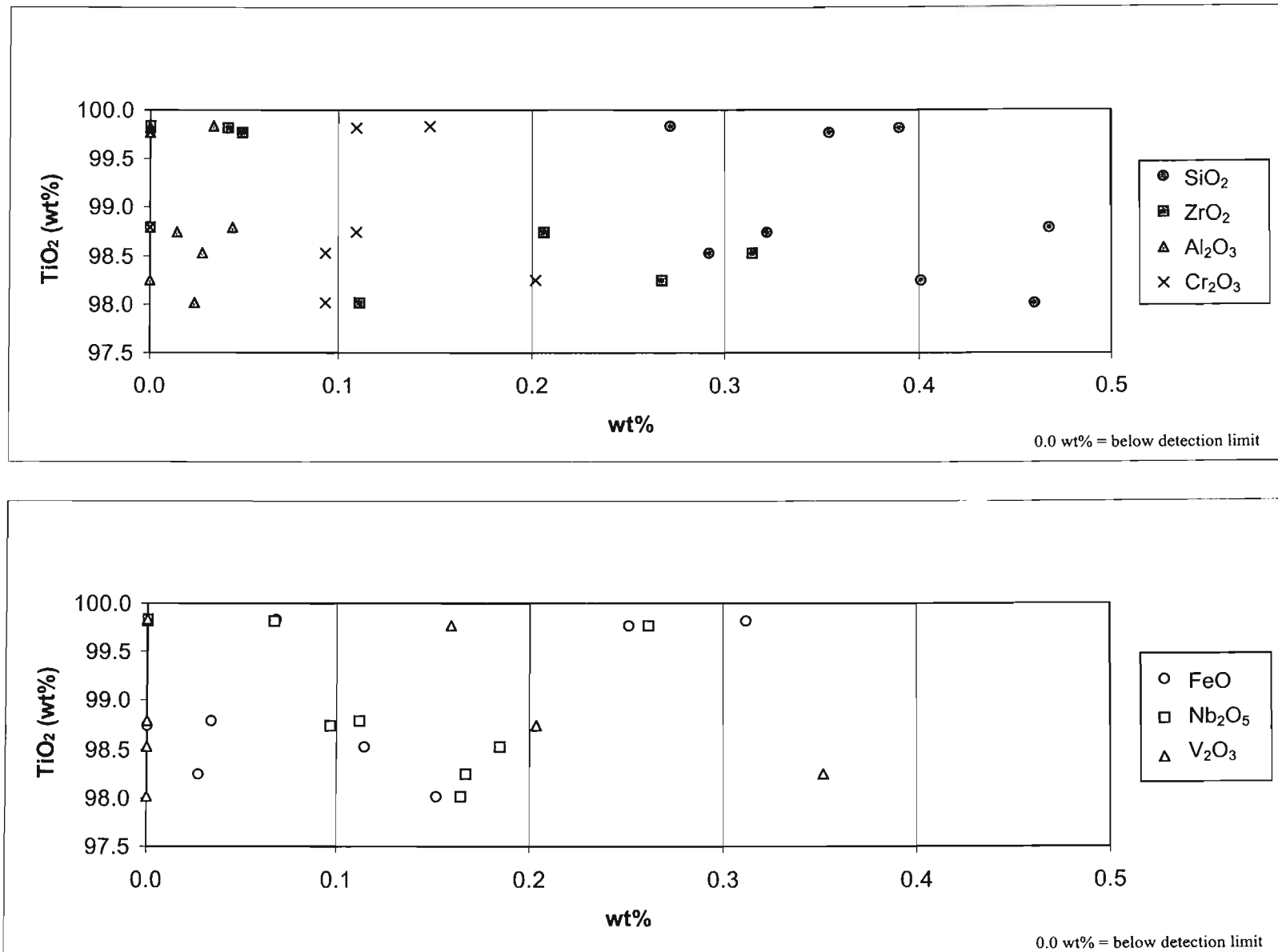
Fig. 5.6.2 Geochemistry of homogenous rutile grains in the primary HT'S conductors fraction of Pond B.

| Oxides | Minimum (wt%) | Maximum (wt%) | *Mean (wt%) |
|---|---|---|---|
| $TiO_2$ | 98.010 | 99.827 | 98.967 |
| $SiO_2$ | 0.271 | 0.468 | 0.370 |
| $ZrO_2$ | # | 0.314 | 0.165 |
| $V_2O_3$ | # | 0.352 | 0.238 |
| $Nb_2O_5$ | # | 0.261 | 0.150 |
| $Al_2O_3$ | # | 0.044 | 0.029 |
| FeO | # | 0.312 | 0.137 |
| $Cr_2O_3$ | # | 0.202 | 0.126 |

Table 5.6.2 A summary of electron microprobe results from 'primary HT'S conductors' fraction of Pond B.

*Mean:       Mean values exclude values that are below the detection limit and very high or low values (see details in text).

#       Lowest values are below the lld

## 5.6.3 Pond C

The distribution of $TiO_2$, $SiO_2$, $ZrO_2$, $V_2O_3$, $Nb_2O_5$, $Al_2O_3$ and FeO from the 'primary HT'S conductors' fraction of Pond C is presented in Fig. 5.6.3 and Table 5.6.3 the analytical data. All eight grains from this fraction had relatively high $TiO_2$ contents of 96.956wt% to 98.050wt%, with a mean of 97.409wt%. Grains all contained varying amounts of $SiO_2$, $ZrO_2$, $V_2O_3$, $Nb_2O_5$ and FeO. The $SiO_2$ content ranged from 0.299wt% to 0.589wt%, with
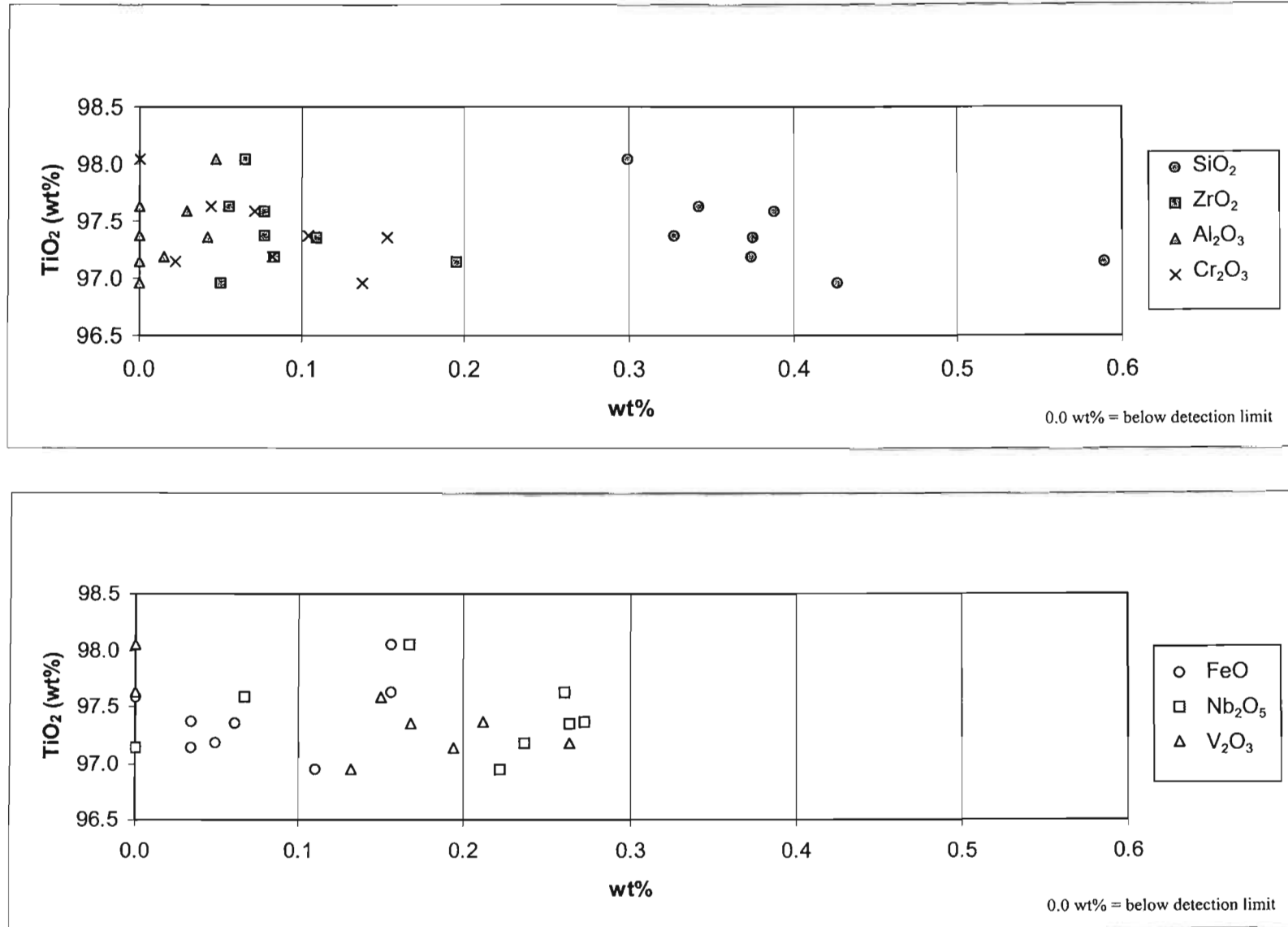
Fig. 5.6.3 Geochemistry of homogenous rutile grains in the primary HT'S conductors fraction of Pond C.

with a mean of 0.390wt%. The $ZrO_2$ content in these rutile grains was much lower than the $SiO_2$ content, varying from 0.050wt% to 0.195wt% and having an average $ZrO_2$ content of 0.089wt%. $V_2O_3$ had five values below the lld (0.133wt%) with the other three having as much as 0.264wt%, with an average of 0.187wt%. One rutile grain contained $Nb_2O_5$ below the lld while the other seven varied up to 0.273wt%, with an average content of 0.213wt% $Nb_2O_5$. Four grains contained $Al_2O_3$ below the lld (<0.011wt%), the remaining four grains had $Al_2O_3$ confined to a narrow range of 0.015wt% to 0.047wt%, with a mean of 0.033wt%. Most of the grains (seven grains) contained FeO, ranging up to a maximum of only 0.156wt% and a mean of 0.077wt%. Only two grains contained detectable quantities of $Ta_2O_5$, at 0.068 and 0.168wt% respectively. Seven of the grains contained $Cr_2O_3$ (albeit at low concentrations) from the lld (0.021wt%) to 0.153wt% with the average $Cr_2O_3$ content at 0.077wt% (Table 5.6.3).

| Oxides | Minimum (wt%) | Maximum (wt%) | *Mean (wt%) |
|---|---|---|---|
| $TiO_2$ | 96.956 | 98.05 | 97.409 |
| $SiO_2$ | 0.299 | 0.589 | 0.390 |
| $ZrO_2$ | 0.050 | 0.195 | 0.089 |
| $V_2O_3$ | # | 0.264 | 0.187 |
| $Nb_2O_5$ | # | 0.273 | 0.213 |
| $Al_2O_3$ | # | 0.047 | 0.033 |
| FeO | # | 0.156 | 0.086 |
| $Cr_2O_3$ | # | 0.153 | 0.088 |

Table 5.6.3 A summary of electron microprobe results from 'primary HT'S conductors' fraction of Pond C.

*Mean:    Mean values exclude values that are below the detection limit and very high or low values (see details in text).

#    Lowest values are below the lld

The proportion of substituting elements into the rutile lattice of the 'primary HT'S conductors was restricted because of the high $TiO_2$ content. Other than $TiO_2$, $SiO_2$ formed the highest proportion in the rutile grains and $Al_2O_3$ had the lowest concentration in rutile grains.

## 5.7 HT'S Scavengers

The HT'S scavengers, non-conductors and mids fraction, was the fraction removed when the Primary HT'S non-conductors fraction was used as the feed for the roller magnets at the same settings as the feed to the Primary HT'S stage. This step ensured that grains caught by entrapment and accidentally reporting as non-conductors were removed and returned to the zircon circuit. Thus this fraction consisted almost exclusively of non-conducting zircon grains. Very few rutile grains were found in this fraction, as rutile is a conducting mineral. Rutile grains were only recovered from the HT'S Scavengers of Pond B, no rutile grains were encountered in this fraction from Ponds A and C.

The distribution of $TiO_2$, $SiO_2$, $ZrO_2$, $V_2O_3$, $Nb_2O_5$, $Al_2O_3$ and FeO from the 'HT'S scavengers non-conductors and mids' fraction of Pond B is presented in Fig. 5.7.1 and in Table 5.7.1 the analytical data The rutile grains had a relatively high $TiO_2$ content in the range of 97.389 to 98.488 wt%, and an average $TiO_2$ content of 97.830wt%. The $SiO_2$ content was restricted to a very narrow range between 0.210wt% to 0.344wt% with a mean of 0.271wt%. $ZrO_2$ varied from a minimum of 0.038wt% to a maximum of 0.343wt%, with a mean $ZrO_2$ content of 0.182wt%. $V_2O_3$ contents differed significantly, with two grains having values below the detection limit (0.133wt%) and the other seven ranging up to 0.946wt%, with an average $V_2O_3$ content of 0.628wt%. $Nb_2O_5$ was detectable in seven of the nine rutile grains with values ranging from below the lld (0.049wt%) to 0.249wt%. The mean $Nb_2O_5$ content was 0.174wt%. The $Al_2O_3$ content of all rutile grains from this fraction was very low, with two grains containing $Al_2O_3$ below the lld while the other seven ranged up to 0.033wt%.

114
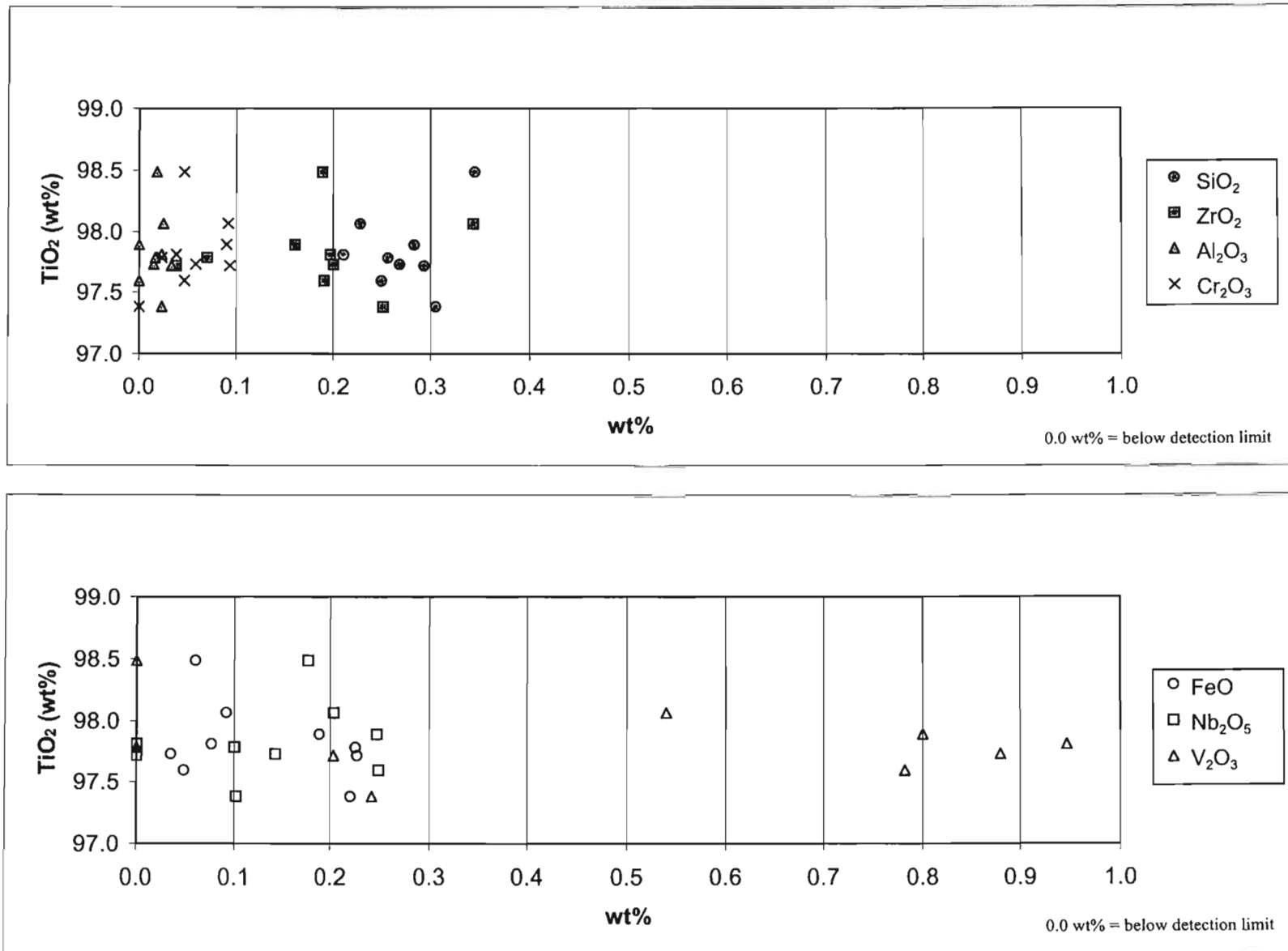
Fig. 5.7.1 Geochemistry of homogenous rutile grains in the HT'S scavengers fraction of Pond B.

The average $Al_2O_3$ content was 0.022wt%. Even though all grains had FeO values above the detection limit these were restricted to a very narrow range of 0.035wt% to 0.226wt%. The mean FeO content was 0.130wt% $Cr_2O_3$ was detected in most of the grains (eight grains) ranging from 0.024wt% to 0.094wt%, with an average of 0.061wt%. $Ta_2O_5$ content in rutile grains was below the lower limit of detection (0.036wt%) in seven of the nine grains, with only two grains having values of 0.067 and 0.065wt%(Table 5.7.1).

| Oxides | Minimum (wt%) | Maximum (wt%) | *Mean (wt%) |
|--------|---------------|---------------|-------------|
| $TiO_2$ | 97.389 | 98.488 | 97.830 |
| $SiO_2$ | 0.210 | 0.344 | 0.271 |
| $ZrO_2$ | 0.038 | 0.343 | 0.182 |
| $V_2O_3$ | # | 0.946 | 0.628 |
| $Nb_2O_5$ | # | 0.249 | 0.174 |
| $Al_2O_3$ | # | 0.033 | 0.022 |
| FeO | 0.035 | 0.226 | 0.130 |
| $Cr_2O_3$ | # | 0.094 | 0.061 |

Table 5.7.1 A summary of electron microprobe results from 'HT'S scavengers' fraction of Pond B.

*Mean:     Mean values exclude values that are below the detection limit and very high or low values (see details in text).

#          Lowest values are below the lld

All grains in the HT'S Scavengers fraction were composed almost entirely of $TiO_2$, with only $V_2O_3$ occurring at concentrations greater than 0.400wt%. However, every grain contained some $SiO_2$, $ZrO_2$ and FeO.


## 5.8 HT'S Cleaner Mids

## 5.8.1 Pond A

The distribution of $TiO_2$, $SiO_2$, $ZrO_2$, $V_2O_3$, $Nb_2O_5$, $Al_2O_3$ and FeO from the 'HT'S cleaner mids' fraction of Pond A is presented in Fig. 5.8.1 and in Table 5.8.1 the analytical data. All grains had relatively high $TiO_2$ contents, between 96.688 and 98.164wt%, with an average of 97.203wt% $TiO_2$. All thirteen grains contained $SiO_2$, ranging from 0.151wt% to 0.456wt%, with the average $SiO_2$ composition for all grains of 0.331wt%. $ZrO_2$ content occupied a range between 0.051 and 0.475wt%, with an overall average of 0.180wt%. $V_2O_3$ had a varied distribution in this fraction, one grain had a value below the lld (0.133wt%) but the other thirteen had up to a maximum of 0.797wt%. The mean $V_2O_3$ content for grains from this fraction was 0.446wt%. $Nb_2O_5$ constituted as much as 0.302wt%; however six grains contained $Nb_2O_5$ below the detection limit. The average $Nb_2O_5$ for grains from this fraction was 0.156wt%. The $Al_2O_3$ content of rutile grains did not display much variation, five grains had values below the lld (0.011wt%) and the other eight had values up to 0.045wt%. The average $Al_2O_3$ content was 0.025wt%. The FeO content varied from below the detection limit, (one grain) to a maximum of 0.272wt%. The average FeO content was 0.118wt%. Most grains (eleven grains) contained $Cr_2O_3$ at levels above the detection limit of 0.021wt% but values did not exceed a maximum of 0.218wt%, with a mean $Cr_2O_3$ content of 0.127wt%. Majority of the grains (eight grains) did not contain detectable quantities of $Ta_2O_5$. Of the five $Ta_2O_5$ bearing grains, one grain had a $Ta_2O_5$ content of 0.215wt% with the average for all grains being 0.098wt% $Ta_2O_5$ (Table 5.8.1).
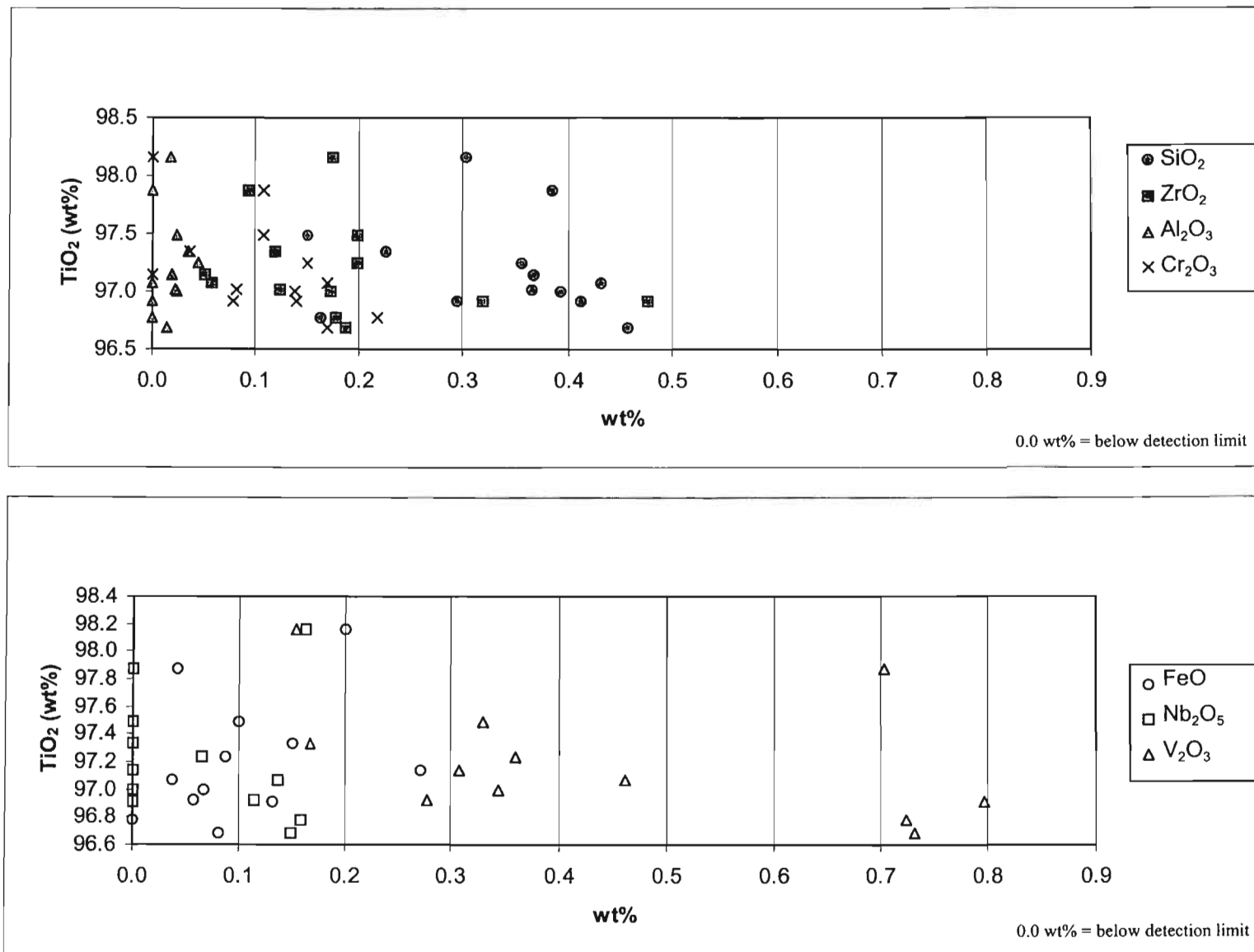
Fig. 5.8.1 Geochemistry of homogenous rutile grains in the HT'S cleaner mids fraction of Pond A.

| Oxides | Minimum (wt%) | Maximum (wt%) | *Mean (wt%) |
|--------|---------------|---------------|-------------|
| $TiO_2$ | 96.688 | 98.164 | 97.203 |
| $SiO_2$ | 0.151 | 0.456 | 0.331 |
| $ZrO_2$ | 0.051 | 0.475 | 0.180 |
| $V_2O_3$ | # | 0.797 | 0.446 |
| $Nb_2O_5$ | # | 0.302 | 0.156 |
| $Al_2O_3$ | # | 0.045 | 0.025 |
| FeO | # | 0.272 | 0.118 |
| $Cr_2O_3$ | # | 0.218 | 0.127 |

Table 5.8.1 A summary of electron microprobe results from 'HT'S cleaner mids' fraction of Pond A.

*Mean:     Mean values exclude values that are below the detection limit and very high or low values (see details in text).

\#          Lowest values are below the lld

Rutile grains from the 'HT'S cleaner mids' fraction of Pond A contained a significant proportion of $SiO_2$ and $ZrO_2$. Although the mean $V_2O_3$ content was higher than either $SiO_2$ or $ZrO_2$, not all the grains contained a higher portion of $V_2O_3$.


## 5.8.2 Pond B

The distribution of $TiO_2$, $SiO_2$, $ZrO_2$, $V_2O_3$, $Nb_2O_5$, $Al_2O_3$ and FeO from the 'HT'S cleaner mids' fraction of Pond B is presented in Fig. 5.8.2 and in Table 5.8.2 the analytical data. $TiO_2$ content of the grains from this fraction varied from 96.758wt% to 98.794wt%, with the average being 97.731wt%. All twenty grains from this fraction contained significant amounts of $SiO_2$ and $ZrO_2$. Rutile grains from this fraction contained $SiO_2$ at
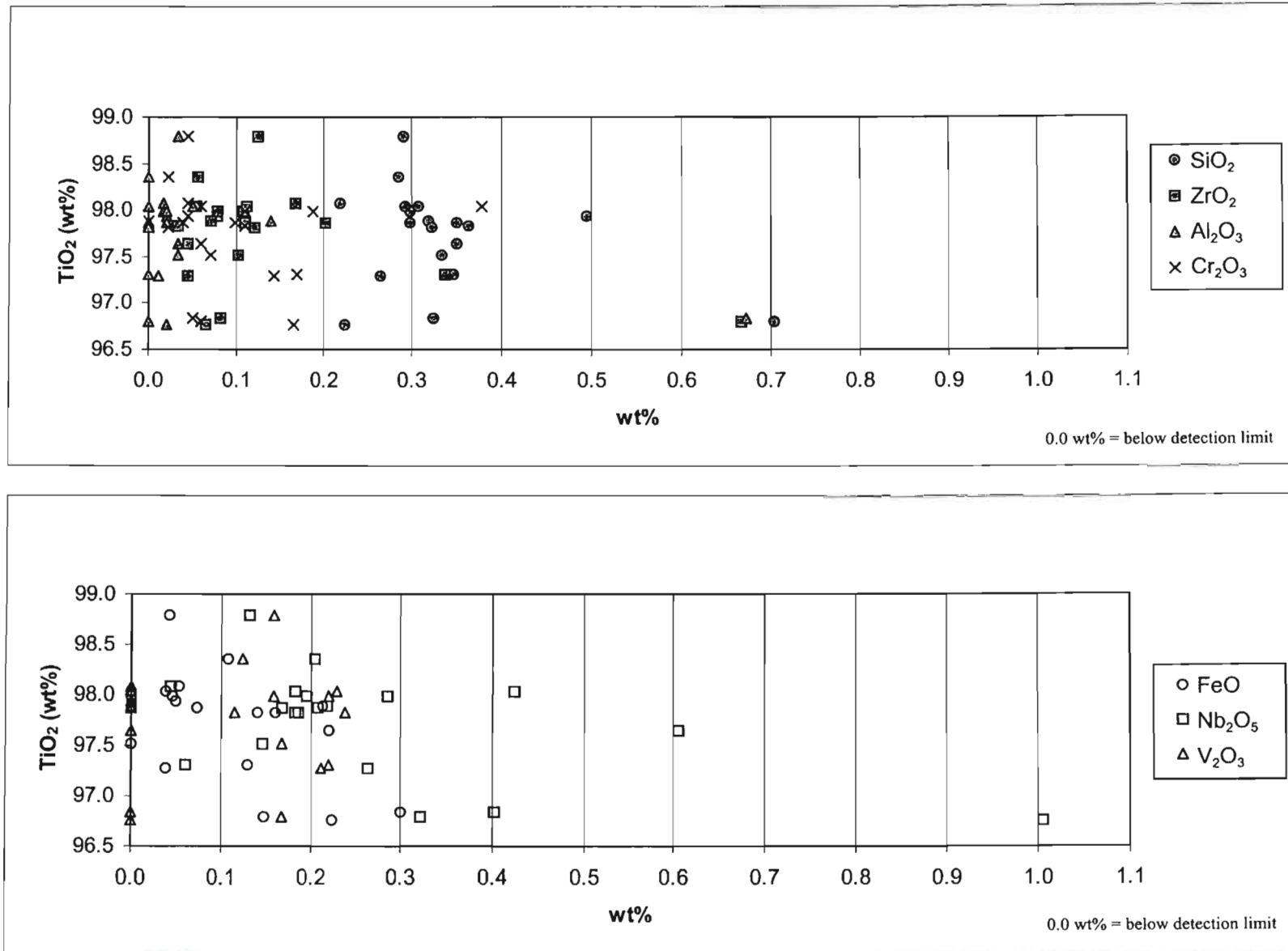
Fig. 5.8.2 Geochemistry of homogenous rutile grains in the HT'S cleaner mids fraction of Pond B.

concentrations from 0.219wt% to 0.704wt%, though only two grains contained higher $SiO_2$ than the other grains, (0.493 and 0.704wt%). The average $SiO_2$ for the other grains (i.e. excluding high $SiO_2$ grains) was 0.304wt%. Two grains had relatively higher $ZrO_2$ concentrations of 0.336 and 0.668wt%. The other grains had an average of 0.091wt% confined to a range of 0.034wt% to 0.202wt%. The $V_2O_3$ content was below the detection limit for nine of the twenty grains analysed and was restricted to a range from below the lld (0.133wt%) to 0.238wt%. The average $V_2O_3$ content for grains from this fraction was 0.183wt%. $Nb_2O_5$ had a larger spread of values, with one grain below the detection limit of 0.049wt% and the other nineteen grains varying up to 1.005wt%. The average $Nb_2O_5$ content was 0.275wt%. Most of the grains contained little or no $Al_2O_3$; however one contained 0.673wt% $Al_2O_3$. Apart from the single grain that had over 1.00wt% $Al_2O_3$, all the other grains (nineteen) had an average of 0.035wt%. FeO content of rutile grains from this fraction fluctuated in a narrow range from below the detection limit of 0.027wt% (four grains) to 0.301wt%, with a mean FeO content of 0.124wt%. Though $Ta_2O_5$ was below the detection limit for most grains, there were eight grains that contained significant $Ta_2O_5$ concentrations (up to 0.260wt%), with the average $Ta_2O_5$ content of 0.127wt%. $Cr_2O_3$ was also present at low concentrations in most grains ranging from a minimum of 0.022wt% to 0.377wt%. The average $Cr_2O_3$ content for the analysed grains from this fraction was 0.098wt% (Table 5.8.2).

In the 'HT'S cleaner mids' fraction of Pond B, $SiO_2$ and $ZrO_2$ were found at levels significantly above the detection limit in all of the analysed rutile grains. Although the $Nb_2O_5$ content sometimes far exceed that of $SiO_2$ not all grains contained $Nb_2O_5$, and only one grain had a high $Al_2O_3$ content.

| Oxides | Minimum (wt%) | Maximum (wt%) | *Mean (wt%) |
|---|---|---|---|
| $TiO_2$ | 96.758 | 98.794 | 97.731 |
| $SiO_2$ | 0.219 | 0.362 | 0.304 |
| $ZrO_2$ | 0.034 | 0.202 | 0.091 |
| $V_2O_3$ | # | 0.238 | 0.183 |
| $Nb_2O_5$ | # | 1.005 | 0.275 |
| $Al_2O_3$ | # | 0.139 | 0.035 |
| FeO | # | 0.301 | 0.124 |
| $Cr_2O_3$ | # | 0.377 | 0.098 |

Table 5.8.2 A summary of electron microprobe results from 'HT'S cleaner mids' fraction of Pond B.

*Mean:     Mean values exclude values that are below the detection limit and very high or low values (see details in text).

\#     Lowest values are below the lld

## 5.8.3 Pond C

The distribution of $TiO_2$, $SiO_2$, $ZrO_2$, $V_2O_3$, $Nb_2O_5$, $Al_2O_3$ and FeO from the 'HT'S cleaner mids' fraction of Pond C is presented in Fig. 5.8.3 and the analytical data in Table 5.8.1. As expected, the rutile grains from this fraction had a very high $TiO_2$ content, as most of these grains were virtually pure with the $TiO_2$ content varying from 97.739wt% to 99.633wt%, with an average $TiO_2$ content of 98.438wt%. All nine analysed rutile grains contained a little $SiO_2$, ranging from 0.034wt% to 0.202wt%, with an average $SiO_2$ content for all the grains is 0.110wt%. The distribution of $ZrO_2$ varied significantly, with only one grain reporting a value below the detection limit (0.017wt%), the other eight containing up to 0.433wt%, with a mean $ZrO_2$ content of 0.261wt%.
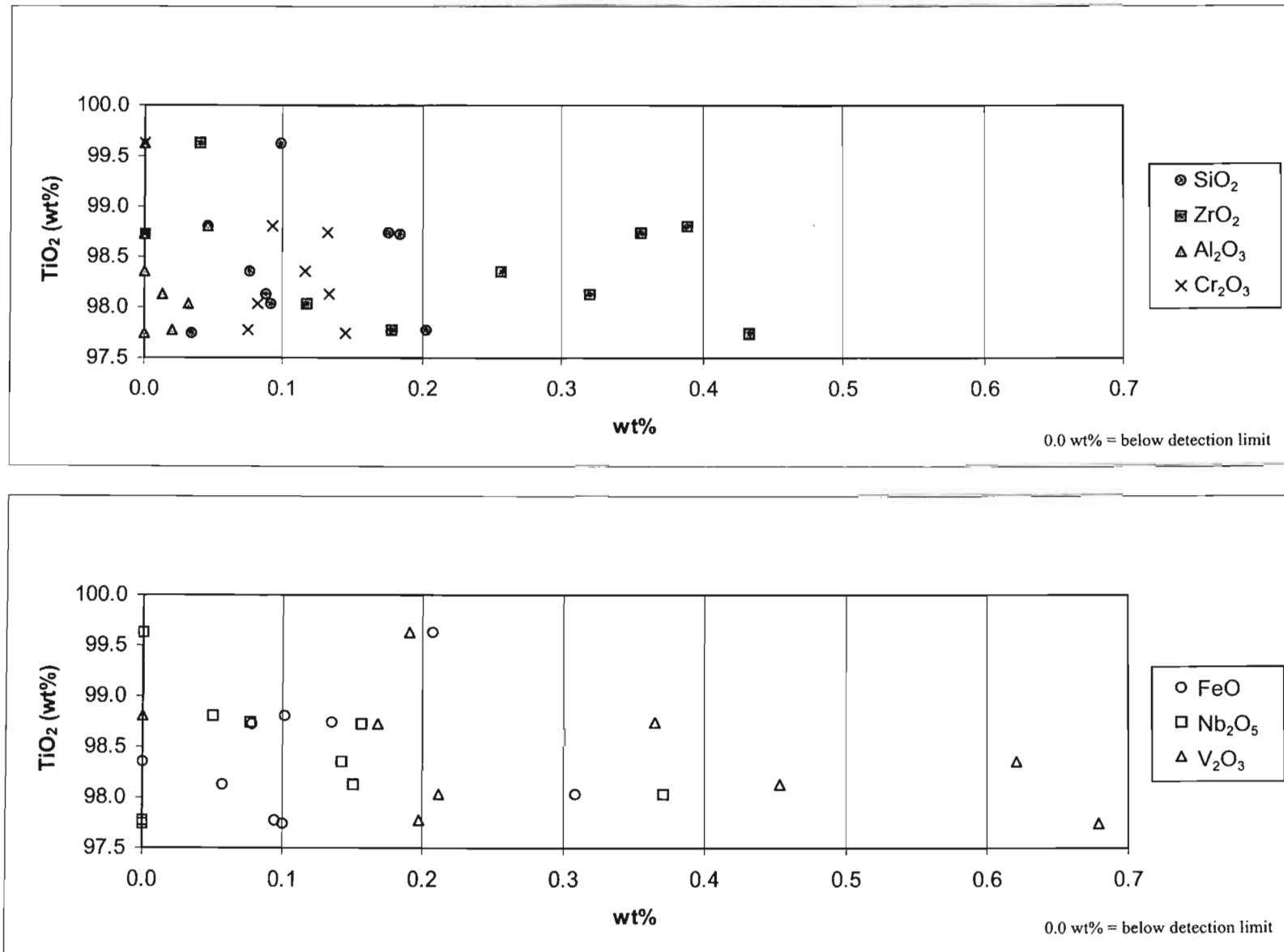
Fig. 5.8.3 Geochemistry of homogenous rutile grains in the HT'S cleaner mids fraction of Pond C.

Rutile grains also contained varying concentrations of $V_2O_3$, from below the detection limit in one grain (0.133wt%) to 0.679wt%, with an average of 0.361wt%. $Nb_2O_5$ content of the six grains that contained $Nb_2O_5$ above the lld averaged 0.116wt% with one grain that contained 0.370wt% $Nb_2O_5$. However, three grains contained $Nb_2O_5$ below the lld of 0.133wt%. Only four of the nine rutile grains contained $Al_2O_3$ at concentration above the detection limit. Values ranged up to a maximum of 0.046wt% with the four grains having a mean of 0.028wt%. Only one grain had FeO below the lld. The other eight grains contained FeO compositions that ranged up to 0.308wt%. The overall average FeO content was 0.135wt%. Only two grains had a significant $Ta_2O_5$ content, (0.219wt% and 0.142wt% respectively), all the other grains had $Ta_2O_5$ below the detection limit (0.036wt%). $Cr_2O_3$ content in rutiles varied from below the detection limit in two grains to 0.145wt%. The average $Cr_2O_3$ content was 0.111wt% (Table 5.8.3).

| Oxides | Minimum (wt%) | Maximum (wt%) | *Mean (wt%) |
|---|---|---|---|
| $TiO_2$ | 97.739 | 99.633 | 98.438 |
| $SiO_2$ | 0.034 | 0.202 | 0.110 |
| $ZrO_2$ | 0.017 | 0.433 | 0.261 |
| $V_2O_3$ | 0.133 | 0.679 | 0.361 |
| $Nb_2O_5$ | 0.049 | 0.157 | 0.116 |
| $Al_2O_3$ | 0.011 | 0.046 | 0.028 |
| FeO | 0.027 | 0.308 | 0.135 |
| $Cr_2O_3$ | 0.021 | 0.145 | 0.111 |

Table 5.8.3 A summary of electron microprobe results from 'HT'S cleaner mids' fraction of Pond C.

*Mean:     Mean values exclude values that are below the detection limit and very high or low values (see details in text).

\#          Lowest values are below the lld

The grains from the 'HT'S cleaner mids' fraction of Pond C are composed almost entirely of $TiO_2$, with the other elements making up only a very small percentage of the rutile grains. Some grains from this fraction contained a high percentage of $V_2O_3$ and $ZrO_2$. Grains contain almost no $Al_2O_3$.

## 5.9 HT'S Cleaner Non-Conductors

## 5.9.1 Pond A

The distribution of $TiO_2$, $SiO_2$, $ZrO_2$, $V_2O_3$, $Nb_2O_5$, $Al_2O_3$ and FeO from the 'HT'S cleaner non-conductors' fraction of Pond A is presented in Fig. 5.9.1 and in Table 5.9.1 the analytical data. The rutile grains from this fraction had a fairly high $TiO_2$ content, which was confined to a narrow range from 97.172 to 98.41wt%, with a mean $TiO_2$ content of 97.823wt%. All thirteen grains from this fraction contained $SiO_2$, in the range from 0.138 to 0.429wt%, with an average $SiO_2$ content for all grains of 0.243wt%. Most of the grains contained measurable amounts of $ZrO_2$; only two grains had $ZrO_2$ below the detection limit of 0.017wt%, the values of the other grains ranged up to 0.263wt%, with a mean $ZrO_2$ content of 0.133wt%. The $V_2O_3$ content of rutile grains varied from eight grains containing $V_2O_3$ below the detection limit (0.133wt%) to as much as 0.414wt%, with an average $V_2O_3$ content of 0.296wt%. $Nb_2O_5$ had the largest range within these rutile grains, three values were below the detection limit (0.049wt%) while another grain contained up to 0.629wt%. Discounting this grain with the exceptionally higher $Nb_2O_5$ content, the remaining grains had a mean of 0.160wt%. $Al_2O_3$ in the rutile grains occurred at very low concentrations, and was found above the detection limit in nine grains, and ranged up to 0.120wt%. The average $Al_2O_3$ content was 0.044wt%. Only one of the thirteen grains contained less than the detection limit of (0.027wt%) FeO. The maximum FeO hosted within a rutile grain in this fraction was 0.407wt%, with a mean FeO content of 0.168wt%. Only two of the thirteen grains contained $Ta_2O_5$ at levels above the detection limit, giving values of 0.203 and 0.125wt% respectively. $Cr_2O_3$ was present in all the grains, at concentrations of 0.027 to 0.147wt%. The mean $Cr_2O_3$ content for all grains was 0.077wt% (Table 5.9.1).
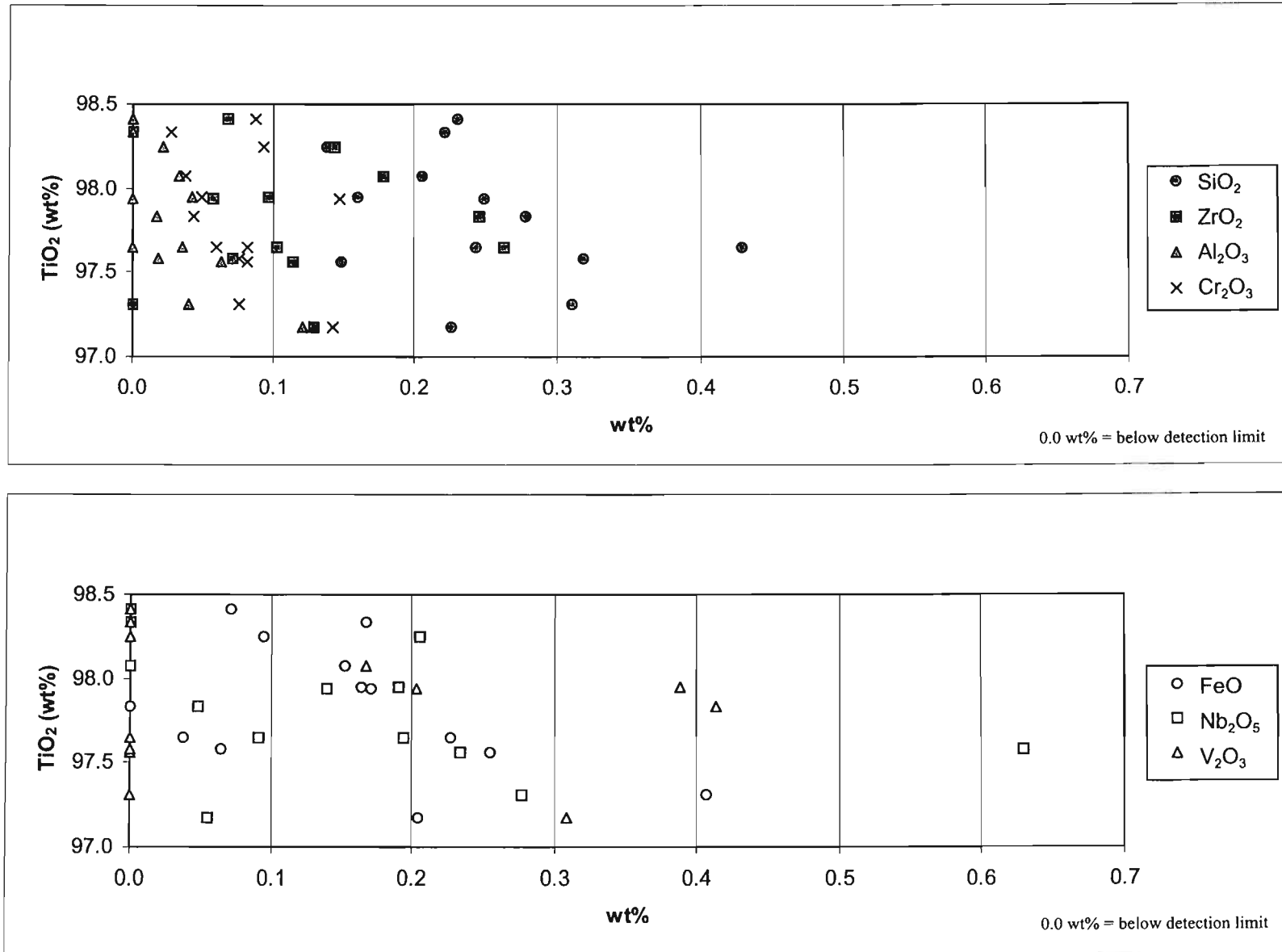
Fig. 5.9.1 Geochemistry of homogenous rutile grains in the HT'S cleaner non-conductors fraction of Pond A.

| Oxides | Minimum (wt%) | Maximum (wt%) | *Mean (wt%) |
|---|---|---|---|
| $TiO_2$ | 97.172 | 98.41 | 97.823 |
| $SiO_2$ | 0.138 | 0.429 | 0.243 |
| $ZrO_2$ | 0.057 | 0.263 | 0.133 |
| $V_2O_3$ | # | 0.414 | 0.296 |
| $Nb_2O_5$ | # | 0.629 | 0.160 |
| $Al_2O_3$ | # | 0.120 | 0.044 |
| FeO | 0.038 | 0.407 | 0.168 |
| $Cr_2O_3$ | 0.027 | 0.147 | 0.077 |

Table 5.9.1 A summary of electron microprobe results from 'HT'S cleaner non-conductors' fraction of Pond A.

*Mean:     Mean values exclude values that are below the detection limit and very high or low values (see details in text).

#          Lowest values are below the lld

Significant amounts of $SiO_2$, $ZrO_2$ and $Cr_2O_3$, were found in all the analysed grains from the 'HT'S cleaner non-conductors' fraction of Pond A. Most grains had low concentrations of substituting ions; however, one grain contained 0.629wt% $Nb_2O_5$. $Al_2O_3$ and $Cr_2O_3$ occurred at concentrations that did not exceed 0.200wt%. However, $SiO_2$, $V_2O_3$, $Nb_2O_5$ and FeO concentrations in some grains exceeded 0.400wt%.

## 5.9.2 Pond B

The distribution of $TiO_2$, $SiO_2$, $ZrO_2$, $V_2O_3$, $Nb_2O_5$, $Al_2O_3$ and FeO from the 'HT'S cleaner non-conductors' fraction of Pond B is presented in Fig. 5.9.2 and in Table 5.9.2 the

Fig. 5.9.2 Geochemistry of homogenous rutile grains in the HT'S cleaner non-conductors fraction of Pond B.
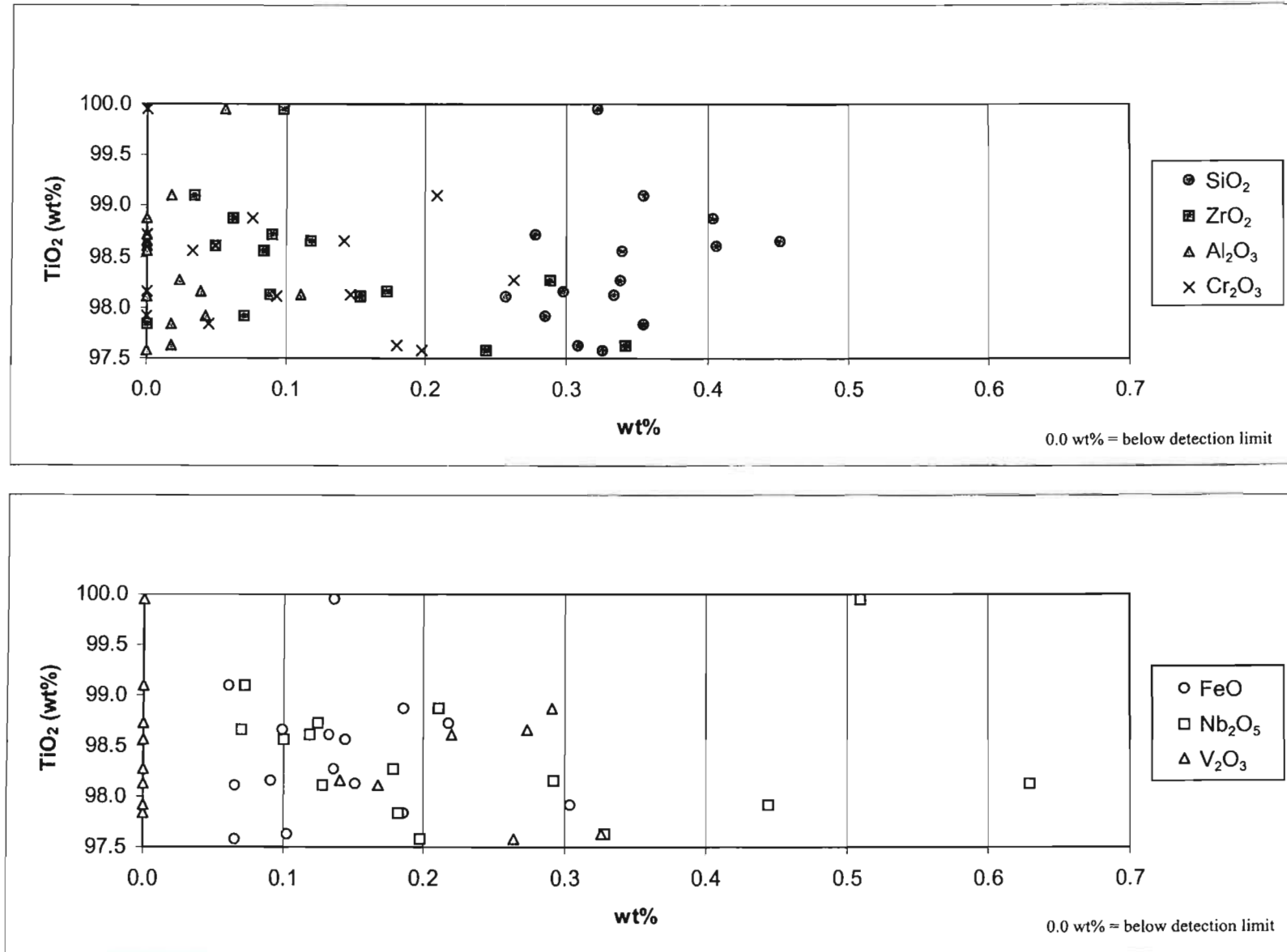
analytical data. All fifteen grains had a high concentration of $TiO_2$ ranging from 97.585wt% to 99.946wt%. The mean $TIO_2$ content was 98.407wt%. Although $SiO_2$ was present at levels above the detection limit in all the grains, it had a limited range of 0.257wt% to 0.451wt%, with an average of 0.337wt%. Only one of the analysed grains reported $ZrO_2$ below the detection limit, whereas most of the other fourteen grains contained substantial $ZrO_2$, one grain containing as much as 0.342wt%. The mean $ZrO_2$ content for grains was 0.135wt%. Most of the grains (eight grains) contained $V_2O_3$ below the lld, and the remaining seven grains had an average of 0.240wt%. $Nb_2O_5$ was present in all grains above the lld, the distribution varied from a minimum of 0.070wt% to a maximum of 0.629wt% with an average of 0.239wt%. Most of the rutile grains had $Al_2O_3$ contents that were below the detection limit (0.011wt%), but seven grains contained low levels of $Al_2O_3$ (from just above the lld to 0.111wt%) with a mean of 0.023wt%. FeO was also present in all the grains, at concentrations above the detection levels with values that differ from 0.061 to 0.304wt%, with an average FeO content of 0.139wt%. From all the grains analysed only two grains contained $Ta_2O_5$ above the lld (0.139 and 0.078wt%). $Cr_2O_3$ ranged from below the detection limit (0.021wt%) in four grains to 0.262wt%, for the other eleven grains, which had a mean $Cr_2O_3$ content of 0.130wt% (Table 5.9.2).


All grains from the 'HT'S cleaner non-conductors' fraction of Pond B contained $SiO_2$, $Nb_2O_5$ and FeO, but $Nb_2O_5$ had the largest range of values within rutile grains.

| Oxides | Minimum (wt%) | Maximum (wt%) | *Mean (wt%) |
|---|---|---|---|
| $TiO_2$ | 97.585 | 99.946 | 98.407 |
| $SiO_2$ | 0.257 | 0.451 | 0.337 |
| $ZrO_2$ | # | 0.342 | 0.135 |
| $V_2O_3$ | # | 0.326 | 0.240 |
| $Nb_2O_5$ | 0.070 | 0.629 | 0.239 |
| $Al_2O_3$ | # | 0.111 | 0.023 |
| FeO | 0.061 | 0.304 | 0.139 |
| $Cr_2O_3$ | # | 0.262 | 0.130 |

Table 5.9.2 A summary of electron microprobe results from 'HT'S cleaner non-conductors' fraction of Pond B.

*Mean:      Mean values exclude values that are below the detection limit and very high or low values (see details in text).

\#      Lowest values are below the lld

## 5.9.3 Pond C

The distribution of $TiO_2$, $SiO_2$, $ZrO_2$, $V_2O_3$, $Nb_2O_5$, $Al_2O_3$ and FeO from the 'HT'S cleaner non-conductors' fraction of Pond C is presented in Fig. 5.9.3 and Table 5.9.3 contains the analytical data. The rutile grains from this fraction had high $TiO_2$ contents, with value's ranging from 97.772wt% to 99.016wt%, and an average of 98.469wt%. $SiO_2$ was present in all the grains and ranged from 0.202wt% to 0.598wt%, with a mean $SiO_2$ content of 0.317wt%. $ZrO_2$ was present in eight of the nine grains, at concentrations above the detection limit of 0.017wt%, ranging up to 0.298wt% with an average $ZrO_2$ content of 0.173wt%. Although five of the analysed rutile grains had $V_2O_3$ contents that were below the detection limit, four grains had $V_2O_3$ contents above the detection limits,

TiO$_2$ (wt%)

99.5
99.0
98.5
98.0
97.5

0.0  0.1  0.2  0.3  0.4  0.5  0.6  0.7  0.8  0.9  1.0

wt%

- • SiO$_2$
- ▣ ZrO$_2$
- △ Al$_2$O$_3$
- × Cr$_2$O$_3$

0.0 wt% = below detection limit

TiO$_2$ (wt%)

99.5
99.0
98.5
98.0
97.5

0.0  0.1  0.2  0.3  0.4  0.5  0.6  0.7  0.8  0.9  1.0

wt%

- ○ FeO
- ▢ Nb$_2$O$_5$
- △ V$_2$O$_3$

0.0 wt% = below detection limit
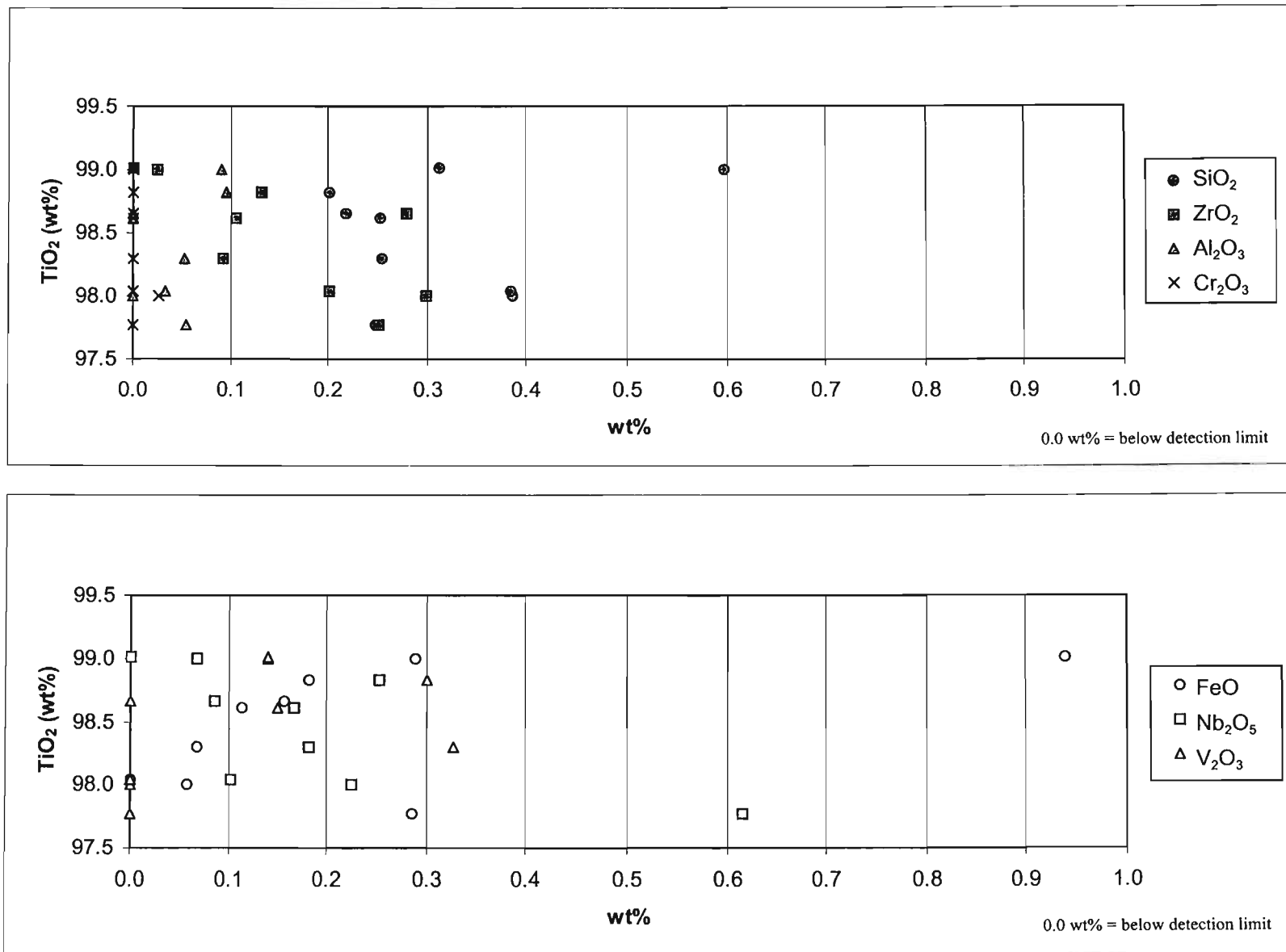
Fig. 5.9.3 Geochemistry of homogenous rutile grains in the HT'S cleaner non-conductors fraction of Pond C.

with values extending from 0.141wt% to 0.326wt%. The average $V_2O_3$ content for these four grains was 0.212wt%. $Nb_2O_5$ was present in seven of the nine grains, and ranged from a minimum of 0.067wt% to a maximum of 0.616wt%. With the exception of a single grain that had a much higher $Nb_2O_5$ (four times the mean) the remaining grains had an average of 0.154wt% $Nb_2O_5$. Four grains had $Al_2O_3$, content below the detection limit of 0.011wt%; the remaining five grains with significant $Al_2O_3$ content had values restricted to a narrow range of 0.033wt% to 0.095wt%, with an average of 0.065wt%. FeO was present in eight of the grains, varying from 0.057wt% to 0.939wt%. The average FeO content, with the exception of the grain with the high FeO content (0.939wt%), was 0.164wt%. Four grains contained $Ta_2O_5$ with values from 0.039wt% to 0.185wt%, with an average of 0.099wt%. Only one grain contained $Cr_2O_3$ above the detection limit (0.021wt%) of 0.027wt% (Table 5.9.3).

| Oxides | Minimum (wt%) | Maximum (wt%) | *Mean (wt%) |
|--------|---------------|---------------|-------------|
| $TiO_2$ | 97.772 | 99.016 | 98.469 |
| $SiO_2$ | 0.202 | 0.598 | 0.317 |
| $ZrO_2$ | # | 0.298 | 0.173 |
| $V_2O_3$ | # | 0.326 | 0.212 |
| $Nb_2O_5$ | # | 0.252 | 0.154 |
| $Al_2O_3$ | # | 0.095 | 0.065 |
| FeO | # | 0.939 | 0.164 |
| $Cr_2O_3$ | # | 0.027 | 0.027 |

Table 5.9.3 A summary of electron microprobe results from 'HT'S cleaner non-conductors' fraction of Pond C.

*Mean:     Mean values exclude values that are below the detection limit and very high or low values (see details in text).

#          Lowest values are below the lld

Notably $SiO_2$ was present in all of the analysed grains in this fraction. The highest proportion of a substituting element in this fraction was FeO with an individual grain containing 0.939 wt%; FeO also had the largest range of values.

## 5.10 HT'S Cleaner Conductors

### 5.10.1 Pond A

The distribution of $TiO_2$, $SiO_2$, $ZrO_2$, $V_2O_3$, $Nb_2O_5$, $Al_2O_3$ and FeO from the 'HT'S cleaner conductors' fraction of Pond A is presented in Fig. 5.10.1 and in Table 5.10.1 the analytical data. Fourteen rutile grains from this fraction were analysed, of which thirteen grains contained a high $TiO_2$ content (96.48 to 97.938wt%); however, one grain had a lower than expected $TiO_2$ content (94.711wt%). The average $TiO_2$ content, with the exception of the low $TiO_2$ grain, was 97.192wt%. $SiO_2$ was found in all of the grains within a narrow range, at concentrations from 0.128wt% to 0.377wt%, with an average of 0.290wt% $SiO_2$. The $ZrO_2$ content in grains was above the lld and ranged from 0.057wt% to 0.464wt%, with a mean $ZrO_2$ content of 0.205wt%. $V_2O_3$ had a large array in concentrations, varying from 0.146wt% to 0.651wt%, with an average of 0.430wt%. Five grains had $Nb_2O_5$ below the detection limit; the balance (nine grains) had a distribution that ranged from 0.052wt% to 0.564wt%, with a mean of 0.200wt%. The $Al_2O_3$ content in rutile grains had a limited range of 0.012wt% to 0.056wt% (mean of 0.026wt%), with the exception of one grain that had an $Al_2O_3$ content 0.213wt%. FeO ranged from a minimum of 0.027wt% to a maximum of 1.167wt% with one grain having a FeO content that was far higher (1.167wt%) than the other grains. The rest of the grains had a mean FeO content of 0.149wt%. Seven grains had $Ta_2O_5$ contents below the detection limit, the remaining seven grains contained $Ta_2O_5$ with a distribution of 0.053wt% to 0.272wt% and a mean of 0.168wt%. All the grains contained $Cr_2O_3$, varying from 0.055wt% to a single enriched grain with 0.569wt%. The average $Cr_2O_3$ content was 0.131wt% (excluding the enriched grain) (Table 5.10.1).

133
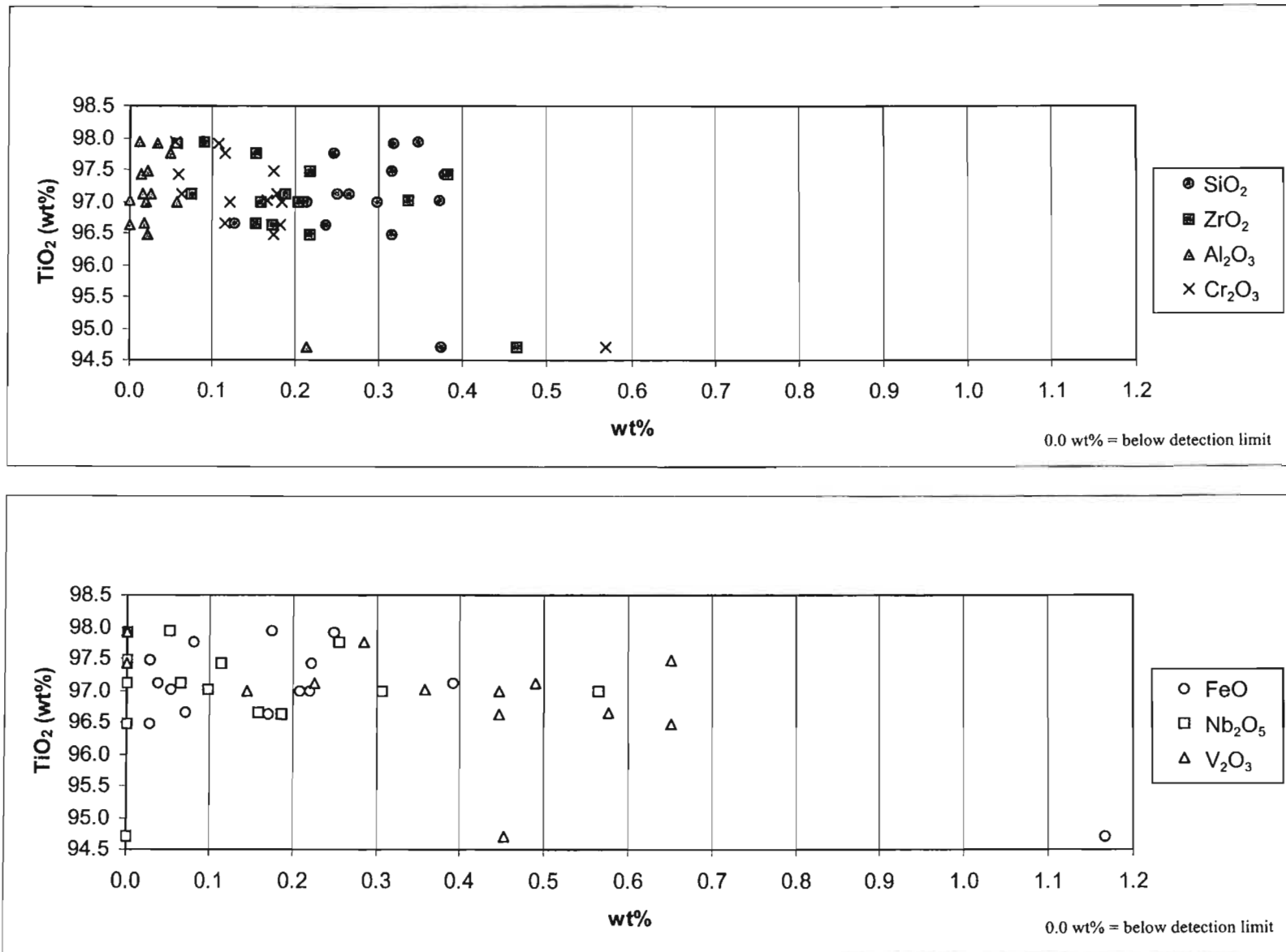
Fig. 5.10.1 Geochemistry of homogenous rutile grains in the HT'S cleaner conductors fraction of Pond A.

| Oxides | Minimum (wt%) | Maximum (wt%) | *Mean (wt%) |
|---|---|---|---|
| $TiO_2$ | 96.480 | 97.938 | 97.192 |
| $SiO_2$ | 0.128 | 0.377 | 0.290 |
| $ZrO_2$ | 0.057 | 0.464 | 0.205 |
| $V_2O_3$ | # | 0.651 | 0.430 |
| $Nb_2O_5$ | # | 0.564 | 0.200 |
| $Al_2O_3$ | # | 0.056 | 0.026 |
| $FeO$ | # | 1.167 | 0.222 |
| $Cr_2O_3$ | 0.055 | 0.184 | 0.131 |

Table 5.10.1 A summary of electron microprobe results from 'HT'S cleaner conductors' fraction of Pond A.

*Mean:   Mean values exclude values that are below the detection limit and very high or low values (see details in text).

\#   Lowest values are below the lld

All the grains analysed contained $SiO_2$, $ZrO_2$ and FeO, and very little $Al_2O_3$. FeO had the largest range in values, with one grain containing 1.167wt%.

## 5.10.2 Pond B

The distribution of $TiO_2$, $SiO_2$, $ZrO_2$, $V_2O_3$, $Nb_2O_5$, $Al_2O_3$ and FeO from the 'HT'S cleaner conductors' fraction of Pond B is presented in Fig. 5.10.2 and in Table 5.10.2 the analytical data. $TiO_2$ had a range of 95.84 to 98.847wt%, however one grain had a significantly lower $TiO_2$ content of 95.84wt%. With the exception of the single low $TiO_2$ grain the others had a mean $TiO_2$ content of 97.973wt%. $SiO_2$ was detectable in all
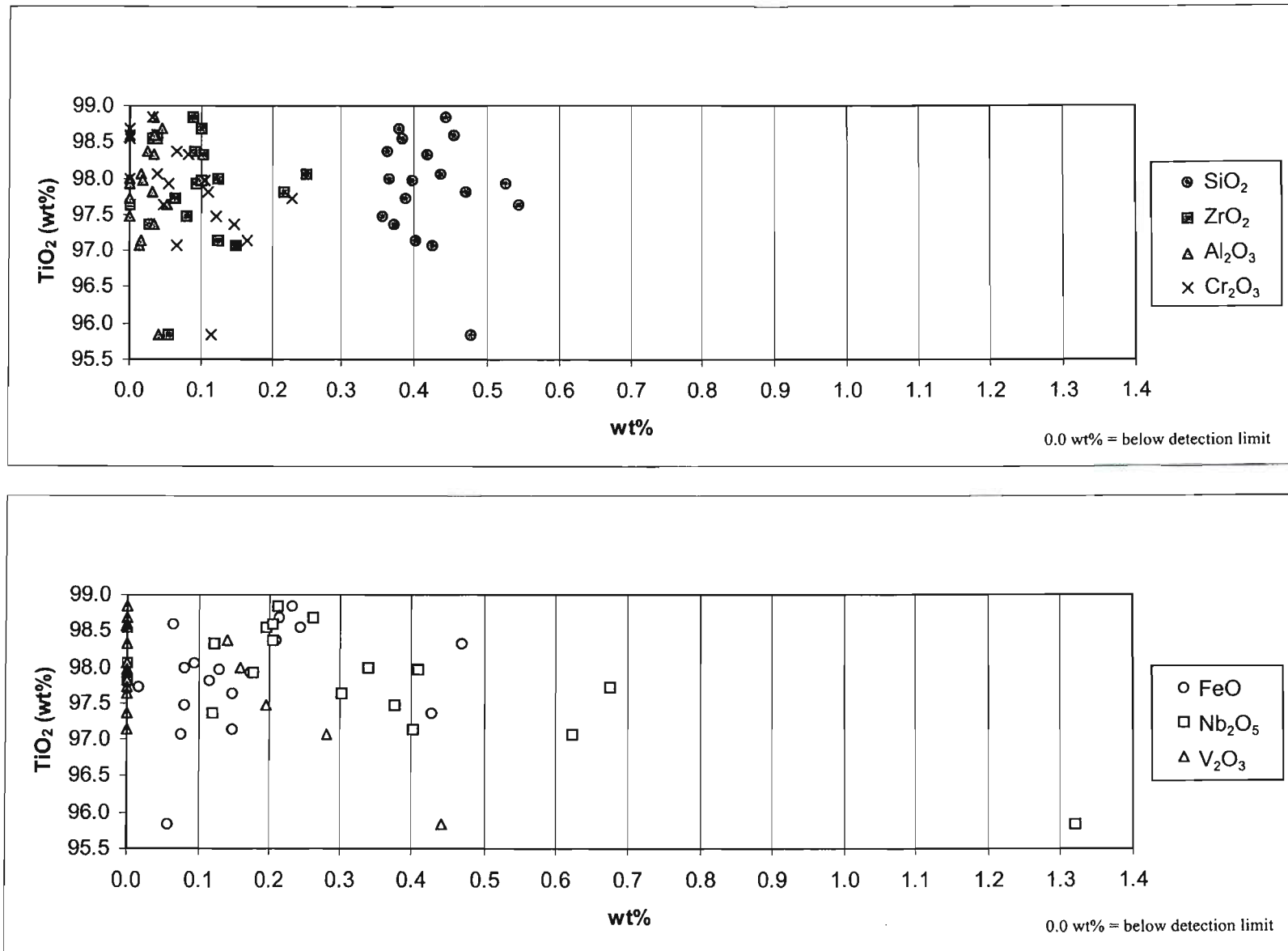
Fig. 5.10.2 Geochemistry of homogenous rutile grains in the HT'S cleaner conductors fraction of Pond B.

eighteen rutile grains, at concentrations ranging from 0.357wt% to 0.544wt%, with an average of 0.422wt% $SiO_2$. $ZrO_2$ was below the lld in only one grain, the other seventeen grains contained from 0.057wt% to 0.250wt% $ZrO_2$ with a mean of 0.102wt%. All but five grains had $V_2O_3$ at levels below the detection limit (0.133wt%). These five significant values were spread between 0.141wt% and 0.44wt%, with the mean at 0.243wt%. Three grains had very high $Nb_2O_5$ contents of 1.319wt%, 0.623wt% and 0.675wt%, of the other fifteen grains only two grains reported $Nb_2O_5$ contents below the detection limit (0.049wt%) with the others had up to 0.408wt% and a mean of 0.255wt%. $Al_2O_3$ contents were confined to a narrow range; four grains were below the lld, the other fourteen grains ranged from 0.013wt% to 0.052wt%, with a mean of 0.031wt%. Only one grain reported a FeO content below the detection limit, the other seventeen grains had a distribution varying from 0.057wt% to 0.468wt%, with an average FeO content for seventeen grains of 0.174wt%. $Ta_2O_5$ was below the lld in all but four grains, and the highest concentrations did not exceed 0.217wt%. Four grains contained $Cr_2O_3$ levels that were below detection limit of 0.027wt%, but the other fourteen varied between 0.033wt% and 0.229wt% of $Cr_2O_3$ with an average of 0.098wt% (Table 5.10.2).

All the rutile grains from 'HT'S cleaner conductors' fraction of Pond B had a high proportion of $SiO_2$. Most of the grains contained a significant proportion $ZrO_2$, $Nb_2O_5$ and FeO.

| Oxides | Minimum (wt%) | Maximum (wt%) | *Mean (wt%) |
|---|---|---|---|
| $TiO_2$ | 97.073 | 98.847 | 97.973 |
| $SiO_2$ | 0.357 | 0.544 | 0.422 |
| $ZrO_2$ | # | 0.250 | 0.102 |
| $V_2O_3$ | # | 0.440 | 0.243 |
| $Nb_2O_5$ | # | 0.408 | 0.255 |
| $Al_2O_3$ | # | 0.052 | 0.031 |
| FeO | 0.057 | 0.468 | 0.174 |
| $Cr_2O_3$ | # | 0.229 | 0.098 |

Table 5.10.2 A summary of electron microprobe results from 'HT'S cleaner conductors' fraction of Pond B.

*Mean:      Mean values exclude values that are below the detection limit and very high or low values (see details in text).

\#          Lowest values are below the lld

## 5.10.3 Pond C

The distribution of $TiO_2$, $SiO_2$, $ZrO_2$, $V_2O_3$, $Nb_2O_5$, $Al_2O_3$ and FeO from the 'HT'S cleaner conductors' fraction of Pond C is presented in Fig. 5.10.3 and in Table 5.10.3 the analytical data. The $TiO_2$ content of the analysed grains from this fraction varied from 96.677wt% to 99.802wt%, with an average of 98.641wt% $TiO_2$. All twenty grains contained $SiO_2$ that was well above the detection limit of 0.018wt%. There appeared to be significant variation in the $SiO_2$ content with values ranging from 0.058wt% to 0.535wt%; however, the mean $SiO_2$ content was 0.196wt%. Nineteen grains contain significant amounts of $ZrO_2$, at concentrations from 0.019wt% to 0.458wt%, with the average $ZrO_2$ content of 0.144wt%. Most of the grains (sixteen grains) contained
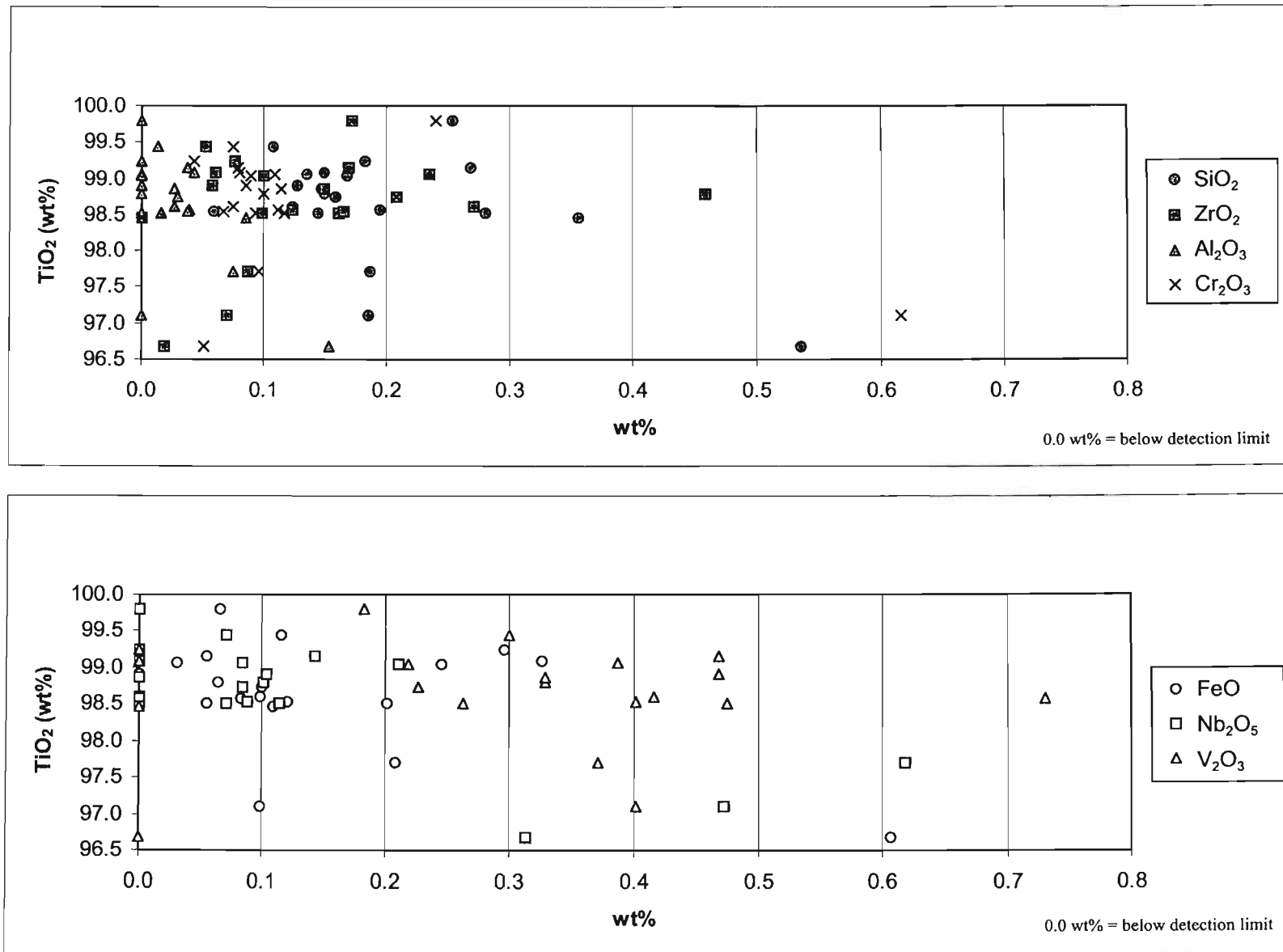
Fig. 5.10.3 Geochemistry of homogenous rutile grains in the HT'S cleaner conductors fraction of Pond C.

detectable $V_2O_3$ at levels of 0.183wt% to 0.731wt%. The average $V_2O_3$ content was 0.373wt%. Only thirteen grains contained Nb2O5, above the lld in the range of 0.070wt% to 0.618wt% with a mean $Nb_2O_5$ content of 0.190wt%. $Al_2O_3$ occurred at relatively low levels; with only twelve grains containing $Al_2O_3$ above the detection limit, (ranged from 0.013wt% to 0,154wt%), with an average of 0.048wt%. Almost all the grains (eighteen grains) contained FeO. The distribution of FeO varied from 0.030wt% to 0.606wt%. However, with the exception of the single grain that had a high FeO content (0.606wt%), the other grains had an average FeO content of 0.134wt%. $Ta_2O_5$ was only present in nine grains, varying from 0.044wt% to 0.323wt%. The average $Ta_2O_5$ content was 0.169wt%. $Cr_2O_3$ occurred in almost all grains (nineteen grains) at concentrations of 0.042wt% to 0.617wt%; however, only one grain had a high $Cr_2O_3$ (0.617wt%), the other grains had an average of 0.102wt% (Table 5.10.3).

| Oxides | Minimum (wt%) | Maximum (wt%) | *Mean (wt%) |
|---|---|---|---|
| $TiO_2$ | 96.677 | 99.802 | 98.641 |
| $SiO_2$ | 0.058 | 0.535 | 0.196 |
| $ZrO_2$ | # | 0.458 | 0.144 |
| $V_2O_3$ | # | 0.731 | 0.373 |
| $Nb_2O_5$ | # | 0.618 | 0.190 |
| $Al_2O_3$ | # | 0.154 | 0.048 |
| FeO | 0.057 | 0.606 | 0.160 |
| $Cr_2O_3$ | # | 0.617 | 0.129 |

Table 5.10.3 A summary of electron microprobe results from 'HT'S cleaner conductors' fraction of Pond C.

*Mean:     Mean values exclude values that are below the detection limit and very high or low values (see details in text).

#          Lowest values are below the lld

$SiO_2$ was present in all the grains, but not at very high concentrations. Some of the rutile grains from the 'HT'S cleaner conductors' fraction of Pond C had high concentrations of $V_2O_3$, $Nb_2O_5$ and FeO. However, $Al_2O_3$ occurred only in minor concentrations.

.

# 6. Discussion

## 6.1 Rutile Chemistry in relation to physical properties

During mineral separation four magnetic fractions were produced:

1. ilmenite fraction - magnetic and non magnetic (most magnetic)
2. mag others fraction – magnetic and non-magnetic
3. cleaner mags
4. primary mags (least magnetic)

and five electrostatic fractions were produced:

5. primary HT'S conductors (most conductive)
6. HT'S scavengers
7. HT'S cleaner mids
8. HT'S cleaner conductors
9. HT'S cleaner non-conductors (least conductive).

The oxides commonly found to be substituting for $TiO_2$ within rutile are $SiO_2$, $ZrO_2$, $V_2O_3$, $Nb_2O_5$, $Al_2O_3$, FeO and $Cr_2O_3$, although there are significant variations between the different fractions.

## 6.1.1 Magnetic effect

Ternary plots were compiled for the magnetic fractions listed above, these show the composition range of rutile grains in terms of, $TiO_2$, FeO, and 'others' (all the other oxides that occur in rutile).

The majority of the grains (15) from the 'magnetic ilmenite' fraction (Fig. 6.1.1.1) were composed of almost pure $TiO_2$ with the substituting oxides making up less than 1wt% of
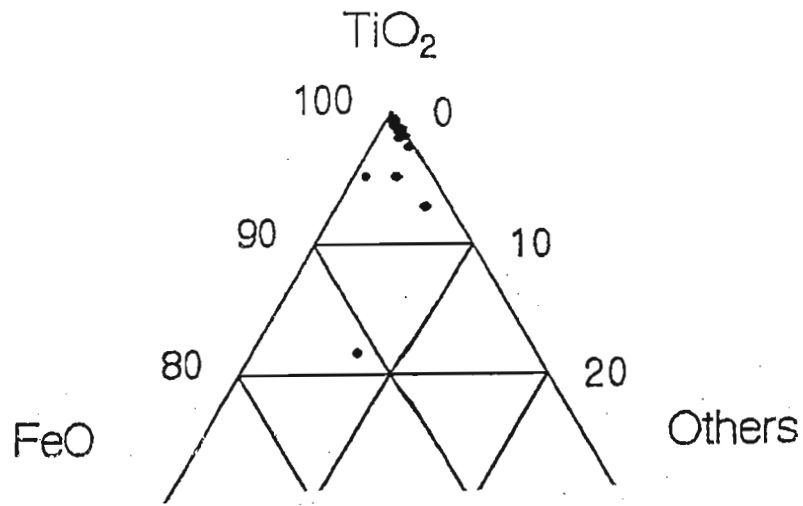
Fig. 6.1.1.1 Ternary plot of TiO$_2$, FeO and other oxides for rutile grains from the 'magnetic ilmenite' fraction
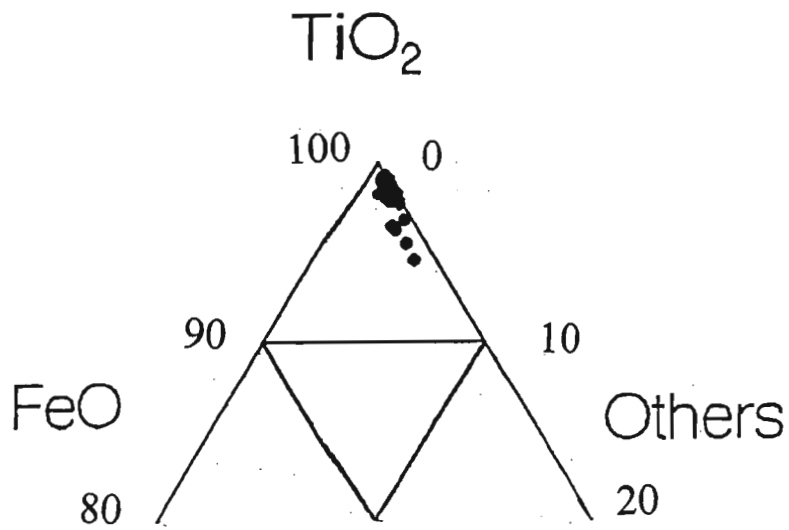


Fig. 6.1.1.2 Ternary plot of TiO$_2$, FeO and other oxides for rutile grains from the 'non magnetic ilmenite' fraction

the grain. Three grains (22%), however, did contain a high percentage of FeO, and 'other' oxides but had a correspondingly low $TiO_2$ content. None of the grains contained more than 10% 'others'. The magnetic ilmenite showed variability in FeO content rather than in the 'other' oxides with a high FeO:others ratio.

The non-magnetic ilmenite fraction (Fig. 6.1.1.2) grains all contained well over 90wt% $TiO_2$. All the grains had less than 1wt% FeO. Although most grains had a low 'others' component, some grains had as much as much as 5wt% others. The non-magnetic ilmenite showed a distinct trend in the 'other' oxides, with very little variation in the FeO (low FeO:others ratio).

The grains of the 'magnetic mag others' fraction (Fig. 6.1.1.3) consisted of $TiO_2$ in the range of 70 to 99wt%, with substitutions of both FeO and 'other' oxides. Although some grains had much higher compositions of other oxides than FeO, most of the grains had less than 10% of 'other' oxides. However, a single grain had about 14% 'other' oxides, 12wt% of which was $SiO_2$.

Most of the grains in the non-magnetic mag others fraction (Fig. 6.1.1.4) had $TiO_2$ in the range of 90 to 100wt%, with the exception of one grain with approximately 82% $TiO_2$. This single grain had a high FeO content (approximately 12wt%), although majority of the grains had less than 5wt% FeO. Most of the 'other' oxides constituted less than 5wt% of the grains; only two grains had about 7wt% 'others'. Grains from the non-magnetic mag others had a high FeO:others ratio.

Grains from the 'primary mags' fraction (Fig. 6.1.1.5) all had high $TiO_2$ content of 95 to 100%. Rutile grains from this fraction had low FeO contents, ranging from below the detection limit of 0.027wt% to approximately 1.6wt%. The proportion of other oxides that substituted into the rutile structure made up less than 5wt%, of which $SiO_2$ was the highest substituting element at 2.203wt% and $V_2O_3$ at 1.746wt%. Grains from the 'primary mags' fraction had a low FeO:others ratio.

144
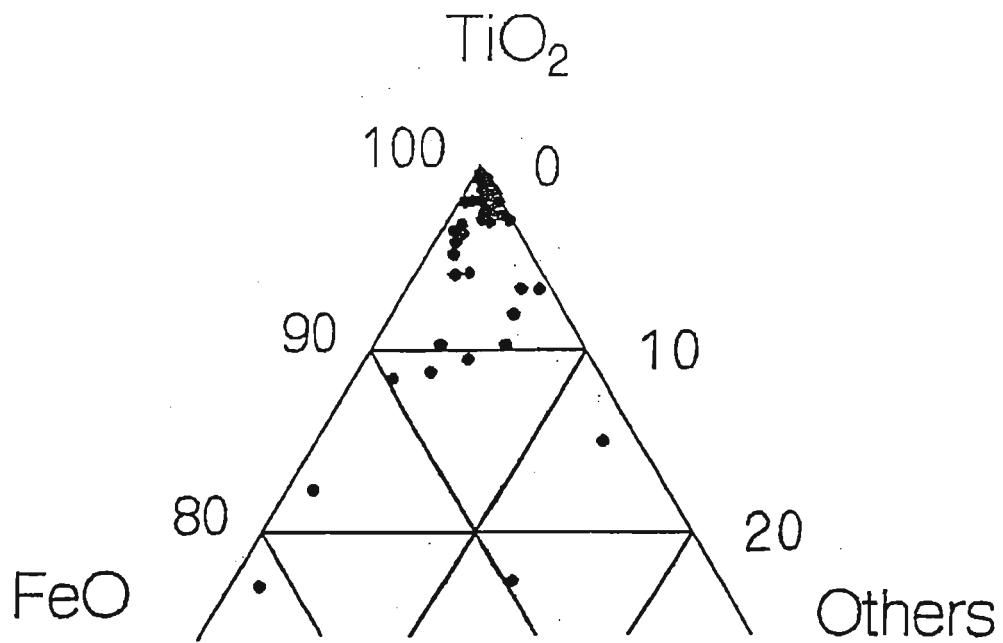
Fig. 6.1.1.3 Ternary plot of $TiO_2$, FeO and other oxides for rutile grains from the 'magnetic mag others' fraction
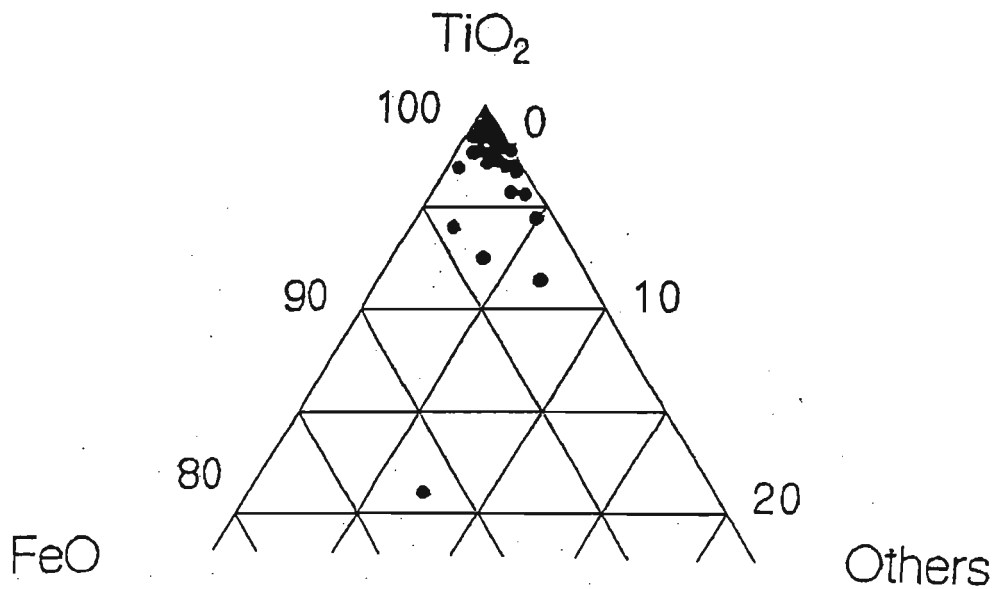


Fig. 6.1.1.4 Ternary plot of $TiO_2$, FeO and other oxides for rutile grains from the 'non magnetic mag others' fraction
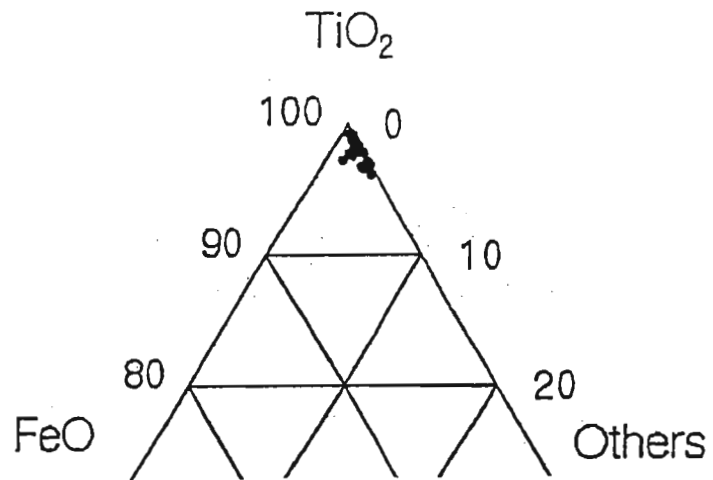
Fig. 6.1.1.5 Ternary plot of $TiO_2$, FeO and other oxides for rutile grains from the 'primary mags' fraction
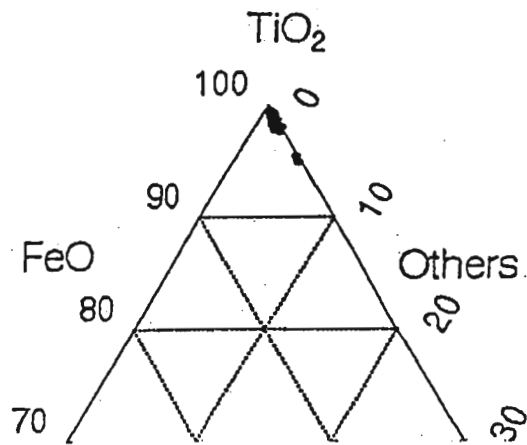


Fig. 6.1.1.6 Ternary plot of $TiO_2$, FeO and other oxides for rutile grains from the 'cleaner mags' fraction

Rutile grains from the cleaner mags fraction plot in the upper most region of the ternary diagram (Fig. 6.1.1.6), with 96 – 100wt% $TiO_2$. All grains had very low FeO with the maximum FeO content being 0.593wt%. All the other oxides in the rutile grains accounted for approximately 5wt% of the grain. One grain contained a very high $Al_2O_3$ content of 1.522wt% and a correspondingly high $SiO_2$ content of 1.076wt%. This fraction had a trend of variability in the 'others' and was characterised by a very low FeO:others ratio.

The more magnetic fractions (i.e., magnetic ilmenite and mag others fraction), as expected contained high FeO. However, these fractions also contained higher proportions of 'others' (notably $V_2O_3$ and $Nb_2O_5$). Magnetic effect although influenced by FeO, also appears to be enhanced by substitutions of other oxides.

## 6.1.2 Electrostatic effect

Ternary diagrams were compiled of $TiO_2$, FeO and 'others' in the electrostatic fractions, 'primary HT'S conductors', 'HT'S Scavengers', 'HT'S cleaner mids', 'HT'S cleaner non-conductors' and 'HT'S cleaner conductors'.

Rutile grains from the 'primary HT'S conductors' fraction (Fig. 6.1.2.1) showed rutile grains were composed of almost entirely $TiO_2$. FeO was less than 0.5wt% in any of the grains. The other oxides combined made up only about 2% in rutile grains. The 'others' showed a greater variability than the FeO.

The HT'S scavengers ternary plot (Fig. 6.1.2.2) showed most grains were almost entirely composed of $TiO_2$ with virtually no FeO. This fraction contained only a trace less FeO than the 'primary HT'S conductors'. Some grains, however, contained up to 1.5wt% of other oxides. The HT'S scavengers showed a trend of slight variability in the concentration of the 'other' oxides.
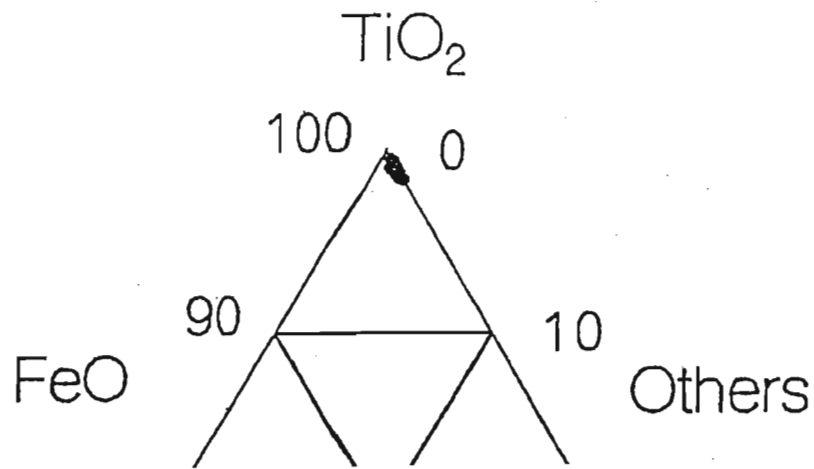
Fig. 6.1.2.1 Ternary plot of $TiO_2$, FeO and other oxides for rutile grains from the 'primary HT's conductors' fraction
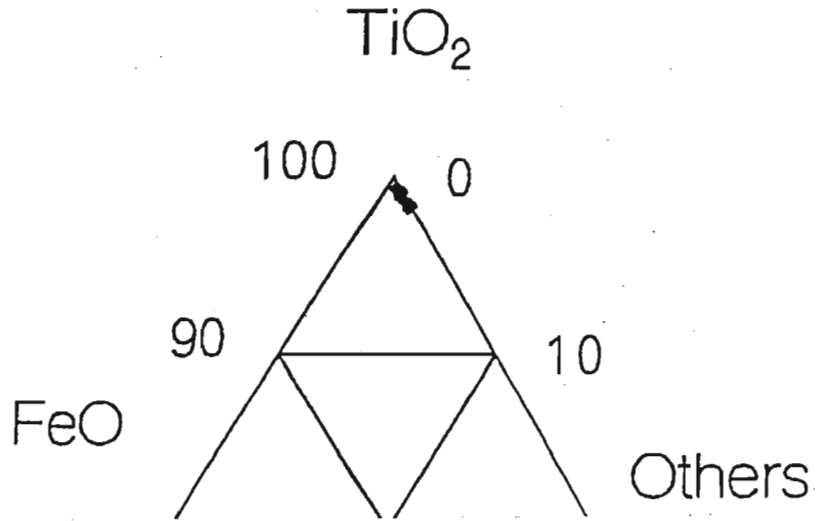


Fig. 6.1.2.2 Ternary plot of $TiO_2$, FeO and other oxides for rutile grains from the 'HT's scavengers' fraction

All the grains from the 'HT'S cleaner mids' fraction (Fig. 6.1.2.3) had $TiO_2$ contents of between 97 to 100wt%. The FeO content of grains was found to be lower than 0.3wt%. The other oxides made up approximately 2.5wt% of the rutile grains. This fraction had a very low FeO:others ratio.

Grains from the 'HT'S cleaner non-conductors' fraction, (Fig. 6.1.2.4) were made up dominantly of $TiO_2$ (97 to 99wt%) with very little FeO. Only one grain contained approximately 1wt% FeO. The other substituting oxides made up at most 2.5wt% of the grain yielding very low FeO:others ratio.

The $TiO_2$ content of rutile grains from the 'HT'S cleaner conductors' (Fig. 6.1.2.5) varied from 94 to 100wt%. Apart from $TiO_2$ the grains from the 'HT'S cleaner conductors' (Fig. 6.1.2.5) appeared to be dominated by the other oxides (approximately 5wt%) substituting into the rutile lattice. Only one grain had FeO content exceeding 1wt% giving a very low FeO:others ratio.

All the electrostatic fractions had very high $TiO_2$ contents, mostly above 96wt%. All grains contained $SiO_2$ and $ZrO_2$, while FeO occurred at much lower concentrations than in the magnetic fractions. The electrostatic fractions were more pure (had higher $TiO_2$ content) and contained fewer substitutions of FeO and 'others'. The magnetic fraction conversely was less pure (lower $TiO_2$ content) and contained a higher proportion of FeO and 'others'.

## 6.1.3 Rutile colour

Grains were selected according to colour from the final rutile product. The most common colours for rutile grains were reddish brown and black followed by yellows and blues respectively (see Appendix A5 for colour plates).

The reddish brown grains (10R ¾ - Rock and Colour Chart Committee, 1979) were the

149
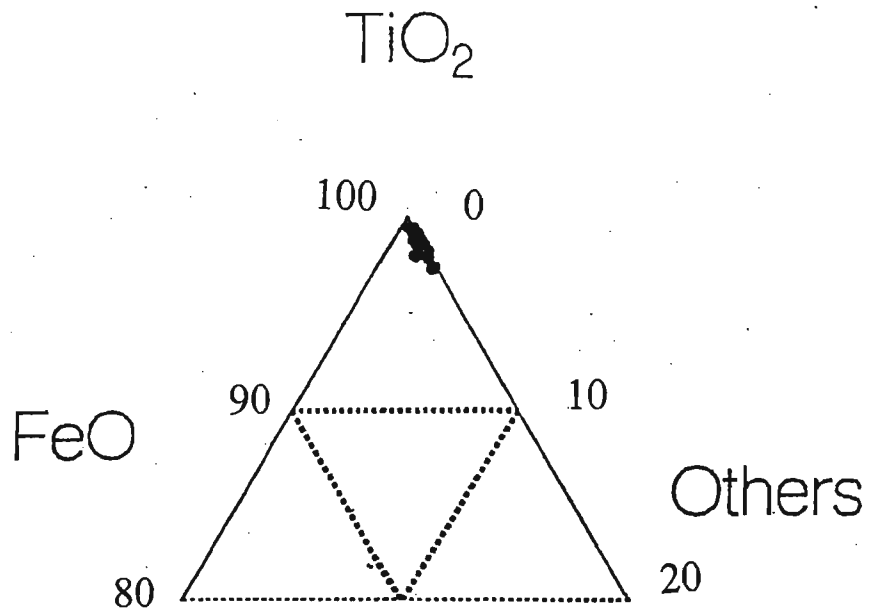
Fig. 6.1.2.3 Ternary plot of $TiO_2$, FeO and other oxides for rutile grains from the 'HT's cleaner mids' fraction
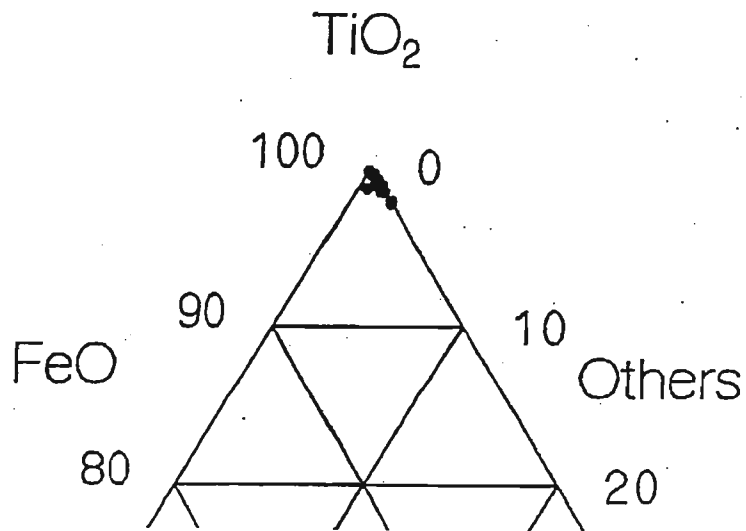


Fig. 6.1.2.4 Ternary plot of $TiO_2$, FeO and other oxides for rutile grains from the 'HT's cleaner non conductors' fraction
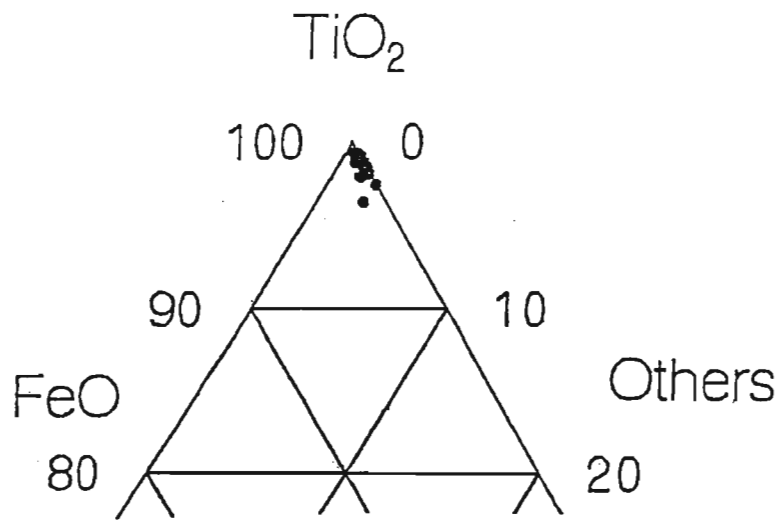
Fig. 6.1.2.5 Ternary plot of $TiO_2$, FeO and other oxides for rutile grains from the 'HT's cleaner conductors' fraction
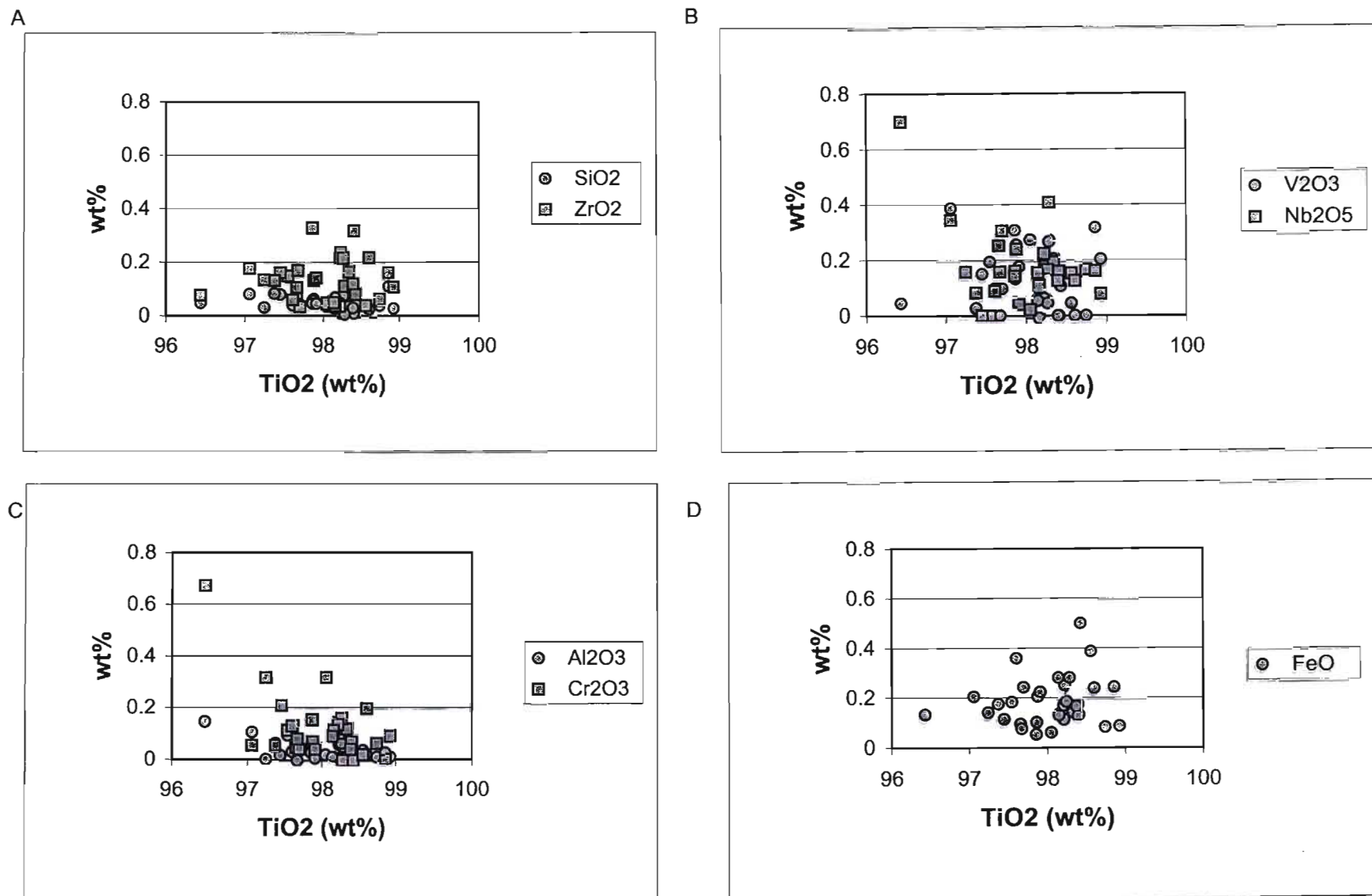
Fig 6.1.3.1 Geochemistry of reddish brown rutile grains from the rutile product.

most abundant. Fig. 6.1.3.1 depicts the geochemical results for the reddish brown grains. Red colouration is generally attributed to high FeO contents (Deer et. al., 1983). However in all the reddish brown rutile grains this high FeO content was not evident. but some grains did contain slightly higher $Nb_2O_5$ and $Cr_2O_3$ values.

The geochemical data for black rutile grains (brownish black 5YR 2/1 – Rock and Colour Chart Committee, 1979) is presented in Fig. 6.1.3.2. Black rutile grains were generally $V_2O_3$ and $Nb_2O_5$ enriched. Many grains had $V_2O_3$ in excess of 1wt%. FeO was not present in all the grains; the maximum FeO content of black rutile was approximately 0.6wt%, which was the same for red rutile grains.

Fig. 6.1.3.3 displays the geochemical data for blue rutile grain (pale blue 5PB 7/2 – Rock and Colour Chart Committee, 1979). All grains contained significant amounts of $Nb_2O_5$, but not all grains contained enhanced concentrations of $Al_2O_3$. There appears therefore to be a correlation between the $Al_2O_3$ and $SiO_2$ content and the blue colour of rutile grains. The colour appears to be the result of a multiple substitution of $SiO_2$, $Al_2O_3$ and $Nb_2O_5$ or an interaction of these oxides.

The graphical representation of the geochemical data for the yellow rutile grains (dark yellowish orange 10YR 6/6 – Rock and Colour Chart Committee, 1979) is Fig. 6.1.3.4. The yellow rutile grains had a higher FeO and $Nb_2O_5$ content in comparison to the other oxides. The yellow colour of rutile grains may therefore be the result of FeO and $Nb_2O_5$ substitution into the rutile lattice.

## 6.2 Overview of rutile geochemistry in the magnetic fractions

Radar diagrams were compiled for each fraction, with the means plotted from all three ponds for the oxides $SiO_2$, $ZrO_2$, $V_2O_3$, $Ta_2O_5$, $Nb_2O_5$, $Al_2O_3$, $Cr_2O_3$ and FeO. The trace oxide patterns all show the same overall distribution for each Pond, although in some cases one pond may show a significantly higher oxide content.
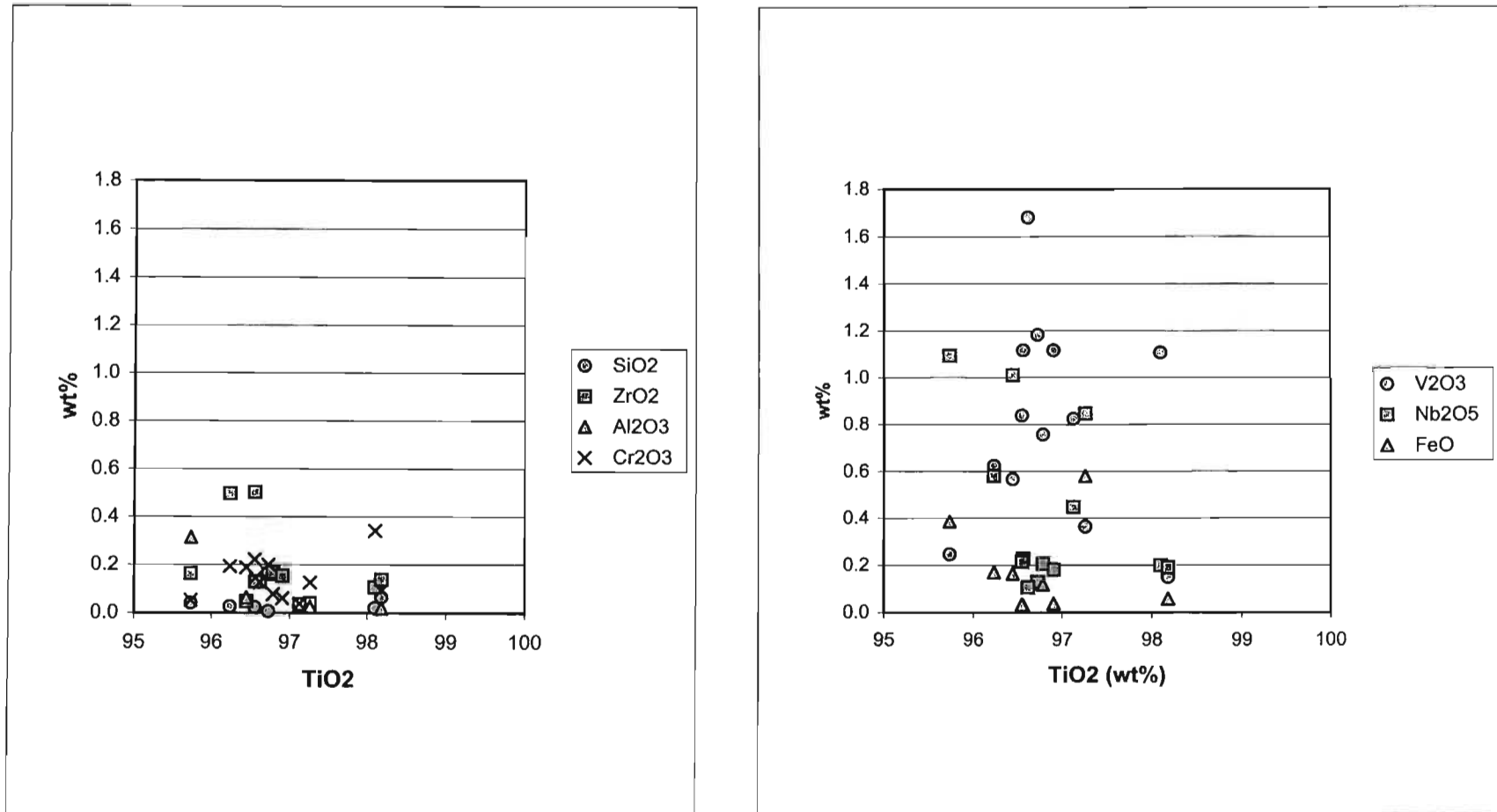
Fig 6.1.3.2 Geochemistry of black rutile grains from the rutile product.
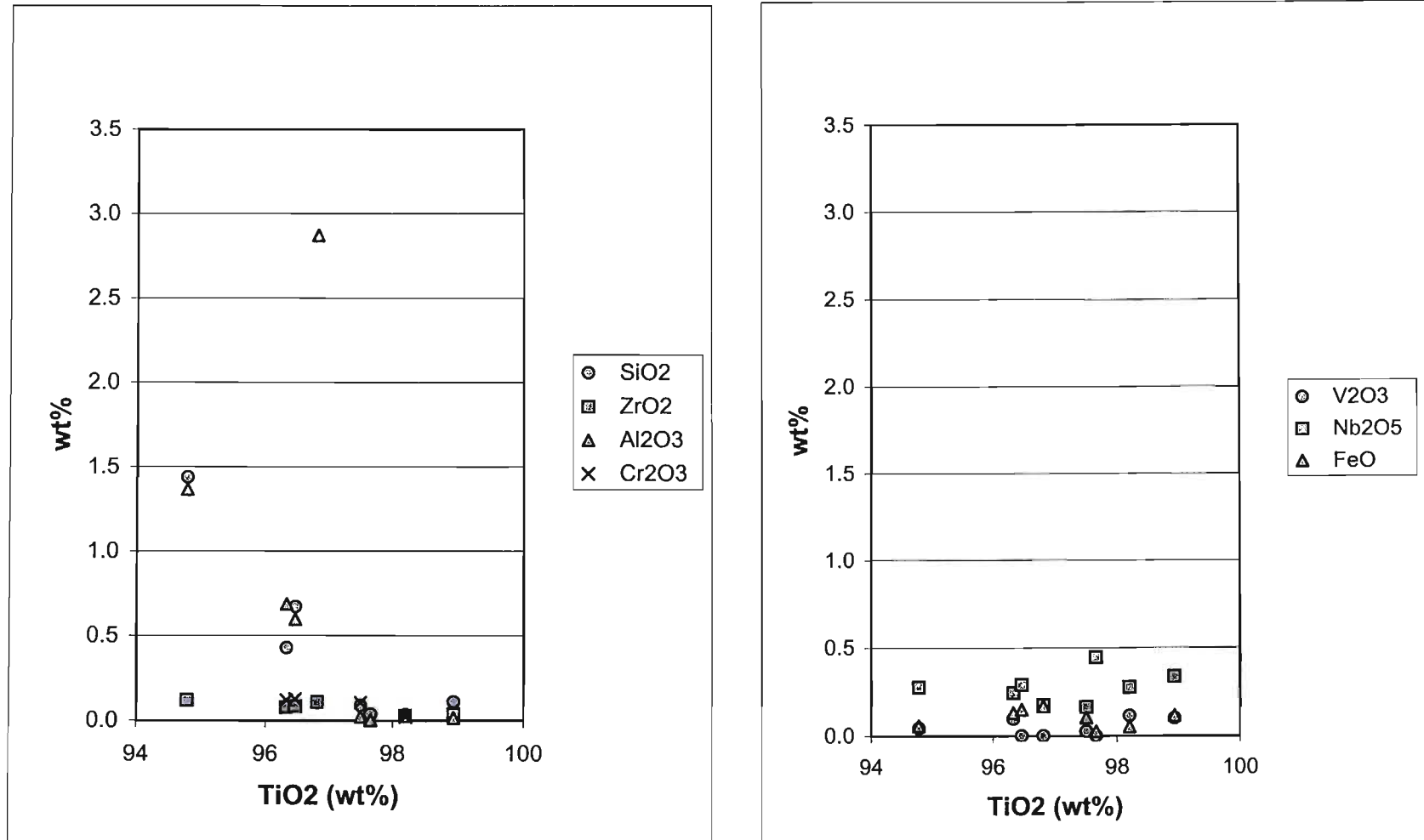
Fig 6.1.3.3 Geochemistry of blue rutile grains from the rutile product.
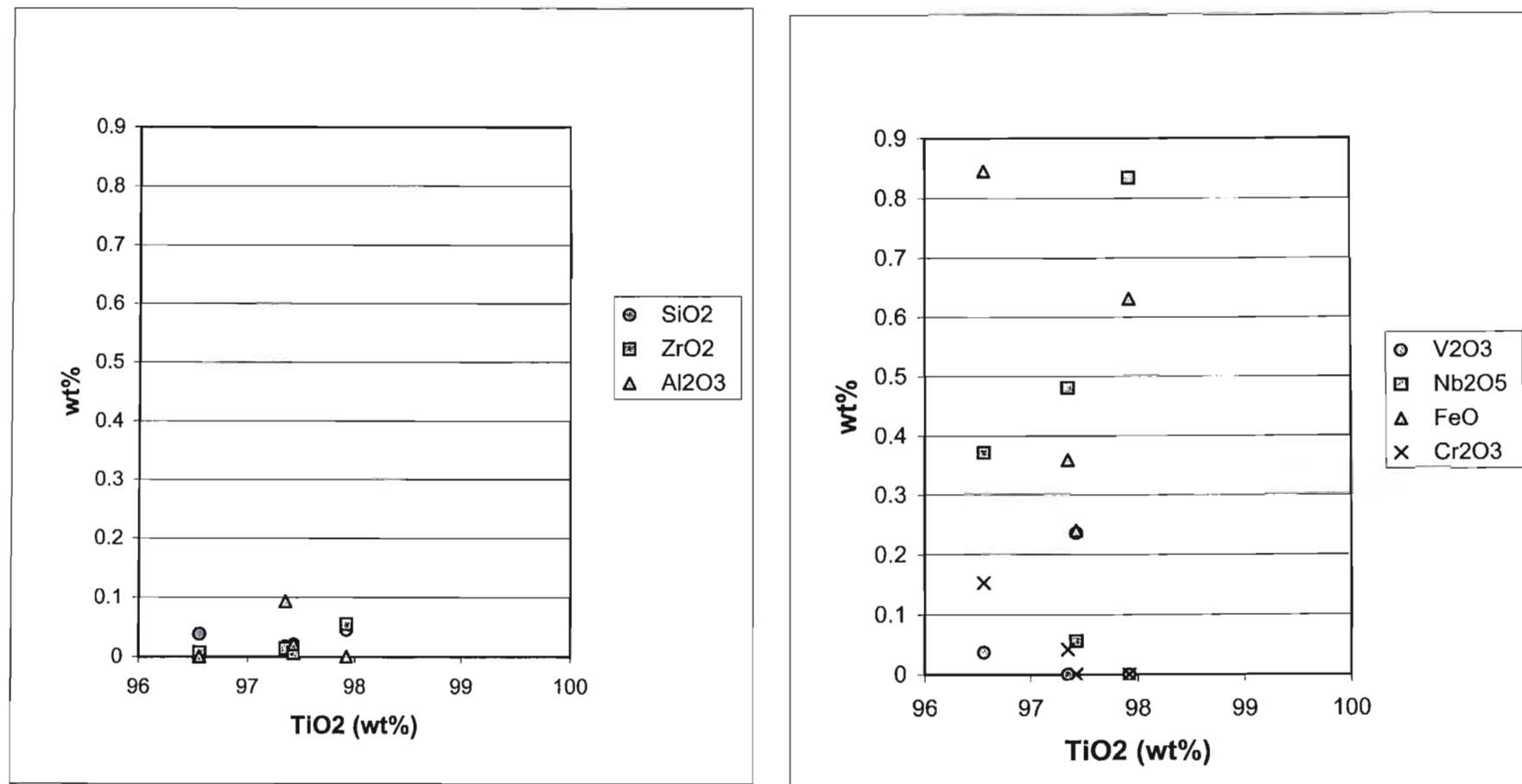
Fig 6.1.3.4 Geochemistry of yellow rutile grains from the rutile product.

## 6.2.1 Magnetic ilmenite fraction

This fraction had a high proportion of impurities in the rutile grain. Pond B showed the largest variation with respect to FeO (2.0wt%); $SiO_2$ of 0.6wt% and $Al_2O_3$ of 0.5wt%. Pond A had three main components, $SiO_2$ (0.5wt%); FeO (>0.5wt%) and $V_2O_3$ (0.5wt%). Pond C appeared to be $SiO_2$ (>0.75wt%); $V_2O_3$ (0.5wt%) and $Al_2O_3$ (0.6wt%) enriched (Fig. 6.2.1).

## 6.2.2 Non-magnetic ilmenite fraction

All three ponds had relatively pure rutile grains, with impurities making up less than 0.75wt%. The three ponds showed enrichment trends towards $SiO_2$, FeO and $V_2O_3$. Ponds B and C were $Nb_2O_5$ enriched, whereas Pond A was distinctly $Nb_2O_5$ poor. Only Pond A had significant $Al_2O_3$, where as rutile grains from Ponds B and C contained virtually no $Al_2O_3$ (Fig. 6.2.2).

.

## 6.2.3 Magnetic mag others fraction

All three ponds showed similar trends. Ponds B and C had a strong preponderance for FeO, with grains containing 2.45 and 2.4wt% respectively. Pond A contained FeO at a much lower concentration (less than 0.75wt%), with a higher $SiO_2$ composition of 1.0wt%. Pond C also had a $SiO_2$ content of 1.0wt%, however Pond B had a lower $SiO_2$ content (0.3wt%). All three ponds had a $V_2O_3$ component of 0.5wt%. Only Pond B had an $Al_2O_3$ composition of 0.3wt% (Fig. 6.2.3).
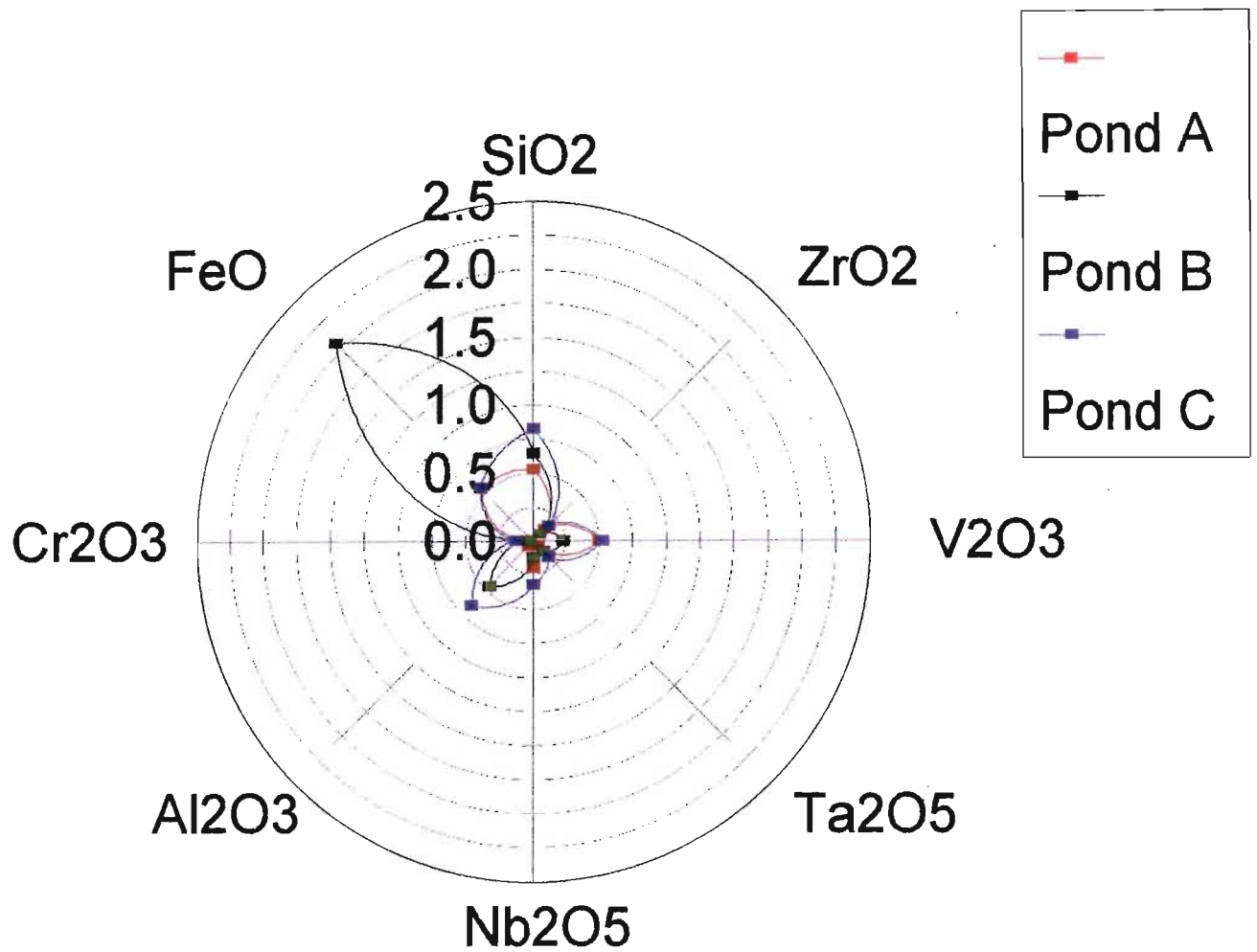
Fig. 6.2.1 Radar plot depicting the mean oxide values for Ponds A, B and C in the 'magnetic ilmenite' fraction
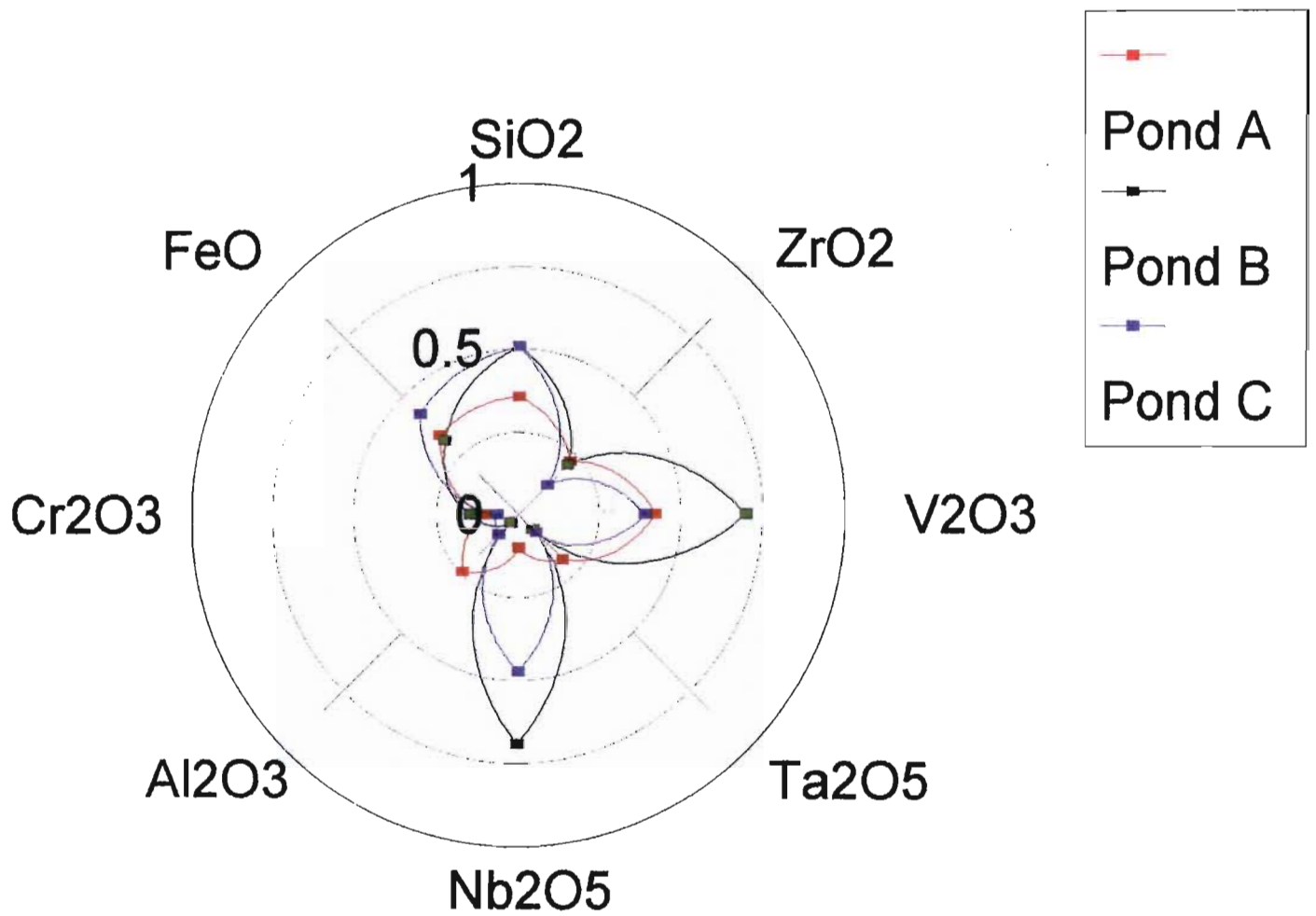
Fig. 6.2.2 Radar plot depicting the mean oxide values for Ponds A, B and C in the 'non magnetic ilmenite' fraction
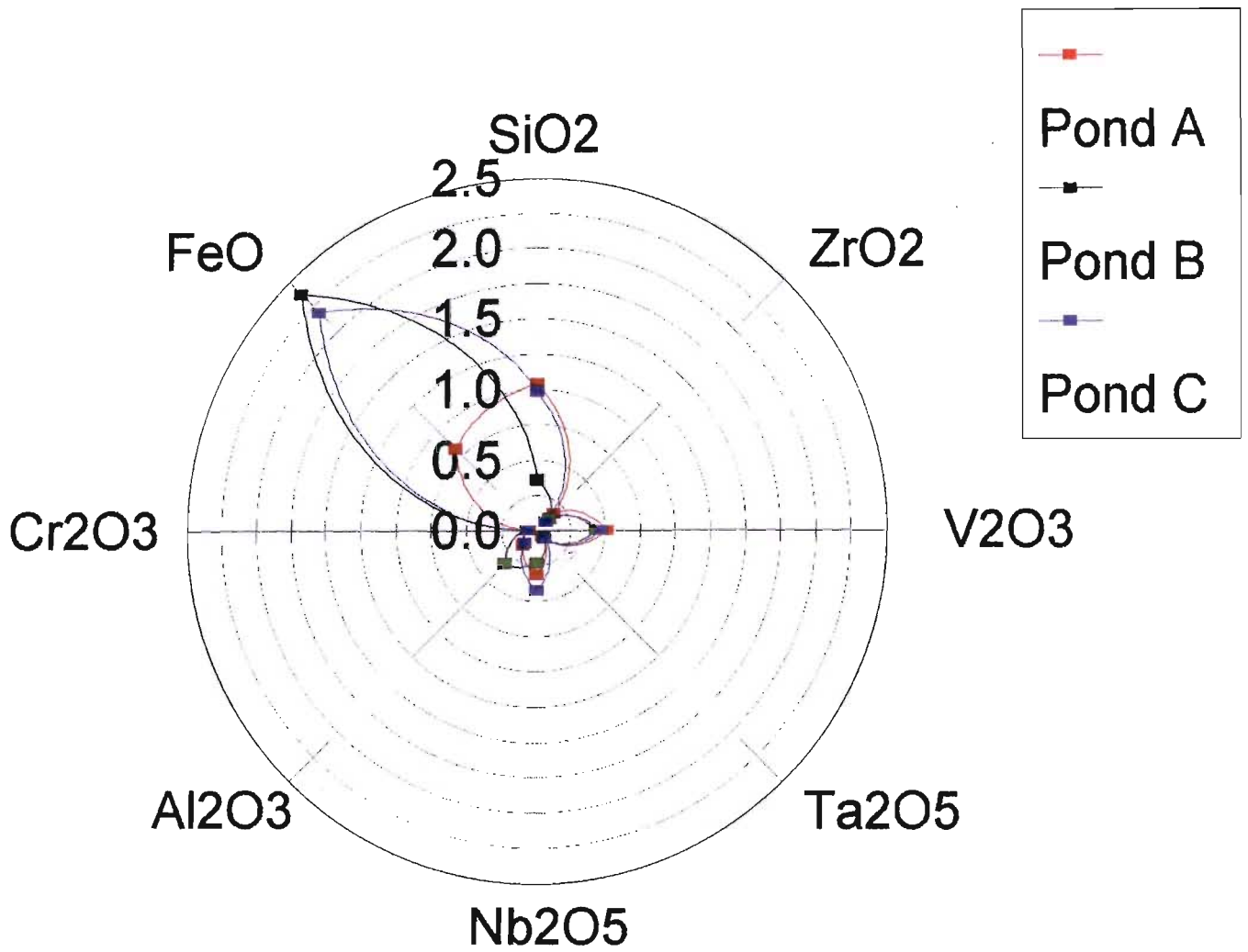
Fig. 6.2.3 Radar plot depicting the mean oxide values for Ponds A, B and C in the 'magnetic mag others fraction

## 6.2.4 Non magnetic mag others fraction

All three ponds had very similar trends (Fig. 6.2.4) with three distinct leaves towards, FeO, $V_2O_3$ and $Nb_2O_5$ enrichment. Pond A showed the most variation with FeO of 1.25wt%, $V_2O_3$ 0.75 and $Nb_2O_5$ 0.5wt%. Pond B had a FeO composition of less than 0.5wt%, $V_2O_3$ at 0.5wt% and $Nb_2O_5$ of 0.7wt%. Pond C showed the least variation, with a FeO content of 0.4wt%, $V_2O_3$ of 0.3wt%, and $Nb_2O_5$ of 0.35wt%. Pond A had a $Ta_2O_5$ composition of 0.3wt% (Fig. 6.2.4).

## 6.2.5 Cleaner mags fraction

The rutile grains from all three ponds had an almost identical trend on the radar plot (Fig. 6.2.5), and were dominated by $SiO_2$, $V_2O_3$ and $Nb_2O_5$. Pond C had a higher $SiO_2$ content (0.6wt%) as well as a higher $Al_2O_3$ content than Ponds A and B. Pond A had a slightly higher $Ta_2O_5$ content than the other two Ponds.

## 6.2.6 Primary mags fraction

All ponds showed a distinct trend in the $V_2O_3$ content (Fig. 6.2.6), with $V_2O_3$ the dominating oxide in all three ponds. Pond A was more $ZrO_2$ enriched than the other ponds. Pond B had a higher proportion of most oxides in comparison to Ponds A and C. All three ponds contained significant amounts of FeO.
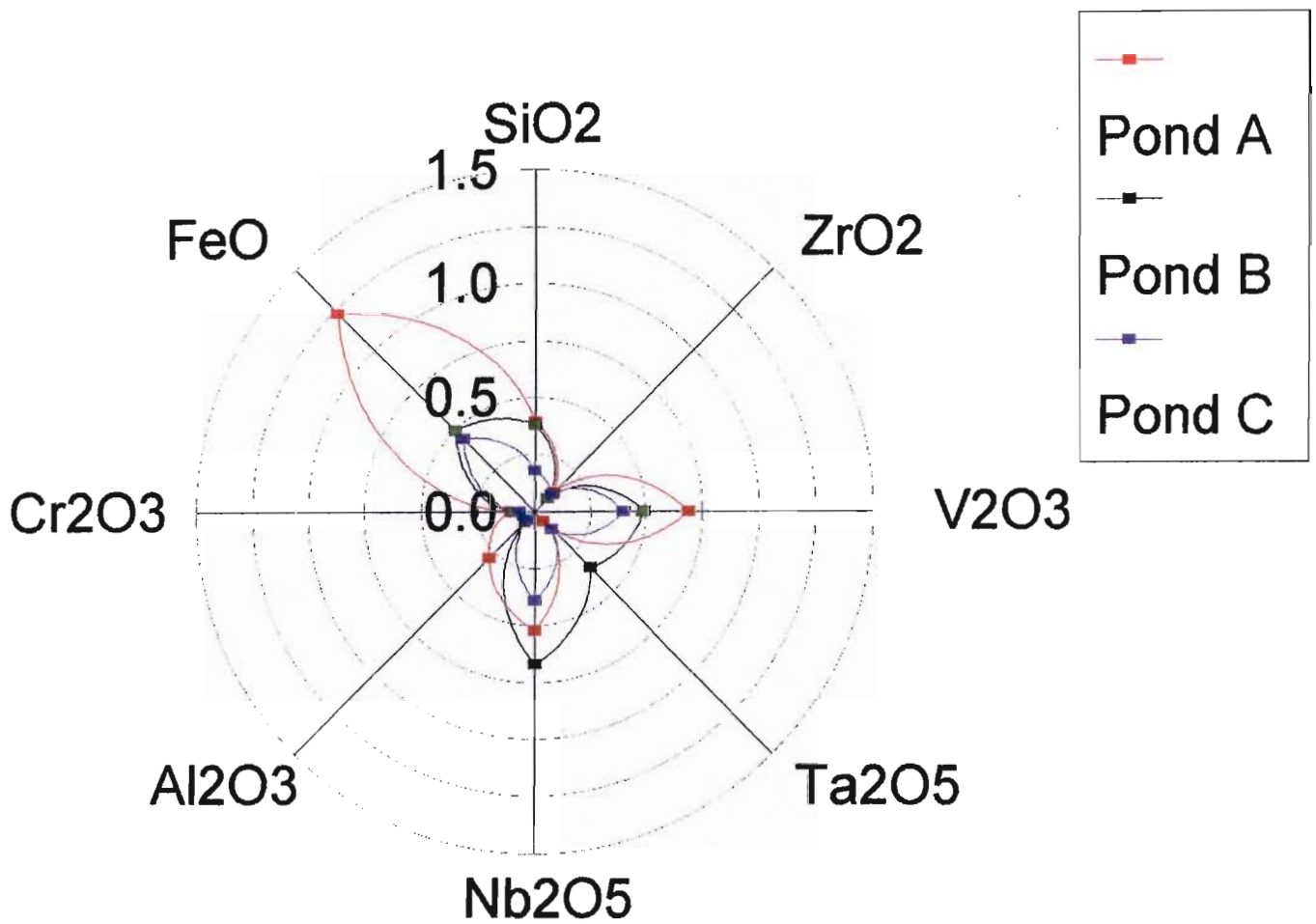
Fig. 6.2.4 Radar plot depicting the mean oxide values for Ponds A, B and C in the 'non magnetic mag others' fraction
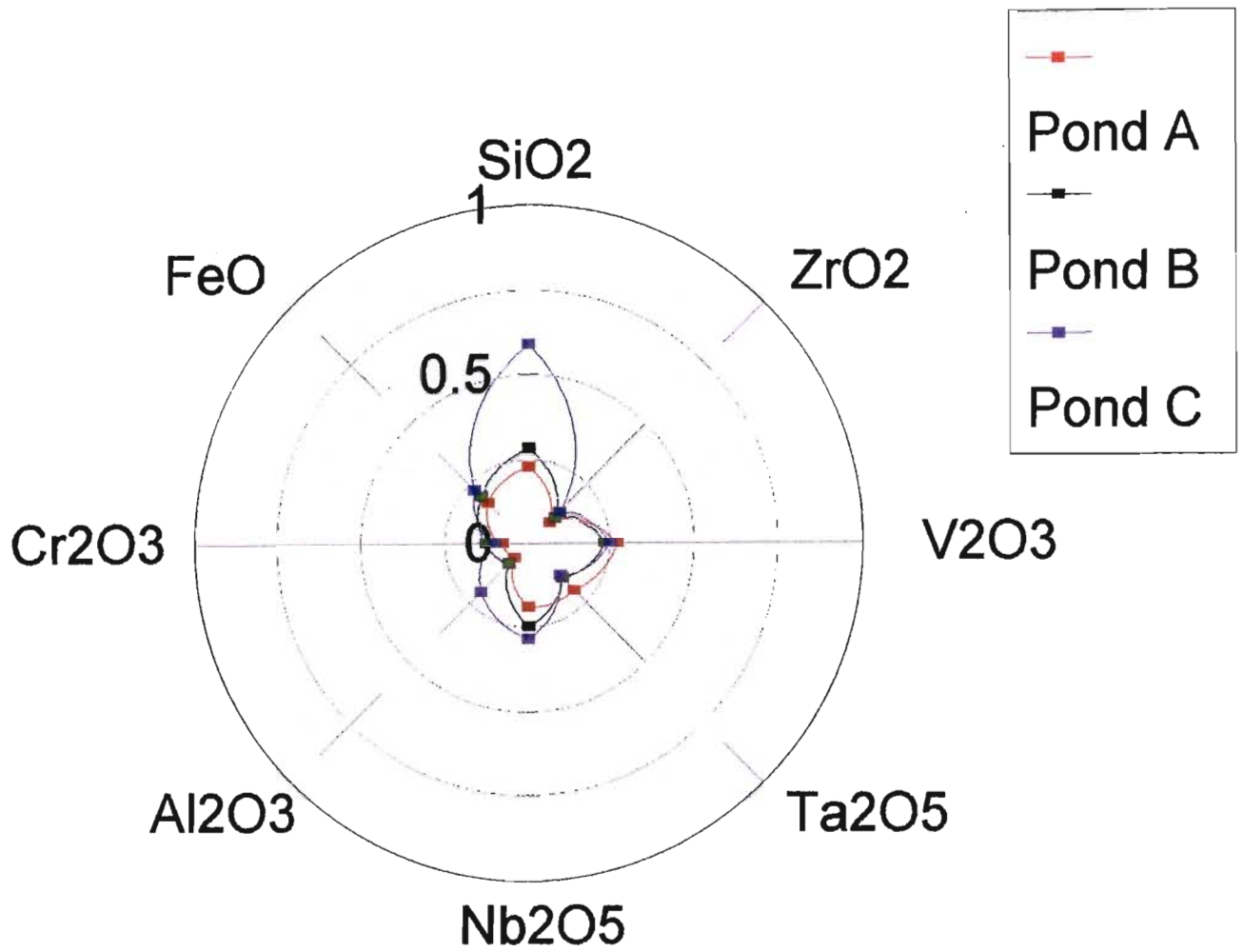
Fig. 6.2.5 Radar plot depicting the mean oxide values for Ponds A, B and C in the 'cleaner mags' fraction
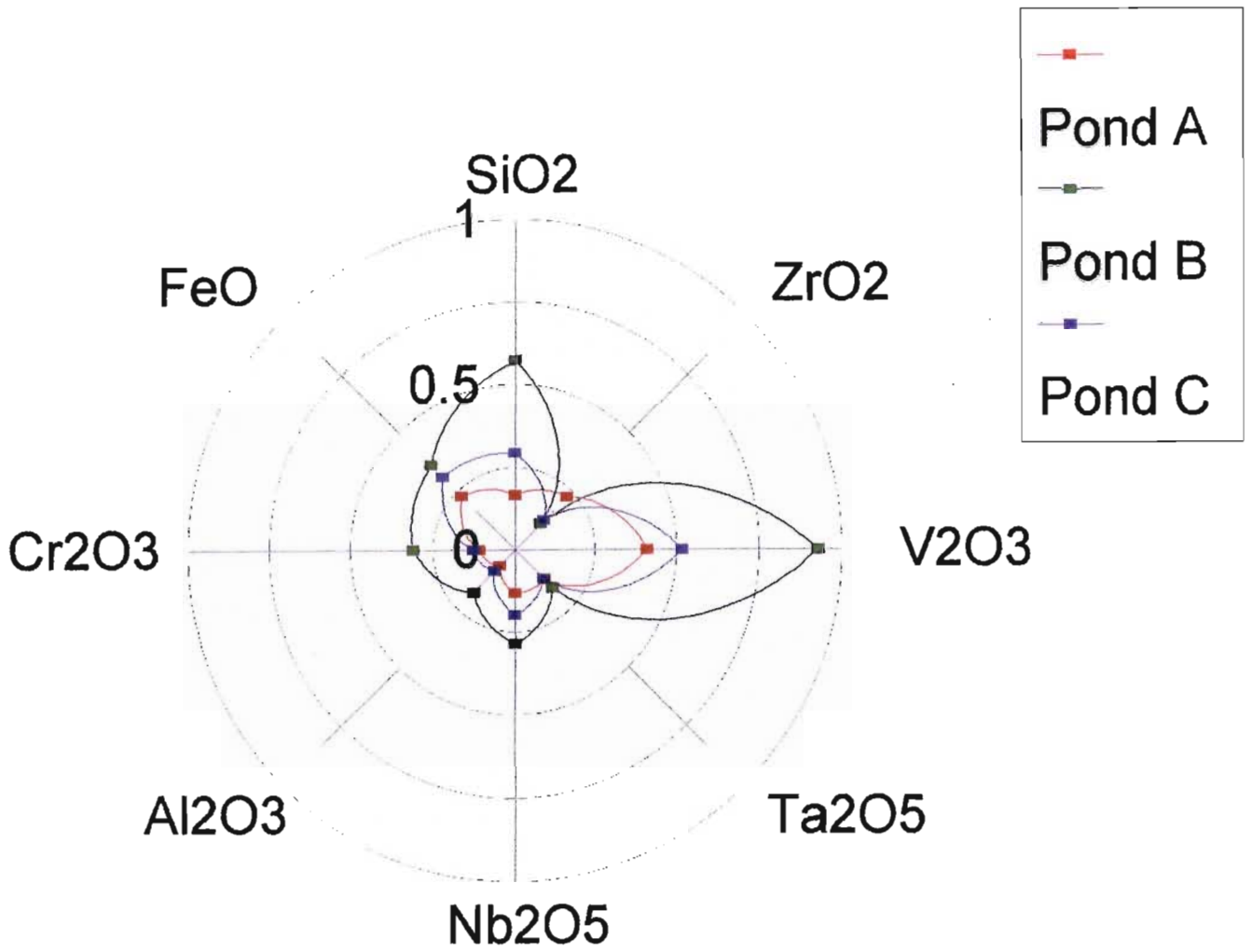
Fig. 6.2.6 Radar plot depicting the mean oxide values for Ponds A, B and C in the 'primary mags' fraction

## 6.3 Overview of rutile geochemistry in the electrostatic fractions

### 6.3.1 Primary HT'S conductors fraction

All ponds had very similar trends (Fig. 6.3.1), with $SiO_2$ being the dominant component in the rutile grains, at approximately 0.38wt% for all Ponds. The diagram (Fig. 6.3.1) also revealed a trend in $V_2O_3$ and $Nb_2O_5$ content. Also evident was the lower FeO and $ZrO_2$ content of rutile grains from all three ponds. Pond B had a notably higher $Ta_2O_5$ content.

### 6.3.2 HT'S scavengers fraction of Pond B

The Radar plot (Fig 6.3.2) shows that $SiO_2$ and $V_2O_3$ were the only oxides that occurred at concentrations greater than 0.25wt%. Grains from this fraction contained virtually no $Al_2O_3$, $Cr_2O_3$ and $Ta_2O_5$.

### 6.3.3 HT'S cleaner mids fraction

No distinct trend was observed between the three ponds A, B and C (Fig. 6.3.3). Rutile grains from Pond A consisted of $SiO_2$ and $V_2O_3$, whereas grains from Pond B were dominated by $SiO_2$ and $Nb_2O_5$. Pond C contained $V_2O_3$, and $ZrO_2$ but had a low $SiO_2$ content. All three ponds however contained much lower FeO contents than the magnetic fractions.

### 6.3.4 HT'S cleaner non-conductors fraction

All three ponds had similar oxide trends with regards to $SiO_2$, $V_2O_3$ and $Nb_2O_5$ (Fig. 6.3.4). Pond A had a higher $V_2O_3$ content than the other ponds. Pond B had a high $SiO_2$ and $Nb_2O_5$ content. All three ponds contained virtually no $Al_2O_3$, as well as a much lower FeO content than the magnetic fractions.
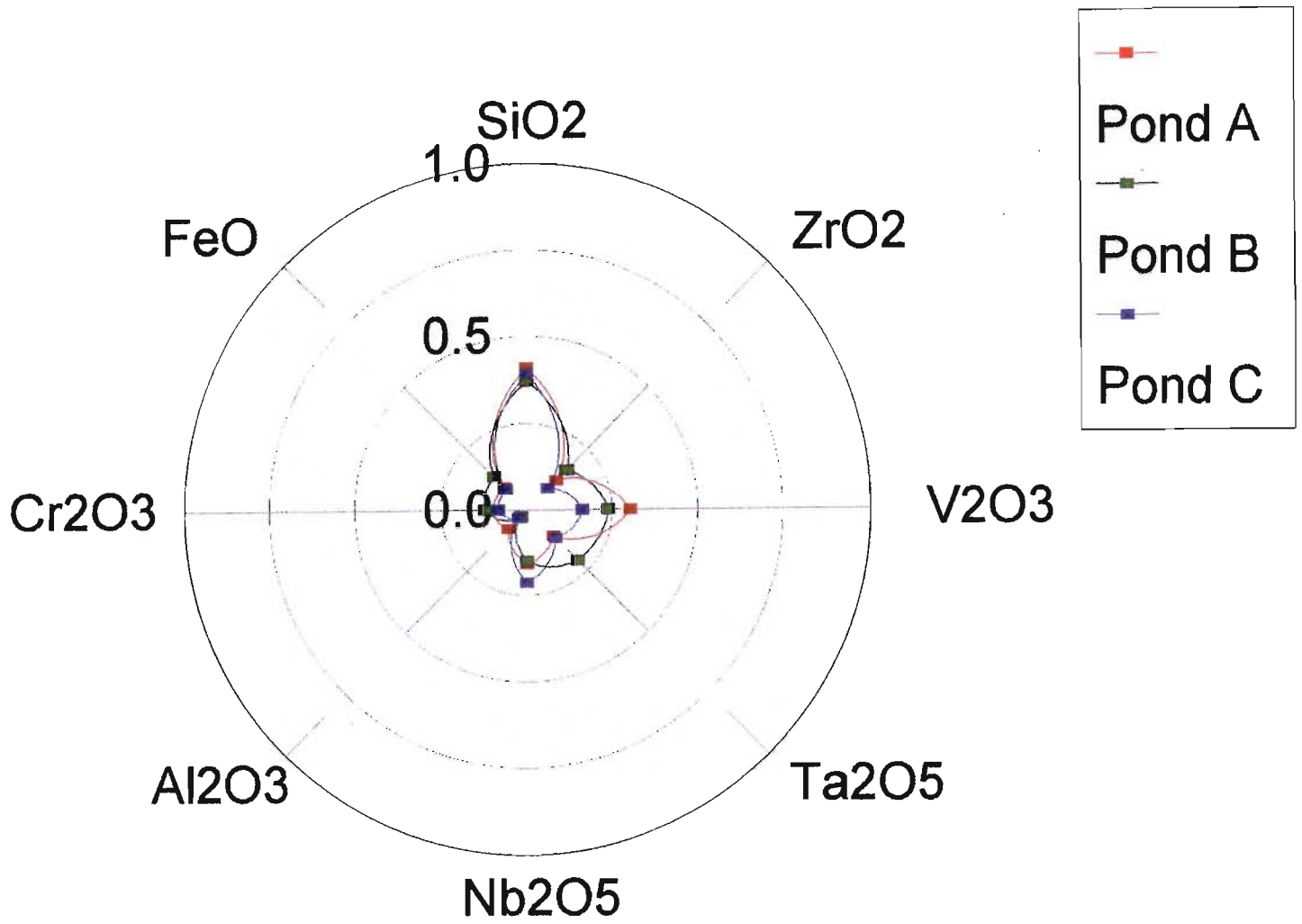
Fig. 6.3.1 Radar plot depicting the mean oxide values for Ponds A, B and C in the 'primary HT's conductors' fraction
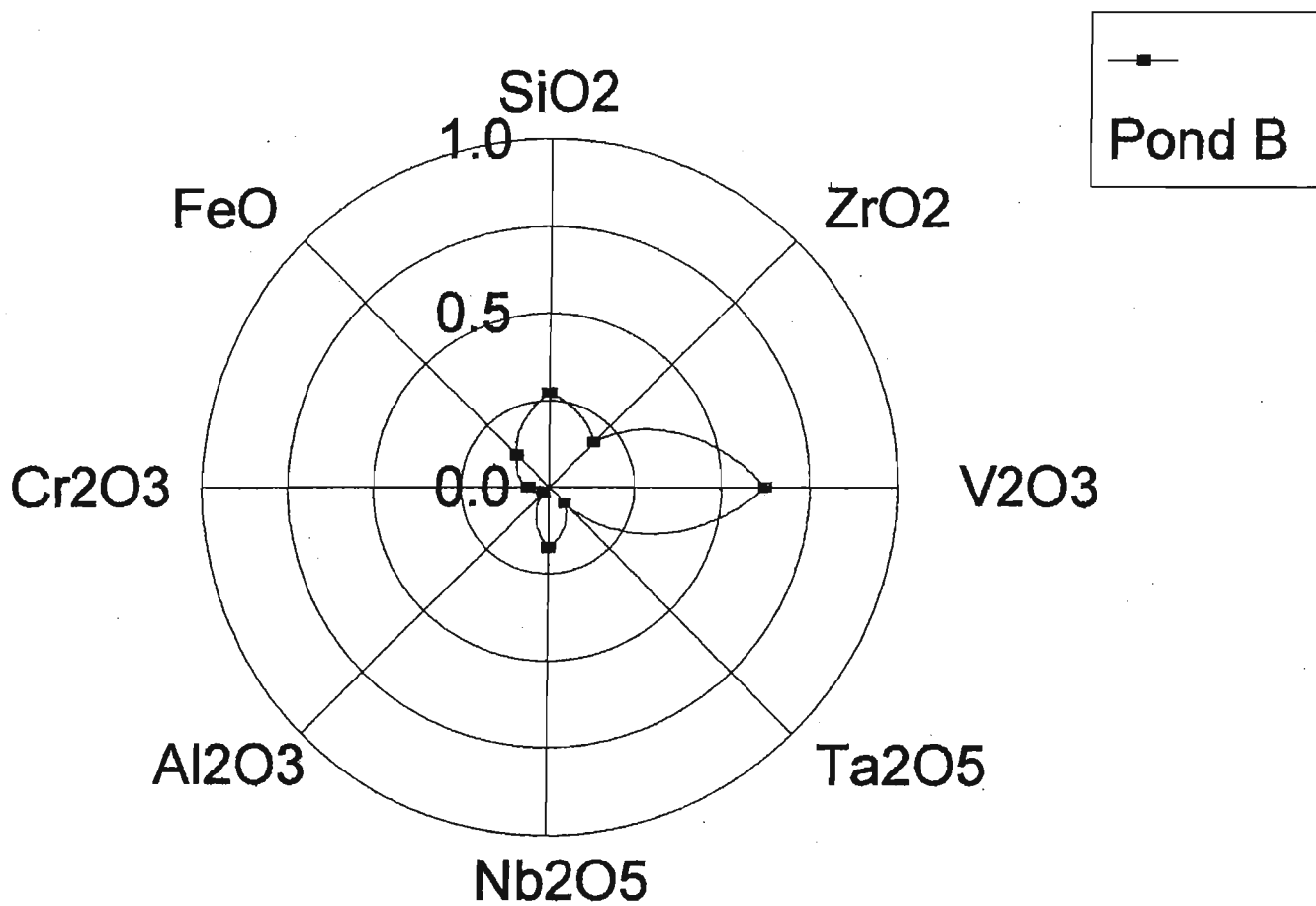
Fig. 6.3.2 Radar plot depicting the mean oxide values for Ponds A, B and C in the 'HT's scavengers' fraction
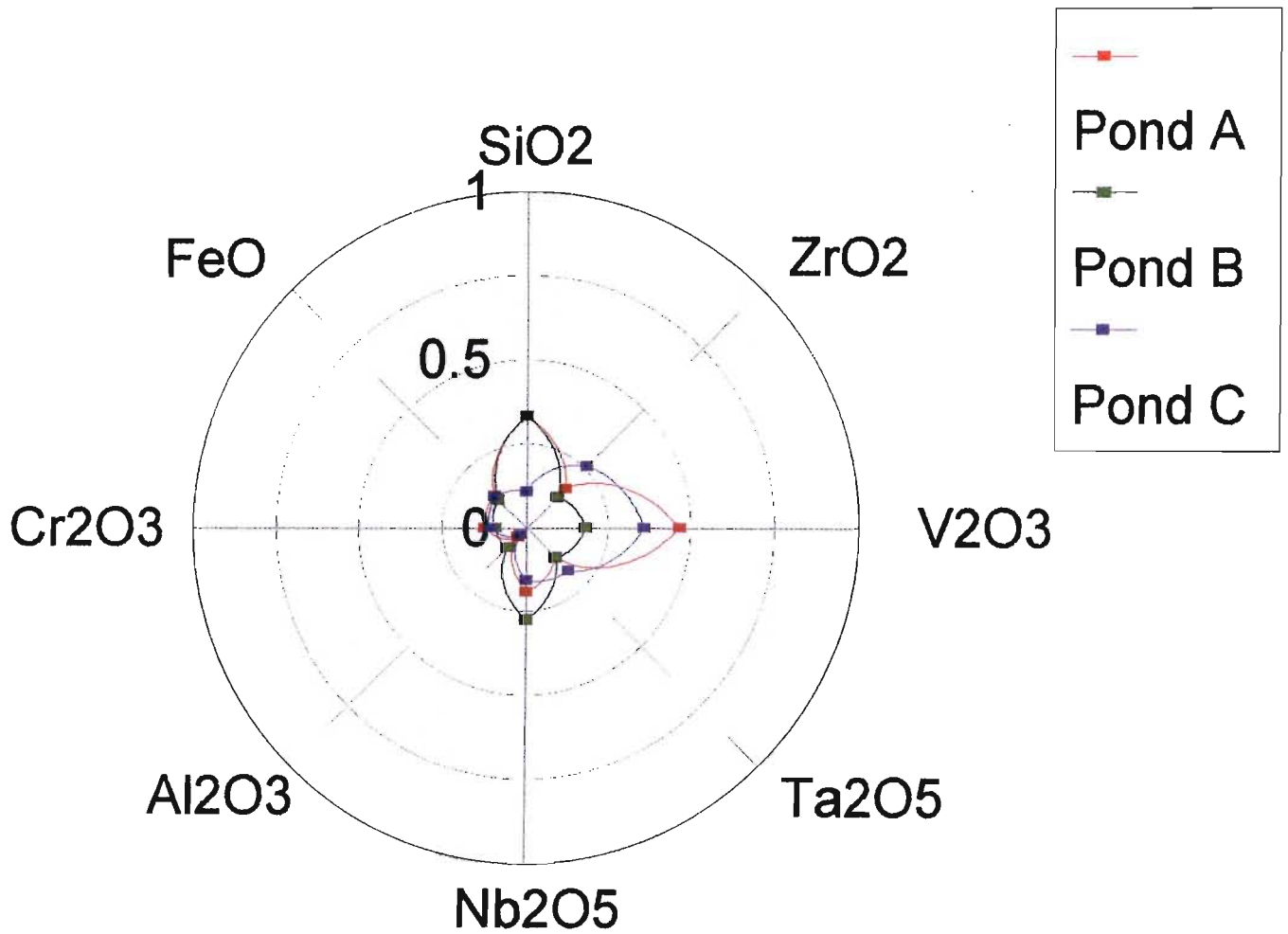
Fig. 6.3.3 Radar plot depicting the mean oxide values for Ponds A, B and C in the 'HT's cleaner mids' fraction
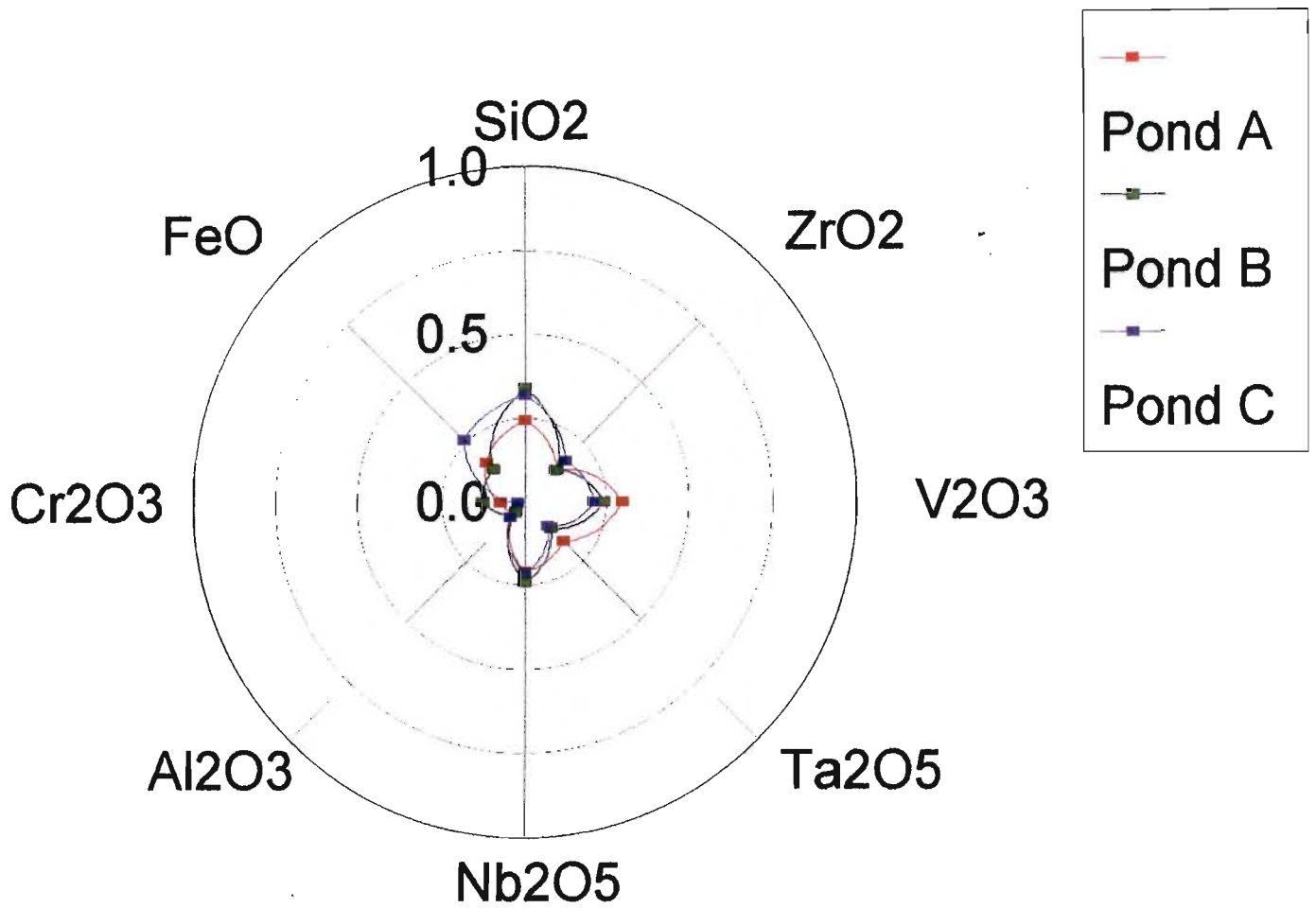
Fig. 6.3.4 Radar plot depicting the mean oxide values for Ponds A, B and C in the 'HT's cleaner non conductors' fraction
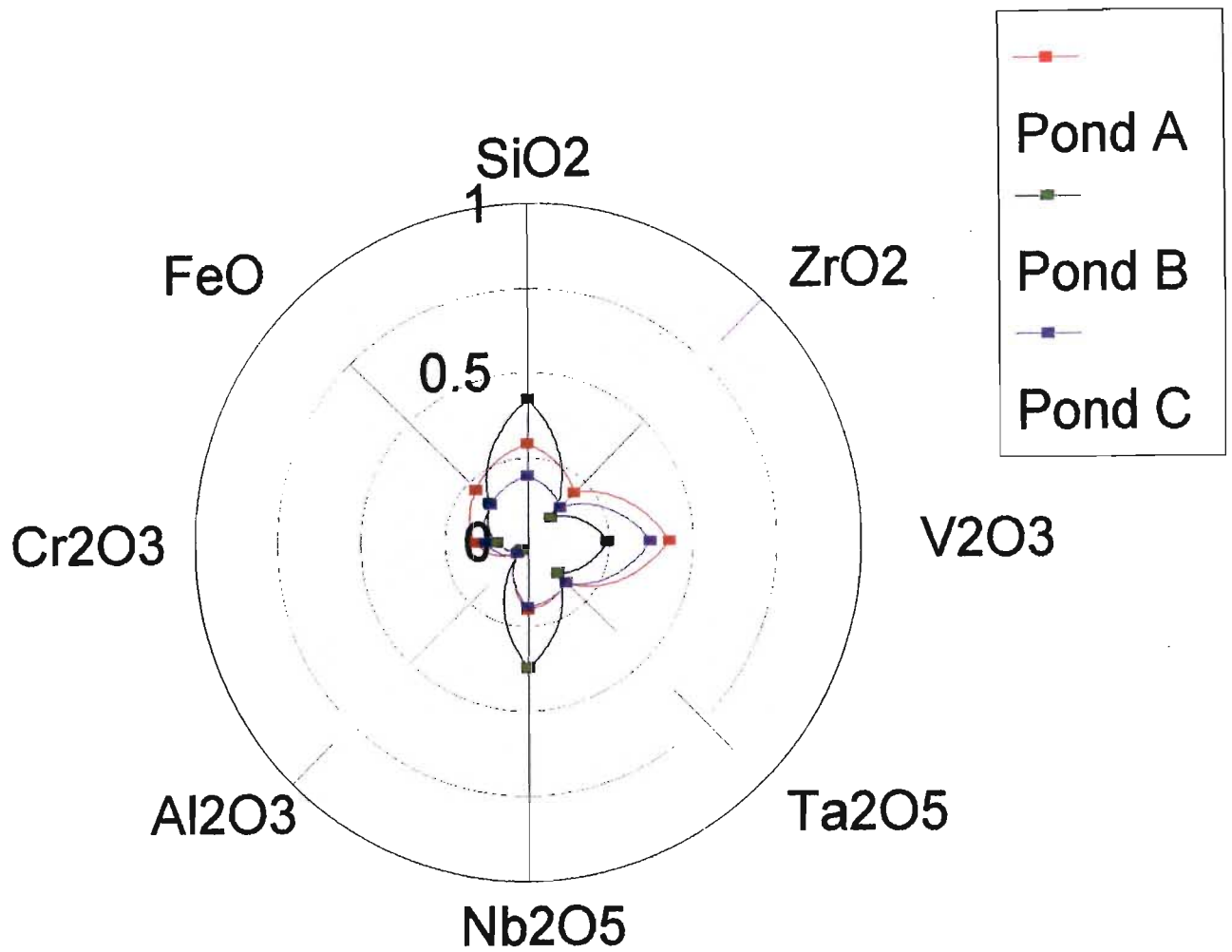
Fig. 6.3.5 Radar plot depicting the mean oxide values for Ponds A, B and C in the
'HT's cleaner conductors' fraction

## 6.3.5 HT'S cleaner conductors fraction

All three ponds showed a similar trend with regards the oxides $SiO_2$, $V_2O_3$ and $Nb_2O_5$ (Fig. 6.3.5). This fraction was relatively pure, with very few impurities, (less than 0.3wt%). Only Pond A shows a higher FeO content (0.25wt%) than Ponds B and C. All grains from all three ponds contained virtually no $Al_2O_3$ and $Cr_2O_3$.

## 6.3.6 A brief summary on Radar graphs

The magnetic fractions contained more impurities than the electrostatic fractions, with the magnetic fractions having at least one oxide above 0.5wt%. The electrostatic fractions however, had with exception to $V_2O_3$ in the HT'S scavengers; all oxide contents below 0.5wt%.

The strong presence of FeO in the magnetic fractions, suggested that this element had a significant influence on the magnetic properties of the rutile grains. This was further reinforced, by the distinct absence of FeO in the electrostatic fractions. Similarly the presence of a slightly higher $Al_2O_3$ content in rutiles from the magnetic fractions implied that small amounts of $Al_2O_3$ might enhance the magnetic influence of FeO.

The electrostatic fractions were purer in terms of $TiO_2$ content, with very few impurities. There appeared to be no single oxide that had a marked affect on conductivity. However, $V_2O_3$ and $SiO_2$ appeared to have some influence on conductivity, as almost all grains in the electrostatic fraction had an enhanced $V_2O_3$ and $SiO_2$ content.

171

# 7. Conclusions

## 7.1 Special features of Ponds A, B and C

In many ways the chemical composition of the rutile grains from all three ponds were very similar, however, certain distinct features were noted in the different fractions.

### 7.1.1 Magnetic ilmenite fraction

The 'magnetic ilmenite fraction' of Pond A contained a single grain that had a very high $SiO_2$ content of 1.2wt%. This grain also had a high FeO content of 2.079wt%. In Pond B, one grain had an uncharacteristically high $SiO_2$ value of 4.016wt% and two grains had very high FeO content of 4.080wt% and 11.118wt%. Rutile grains from Pond C were relatively $TiO_2$ pure and had no anomalous grains.

### 7.1.2 Non-magnetic ilmenite fraction

The 'non magnetic ilmenite fraction' of Pond A had one grain containing $SiO_2$ at 1.185wt% and three grains with high FeO values (0.811, 1.082, and 1.085 wt%) but Pond B had no grains with anomalous $SiO_2$ or FeO values, although Pond C yielded a FeO enriched grain (up to 1.002wt%). In contrast to Pond A, Pond B and C contained grains with very high $Nb_2O_5$ concentrations (2.185wt% and 2.825wt% respectively). Unlike Ponds A and C, Pond B rutile grains had a large range in $V_2O_3$, with most grains having $V_2O_3$ over 0.4wt%.

### 7.1.3 Magnetic mag others fraction

The 'magnetic mag others' fraction of Ponds A, B and C all showed a preponderance for FeO. The most FeO enriched grain came from Pond B and contained 21.5wt% FeO, whilst Pond A yielded a grain with an FeO content of 3.54wt% and Pond C had four FeO enriched grains.

### 7.1.4 Non magnetic mag others fraction

Rutile grains in the 'non magnetic mag others' fraction of Pond A, were $Al_2O_3$ (3.456wt%), $SiO_2$ (2.933wt%), $V_2O_3$ (1.225wt%), $Nb_2O_5$ (2.778wt%) and FeO (11.59wt%) enriched. The $Al_2O_3$ content in this fraction from Pond A was higher than in any other fraction. Unlike the non magnetic mag others fraction of Pond A this fraction from Ponds B and C contained rutile grains that were $Nb_2O_5$ (5.057 and 3.160 wt%) and FeO (1.974 and 1.635wt%) enriched.

### 7.1.5 Cleaner mags fraction

No element in particular dominated the 'cleaner mags' fraction of Ponds A, B and C, although, most grains contained varying concentrations of other ions. Virtually all grains had significant quantities of $SiO_2$, $Nb_2O_5$ and FeO. Only Pond C contained a grain with a high $Al_2O_3$ content (1.522wt%).

### 7.1.6 Primary mags fraction

All the rutile grains analysed in the 'primary mags' fraction of Pond A contained some $SiO_2$ and FeO. However, one grain from Pond A reported a very high $V_2O_3$ value of 1.162wt%. Conversely, Pond B contained grains enriched in $SiO_2$ (2.203wt%), $V_2O_3$ (1.746wt%) and FeO (1.664wt%). Like Pond A, Pond C also contained $SiO_2$ (1.188wt%) and FeO (1.028wt%) enriched grains.

### 7.1.7 Primary HT'S conductors fraction

The rutile grains from 'primary HT'S conductors' fraction of Ponds A, B and C, are almost pure $TiO_2$, and contained very limited substitutions of any other oxides. Although all grains had minor quantities of $SiO_2$, $ZrO_2$, $Nb_2O_5$, $Cr_2O_3$ and FeO, no grain contains more than 0.6wt% of any oxide.

## 7.1.8 HT'S scavengers fraction of Pond B

Grains from the HT'S scavengers fraction of Pond B all contained $SiO_2$, $ZrO_2$ and FeO at low concentrations with only $V_2O_3$ having concentrations close to 1wt%. Ponds A and C contained no rutile grains.

## 7.1.9 HT'S cleaner mids fraction

Rutile grains from the "HT'S cleaner mids' fraction of all three ponds contained significant amounts of $SiO_2$ and $ZrO_2$. Ponds A and C contained slightly higher $V_2O_3$ and $ZrO_2$ concentrations than Pond B. Although the mean $V_2O_3$ content of grains from all ponds was higher than either $SiO_2$ or $ZrO_2$, not all the grains contained a higher proportion of $V_2O_3$. Pond B unlike Ponds A and C yielded some grains, that contained higher levels of $Nb_2O_5$.

## 7.1.10 HT'S cleaner non-conductors fraction

A notable quantity of $SiO_2$ was present in all of the 'HT'S cleaner non-conductors' grains analysed from Ponds A, B and C. All grains of Pond A had low concentrations $ZrO_2$, and $Cr_2O_3$, however, one grain contained 0.629wt% $Nb_2O_5$. Grains from Pond B all contained enriched $Nb_2O_5$ and FeO, with $Nb_2O_5$ in the highest proportion in grains, while those from Pond C had the highest proportion of FeO.

## 7.1.11 HT'S cleaner conductors fraction

All the grains analysed in the 'HT'S cleaner conductors' fraction of Ponds A, B and C contained significant amounts of $SiO_2$ and FeO, with one grain in Pond A containing 1.167wt% FeO. Pond B grains contained significant $ZrO_2$ and $Nb_2O_5$ compared to the other two ponds, while Pond C had a higher $V_2O_3$ and $Nb_2O_5$ content.

## 7.2 Rutile chemistry in relation to magnetic susceptibility, electrostatic conductivity and colour

### 7.2.1 Magnetic Susceptibility

The most magnetic fractions contained a higher proportion of FeO as well as a higher proportion of 'others' (particularly $V_2O_3$, $Nb_2O_5$ and $Al_2O_3$). Magnetic effects although clearly influenced by FeO content are also enhanced by the substitution of other oxides.

### 7.2.2 Electrostatic Conductivity

The electrostatic fractions are more $TiO_2$ pure and contain lower concentrations of other oxides notably $SiO_2$, $ZrO_2$ and FeO. No direct correlation can be made between any of the analysed oxide phases and conductivity. However $SiO_2$ and $V_2O_3$ appear to contribute to electrostatic conductivity as almost all grains in the electrostatic fraction contain notable quantities of these oxides.

### 7.2.3 Colour

Red rutile grains have a slightly higher $Cr_2O_3$ and $Nb_2O_5$ contents, whereas black rutile grains are generally $V_2O_3$ and $Nb_2O_5$ enriched. The blue colouration of rutile grains appears to be the product of multiple substitutions by $SiO_2$, $Al_2O_3$ and $Nb_2O_5$. While yellow colouration is most probably caused by FeO and $Nb_2O_5$ substitutions into the rutile lattice.

Colour may also be influenced by elements such as $C^{4+}$ and $H^+$, which cannot be determined by electron microprobe analysis, or by the interaction of these, and other elements. Colouration may also be due to lattice defects related to ionising radiation and therefore colour and trace element composition relationships must be considered as tentative.

# REFERENCES

Banfield, J.F. and Veblen, D.R. (1991) The structure and origin of Fe-bearing platelets in metamorphic rutile. *Amer. Mineral.*, 76, 113-127.

Barkov, A., Laajoki, K.V.O., Menshikov, Y.P., Alapieti, T.T., Sivonen, S.J. (1997) First terrestrial occurrence of titanium-rich pyrrhottite, marcasite and pyrite in a fenitized xenolith from the Khibina Alkaline Complex, Russia, *Can. Mineral* 35, 875-885.

Bates, R.L. and Jackson J.A. (1980) Glossary of Geology. Am. Geol. Inst. Falls Church, Virginia, 749pp.

Blanchin, M.G., and Bursill, L.A. (1989) Non-classical twinning of alumina precipitates in rutile. *Phil. Mag,* 60, (5), 619-630.

Bloss, D.F. (1971) Crystallography and Crystal Chemistry. Holt, Rinehort and Winston Inc. 543pp.

Botha, G.A. (1987) The Maputaland Group: a provisional lithostratigraphy for coastal KwaZulu-Natal. In: *Maputaland. Focus on the Quaternary evolution of the south-east African coastal plain. Field Guide and Conference Abstracts.* Botha, G.A.(ed.). Pietermaritzburg. International Union for Quaternary Research. Commission on Quaternary Shorelines. African Subcommission.

Bursill, L.A. and Blanchin, M.G. (1989) Interphase structures observed as alumina precipitates in rutile. *Phil. Mag. A,* 60, No.5, 631-642.

Bursill, L.A., Blanchin, M.G., and Smith, D.J. (1984) Precipitation phenomena in non stoichiometric oxides II. {100} Platelet defects in reduced rutiles. *Proc. Royal Soc. of Lon.,* A 391, 373-391.

Bramdeo, S. and Dunlevey, J.N. (1999) The mineral chemistry of rutile. *S. Afr. Inst. Mining Metal.* Symposium Series S23, 63-65.

Bramdeo, S. and Dunlevey, J.N. (2000) The geochemistry of detrital rutile. *Afr. J. Earth Sci.,* 31 (1A), 8-9.

Coastal and Environmental Services (1993) *Environmental Impact Assessment, Eastern Shores of Lake St Lucia (Kingsa/Tojan Lease Area).* Volume 3. Environmental Impact Report, CSIR Env. Serv., 185pp.

Coastal and Environmental Services (1982) *Environmental Impact Assessment, Eastern Shores of Lake St Lucia (Kingsa/Tojan Lease Area).* Volume 1, Part 1. Special reports, CSIR Env. Serv., 741pp.

Deer, W.A., Howie, R.A., and Zussman, J. (1985) *An Introduction to the Rock Forming Minerals.* Longmans 528pp.

Fockema, P.D. (1986) *The heavy mineral deposits north of Richards Bay.* In: Anhaeusser, C.R. and Maske, S. (Eds.), Mineral Deposits of Southern Africa, Geol. Soc. S. Afr., Johannesburg, 2301-2307pp.

Force, E.R. (1991) *Geology of titanium mineral deposits.* Geol. Soc. Am., Special Paper, 259, 112pp.

Graham, J. and Morris, R.C. (1973) Tungsten and antimony-substituted rutile. *Min. Mag.,* 39, 470-473pp.

Gribble, C.D. (1988) *Rutley's Elements of Mineralogy.* Unwin and Hyman, London, 482pp.

------- and Hall, A.J. (1992) *Optical Mineralogy; Principles and Practice.* UCL Press, London, 302pp.

Harris, D.C. (1986) Mineralogy and geochemistry of the main Hemlo Gold Deposit, Hemlo, Ontario, Canada. *Proc. of Gold '86 Symposium, Toronto*, 297-310.

Hassan, W.F. (1994) Geochemistry and mineralogy of Ta-Nb rutlie from Peninsular Malaysia. *J. SE. Asian. Earth. Sc.,* 10, 11-23.

Hobday, D.K. and Orme, A.R. (1974) The Port Durnford Formation. A major Pleistocene barrier lagoon complex along the Zululand coast. *Trans. Geol. Soc. S. Afr.,* 77, 141 - 149.

Hobday, D.K. and Jackson, M.P.A. (1979) Transgressive shore zone sedimentation and syndepositional deformation in the Pleistocene of Zululand, South Africa. *J. Sed. Pet., 49,* 145-158.

Hugo, V.E. (1993) *The study of titanium-bearing oxides in heavy minerals deposited along the east coast of South Africa.* PhD thesis (unpubl.), Univ. Natal, (Durban) 357pp.

Hutchison, C.S. (1974) *Laboratory Handbook of Petrographic Techniques*: John Wiley and Sons, Canada, 527pp

Ishida, S., Hayashi, M., Fujimura, Y. and Fujiyoshi, K. (1990) Spectroscopic study of the chemical state and coloration of chromium in rutile. *J. Amer. Ceramic Soc.,* 73 (11), 3351-3355.

Johnson, M.R. (1994) *Lexicon of South African Stratigraphy Part 1: Phanerozoic Units.* South African Council for Stratigraphy, Council for Geoscience, Pretoria, RSA.

Joseph, K.R. (2000) Titanium. *In:* South Africa's Mineral Industry 1998/1999. 16th Revised Edition, Department of Minerals and Energy, Directorate: Mineral Economics, Pretoria, 115-118.

Linnen, R.L., and Keppler, H. (1997) Columbite solubility in granitic melts: consequences for the enrichment and fractionation of Nb and Ta in the earth's crust. *Contrib. Mineral. Pet.,* 128, 213-227.

Lindsley, D.H. (1976) The crystal structure of the oxide minerals as exemplified by the Fe-Ti oxides. *Reviews in Mineral.,* 3, L1-L60.

------, Rumble III, D., Haggerty, S.E. El Goresy, A., and Huebner, S.J. (1976) Oxide Minerals *Mineralogical Society of America Short Course Notes* Vol 3. Rumble III, D.(ed.). Southern Printing Company, Virginia L1-Hg300.

Maud, R.R. and Botha, G.A. (2000) *Deposits of the South Eastern and Southern coasts,* 19-32, (*In* Partridge T.C. and Maud, R.R., The Cenozoic of Southern Africa. Monograph 40), Oxford University Press. 406pp.

Mdludlu, S. (1997) *Mineralogy of the titanium oxide and associated minerals of the Sibaya Formation.* M.Sc thesis (unpubl.) Univ. Durban-Westville. 128pp.

Michailidis, K.M. (1997) An EPMA and SEM study of niobian - tungstenian rutile from the Fanos Aplitic Granite, Central Macedonia, Northern Greece. *N. Jb. Miner.,* 12, 549-563.

Murphy, P.W. and Taylor, R.K.A. (1999) Market Opportunities for titanium mineral Projects in South Africa. Heavy Minerals 1999, *S. Afr. Inst. Mining Metal. Symposium Series, S23* .

Putnis, A. and McConnell, J.D.C. (1980) *Principles of Mineral Behaviour*. Blackwell Scientific Publications, Oxford, 257pp.

Ramdohr, P. (1969) *The ore minerals and their intergrowths.* Vol. 1, Pergamon Press, London. 174pp.

----- (1980) *The ore minerals and their intergrowths.* Vol. 2 Pergamon Press, Oxford, 207pp.

Rice, C.M., Darke, K.E., Still, J.W. and Lachowski, E.E. (1998) Tungsten-bearing rutile from the Kori Kollo gold mine, Bolivia. *Mineral. Mag.,* 62(3), 421-429.

Rock and Colour Chart Committee (1979). *Rock-colour chart with Munsel colour chips.* The Geological Society of America, Boulder, Colorado.

Rozendaal, A., Philander, C. and de Meijer, R.J. (1999) *Mineralogy of heavy mineral placers along the West Coast of South Africa*. Heavy Minerals 1999, *S. Afr. Inst. Min. Metal.* Symposium Series S23, Symposium Series S23, 67-73.

Smith, R.M.H. (1990) A review of stratigraphy and sedimentary environments of the Karoo Basin of South Africa. *J. Afr. Earth Sci.,* 10, (1/2), 117-137.

Smith, R.H., Eriksson, P.G. and Botha, W.J. (1993) A review of the stratigraphy and sedimentary environments of the Karoo-aged basins of Southern Africa. *J. Afr. Earth Sc.,* 16, (1/2), 143-169.

Singh, V. (1995) *Mineral Stratigraphy of the Kosi Bay Formation*. M.Sc thesis (unpubl) Univ. Durban-Westville. 148pp.

South African Committee for Stratigraphy (SACS) (1980) *Stratigraphy of South Africa.*
*Part 1* (comp. L.E. Kent). Lithostratigraphy of the Republic of South Africa, South
West Africa/Namibia, and the Republics of Bophuthatswana, Transkei and Venda.
Handbook 8. Geol. Surv. S. Afr., 690pp

Tollo, R.P. and Haggerty, S.E. (1987) Nb-Cr - rutile in the Orapa kimberlite, Botswana.
*Can. Mineral.*, 25, 251-264.

Uken R. (2000) KwaZulu-Natal. *In: An Introduction to South Africa's geological and*
*mining Heritage.* (M.J. Viljoen and W.U. Reimold, eds) Geol. Soc. S. Afr., 42-54.

Vlassopoulos, D., Rossman, G.R., and Haggerty, S.E. (1993) Coupled substitution of $H^+$
and minor elements in rutile and the implications of high OH contents in Nb and
Cr-rich rutile from the upper mantle. *Amer. Mineral.*, 78, 1181-1191.

Wenger, M. and Armbruster, T. (1993) Phase relations of columbite and rutile – type
compounds in the system $NiNb_2O_6$ - $TiO_2$. *N. Jb. Miner. Mh.*, 5, 224-232.

Wipplinger, P.E. (1998) Titanium *In:* The Mineral Resources of South Africa. (M.G.C.
Wilson and C.R. Anhaeusser, eds) Handbook16, Council for Geoscience, 621 –
632.

Wilson, M.G.C. and Anhaeusser, C.R. (eds) (1998) *Mineral Resources of South Africa*,
*Handbook* 16, Council for Geoscience, 740pp.

# APPENDIX A1

## Electron microprobe analysis

Appendix A1

The chemical analyses of rutile grains reported in this dissertation were analysed using the JEOL 8800 RXL Superprobe Electron Microprobe in the Discipline of Geology at the University of Durban-Westville working at the operating conditions detailed in Table A1.1 The MAC corrections were carried out using the proprietary software supplied with the JEOL 8800 RXL Super Electron Microprobe. The instrument calibration was checked prior to the commencement of each probe session against a rutile standard.

**Operating conditions:**

Accelerating voltage: 15kV

Probe current: $2.00 \times 10^{-8}$ Amp

Probe diameter: 4 micron

| Oxide | X-ray line | Counting time | Detection Limit | Standard Deviation |
|-------|-----------|---------------|-----------------|--------------------|
| $Nb_2O_5$ | Kα | 40s | 0.049wt% | 0.0163 |
| $Ta_2O_5$ | Kα | 20s | 0.036wt% | 0.0120 |
| $TiO_2$ | Kα | 20s | 0.030wt% | 0.0100 |
| $Al_2O_3$ | Kα | 20s | 0.011wt% | 0.0036 |
| $ZrO_2$ | Kα | 20s | 0.017wt% | 0.0056 |
| $SiO_2$ | Kα | 20s | 0.018wt% | 0.0059 |
| FeO | Kα | 20s | 0.027wt% | 0.0089 |
| $Cr_2O_3$ | Kα | 40s | 0.021wt% | 0.0069 |
| $V_2O_3$ | Kβ | 40s | 0.133wt% | 0.0443 |

Table A1.1 Electron Microprobe operating conditions.

## Standards:

| | |
|---|---|
| $Nb_2O_5$ | Niobium (metal) |
| $Ta_2O_5$ | Tantalum (metal) |
| $TiO_2$ | Titanium (metal) |
| $Al_2O_3$ | Spinel |
| $ZrO_2$ | Baddeleyite |
| $SiO_2$ | Silicon |
| FeO | Magnetite |
| $Cr_2O_3$ | Chromite |
| $V_2O_3$ | Vanadium (metal) |
| MnO | Spessartine |

## Problems encountered

Analysis for V and Cr, are problematic due to the high concentratons of Ti that cause overlap problems with V and Cr peaks. There is an overlap of the very strong $Ti_{k\beta}$ line on the $V_{k\alpha}$ line. A solution to this problem is to use the K$\beta$ line of V for analysis. However, this still poses a problem because of the interference and an overlap of $Cr_{k\alpha}$ on $V_{k\beta}$ line. A Cr-diopside standard was used to assess the the influence of Cr on V. It was found that at low concentrations of Cr (less than 0.5wt%) the of Cr had virtually no affect on $V_2O_3$. However the smaller K$\beta$ line used for V analysis, had a significantly lower count rate and hence the higher detection limit for $V_2O_3$.

## Homogeneity of rutile grains

The homogeneity of grains was assessed using electron backscatter imaging. Element mapping was done on a JEOL Electron Microprobe, for $SiO_2$, FeO, $TiO_2$, $ZrO_2$. Images showed that rutile grain were free from any inclusions.

# APPENDIX A2
## Mineral separation techniques

Appendix A2

Mineral Separation Techniques

1. Magnetic Separation

Frantz Isodynamic Magnetic Separator uses a magnetic field generated by a electric current to exploit the magnetic tendencies of grains. Adjusting this current controls the strength of the magnetic field. A low current induces a low intensity magnetic field and can be used to extract more magnetic minerals. Details of this technique are given in Hutchison (1974).

The Frantz Isodynamic Magnetic Separator was used to separate the 'ilmenite fraction' into 'magnetic ilmenite' and 'non magnetic ilmenite'. The 'mag others' fraction was also split into 'magnetic mag others' and 'non magnetic mag others'.

2. Electrostatic Separation

Electrical separation employs an electrostatic field to separate minerals of different electrical properties by exploiting the attraction between unlike charges and the repulsion between like charges. High-tension separators use a high rate of electrical discharge with electron flow and gaseous ionization. Commercial use has been made possible by employing the "pinning effect" in which non-conducting mineral particles receive a surface charge from the electrode, retain this charge and are "pinned" to the oppositely charged separator surface by positive-negative attraction. When ionization occurs minerals are sprayed with a discharge of electrons, which gives poor conductors a high surface charge, causing them to become "pinned" to the rotor surface

3. Density separation

This technique uses differences in the specific gravity. The dense heavy liquid; tetrabromoethane (TBE) which has a specific gravity of 2.95g/ml at 20°C, causes minerals with a density less than that of the liquid to float and minerals with a density greater than the liquid will sink. Due to the toxicity and high cost of TBE this technique cannot be used on an industrial scale, but in the laboratory provides a relatively quick and efficient method of removing any light mineral grains that were entrained by the Humphries Spirals.

# APPENDIX A3

## Electron microprobe analyses of rutile

## APPENDIX A3 – ELECTRON MICROPROBE ANALYSES OF RUTILE

**Magnetic ilmenite**

**Pond A**

| No. | 1 | 2 | 3 | 4 | 5 | 6 |
|---|---|---|---|---|---|---|
| $SiO_2$ | 0.565 | 1.167 | 0.351 | 0.342 | 0.331 | 0.420 |
| $TiO_2$ | 97.477 | 93.292 | 97.963 | 98.409 | 98.232 | 98.514 |
| $ZrO_2$ | 0.135 | 0.096 | 0.219 | 0.155 | 0.112 | 0.053 |
| $V_2O_3$ | 0.521 | 0.731 | 0.280 | 0.357 | 0.892 | 0.227 |
| $Ta_2O_5$ | nd | 0.052 | nd | nd | nd | nd |
| $Nb_2O_5$ | 0.110 | 0.412 | 0.106 | 0.280 | 0.169 | 0.124 |
| $Al_2O_3$ | 0.011 | 0.162 | 0.033 | 0.028 | nd | nd |
| $Cr_2O_3$ | 0.068 | 0.063 | 0.028 | nd | 0.154 | 0.070 |
| FeO | 0.492 | 2.079 | 0.318 | 0.132 | 0.126 | 0.186 |
| Total | 99.379 | 98.054 | 99.298 | 99.703 | 100.016 | 99.594 |

**Pond B**

| No. | 1 | 2 | 3 | 4 |
|---|---|---|---|---|
| $SiO_2$ | 0.107 | 0.147 | 0.092 | 0.076 |
| $TiO_2$ | 98.248 | 98.415 | 98.145 | 99.985 |
| $ZrO_2$ | 0.052 | 0.065 | 0.073 | 0.060 |
| $V_2O_3$ | 0.270 | 0.203 | nd | nd |
| $Ta_2O_5$ | nd | nd | 0.075 | 0.064 |
| $Nb_2O_5$ | 0.121 | 0.079 | 0.249 | nd |
| $Al_2O_3$ | nd | 0.026 | 0.079 | nd |
| $Cr_2O_3$ | nd | 0.034 | nd | 0.022 |
| FeO | 0.252 | 0.291 | 0.388 | 0.224 |
| Total | 99.050 | 99.260 | 99.101 | 100.431 |

**Pond B**

| No. | 5 | 6 | 7 | 8 |
|---|---|---|---|---|
| $SiO_2$ | 0.356 | 4.061 | 0.118 | 0.229 |
| $TiO_2$ | 95.306 | 80.424 | 97.992 | 99.252 |
| $ZrO_2$ | 0.020 | nd | 0.160 | 0.094 |
| $V_2O_3$ | nd | nd | nd | nd |
| $Ta_2O_5$ | 0.206 | nd | nd | nd |
| $Nb_2O_5$ | nd | nd | 0.067 | 0.124 |
| $Al_2O_3$ | 0.060 | 2.601 | 0.031 | 0.029 |
| $Cr_2O_3$ | nd | nd | nd | 0.033 |
| FeO | 4.080 | 11.118 | 0.065 | 0.152 |
| Total | 100.028 | 98.204 | 98.433 | 99.913 |

**Pond C**

| No. | 1 | 3 | 4 | 5 |
|---|---|---|---|---|
| $SiO_2$ | 0.238 | 0.206 | 0.256 | 0.213 |
| $TiO_2$ | 97.854 | 97.243 | 97.681 | 97.596 |
| $ZrO_2$ | 0.035 | 0.243 | 0.249 | 0.208 |
| $V_2O_3$ | 0.706 | 0.554 | 0.547 | nd |
| $Ta_2O_5$ | 0.260 | nd | nd | 0.083 |
| $Nb_2O_5$ | 0.849 | nd | 0.126 | 0.199 |
| $Al_2O_3$ | 0.024 | nd | nd | 0.013 |
| $Cr_2O_3$ | 0.218 | 0.154 | 0.120 | 0.151 |
| FeO | 0.267 | nd | 0.193 | 0.197 |
| Total | 100.451 | 98.400 | 99.172 | 98.660 |

## Non magnetic ilmenite
### Pond A

| No. | 1 | 2 | 3 | 4 | 5 | 6 | 7 | 8 | 9 | 10 | 11 |
|-----|-----|-----|-----|-----|-----|-----|-----|-----|-----|-----|-----|
| $SiO_2$ | 0.298 | 0.077 | 0.245 | 0.928 | 0.201 | 0.074 | 0.131 | 0.134 | 1.185 | 0.098 | 0.116 |
| $TiO_2$ | 99.363 | 99.766 | 99.464 | 98.698 | 99.133 | 99.881 | 99.993 | 99.086 | 94.759 | 99.823 | 99.499 |
| $ZrO_2$ | 0.225 | 0.092 | 0.200 | 0.260 | 0.272 | 0.218 | 0.048 | nd | 0.239 | 0.223 | 0.475 |
| $V_2O_3$ | 0.571 | 0.402 | nd | 0.322 | 0.834 | 0.146 | 0.154 | 0.445 | nd | 0.270 | 0.745 |
| $Ta_2O_5$ | nd | nd | nd | nd | nd | 0.217 | nd | nd | nd | 0.193 | 0.136 |
| $Nb_2O_5$ | 0.087 | 0.068 | 0.110 | nd | 0.056 | nd | 0.091 | 0.112 | 0.167 | 0.085 | nd |
| $Al_2O_3$ | 0.062 | 0.023 | 0.020 | 0.384 | nd | 0.013 | nd | 0.020 | 0.694 | nd | nd |
| $Cr_2O_3$ | 0.125 | 0.119 | 0.021 | 0.211 | 0.144 | 0.098 | 0.068 | 0.128 | 0.034 | 0.038 | 0.137 |
| FeO | 0.135 | 0.084 | 0.394 | 0.167 | 0.049 | 0.054 | 0.119 | 0.069 | 1.085 | 0.811 | 0.033 |
| Total | 100.866 | 100.631 | 100.454 | 100.970 | 100.689 | 100.701 | 100.604 | 99.994 | 98.163 | 101.541 | 101.141 |

### Pond A

| No. | 12 | 13 |
|-----|-----|-----|
| $SiO_2$ | 0.952 | 0.165 |
| $TiO_2$ | 95.650 | 99.737 |
| $ZrO_2$ | 0.355 | 0.106 |
| $V_2O_3$ | nd | 0.344 |
| $Ta_2O_5$ | 0.303 | 0.105 |
| $Nb_2O_5$ | 0.136 | nd |
| $Al_2O_3$ | 0.717 | nd |
| $Cr_2O_3$ | 0.044 | 0.125 |
| FeO | 1.082 | nd |
| Total | 99.239 | 100.582 |

### Pond B

| No. | 1 | 2 | 3 | 4 |
|-----|-----|-----|-----|-----|
| $SiO_2$ | 0.541 | 0.531 | 0.468 | 0.491 |
| $TiO_2$ | 94.343 | 96.143 | 97.489 | 96.555 |
| $ZrO_2$ | 0.091 | 0.106 | 0.128 | 0.527 |
| $V_2O_3$ | 0.479 | 0.964 | 0.737 | 0.616 |
| $Ta_2O_5$ | 0.063 | nd | nd | nd |
| $Nb_2O_5$ | 2.185 | 0.219 | 0.164 | 0.193 |
| $Al_2O_3$ | 0.059 | 0.021 | 0.042 | 0.015 |
| $Cr_2O_3$ | 0.152 | 0.147 | 0.158 | 0.133 |
| FeO | 0.916 | 0.116 | 0.037 | 0.205 |
| Total | 98.829 | 98.247 | 99.223 | 98.735 |

## Pond C

| No. | 1 | 2 | 3 | 4 | 5 | 6 | 7 | 8 | 9 | 10 | 11 |
|---|---|---|---|---|---|---|---|---|---|---|---|
| $SiO_2$ | 1.076 | 0.158 | 0.120 | 0.147 | 0.825 | 0.163 | 1.386 | 0.383 | 0.484 | 0.377 | 0.402 |
| $TiO_2$ | 98.682 | 97.901 | 97.520 | 97.727 | 97.113 | 98.210 | 95.297 | 92.989 | 98.733 | 98.652 | 99.202 |
| $ZrO_2$ | nd | 0.030 | 0.237 | 0.097 | nd | nd | 0.037 | 0.343 | 0.058 | 0.080 | nd |
| $V_2O_3$ | 0.135 | 0.367 | 0.154 | 0.135 | 0.396 | 0.858 | 0.656 | 0.644 | 0.569 | 0.212 | 0.183 |
| $Ta_2O_5$ | nd | 0.057 | nd | nd | nd | 0.039 | nd | nd | nd | nd | nd |
| $Nb_2O_5$ | 0.122 | 0.474 | 0.194 | 0.134 | 0.231 | 0.246 | 0.284 | 2.825 | 0.304 | 0.389 | 0.058 |
| $Al_2O_3$ | 0.022 | nd | nd | nd | 0.048 | nd | 0.240 | 0.082 | 0.022 | nd | 0.054 |
| $Cr_2O_3$ | 0.033 | 0.087 | 0.053 | 0.057 | 0.125 | 0.029 | 0.185 | 0.094 | 0.036 | nd | 0.027 |
| $FeO$ | 0.591 | 0.273 | 0.253 | 0.206 | 0.519 | 0.395 | 0.402 | 1.002 | 0.265 | 0.277 | 0.306 |
| Total | 100.661 | 99.347 | 98.531 | 98.503 | 99.257 | 99.940 | 98.487 | 98.362 | 100.471 | 99.987 | 100.232 |

## Pond C

| No. | 12 |
|---|---|
| $SiO_2$ | 0.559 |
| $TiO_2$ | 97.530 |
| $ZrO_2$ | nd |
| $V_2O_3$ | nd |
| $Ta_2O_5$ | 0.137 |
| $Nb_2O_5$ | 0.411 |
| $Al_2O_3$ | 0.134 |
| $Cr_2O_3$ | 0.039 |
| $FeO$ | 0.663 |
| Total | 99.473 |

**Magnetic Mag-other**

## Pond A

| No. | 1 | 2 | 3 | 4 | 5 | 6 | 7 |
|---|---|---|---|---|---|---|---|
| $SiO_2$ | 0.627 | 0.714 | 0.730 | 4.525 | 0.193 | 0.135 | 0.390 |
| $TiO_2$ | 98.128 | 94.779 | 98.522 | 95.166 | 97.379 | 97.376 | 96.048 |
| $ZrO_2$ | nd | nd | 0.023 | 0.147 | nd | 0.283 | 0.264 |
| $V_2O_3$ | nd | 0.308 | nd | 0.255 | nd | 0.763 | 0.733 |
| $Ta_2O_5$ | 0.057 | 0.049 | 0.110 | nd | nd | 0.044 | 0.047 |
| $Nb_2O_5$ | 0.109 | nd | nd | 0.573 | 0.422 | nd | 0.155 |
| $Al_2O_3$ | 0.011 | 0.035 | 0.018 | 0.732 | 0.025 | nd | 0.043 |
| $Cr_2O_3$ | nd | nd | nd | nd | 0.036 | 0.067 | 0.093 |
| FeO | 0.121 | 3.540 | 0.087 | 0.594 | 0.459 | 0.201 | 0.757 |
| Total | 99.053 | 99.425 | 99.490 | 101.992 | 98.514 | 98.869 | 98.530 |

## Pond B

| No. | 1 | 2 | 3 | 4 |
|---|---|---|---|---|
| $SiO_2$ | 1.689 | 0.166 | 1.029 | 0.100 |
| $TiO_2$ | 87.773 | 99.138 | 96.345 | 98.113 |
| $ZrO_2$ | 0.067 | 0.039 | nd | 0.117 |
| $V_2O_3$ | 0.325 | 0.367 | 0.251 | 0.377 |
| $Ta_2O_5$ | nd | nd | nd | nd |
| $Nb_2O_5$ | 0.342 | 0.285 | 0.146 | 0.137 |
| $Al_2O_3$ | 2.163 | 0.047 | 0.125 | 0.022 |
| $Cr_2O_3$ | 0.100 | 0.053 | nd | 0.060 |
| FeO | 5.562 | 0.219 | 1.277 | 0.069 |
| Total | 98.021 | 100.314 | 99.173 | 98.995 |

## Pond B

| | 5 | 6 | 7 | 8 | 9 | 10 | 11 | 12 | 13 |
|---|---|---|---|---|---|---|---|---|---|
| | 0.093 | 0.153 | 0.674 | 0.091 | 0.048 | 0.065 | 0.062 | 0.046 | 0.494 |
| | 97.529 | 98.458 | 95.344 | 98.127 | 98.128 | 97.685 | 96.378 | 97.286 | 76.844 |
| | 0.209 | 0.046 | 0.236 | 0.219 | 0.122 | nd | 0.095 | 0.236 | 0.022 |
| | 0.589 | 0.512 | nd | nd | 0.328 | nd | 0.801 | 0.396 | 0.382 |
| | nd | nd | nd | nd | nd | nd | nd | 0.075 | nd |
| | 0.176 | nd | 0.399 | 0.155 | 0.158 | 0.134 | 0.556 | 0.234 | 0.078 |
| | 0.082 | 0.054 | 0.604 | 0.033 | 0.037 | nd | 0.044 | nd | 0.399 |
| | 0.039 | 0.099 | nd | nd | 0.078 | nd | 0.166 | nd | 0.035 |
| | 0.198 | 0.079 | 1.012 | 0.299 | 0.159 | 0.158 | 0.175 | 0.152 | 21.509 |
| | 98.915 | 99.401 | 98.269 | 98.924 | 99.058 | 98.042 | 98.277 | 98.425 | 99.763 |

## Pond C

| No. | 1 | 2 | 3 |
|---|---|---|---|
| $SiO_2$ | 1.081 | 0.808 | 0.770 |
| $TiO_2$ | 87.330 | 82.519 | 94.347 |
| $ZrO_2$ | 0.114 | 0.055 | 0.030 |
| $V_2O_3$ | 0.223 | nd | nd |
| $Ta_2O_5$ | 0.099 | nd | 0.092 |
| $Nb_2O_5$ | 0.071 | 0.063 | 0.675 |
| $Al_2O_3$ | 0.161 | 0.176 | 0.092 |
| $Cr_2O_3$ | 0.065 | 0.043 | 0.102 |
| FeO | 9.544 | 16.482 | 4.031 |
| Total | 98.688 | 100.146 | 100.139 |

**Pond C**

| No. | 4 | 5 | 6 | 7 | 8 | 9 | 10 | 11 | 12 | 13 | 14 | 15 | 16 |
|---|---|---|---|---|---|---|---|---|---|---|---|---|---|
| $SiO_2$ | 0.139 | 0.748 | 0.092 | 0.312 | 0.077 | 0.088 | 0.118 | 0.195 | 1.297 | 0.337 | 0.555 | 0.386 | 12.431 |
| $TiO_2$ | 96.083 | 97.577 | 98.434 | 96.726 | 97.568 | 97.420 | 99.020 | 97.209 | 94.121 | 99.740 | 98.810 | 99.043 | 85.574 |
| $ZrO_2$ | 0.054 | nd | 0.121 | 0.024 | 0.308 | 0.322 | nd | 0.033 | 0.104 | nd | nd | 0.036 | 0.027 |
| $V_2O_3$ | nd | nd | 0.734 | nd | 0.598 | 0.695 | nd | nd | nd | 0.351 | nd | nd | 0.357 |
| $Ta_2O_5$ | 0.103 | nd | nd | nd | nd | nd | 0.054 | nd | nd | nd | nd | nd | nd |
| $Nb_2O_5$ | 0.084 | 0.053 | 0.182 | 0.155 | 0.282 | 0.228 | 0.079 | nd | 0.260 | nd | 0.068 | 0.479 | 0.554 |
| $Al_2O_3$ | 0.036 | 0.016 | nd | 0.027 | 0.013 | 0.026 | 0.029 | nd | 0.533 | 0.016 | 0.020 | 0.070 | 0.020 |
| $Cr_2O_3$ | 0.034 | nd | nd | nd | 0.054 | 0.090 | nd | nd | 0.098 | 0.095 | 0.072 | nd | 0.063 |
| FeO | 2.952 | 3.207 | 0.069 | 1.262 | 0.059 | 0.057 | 0.405 | 1.646 | 3.342 | 0.506 | 0.527 | 0.567 | 1.644 |
| Total | 99.485 | 101.601 | 99.632 | 98.506 | 98.959 | 98.926 | 99.705 | 99.083 | 99.755 | 101.045 | 100.052 | 100.581 | 100.67 |

**Pond C**

| No. | 17 | 18 | 19 | 20 | 21 | 22 | 23 | 24 | 25 | 26 | 27 | 28 | 29 |
|---|---|---|---|---|---|---|---|---|---|---|---|---|---|
| $SiO_2$ | 0.077 | 0.089 | 0.084 | 4.816 | 0.392 | 1.426 | 0.481 | 2.350 | 2.165 | 1.826 | 0.449 | 0.415 | 0.230 |
| $TiO_2$ | 96.129 | 98.494 | 97.648 | 91.062 | 99.107 | 96.925 | 96.278 | 96.219 | 90.531 | 87.529 | 98.851 | 99.032 | 95.235 |
| $ZrO_2$ | 0.075 | 0.035 | 0.046 | 0.027 | 0.108 | 0.065 | 0.038 | 0.099 | 0.062 | 0.314 | nd | 0.186 | 0.023 |
| $V_2O_3$ | 0.337 | nd | nd | 0.615 | 0.447 | 0.300 | nd | nd | nd | 0.498 | nd | 0.425 | nd |
| $Ta_2O_5$ | 0.054 | nd | nd | nd | nd | nd | nd | nd | 0.193 | nd | nd | nd | nd |
| $Nb_2O_5$ | 0.332 | 0.091 | 0.796 | 0.192 | 0.194 | 0.183 | 0.177 | 0.105 | 0.077 | 0.387 | 0.128 | nd | 0.289 |
| $Al_2O_3$ | 0.124 | 0.031 | 0.117 | 0.467 | nd | 0.320 | nd | 0.166 | 0.583 | 0.258 | 0.028 | nd | 0.023 |
| $Cr_2O_3$ | 0.04 | 0.041 | nd | 0.044 | 0.143 | 0.076 | nd | 0.032 | 0.042 | 0.155 | nd | 0.106 | 0.044 |
| FeO | 2.581 | 0.244 | 0.837 | 3.654 | 0.081 | 0.295 | 2.407 | 0.147 | 6.559 | 7.583 | nd | 0.065 | 2.627 |
| Total | 99.749 | 99.025 | 99.528 | 100.877 | 100.472 | 99.590 | 99.381 | 99.118 | 100.212 | 98.550 | 99.456 | 100.229 | 98.471 |

**Pond C**

| No. | 30 | 31 | 32 | 33 | 34 | 35 | 36 | 37 |
|-----|-----|-----|-----|-----|-----|-----|-----|-----|
| $SiO_2$ | 0.258 | 0.212 | 0.238 | 0.654 | 0.250 | 0.277 | 0.206 | 0.209 |
| $TiO_2$ | 96.728 | 98.033 | 97.938 | 96.419 | 91.320 | 97.262 | 97.762 | 98.148 |
| $ZrO_2$ | 0.185 | nd | nd | 0.074 | 0.094 | 0.061 | 0.082 | 0.041 |
| $V_2O_3$ | 0.704 | nd | nd | nd | 0.355 | nd | 0.406 | nd |
| $Ta_2O_5$ | nd | 0.052 | 0.036 | nd | nd | nd | nd | 0.057 |
| $Nb_2O_5$ | 0.395 | 0.222 | 0.383 | 0.235 | 4.741 | 1.167 | 0.401 | 0.602 |
| $Al_2O_3$ | 0.041 | nd | 0.028 | 0.382 | 0.051 | 0.018 | 0.043 | nd |
| $Cr_2O_3$ | 0.036 | nd | 0.101 | nd | 0.057 | nd | nd | nd |
| FeO | 0.156 | 0.193 | 0.165 | 1.007 | 2.450 | 0.812 | 0.159 | 0.605 |
| Total | 98.503 | 98.712 | 98.889 | 98.771 | 99.318 | 99.597 | 99.059 | 99.662 |

**Non magnetic mag others**

## Pond A

| No. | 1 | 2 | 3 | 4 | 5 | 6 | 7 | 8 | 9 | 10 | 11 | 12 | 13 |
|-----|---|---|---|---|---|---|---|---|---|----|----|----|----|
| $SiO_2$ | 0.911 | 0.097 | 2.933 | 0.079 | 0.078 | 0.176 | 0.756 | 0.124 | 0.162 | 0.152 | 0.108 | 0.146 | 0.162 |
| $TiO_2$ | 92.933 | 100.354 | 79.873 | 98.692 | 91.108 | 99.409 | 96.822 | 99.086 | 98.608 | 98.615 | 98.282 | 97.655 | 96.854 |
| $ZrO_2$ | nd | 0.185 | 0.133 | 0.028 | 0.130 | 0.160 | 0.047 | 0.121 | 0.100 | 0.197 | 0.118 | 0.114 | 0.080 |
| $V_2O_3$ | 0.576 | nd | 0.379 | 0.221 | 0.479 | 0.724 | nd | 1.215 | 0.174 | 1.023 | 0.791 | 0.955 | 0.886 |
| $Ta_2O_5$ | nd | nd | 0.067 | nd | 0.070 | nd | nd | 0.044 | nd | nd | nd | nd | nd |
| $Nb_2O_5$ | 0.138 | 0.155 | nd | 0.125 | 2.778 | 0.270 | 0.201 | 0.279 | 0.097 | 0.179 | 0.282 | 0.522 | 1.654 |
| $Al_2O_3$ | 0.140 | nd | 3.456 | 0.040 | 0.136 | 0.020 | 0.503 | 0.022 | nd | 0.017 | 0.014 | 0.022 | nd |
| $Cr_2O_3$ | nd | 0.033 | 0.153 | nd | 0.046 | 0.060 | nd | 0.055 | nd | 0.148 | 0.065 | 0.073 | 0.106 |
| $FeO$ | 4.139 | 0.242 | 11.590 | 2.622 | 3.705 | 0.085 | 1.288 | nd | 0.033 | 0.092 | 0.127 | 0.137 | 0.379 |
| Total | 98.837 | 101.066 | 98.584 | 101.807 | 98.530 | 100.904 | 99.617 | 100.946 | 99.174 | 100.423 | 99.787 | 99.624 | 100.121 |

## Pond A

| No. | 14 | 15 | 16 | 17 | 18 | 19 | 20 | 21 | 22 | 23 | 24 | 25 | 26 |
|-----|----|----|----|----|----|----|----|----|----|----|----|----|----|
| $SiO_2$ | 0.158 | 0.189 | 0.205 | 0.164 | 0.180 | 0.175 | 2.109 | 0.193 | 0.291 | 0.310 | 0.182 | 0.184 | 0.284 |
| $TiO_2$ | 98.207 | 97.594 | 97.665 | 95.614 | 98.522 | 97.747 | 98.110 | 97.026 | 97.335 | 97.065 | 96.422 | 97.326 | 98.036 |
| $ZrO_2$ | 0.116 | 0.133 | 0.152 | 0.257 | 0.155 | 0.179 | nd | 0.102 | nd | 0.021 | nd | 0.052 | nd |
| $V_2O_3$ | 1.225 | 0.482 | 0.521 | 0.683 | 0.888 | 1.109 | nd | 0.801 | 0.338 | 0.550 | 0.713 | 0.993 | nd |
| $Ta_2O_5$ | nd | 0.067 | nd | 0.059 | nd | 0.052 | nd | nd | nd | nd | nd | nd | nd |
| $Nb_2O_5$ | 0.164 | 0.283 | 0.552 | 2.268 | 0.173 | 0.100 | 0.284 | 0.161 | 0.058 | 0.529 | 1.172 | 0.425 | 0.547 |
| $Al_2O_3$ | nd | nd | nd | 0.242 | nd | 0.017 | 0.278 | 0.011 | 0.064 | 0.076 | nd | nd | 0.060 |
| $Cr_2O_3$ | 0.138 | 0.068 | nd | 0.163 | 0.069 | 0.052 | nd | 0.114 | 0.034 | 0.226 | 0.220 | 0.230 | nd |
| $FeO$ | nd | 0.545 | 0.065 | 0.577 | 0.108 | 0.116 | 0.348 | 0.080 | 0.239 | 0.343 | 0.659 | 0.152 | 0.562 |
| Total | 100.008 | 99.361 | 99.160 | 100.027 | 100.095 | 99.547 | 101.129 | 98.488 | 98.359 | 99.120 | 99.368 | 99.362 | 99.489 |

## Pond B

| No. | 1 | 2 | 3 | 4 | 5 | 6 | 7 | 8 | 9 | 10 | 11 | 12 | 13 |
|---|---|---|---|---|---|---|---|---|---|---|---|---|---|
| $SiO_2$ | 0.629 | 0.340 | 0.249 | 0.564 | 0.329 | 0.273 | 0.286 | 0.288 | 0.496 | 0.592 | 0.463 | 0.462 | 0.231 |
| $TiO_2$ | 98.439 | 98.043 | 98.843 | 96.614 | 89.703 | 97.705 | 97.453 | 96.643 | 96.364 | 94.548 | 96.115 | 97.258 | 98.371 |
| $ZrO_2$ | 0.097 | 0.048 | 0.124 | 0.103 | 0.046 | 0.100 | 0.119 | 0.091 | nd | nd | nd | nd | nd |
| $V_2O_3$ | 0.666 | 0.550 | nd | 0.386 | 0.767 | 0.849 | nd | 0.232 | 0.704 | 0.264 | nd | nd | nd |
| $Ta_2O_5$ | nd | nd | nd | nd | nd | nd | nd | nd | 0.800 | 0.103 | 0.542 | 0.568 | nd |
| $Nb_2O_5$ | 0.365 | 0.185 | 0.212 | 0.310 | 5.057 | 0.282 | 0.112 | 0.550 | 0.061 | 1.614 | 0.914 | 0.244 | 0.070 |
| $Al_2O_3$ | 0.012 | 0.027 | nd | 0.028 | 0.168 | 0.026 | 0.036 | nd | 0.037 | 0.261 | nd | nd | 0.074 |
| $Cr_2O_3$ | 0.045 | 0.061 | nd | nd | 0.115 | 0.060 | nd | 0.075 | nd | 0.326 | nd | nd | nd |
| $FeO$ | 0.080 | 0.211 | 0.109 | 0.327 | 1.974 | 0.190 | 0.094 | 0.512 | 0.114 | 1.063 | 0.835 | nd | 0.174 |
| Total | 100.333 | 99.465 | 99.537 | 98.332 | 98.159 | 99.485 | 98.100 | 98.391 | 98.576 | 98.771 | 98.869 | 98.532 | 98.920 |

## Pond B

| No. | 14 | 15 | 16 | 17 | 18 |
|---|---|---|---|---|---|
| $SiO_2$ | 0.309 | 0.374 | 0.265 | 0.336 | 0.342 |
| $TiO_2$ | 97.569 | 97.452 | 96.159 | 96.840 | 97.112 |
| $ZrO_2$ | 0.068 | nd | 0.047 | nd | nd |
| $V_2O_3$ | 0.342 | nd | nd | nd | 0.141 |
| $Ta_2O_5$ | 0.265 | nd | 0.271 | 0.098 | 0.132 |
| $Nb_2O_5$ | nd | 0.191 | 0.745 | 0.140 | 0.285 |
| $Al_2O_3$ | nd | nd | 0.058 | 0.026 | 0.046 |
| $Cr_2O_3$ | 0.060 | 0.071 | nd | 0.082 | 0.082 |
| $FeO$ | 0.144 | 0.693 | 0.891 | 0.961 | 0.167 |
| Total | 98.757 | 98.781 | 98.436 | 98.483 | 98.307 |

## Pond C

| No. | 1 | 2 | 3 | 4 | 5 | 6 |
|---|---|---|---|---|---|---|
| $SiO_2$ | 0.238 | 0.153 | 0.210 | 0.223 | 0.172 | 0.222 |
| $TiO_2$ | 93.092 | 97.927 | 97.681 | 98.283 | 98.056 | 97.327 |
| $ZrO_2$ | nd | 0.055 | 0.149 | 0.136 | 0.167 | 0.298 |
| $V_2O_3$ | 0.644 | 0.627 | 0.589 | 0.135 | 0.145 | 0.743 |
| $Ta_2O_5$ | nd | nd | nd | 0.070 | nd | 0.067 |
| $Nb_2O_5$ | 3.616 | 0.219 | 0.191 | 0.270 | 0.079 | 0.352 |
| $Al_2O_3$ | 0.213 | 0.024 | 0.040 | 0.034 | nd | 0.037 |
| $Cr_2O_3$ | 0.103 | nd | 0.044 | 0.040 | 0.075 | 0.055 |
| $FeO$ | 0.664 | 0.222 | 0.118 | 0.180 | 0.103 | 0.081 |
| Total | 98.570 | 99.227 | 99.022 | 99.371 | 98.797 | 99.182 |

## Pond C

| No. | 7 | 8 | 9 | 10 | 11 | 12 | 13 | 14 | 15 | 16 | 17 | 18 | 19 |
|---|---|---|---|---|---|---|---|---|---|---|---|---|---|
| $SiO_2$ | 0.226 | 0.160 | 0.128 | 0.281 | 0.262 | 0.288 | 0.361 | 0.248 | 0.082 | 0.168 | 0.062 | 0.086 | 0.091 |
| $TiO_2$ | 97.661 | 97.970 | 98.826 | 97.709 | 96.271 | 96.968 | 97.325 | 97.471 | 97.128 | 96.513 | 96.829 | 96.958 | 97.655 |
| $ZrO_2$ | 0.028 | nd | 0.094 | 0.159 | 0.020 | 0.019 | nd | nd | 0.120 | 0.065 | 0.085 | 0.068 | 0.094 |
| $V_2O_3$ | 0.222 | 0.135 | 0.270 | 0.444 | 0.289 | nd | nd | nd | nd | 0.376 | nd | 0.724 | 0.117 |
| $Ta_2O_5$ | nd | nd | nd | nd | nd | nd | nd | nd | 0.057 | nd | nd | 0.116 | 0.232 |
| $Nb_2O_5$ | 0.246 | 0.731 | 0.167 | 0.155 | 0.283 | nd | 0.061 | 0.204 | 0.291 | nd | 0.085 | 0.134 | 0.180 |
| $Al_2O_3$ | 0.038 | nd | 0.033 | 0.032 | 0.022 | 0.053 | 0.116 | nd | 0.030 | nd | 0.063 | nd | 0.030 |
| $Cr_2O_3$ | 0.078 | nd | 0.036 | 0.055 | 0.033 | 0.022 | 0.021 | nd | nd | 0.079 | 0.031 | 0.213 | 0.052 |
| FeO | 0.156 | 0.177 | 1.635 | 0.255 | 1.290 | 0.711 | 0.374 | 0.534 | 0.369 | 0.869 | 1.203 | 0.068 | 0.194 |
| Total | 98.655 | 99.173 | 101.189 | 99.090 | 98.470 | 98.061 | 98.258 | 98.457 | 98.077 | 98.070 | 98.358 | 98.367 | 98.645 |

## Pond C

| No. | 20 | 21 |
|---|---|---|
| $SiO_2$ | 0.061 | 0.045 |
| $TiO_2$ | 97.616 | 97.681 |
| $ZrO_2$ | 0.157 | 0.132 |
| $V_2O_3$ | 0.592 | 0.402 |
| $Ta_2O_5$ | nd | nd |
| $Nb_2O_5$ | 0.064 | 0.083 |
| $Al_2O_3$ | 0.012 | 0.072 |
| $Cr_2O_3$ | 0.192 | 0.096 |
| FeO | 0.132 | 0.125 |
| Total | 98.826 | 98.636 |

**Cleaner Mags**
**Pond A**

| No. | 1 | 2 | 3 | 4 | 5 | 6 | 7 | 8 | 9 | 10 | 11 | 12 |
|---|---|---|---|---|---|---|---|---|---|---|---|---|
| $SiO_2$ | 0.090 | 0.065 | 0.135 | 0.524 | 0.145 | 0.202 | 0.226 | 0.207 | 0.322 | 0.232 | 0.199 | 0.225 |
| $TiO_2$ | 98.543 | 99.350 | 99.456 | 98.337 | 99.316 | 98.724 | 99.161 | 98.717 | 98.726 | 99.340 | 99.574 | 98.839 |
| $ZrO_2$ | 0.153 | 0.071 | nd | 0.054 | 0.128 | 0.101 | 0.065 | 0.074 | 0.187 | 0.092 | 0.032 | 0.081 |
| $V_2O_3$ | nd | nd | nd | nd | nd | nd | nd | 0.247 | 0.282 | nd | nd | nd |
| $Ta_2O_5$ | nd | 0.153 | 0.068 | 0.335 | nd | nd | nd | 0.128 | 0.274 | nd | nd | 0.221 |
| $Nb_2O_5$ | 0.167 | 0.228 | nd | 0.235 | 0.264 | 0.188 | 0.164 | 0.259 | 0.167 | 0.167 | 0.213 | 0.067 |
| $Al_2O_3$ | 0.035 | 0.028 | nd | 0.371 | 0.031 | nd | 0.017 | nd | 0.012 | 0.048 | 0.013 | 0.020 |
| $Cr_2O_3$ | 0.082 | 0.049 | 0.060 | 0.191 | nd | 0.049 | 0.071 | 0.164 | 0.060 | 0.038 | nd | 0.076 |
| $FeO$ | 0.164 | 0.232 | 0.225 | 0.148 | 0.240 | 0.187 | 0.088 | 0.076 | 0.072 | 0.263 | 0.065 | 0.426 |
| Total | 99.234 | 100.176 | 99.944 | 100.195 | 100.124 | 99.451 | 99.792 | 99.872 | 100.102 | 100.180 | 100.096 | 99.955 |

**Pond A**

| No. | 14 | 15 |
|---|---|---|
| $SiO_2$ | 0.306 | 0.341 |
| $TiO_2$ | 98.590 | 99.138 |
| $ZrO_2$ | 0.101 | 0.079 |
| $V_2O_3$ | nd | nd |
| $Ta_2O_5$ | nd | nd |
| $Nb_2O_5$ | 0.222 | nd |
| $Al_2O_3$ | 0.062 | 0.049 |
| $Cr_2O_3$ | 0.060 | nd |
| $FeO$ | 0.091 | 0.210 |
| Total | 99.432 | 99.817 |

**Pond B**

| No. | 1 | 2 | 3 | 4 | 5 | 6 | 7 | 8 |
|---|---|---|---|---|---|---|---|---|
| $SiO_2$ | 0.334 | 0.287 | 0.257 | 0.326 | 0.295 | 0.245 | 0.245 | 0.210 |
| $TiO_2$ | 99.670 | 99.373 | 98.627 | 98.187 | 99.123 | 99.446 | 99.901 | 99.339 |
| $ZrO_2$ | 0.188 | 0.267 | 0.037 | 0.211 | 0.055 | 0.089 | 0.023 | 0.122 |
| $V_2O_3$ | nd | nd | nd | 0.168 | nd | 0.212 | 0.194 | nd |
| $Ta_2O_5$ | 0.082 | nd | 0.107 | 0.224 | 0.249 | nd | nd | 0.039 |
| $Nb_2O_5$ | 0.152 | 0.097 | 0.356 | nd | 0.222 | 0.243 | 0.070 | 0.146 |
| $Al_2O_3$ | 0.022 | 0.011 | 0.020 | 0.711 | 0.098 | 0.020 | nd | 0.031 |
| $Cr_2O_3$ | 0.159 | 0.049 | 0.033 | 0.055 | 0.082 | 0.071 | nd | 0.082 |
| $FeO$ | 0.107 | 0.107 | 0.152 | 0.168 | 0.590 | 0.171 | 0.320 | 0.046 |
| Total | 100.714 | 100.191 | 99.589 | 100.050 | 100.714 | 100.497 | 100.753 | 100.015 |

## Pond B

| No. | 10 | 11 | 12 | 13 | 14 | 15 |
|---|---|---|---|---|---|---|
| $SiO_2$ | 0.162 | 0.243 | 0.145 | 0.420 | 0.380 | 0.504 |
| $TiO_2$ | 98.882 | 98.575 | 98.870 | 98.832 | 97.845 | 99.144 |
| $ZrO_2$ | 0.087 | 0.075 | 0.038 | 0.099 | 0.159 | 0.097 |
| $V_2O_3$ | nd | 0.362 | nd | nd | nd | nd |
| $Ta_2O_5$ | nd | nd | nd | 0.039 | 0.178 | 0.100 |
| $Nb_2O_5$ | 0.155 | 0.116 | 0.219 | nd | 0.831 | 0.487 |
| $Al_2O_3$ | 0.044 | nd | 0.027 | nd | 0.016 | 0.027 |
| $Cr_2O_3$ | 0.202 | 0.514 | 0.098 | 0.098 | 0.038 | 0.148 |
| $FeO$ | 0.046 | nd | 0.190 | nd | 0.517 | 0.107 |
| Total | 99.578 | 99.885 | 99.587 | 99.488 | 99.964 | 100.614 |

## Pond C

| No. | 1 | 2 | 3 | 4 |
|---|---|---|---|---|
| $SiO_2$ | 0.498 | 0.521 | 0.332 | 0.309 |
| $TiO_2$ | 97.520 | 97.597 | 96.464 | 97.878 |
| $ZrO_2$ | 0.038 | 0.056 | 0.299 | 0.112 |
| $V_2O_3$ | nd | nd | nd | 0.238 |
| $Ta_2O_5$ | 0.171 | nd | 0.140 | 0.153 |
| $Nb_2O_5$ | 0.673 | 0.776 | 0.858 | 0.234 |
| $Al_2O_3$ | 0.028 | 0.019 | 0.112 | nd |
| $Cr_2O_3$ | 0.060 | 0.033 | 0.164 | 0.197 |
| $FeO$ | 0.593 | 0.521 | 0.304 | 0.053 |
| Total | 99.581 | 99.523 | 98.673 | 99.174 |

## Pond C

| No. | 6 | 7 | 8 | 9 | 10 | 11 | 12 | 13 | 14 | 15 | 16 |
|---|---|---|---|---|---|---|---|---|---|---|---|
| $SiO_2$ | 0.224 | 0.342 | 0.435 | 1.076 | 0.379 | 0.368 | 0.377 | 0.331 | 0.242 | 0.335 | 0.601 |
| $TiO_2$ | 98.438 | 97.566 | 98.609 | 96.187 | 98.564 | 98.668 | 98.856 | 98.382 | 97.847 | 98.407 | 97.437 |
| $ZrO_2$ | 0.098 | 0.131 | 0.109 | nd | 0.171 | 0.093 | 0.039 | 0.101 | 0.232 | 0.166 | 0.267 |
| $V_2O_3$ | nd | 0.141 | nd | nd | nd | nd | nd | nd | nd | 0.185 | 0.414 |
| $Ta_2O_5$ | nd | 0.096 | nd | 0.065 | nd | nd | 0.171 | nd | nd | 0.127 | 0.261 |
| $Nb_2O_5$ | 0.255 | 0.049 | 0.234 | 0.101 | 0.055 | 0.207 | 0.067 | 0.112 | 0.359 | 0.155 | 0.222 |
| $Al_2O_3$ | 0.044 | nd | 0.047 | 1.522 | 0.015 | nd | nd | 0.040 | 0.202 | nd | 0.011 |
| $Cr_2O_3$ | 0.071 | 0.153 | 0.055 | 0.137 | 0.115 | 0.104 | 0.093 | 0.066 | 0.066 | 0.060 | 0.175 |
| $FeO$ | 0.168 | 0.506 | 0.228 | 0.290 | 0.065 | 0.049 | nd | 0.103 | 0.213 | 0.145 | nd |
| Total | 99.298 | 98.984 | 99.717 | 99.378 | 99.364 | 99.489 | 99.603 | 99.135 | 99.161 | 99.580 | 99.388 |

## Primary mags
### Pond A

| No. | 1 | 2 | 3 | 4 | 5 | 6 | 7 | 8 | 9 | 10 | 11 | 12 | 13 |
|---|---|---|---|---|---|---|---|---|---|---|---|---|---|
| $SiO_2$ | 0.111 | 0.065 | 0.189 | 0.233 | 0.173 | 0.193 | 0.208 | 0.197 | 0.191 | 0.107 | 0.161 | 0.394 | 0.100 |
| $TiO_2$ | 98.899 | 98.976 | 99.062 | 98.881 | 98.691 | 98.444 | 99.638 | 98.542 | 99.055 | 99.161 | 99.203 | 96.526 | 99.573 |
| $ZrO_2$ | 0.271 | 0.202 | 0.108 | 0.432 | 0.267 | 0.162 | 0.102 | 0.266 | 0.210 | 0.174 | 0.253 | 0.442 | 0.186 |
| $V_2O_3$ | 0.366 | 0.183 | 0.139 | 0.278 | 0.490 | 1.162 | nd | 0.285 | 0.439 | nd | 0.490 | 0.161 | nd |
| $Ta_2O_5$ | nd | 0.149 | nd | 0.072 | 0.081 | nd | 0.050 | nd | 0.208 | 0.289 | nd | 0.077 | 0.167 |
| $Nb_2O_5$ | 0.054 | 0.151 | 0.232 | 0.132 | 0.105 | 0.209 | nd | 0.259 | nd | 0.099 | 0.124 | 0.087 | 0.201 |
| $Al_2O_3$ | nd | 0.024 | nd | 0.043 | 0.014 | nd | 0.067 | 0.016 | 0.072 | nd | nd | 0.401 | nd |
| $Cr_2O_3$ | 0.077 | 0.117 | 0.114 | 0.081 | 0.156 | 0.168 | nd | 0.226 | 0.091 | 0.023 | 0.083 | 0.040 | 0.122 |
| $FeO$ | 0.115 | 0.176 | 0.192 | 0.267 | 0.212 | 0.056 | 0.364 | 0.079 | 0.151 | 0.279 | 0.103 | 0.889 | 0.123 |
| Total | 99.893 | 100.043 | 100.036 | 100.419 | 100.189 | 100.394 | 100.429 | 99.870 | 100.417 | 100.132 | 100.417 | 99.017 | 100.472 |

### Pond A

| No. | 14 | 15 | 16 |
|---|---|---|---|
| $SiO_2$ | 0.130 | 0.105 | 0.105 |
| $TiO_2$ | 99.246 | 98.777 | 99.658 |
| $ZrO_2$ | 0.260 | 0.187 | 0.113 |
| $V_2O_3$ | 0.570 | 0.534 | 0.234 |
| $Ta_2O_5$ | 0.061 | nd | nd |
| $Nb_2O_5$ | 0.091 | 0.054 | 0.052 |
| $Al_2O_3$ | 0.017 | 0.024 | 0.036 |
| $Cr_2O_3$ | 0.167 | 0.171 | 0.057 |
| $FeO$ | nd | 0.111 | 0.352 |
| Total | 100.542 | 99.963 | 100.607 |

### Pond B

| No. | 1 | 2 | 3 | 4 | 5 | 6 | 7 | 8 |
|---|---|---|---|---|---|---|---|---|
| $SiO_2$ | 0.222 | 0.168 | 0.197 | 0.409 | 0.184 | 0.222 | 1.515 | 0.413 |
| $TiO_2$ | 97.442 | 97.858 | 99.358 | 99.959 | 99.539 | 99.702 | 97.580 | 97.978 |
| $ZrO_2$ | 0.104 | 0.138 | 0.105 | nd | 0.123 | 0.223 | 0.043 | 0.047 |
| $V_2O_3$ | 1.746 | 1.519 | 0.709 | 0.403 | 0.680 | 1.090 | 0.154 | nd |
| $Ta_2O_5$ | nd | 0.202 | 0.182 | nd | nd | 0.121 | nd | 0.149 |
| $Nb_2O_5$ | 0.494 | 0.501 | 0.374 | 0.134 | 0.355 | 0.081 | 0.088 | 0.348 |
| $Al_2O_3$ | nd | nd | 0.012 | 0.081 | nd | nd | 0.479 | 0.104 |
| $Cr_2O_3$ | 0.523 | 0.339 | 0.083 | 0.135 | 0.075 | 0.203 | 0.303 | nd |
| $FeO$ | 0.062 | 0.040 | 0.179 | 0.186 | 0.153 | nd | 0.631 | 1.664 |
| Total | 100.593 | 100.765 | 101.199 | 101.307 | 101.109 | 101.642 | 100.793 | 100.703 |

## Pond B

| No. | 9 | 10 |
|---|---|---|
| $SiO_2$ | 0.215 | 2.203 |
| $TiO_2$ | 98.991 | 96.226 |
| $ZrO_2$ | 0.119 | nd |
| $V_2O_3$ | 1.126 | nd |
| $Ta_2O_5$ | nd | nd |
| $Nb_2O_5$ | 0.351 | 0.129 |
| $Al_2O_3$ | 0.028 | 0.395 |
| $Cr_2O_3$ | 0.409 | 0.758 |
| FeO | 0.033 | 0.332 |
| Total | 101.272 | 100.043 |

## Pond C

| No. | 1 | 2 | 3 | 4 | 5 | 6 | 7 | 8 | 9 |
|---|---|---|---|---|---|---|---|---|---|
| $SiO_2$ | 0.288 | 0.283 | 0.293 | 0.265 | 0.338 | 0.246 | 1.188 | 0.258 | 0.200 |
| $TiO_2$ | 97.034 | 98.591 | 99.770 | 99.263 | 96.982 | 98.430 | 97.229 | 99.868 | 99.666 |
| $ZrO_2$ | 0.091 | nd | 0.079 | nd | 0.042 | 0.300 | nd | 0.142 | 0.146 |
| $V_2O_3$ | 0.313 | nd | 0.285 | 0.634 | nd | 0.685 | 0.831 | nd | 0.893 |
| $Ta_2O_5$ | 0.151 | 0.103 | nd | nd | 0.061 | nd | nd | 0.199 | 0.068 |
| $Nb_2O_5$ | 0.344 | 0.153 | 0.095 | 0.230 | 0.103 | 0.124 | nd | nd | 0.217 |
| $Al_2O_3$ | nd | 0.032 | 0.012 | nd | 0.488 | 0.011 | 0.221 | 0.015 | 0.022 |
| $Cr_2O_3$ | nd | 0.076 | 0.053 | 0.192 | 0.065 | 0.140 | 0.303 | 0.045 | 0.208 |
| FeO | 1.028 | 0.382 | 0.112 | 0.083 | 0.992 | 0.037 | 0.165 | 0.209 | 0.059 |
| Total | 99.249 | 99.620 | 100.699 | 100.667 | 99.071 | 99.973 | 99.937 | 100.736 | 101.479 |

## Pond C

| No. | 10 | 11 | 12 | 13 | 14 |
|---|---|---|---|---|---|
| $SiO_2$ | 0.192 | 0.126 | 0.158 | 0.080 | 0.188 |
| $TiO_2$ | 98.100 | 98.103 | 97.492 | 98.356 | 99.424 |
| $ZrO_2$ | 0.042 | 0.175 | 0.099 | 0.252 | 0.020 |
| $V_2O_3$ | 0.220 | 0.176 | nd | 0.864 | 0.271 |
| $Ta_2O_5$ | 0.068 | 0.244 | 0.099 | nd | nd |
| $Nb_2O_5$ | 0.213 | 0.083 | 0.610 | 0.081 | 0.130 |
| $Al_2O_3$ | 0.015 | 0.085 | 0.185 | 0.022 | 0.012 |
| $Cr_2O_3$ | 0.084 | 0.107 | 0.097 | 0.168 | 0.159 |
| FeO | 0.203 | 0.315 | 0.514 | 0.088 | 0.205 |
| Total | 99.137 | 99.414 | 99.254 | 99.911 | 100.409 |

## HT'S Scavengers (mid and non-conductors)
## Pond B

| No. | 1 | 2 | 3 | 4 | 5 | 6 | 7 | 8 | 9 |
|---|---|---|---|---|---|---|---|---|---|
| $SiO_2$ | 0.292 | 0.249 | 0.268 | 0.305 | 0.210 | 0.256 | 0.283 | 0.228 | 0.344 |
| $TiO_2$ | 97.721 | 97.598 | 97.734 | 97.389 | 97.806 | 97.777 | 97.887 | 98.066 | 98.488 |
| $ZrO_2$ | 0.038 | 0.190 | 0.201 | 0.250 | 0.198 | 0.071 | 0.160 | 0.343 | 0.189 |
| $V_2O_3$ | 0.203 | 0.782 | 0.879 | 0.241 | 0.946 | nd | 0.801 | 0.541 | nd |
| $Ta_2O_5$ | 0.067 | nd | 0.065 | nd | nd | nd | nd | nd | nd |
| $Nb_2O_5$ | nd | 0.249 | 0.143 | 0.103 | nd | 0.100 | 0.246 | 0.203 | 0.176 |
| $Al_2O_3$ | 0.033 | nd | 0.015 | 0.023 | 0.023 | 0.016 | nd | 0.025 | 0.018 |
| $Cr_2O_3$ | 0.094 | 0.047 | 0.059 | nd | 0.039 | 0.024 | 0.090 | 0.092 | 0.046 |
| FeO | 0.226 | 0.048 | 0.035 | 0.220 | 0.078 | 0.225 | 0.188 | 0.093 | 0.060 |
| Total | 98.674 | 99.163 | 99.399 | 98.531 | 99.300 | 98.469 | 99.655 | 99.591 | 99.321 |

## Primary HT'S Conductors

### Pond A

| No. | 1 | 2 | 3 | 4 | 5 | 6 | 7 | 8 | 9 |
|---|---|---|---|---|---|---|---|---|---|
| $SiO_2$ | 0.342 | 0.592 | 0.606 | 0.441 | 0.368 | 0.342 | 0.356 | 0.309 | 0.333 |
| $TiO_2$ | 99.000 | 98.704 | 98.876 | 100.439 | 98.713 | 99.678 | 99.252 | 98.749 | 98.839 |
| $ZrO_2$ | 0.110 | 0.117 | 0.163 | 0.040 | 0.097 | 0.083 | 0.093 | 0.321 | 0.059 |
| $V_2O_3$ | nd | 0.300 | nd | nd | 0.335 | nd | nd | 0.273 | nd |
| $Ta_2O_5$ | nd | nd | nd | nd | nd | 0.181 | nd | 0.100 | 0.046 |
| $Nb_2O_5$ | 0.234 | 0.140 | 0.158 | nd | 0.161 | 0.049 | 0.212 | 0.161 | 0.158 |
| $Al_2O_3$ | nd | nd | 0.021 | nd | 0.138 | nd | nd | nd | nd |
| $Cr_2O_3$ | 0.098 | 0.131 | 0.082 | 0.044 | 0.038 | 0.093 | 0.049 | 0.218 | 0.180 |
| FeO | 0.049 | 0.057 | 0.084 | nd | 0.175 | 0.065 | nd | 0.122 | 0.114 |
| Total | 99.833 | 100.041 | 99.990 | 100.964 | 100.025 | 100.491 | 99.962 | 100.253 | 99.729 |

### Pond B

| No. | 1 |
|---|---|
| $SiO_2$ | 0.401 |
| $TiO_2$ | 98.242 |
| $ZrO_2$ | 0.267 |
| $V_2O_3$ | 0.352 |
| $Ta_2O_5$ | 0.199 |
| $Nb_2O_5$ | 0.167 |
| $Al_2O_3$ | nd |
| $Cr_2O_3$ | 0.202 |
| FeO | 0.027 |
| Total | 99.857 |

### Pond B

| No. | 2 | 3 | 4 | 5 | 6 | 7 | 8 |
|---|---|---|---|---|---|---|---|
| $SiO_2$ | 0.322 | 0.460 | 0.390 | 0.291 | 0.271 | 0.468 | 0.354 |
| $TiO_2$ | 98.735 | 98.010 | 99.825 | 98.524 | 99.827 | 98.799 | 99.772 |
| $ZrO_2$ | 0.206 | 0.111 | 0.041 | 0.314 | nd | nd | 0.049 |
| $V_2O_3$ | 0.203 | nd | nd | nd | nd | nd | 0.159 |
| $Ta_2O_5$ | nd | 0.156 | nd | 0.270 | nd | nd | nd |
| $Nb_2O_5$ | 0.097 | 0.164 | 0.067 | 0.185 | nd | 0.112 | 0.261 |
| $Al_2O_3$ | 0.014 | 0.024 | nd | 0.028 | 0.034 | 0.044 | nd |
| $Cr_2O_3$ | 0.109 | 0.093 | 0.109 | 0.093 | 0.147 | nd | nd |
| FeO | nd | 0.152 | 0.312 | 0.114 | 0.068 | 0.034 | 0.251 |
| Total | 99.686 | 99.170 | 100.744 | 99.819 | 100.347 | 99.457 | 100.846 |

### Pond C

| No. | 1 | 2 | 3 |
|---|---|---|---|
| $SiO_2$ | 0.388 | 0.342 | 0.299 |
| $TiO_2$ | 97.587 | 97.632 | 98.050 |
| $ZrO_2$ | 0.077 | 0.055 | 0.065 |
| $V_2O_3$ | 0.150 | 0.123 | 0.062 |
| $Ta_2O_5$ | nd | nd | nd |
| $Nb_2O_5$ | 0.067 | 0.261 | 0.167 |
| $Al_2O_3$ | 0.029 | nd | 0.047 |
| $Cr_2O_3$ | 0.071 | 0.044 | nd |
| FeO | nd | 0.156 | 0.156 |
| Total | 98.369 | 98.613 | 98.846 |

## Pond C

| No. | 4 | 5 | 6 | 7 | 8 |
|---|---|---|---|---|---|
| $SiO_2$ | 0.426 | 0.374 | 0.589 | 0.327 | 0.375 |
| $TiO_2$ | 96.956 | 97.180 | 97.136 | 97.376 | 97.353 |
| $ZrO_2$ | 0.050 | 0.083 | 0.195 | 0.077 | 0.109 |
| $V_2O_3$ | 0.132 | 0.264 | 0.194 | 0.212 | 0.168 |
| $Ta_2O_5$ | nd | 0.167 | nd | 0.068 | nd |
| $Nb_2O_5$ | 0.222 | 0.237 | nd | 0.273 | 0.264 |
| $Al_2O_3$ | nd | 0.015 | nd | nd | 0.042 |
| $Cr_2O_3$ | 0.137 | 0.082 | 0.022 | 0.104 | 0.153 |
| FeO | 0.110 | 0.049 | 0.034 | 0.034 | 0.061 |
| Total | 98.033 | 98.451 | 98.170 | 98.471 | 98.525 |

# HT'S cleaner conductors

## Pond A

| No. | 1 | 2 | 3 | 4 | 5 | 6 | 7 | 8 | 9 | 10 | 11 | 12 |
|---|---|---|---|---|---|---|---|---|---|---|---|---|
| $SiO_2$ | 0.316 | 0.377 | 0.236 | 0.347 | 0.265 | 0.372 | 0.297 | 0.213 | 0.374 | 0.251 | 0.317 | 0.128 |
| $TiO_2$ | 96.480 | 97.433 | 96.639 | 97.938 | 97.128 | 97.001 | 96.975 | 96.975 | 94.711 | 97.127 | 97.915 | 96.650 |
| $ZrO_2$ | 0.218 | 0.381 | 0.172 | 0.090 | 0.075 | 0.335 | 0.158 | 0.203 | 0.464 | 0.188 | 0.057 | 0.153 |
| $V_2O_3$ | 0.651 | nd | 0.446 | nd | 0.227 | 0.358 | 0.446 | 0.146 | 0.452 | 0.490 | nd | 0.577 |
| $Ta_2O_5$ | 0.167 | nd | 0.053 | 0.138 | nd | nd | nd | nd | 0.272 | nd | 0.213 | 0.164 |
| $Nb_2O_5$ | nd | 0.114 | 0.186 | 0.052 | nd | 0.099 | 0.306 | 0.564 | nd | 0.064 | nd | 0.159 |
| $Al_2O_3$ | 0.022 | 0.014 | nd | 0.012 | 0.025 | nd | 0.019 | 0.056 | 0.213 | 0.016 | 0.034 | 0.018 |
| $Cr_2O_3$ | 0.175 | 0.058 | 0.182 | 0.055 | 0.063 | 0.166 | 0.184 | 0.122 | 0.569 | 0.178 | 0.108 | 0.115 |
| $FeO$ | 0.027 | 0.223 | 0.171 | 0.176 | 0.392 | 0.054 | 0.220 | 0.208 | 1.167 | 0.038 | 0.249 | 0.071 |
| Total | 98.056 | 98.600 | 98.085 | 98.808 | 98.175 | 98.385 | 98.605 | 98.487 | 98.222 | 98.352 | 98.893 | 98.035 |

## Pond A                    Pond B

| No. | 13 | 14 | No. | 1 | 2 | 3 | 4 | 5 | 6 | 7 | 8 |
|---|---|---|---|---|---|---|---|---|---|---|---|
| $SiO_2$ | 0.247 | 0.316 | $SiO_2$ | 0.424 | 0.437 | 0.470 | 0.357 | 0.526 | 0.402 | 0.398 | 0.379 |
| $TiO_2$ | 97.758 | 97.480 | $TiO_2$ | 97.073 | 98.049 | 97.806 | 97.474 | 97.934 | 97.127 | 97.964 | 98.689 |
| $ZrO_2$ | 0.153 | 0.218 | $ZrO_2$ | 0.149 | 0.250 | 0.218 | 0.080 | 0.093 | 0.124 | 0.100 | 0.100 |
| $V_2O_3$ | 0.285 | 0.651 | $V_2O_3$ | 0.282 | nd | nd | 0.194 | nd | nd | nd | nd |
| $Ta_2O_5$ | nd | 0.167 | $Ta_2O_5$ | 0.060 | nd | nd | nd | nd | nd | 0.217 | nd |
| $Nb_2O_5$ | 0.256 | nd | $Nb_2O_5$ | 0.623 | nd | nd | 0.377 | 0.176 | 0.401 | 0.408 | 0.261 |
| $Al_2O_3$ | 0.049 | 0.022 | $Al_2O_3$ | 0.013 | 0.017 | 0.033 | nd | nd | 0.015 | 0.019 | 0.045 |
| $Cr_2O_3$ | 0.116 | 0.175 | $Cr_2O_3$ | 0.066 | 0.038 | 0.109 | 0.120 | 0.055 | 0.164 | 0.104 | nd |
| $FeO$ | 0.081 | 0.027 | $FeO$ | 0.076 | 0.095 | 0.114 | 0.080 | 0.171 | 0.148 | 0.129 | 0.213 |
| Total | 98.945 | 99.056 | Total | 98.766 | 98.886 | 98.750 | 98.682 | 98.955 | 98.381 | 99.339 | 99.687 |

**Pond B**

| No. | 9 | 10 | 11 | 12 | 13 | 14 | 15 | 16 | 17 | 18 |
|---|---|---|---|---|---|---|---|---|---|---|
| $SiO_2$ | 0.388 | 0.544 | 0.442 | 0.383 | 0.365 | 0.454 | 0.372 | 0.418 | 0.363 | 0.478 |
| $TiO_2$ | 97.719 | 97.642 | 98.847 | 98.558 | 97.990 | 98.600 | 97.368 | 98.327 | 98.372 | 95.840 |
| $ZrO_2$ | 0.064 | nd | 0.089 | 0.033 | 0.124 | 0.039 | 0.028 | 0.102 | 0.092 | 0.054 |
| $V_2O_3$ | nd | nd | nd | nd | 0.159 | nd | nd | nd | 0.141 | 0.440 |
| $Ta_2O_5$ | 0.036 | 0.203 | nd | nd | nd | nd | nd | nd | nd | nd |
| $Nb_2O_5$ | 0.675 | 0.304 | 0.210 | 0.195 | 0.340 | 0.204 | 0.119 | 0.122 | 0.204 | 1.319 |
| $Al_2O_3$ | nd | 0.052 | 0.034 | 0.039 | nd | 0.034 | 0.035 | 0.034 | 0.024 | 0.040 |
| $Cr_2O_3$ | 0.229 | 0.049 | 0.033 | nd | nd | nd | 0.147 | 0.082 | 0.066 | 0.115 |
| FeO | 0.015 | 0.148 | 0.232 | 0.244 | 0.080 | 0.065 | 0.426 | 0.468 | 0.209 | 0.057 |
| Total | 99.126 | 98.942 | 99.887 | 99.452 | 99.058 | 99.396 | 98.495 | 99.553 | 99.471 | 98.343 |

**Pond C**

| No. | 1 | 2 | 3 | 4 | 5 | 6 | 7 | 8 | 9 | 10 |
|---|---|---|---|---|---|---|---|---|---|---|
| $SiO_2$ | 0.535 | 0.150 | 0.186 | 0.124 | 0.188 | 0.183 | 0.195 | 0.150 | 0.107 | 0.135 |
| $TiO_2$ | 96.677 | 99.081 | 97.112 | 98.599 | 97.711 | 99.244 | 98.566 | 98.797 | 99.449 | 99.068 |
| $ZrO_2$ | 0.019 | 0.060 | 0.069 | 0.271 | 0.087 | 0.076 | 0.124 | 0.458 | 0.052 | 0.235 |
| $V_2O_3$ | nd | nd | 0.402 | 0.417 | 0.372 | nd | 0.731 | 0.329 | 0.300 | 0.387 |
| $Ta_2O_5$ | 0.323 | 0.116 | nd | nd | 0.278 | nd | 0.162 | 0.094 | nd | 0.182 |
| $Nb_2O_5$ | 0.313 | nd | 0.472 | nd | 0.618 | nd | nd | 0.101 | 0.070 | 0.083 |
| $Al_2O_3$ | 0.154 | 0.043 | nd | 0.026 | 0.075 | nd | 0.038 | nd | 0.013 | nd |
| $Cr_2O_3$ | 0.051 | 0.080 | 0.617 | 0.075 | 0.096 | 0.042 | 0.111 | 0.100 | 0.074 | 0.109 |
| FeO | 0.606 | 0.327 | 0.098 | 0.098 | 0.208 | 0.296 | 0.082 | 0.064 | 0.116 | 0.030 |
| Total | 98.678 | 99.857 | 98.956 | 99.610 | 99.633 | 99.841 | 100.009 | 100.093 | 100.181 | 100.229 |

**Pond C**

| No. | 11 | 12 | 13 | 14 | 15 | 16 | 17 | 18 | 19 | 20 |
|---|---|---|---|---|---|---|---|---|---|---|
| $SiO_2$ | 0.169 | 0.269 | 0.356 | 0.254 | 0.145 | 0.058 | 0.127 | 0.148 | 0.160 | 0.280 |
| $TiO_2$ | 99.036 | 99.150 | 98.463 | 99.802 | 98.517 | 98.532 | 98.905 | 98.858 | 98.737 | 98.516 |
| $ZrO_2$ | 0.100 | 0.170 | nd | 0.173 | 0.162 | 0.166 | 0.057 | 0.150 | 0.209 | 0.098 |
| $V_2O_3$ | 0.219 | 0.468 | nd | 0.183 | 0.475 | 0.402 | 0.468 | 0.329 | 0.227 | 0.263 |
| $Ta_2O_5$ | nd | 0.213 | 0.044 | nd | nd | nd | nd | 0.112 | nd | nd |
| $Nb_2O_5$ | 0.211 | 0.143 | nd | nd | 0.114 | 0.087 | 0.103 | nd | 0.083 | 0.070 |
| $Al_2O_3$ | nd | 0.037 | 0.085 | nd | 0.016 | 0.037 | nd | 0.026 | 0.029 | nd |
| $Cr_2O_3$ | 0.089 | 0.079 | nd | 0.241 | 0.117 | 0.067 | 0.085 | 0.114 | 0.208 | 0.093 |
| $FeO$ | 0.246 | 0.055 | 0.109 | 0.065 | 0.055 | 0.121 | nd | nd | 0.100 | 0.201 |
| Total | 100.070 | 100.584 | 99.057 | 100.718 | 99.601 | 99.470 | 99.745 | 99.737 | 99.753 | 99.521 |

**HT'S cleaner mids**

**Pond A**

| No. | 1 | 2 | 3 | 4 | 5 | 6 | 7 | 8 | 9 | 10 | 11 | 12 |
|-----|---|---|---|---|---|---|---|---|---|----|----|----|
| $SiO_2$ | 0.355 | 0.268 | 0.293 | 0.313 | 0.411 | 0.456 | 0.431 | 0.392 | 0.366 | 0.355 | 0.484 | 0.373 |
| $TiO_2$ | 97.241 | 94.303 | 96.491 | 96.123 | 96.915 | 96.688 | 97.073 | 96.996 | 97.143 | 96.338 | 96.210 | 96.297 |
| $ZrO_2$ | 0.198 | 0.217 | 0.203 | 0.097 | 0.318 | 0.188 | 0.058 | 0.173 | 0.051 | 0.109 | 0.058 | 0.232 |
| $V_2O_3$ | 0.359 | 0.497 | 0.329 | 0.585 | 0.797 | 0.731 | 0.461 | 0.344 | 0.307 | 0.622 | nd | 0.826 |
| $Ta_2O_5$ | nd | 0.300 | 0.213 | nd | 0.068 | nd | nd | nd | nd | 0.118 | nd | nd |
| $Nb_2O_5$ | 0.066 | 0.891 | 0.161 | 0.095 | nd | 0.149 | 0.136 | nd | nd | 0.151 | 0.142 | nd |
| $Al_2O_3$ | 0.045 | 0.175 | 0.014 | 0.022 | nd | 0.014 | nd | 0.024 | 0.019 | 0.033 | 0.038 | 0.036 |
| $Cr_2O_3$ | 0.150 | nd | 0.079 | 0.104 | 0.139 | 0.170 | 0.169 | 0.138 | nd | 0.104 | 0.078 | 0.137 |
| FeO | 0.088 | 0.610 | 0.147 | 0.100 | 0.132 | 0.081 | 0.038 | 0.068 | 0.272 | 0.098 | 0.135 | 0.032 |
| Total | 98.502 | 97.261 | 97.930 | 97.439 | 98.780 | 98.477 | 98.366 | 98.135 | 98.158 | 97.928 | 97.145 | 97.933 |

**Pond A**

| No. | 13 | 14 | 15 | 16 | 17 | 18 | 19 | 20 | 21 | 22 | 23 | 24 |
|-----|----|----|----|----|----|----|----|----|----|----|----|----|
| $SiO_2$ | 0.367 | 0.283 | 0.300 | 0.331 | 0.365 | 0.362 | 0.385 | 0.295 | 0.303 | 0.325 | 0.225 | 0.341 |
| $TiO_2$ | 95.557 | 96.491 | 96.685 | 96.615 | 97.021 | 95.568 | 97.878 | 96.920 | 98.164 | 96.265 | 97.336 | 96.608 |
| $ZrO_2$ | 0.184 | 0.167 | 0.053 | 0.250 | 0.124 | 0.098 | 0.093 | 0.475 | 0.174 | 0.259 | 0.118 | 0.099 |
| $V_2O_3$ | 0.848 | 0.322 | 0.176 | 0.359 | nd | 0.563 | 0.702 | 0.278 | 0.154 | 0.322 | 0.168 | 0.402 |
| $Ta_2O_5$ | nd | 0.068 | 0.075 | nd | 0.042 | nd | 0.215 | nd | nd | nd | nd | nd |
| $Nb_2O_5$ | nd | 0.062 | 0.089 | nd | 0.302 | 0.256 | nd | 0.114 | 0.163 | 0.279 | nd | 0.056 |
| $Al_2O_3$ | 0.025 | 0.057 | 0.020 | nd | 0.023 | nd | nd | nd | 0.018 | 0.074 | 0.036 | nd |
| $Cr_2O_3$ | 0.204 | 0.061 | 0.088 | 0.120 | 0.081 | 0.265 | 0.107 | 0.078 | nd | 0.055 | 0.037 | 0.249 |
| FeO | nd | 0.272 | 0.117 | 0.053 | 0.179 | 0.070 | 0.042 | 0.058 | 0.201 | 0.200 | 0.151 | 0.069 |
| Total | 97.185 | 97.783 | 97.603 | 97.728 | 98.137 | 97.182 | 99.422 | 98.218 | 99.177 | 97.779 | 98.071 | 97.824 |

## Pond A

| No. | 25 | 26 |
|---|---|---|
| $SiO_2$ | 0.151 | 0.164 |
| $TiO_2$ | 97.483 | 96.775 |
| $ZrO_2$ | 0.198 | 0.177 |
| $V_2O_3$ | 0.329 | 0.723 |
| $Ta_2O_5$ | 0.059 | 0.107 |
| $Nb_2O_5$ | nd | 0.159 |
| $Al_2O_3$ | 0.024 | nd |
| $Cr_2O_3$ | 0.108 | 0.218 |
| FeO | 0.101 | nd |
| Total | 98.453 | 98.323 |

## Pond B

| No. | 1 | 2 | 3 | 4 | 5 | 6 | 7 | 8 |
|---|---|---|---|---|---|---|---|---|
| $SiO_2$ | 0.493 | 0.362 | 0.318 | 0.291 | 0.298 | 0.297 | 0.333 | 0.264 |
| $TiO_2$ | 97.939 | 97.827 | 97.882 | 98.794 | 97.982 | 97.990 | 97.520 | 97.280 |
| $ZrO_2$ | 0.078 | 0.034 | 0.071 | 0.123 | 0.077 | 0.107 | 0.102 | 0.045 |
| $V_2O_3$ | nd | 0.238 | nd | 0.159 | 0.159 | 0.220 | 0.168 | 0.212 |
| $Ta_2O_5$ | 0.260 | nd | 0.093 | nd | 0.093 | nd | nd | 0.139 |
| $Nb_2O_5$ | nd | 0.185 | 0.219 | 0.131 | 0.194 | 0.286 | 0.146 | 0.264 |
| $Al_2O_3$ | 0.021 | nd | 0.139 | 0.033 | 0.016 | 0.020 | 0.034 | 0.012 |
| $Cr_2O_3$ | 0.044 | 0.109 | nd | 0.044 | 0.109 | 0.186 | 0.071 | 0.142 |
| FeO | 0.049 | 0.160 | 0.213 | 0.042 | 0.046 | nd | nd | 0.038 |
| Total | 98.884 | 98.915 | 98.935 | 99.617 | 98.974 | 99.106 | 98.374 | 98.396 |

## Pond B

| No. | 9 | 10 | 11 | 12 | 13 | 14 | 15 | 16 | 17 | 18 | 19 | 20 |
|---|---|---|---|---|---|---|---|---|---|---|---|---|
| $SiO_2$ | 0.704 | 0.307 | 0.350 | 0.322 | 0.285 | 0.350 | 0.297 | 0.324 | 0.219 | 0.223 | 0.292 | 0.346 |
| $TiO_2$ | 96.790 | 98.039 | 97.870 | 97.819 | 98.361 | 97.641 | 97.864 | 96.838 | 98.081 | 96.758 | 98.035 | 97.305 |
| $ZrO_2$ | 0.668 | 0.054 | 0.202 | 0.121 | 0.056 | 0.044 | 0.109 | 0.082 | 0.166 | 0.064 | 0.111 | 0.336 |
| $V_2O_3$ | 0.167 | 0.229 | nd | 0.115 | 0.123 | nd | nd | nd | nd | nd | nd | 0.220 |
| $Ta_2O_5$ | nd | nd | 0.093 | nd | 0.132 | 0.128 | nd | nd | nd | nd | 0.075 | nd |
| $Nb_2O_5$ | 0.322 | 0.182 | 0.167 | 0.182 | 0.204 | 0.605 | 0.207 | 0.402 | 0.043 | 1.005 | 0.425 | 0.061 |
| $Al_2O_3$ | nd | nd | nd | nd | nd | 0.033 | 0.020 | 0.673 | 0.017 | 0.021 | 0.049 | nd |
| $Cr_2O_3$ | 0.060 | 0.377 | 0.038 | 0.022 | 0.022 | 0.060 | 0.098 | 0.049 | 0.044 | 0.164 | 0.060 | 0.169 |
| FeO | 0.148 | 0.038 | nd | 0.141 | 0.107 | 0.221 | 0.072 | 0.301 | 0.053 | 0.224 | nd | 0.129 |
| Total | 98.859 | 99.226 | 98.720 | 98.722 | 99.290 | 99.082 | 98.667 | 98.669 | 98.623 | 98.459 | 99.047 | 98.566 |

**Pond C**

| No. | 1 | 2 | 3 | 4 | 5 | 6 | 7 | 8 | 9 |
|---|---|---|---|---|---|---|---|---|---|
| $SiO_2$ | 0.098 | 0.088 | 0.034 | 0.175 | 0.076 | 0.091 | 0.046 | 0.184 | 0.202 |
| $TiO_2$ | 99.633 | 98.126 | 97.739 | 98.739 | 98.353 | 98.036 | 98.808 | 98.727 | 97.782 |
| $ZrO_2$ | 0.040 | 0.319 | 0.433 | 0.356 | 0.256 | 0.117 | 0.389 | nd | 0.178 |
| $V_2O_3$ | 0.190 | 0.453 | 0.679 | 0.365 | 0.621 | 0.212 | nd | 0.168 | 0.197 |
| $Ta_2O_5$ | nd | 0.219 | 0.142 | nd | nd | nd | nd | nd | nd |
| $Nb_2O_5$ | nd | 0.151 | nd | 0.077 | 0.143 | 0.370 | 0.050 | 0.157 | nd |
| $Al_2O_3$ | nd | 0.013 | nd | nd | nd | 0.032 | 0.046 | nd | 0.020 |
| $Cr_2O_3$ | nd | 0.134 | 0.145 | 0.132 | 0.116 | 0.082 | 0.092 | nd | 0.075 |
| FeO | 0.207 | 0.057 | 0.100 | 0.136 | nd | 0.308 | 0.102 | 0.078 | 0.095 |
| **Total** | 100.168 | 99.560 | 99.272 | 99.980 | 99.565 | 99.248 | 99.533 | 99.314 | 98.549 |

## HT'S Cleaner Non Conductors

### Pond A

| No. | 1 | 2 | 3 | 4 | 5 | 6 | 7 | 8 | 9 | 10 | 11 | 12 |
|---|---|---|---|---|---|---|---|---|---|---|---|---|
| $SiO_2$ | 0.222 | 0.138 | 0.310 | 0.160 | 0.148 | 0.243 | 0.429 | 0.318 | 0.226 | 0.231 | 0.205 | 0.249 |
| $TiO_2$ | 98.331 | 98.245 | 97.306 | 97.944 | 97.561 | 97.653 | 97.651 | 97.579 | 97.172 | 98.410 | 98.072 | 97.942 |
| $ZrO_2$ | nd | 0.144 | nd | 0.096 | 0.114 | 0.263 | 0.102 | 0.071 | 0.129 | 0.068 | 0.178 | 0.057 |
| $V_2O_3$ | nd | nd | nd | 0.388 | nd | nd | nd | nd | 0.308 | nd | 0.168 | 0.203 |
| $Ta_2O_5$ | nd | nd | nd | nd | nd | nd | nd | nd | 0.203 | nd | nd | nd |
| $Nb_2O_5$ | nd | 0.206 | 0.277 | 0.191 | 0.234 | 0.194 | 0.091 | 0.629 | 0.055 | nd | nd | 0.140 |
| $Al_2O_3$ | nd | 0.022 | 0.040 | 0.043 | 0.063 | 0.036 | nd | 0.018 | 0.120 | nd | 0.033 | nd |
| $Cr_2O_3$ | 0.027 | 0.093 | 0.076 | 0.049 | 0.082 | 0.082 | 0.060 | 0.076 | 0.142 | 0.087 | 0.038 | 0.147 |
| $FeO$ | 0.167 | 0.095 | 0.407 | 0.164 | 0.255 | 0.038 | 0.228 | 0.065 | 0.205 | 0.072 | 0.152 | 0.171 |
| Total | 98.747 | 98.943 | 98.416 | 99.035 | 98.457 | 98.509 | 98.561 | 98.756 | 98.560 | 98.868 | 98.846 | 98.909 |

### Pond A                    Pond B

| No. | 13 | No. | 1 | 2 | 3 | 4 | 5 | 6 | 7 | 8 | 9 |
|---|---|---|---|---|---|---|---|---|---|---|---|
| $SiO_2$ | 0.278 | $SiO_2$ | 0.338 | 0.355 | 0.451 | 0.406 | 0.404 | 0.334 | 0.355 | 0.322 | 0.278 |
| $TiO_2$ | 97.835 | $TiO_2$ | 98.270 | 99.103 | 98.660 | 98.608 | 98.871 | 98.121 | 97.840 | 99.946 | 98.725 |
| $ZrO_2$ | 0.246 | $ZrO_2$ | 0.288 | 0.034 | 0.118 | 0.049 | 0.062 | 0.089 | nd | 0.098 | 0.090 |
| $V_2O_3$ | 0.414 | $V_2O_3$ | nd | nd | 0.273 | 0.220 | 0.291 | nd | nd | nd | nd |
| $Ta_2O_5$ | 0.125 | $Ta_2O_5$ | nd | nd | nd | nd | 0.139 | nd | nd | nd | nd |
| $Nb_2O_5$ | 0.049 | $Nb_2O_5$ | 0.179 | 0.073 | 0.070 | 0.119 | 0.210 | 0.629 | 0.182 | 0.510 | 0.125 |
| $Al_2O_3$ | 0.017 | $Al_2O_3$ | 0.023 | 0.018 | nd | nd | nd | 0.111 | 0.017 | 0.056 | nd |
| $Cr_2O_3$ | 0.044 | $Cr_2O_3$ | 0.262 | 0.208 | 0.142 | 0.049 | 0.076 | 0.147 | 0.044 | nd | nd |
| $FeO$ | nd | $FeO$ | 0.137 | 0.061 | 0.099 | 0.133 | 0.186 | 0.152 | 0.186 | 0.137 | 0.217 |
| Total | 99.008 | Total | 99.497 | 99.852 | 99.813 | 99.584 | 100.239 | 99.583 | 98.624 | 101.069 | 99.435 |

## Pond B

| No. | 10 | 11 | 12 | 13 | 14 | 15 |
|---|---|---|---|---|---|---|
| $SiO_2$ | 0.285 | 0.340 | 0.325 | 0.297 | 0.257 | 0.308 |
| $TiO_2$ | 97.913 | 98.565 | 97.585 | 98.161 | 98.114 | 97.629 |
| $ZrO_2$ | 0.070 | 0.084 | 0.243 | 0.173 | 0.154 | 0.342 |
| $V_2O_3$ | nd | nd | 0.264 | 0.141 | 0.168 | 0.326 |
| $Ta_2O_5$ | nd | nd | 0.078 | nd | nd | nd |
| $Nb_2O_5$ | 0.444 | 0.100 | 0.198 | 0.292 | 0.128 | 0.328 |
| $Al_2O_3$ | 0.042 | nd | nd | 0.039 | nd | 0.018 |
| $Cr_2O_3$ | nd | 0.033 | 0.197 | nd | 0.093 | 0.180 |
| FeO | 0.304 | 0.145 | 0.065 | 0.091 | 0.065 | 0.103 |
| Total | 99.058 | 99.267 | 98.955 | 99.194 | 98.979 | 99.234 |

## Pond C

| No. | 1 | 2 | 3 | 4 |
|---|---|---|---|---|
| $SiO_2$ | 0.202 | 0.253 | 0.218 | 0.386 |
| $TiO_2$ | 98.825 | 98.613 | 98.656 | 97.999 |
| $ZrO_2$ | 0.132 | 0.105 | 0.279 | 0.298 |
| $V_2O_3$ | 0.300 | 0.150 | nd | nd |
| $Ta_2O_5$ | 0.132 | nd | nd | 0.039 |
| $Nb_2O_5$ | 0.252 | 0.167 | 0.085 | 0.225 |
| $Al_2O_3$ | 0.095 | nd | nd | nd |
| $Cr_2O_3$ | nd | nd | nd | 0.027 |
| FeO | 0.182 | 0.114 | 0.156 | 0.057 |
| Total | 100.120 | 99.402 | 99.394 | 99.031 |

## Pond C

| No. | 5 | 6 | 7 | 8 | 9 |
|---|---|---|---|---|---|
| $SiO_2$ | 0.385 | 0.598 | 0.248 | 0.254 | 0.312 |
| $TiO_2$ | 98.041 | 99.003 | 97.772 | 98.294 | 99.016 |
| $ZrO_2$ | 0.202 | 0.025 | 0.251 | 0.093 | nd |
| $V_2O_3$ | nd | 0.141 | nd | 0.326 | 0.141 |
| $Ta_2O_5$ | nd | nd | 0.039 | nd | 0.185 |
| $Nb_2O_5$ | 0.103 | 0.067 | 0.616 | 0.182 | nd |
| $Al_2O_3$ | 0.033 | 0.091 | 0.055 | 0.052 | nd |
| $Cr_2O_3$ | nd | nd | nd | nd | nd |
| FeO | nd | 0.289 | 0.285 | 0.068 | 0.939 |
| Total | 98.764 | 100.214 | 99.266 | 99.269 | 100.593 |

**APPENDIX A4**

**Electron microprobe analyses of reddish brown, black, yellow and blue rutile grains**

# APPENDIX A4 – ELECTRON MICROPROBE ANALYSES OF REDDISH BROWN, BLACK, YELLOW AND BLUE RUTILE GRAINS

**nd – not detected**

## Reddish brown

| No. | 1 | 2 | 3 | 4 | 5 | 6 | 7 | 8 | 9 | 10 | 11 | 12 | 13 |
|---|---|---|---|---|---|---|---|---|---|---|---|---|---|
| SiO2 | 0.049 | nd | 0.033 | 0.040 | 0.041 | nd | nd | 0.026 | 0.061 | 0.043 | 0.109 | 0.078 | 0.142 |
| TiO2 | 98.422 | 98.229 | 98.219 | 98.337 | 98.554 | 98.401 | 98.281 | 98.924 | 97.877 | 98.738 | 98.856 | 98.263 | 97.547 |
| ZrO2 | 0.084 | 0.235 | 0.216 | 0.166 | 0.043 | 0.317 | 0.114 | 0.107 | 0.131 | 0.062 | 0.161 | 0.216 | 0.148 |
| V2O3 | nd | nd | nd | 0.210 | nd | nd | 0.272 | 0.202 | 0.254 | nd | 0.316 | nd | 0.193 |
| Ta2O5 | nd | 0.044 | nd | nd | nd | 0.093 | nd | nd | nd | 0.272 | 0.051 | nd | nd |
| Nb2O5 | 0.160 | 0.184 | 0.223 | 0.199 | 0.160 | 0.166 | 0.408 | 0.078 | 0.239 | 0.166 | 0.160 | 0.172 | nd |
| Al2O3 | nd | 0.060 | nd | 0.013 | 0.038 | nd | 0.051 | nd | 0.050 | 0.013 | 0.029 | 0.064 | 0.095 |
| Cr2O3 | nd | 0.103 | 0.141 | 0.119 | 0.022 | 0.071 | nd | 0.092 | 0.071 | 0.065 | nd | 0.158 | 0.114 |
| FeO | 0.499 | 0.178 | 0.250 | 0.148 | 0.386 | 0.132 | 0.280 | 0.087 | 0.204 | 0.083 | 0.242 | 0.193 | 0.182 |
| Total | 99.214 | 99.033 | 99.082 | 99.232 | 99.244 | 99.180 | 99.406 | 99.516 | 98.887 | 99.442 | 99.924 | 99.144 | 98.421 |

| No. | 14 | 15 | 16 | 17 | 18 | 19 | 20 | 21 | 22 | 23 | 24 | 25 | 26 |
|---|---|---|---|---|---|---|---|---|---|---|---|---|---|
| SiO2 | 0.056 | 0.045 | 0.034 | 0.044 | 0.071 | 0.080 | 0.053 | 0.078 | 0.039 | 0.042 | 0.047 | 0.170 | 0.029 |
| TiO2 | 97.863 | 97.858 | 98.390 | 97.909 | 97.658 | 97.058 | 98.219 | 97.449 | 98.049 | 97.698 | 96.431 | 97.673 | 98.598 |
| ZrO2 | 0.326 | 0.329 | 0.123 | 0.141 | 0.105 | 0.176 | 0.040 | 0.160 | 0.048 | 0.033 | 0.077 | 0.168 | 0.216 |
| V2O3 | nd | 0.307 | nd | 0.175 | nd | 0.386 | 0.167 | 0.149 | 0.272 | nd | nd | nd | nd |
| Ta2O5 | nd | 0.082 | 0.062 | nd | 0.051 | nd | nd | 0.041 | 0.111 | 0.108 | 0.136 | 0.234 | 0.236 |
| Nb2O5 | 0.160 | 0.142 | 0.133 | nd | 0.251 | 0.344 | 0.229 | nd | nd | 0.305 | 0.701 | 0.157 | 0.133 |
| Al2O3 | 0.029 | 0.029 | 0.012 | nd | 0.020 | 0.105 | nd | 0.019 | 0.021 | 0.043 | 0.145 | nd | 0.024 |
| Cr2O3 | 0.152 | 0.152 | 0.043 | 0.043 | 0.049 | 0.054 | 0.136 | 0.206 | 0.315 | 0.043 | 0.673 | 0.081 | 0.195 |
| FeO | 0.102 | 0.053 | 0.174 | 0.223 | 0.095 | 0.204 | 0.121 | 0.114 | 0.061 | 0.242 | 0.132 | 0.076 | 0.238 |
| Total | 98.688 | 98.997 | 98.971 | 98.535 | 98.300 | 98.407 | 98.965 | 98.216 | 98.916 | 98.514 | 98.342 | 98.559 | 99.669 |

# APPENDIX A4 – ELECTRON MICROPROBE ANALYSES OF REDDISH BROWN, BLACK, YELLOW AND BLUE RUTILE GRAINS

## Reddish Brown

| No. | 27 | 28 | 29 | 30 | 31 |
|---|---|---|---|---|---|
| $SiO_2$ | 0.082 | 0.030 | 0.072 | 0.033 | 0.038 |
| $TiO_2$ | 97.373 | 97.245 | 98.158 | 98.141 | 97.607 |
| $ZrO_2$ | 0.131 | 0.134 | 0.042 | 0.054 | 0.059 |
| $V_2O_3$ | nd | 0.158 | nd | nd | nd |
| $Ta_2O_5$ | 0.162 | nd | 0.067 | nd | 0.257 |
| $Nb_2O_5$ | 0.082 | 0.157 | 0.109 | 0.154 | 0.088 |
| $Al_2O_3$ | 0.062 | nd | 0.012 | 0.012 | 0.033 |
| $Cr_2O_3$ | 0.054 | 0.315 | 0.114 | 0.092 | 0.130 |
| FeO | 0.174 | 0.140 | 0.136 | 0.280 | 0.359 |
| Total | 98.120 | 98.179 | 98.710 | 98.766 | 98.571 |

## Black

| No. | 1 | 2 | 3 | 4 | 5 | 6 | 7 | 8 | 9 | 10 | 11 | 12 | 13 |
|---|---|---|---|---|---|---|---|---|---|---|---|---|---|
| $SiO_2$ | 0.020 | nd | nd | nd | 0.040 | 0.026 | nd | nd | nd | nd | 0.023 | 0.040 | 0.064 |
| $TiO_2$ | 98.096 | 96.723 | 96.782 | 96.615 | 97.258 | 96.232 | 96.903 | 96.443 | 97.125 | 96.560 | 96.547 | 95.732 | 98.177 |
| $ZrO_2$ | 0.106 | 0.160 | 0.168 | 0.129 | 0.039 | 0.497 | 0.153 | 0.047 | 0.035 | 0.129 | 0.503 | 0.163 | 0.138 |
| $V_2O_3$ | 1.107 | 1.183 | 0.757 | 1.681 | 0.364 | 0.624 | 1.117 | 0.566 | 0.824 | 1.117 | 0.838 | 0.246 | 0.149 |
| $Nb_2O_5$ | 0.200 | 0.129 | 0.205 | 0.106 | 0.847 | 0.580 | 0.181 | 1.011 | 0.448 | 0.228 | 0.215 | 1.094 | 0.190 |
| $Al_2O_3$ | nd | nd | nd | nd | 0.024 | nd | nd | 0.062 | nd | nd | nd | 0.314 | 0.019 |
| $Cr_2O_3$ | 0.341 | 0.199 | 0.077 | 0.125 | 0.125 | 0.193 | 0.060 | 0.187 | 0.037 | 0.145 | 0.221 | 0.051 | 0.092 |
| FeO | nd | nd | 0.117 | nd | 0.580 | 0.170 | 0.037 | 0.164 | nd | 0.028 | 0.032 | 0.385 | 0.057 |
| Total | 99.870 | 98.394 | 98.106 | 98.656 | 99.277 | 98.322 | 98.451 | 98.480 | 98.469 | 98.207 | 98.379 | 98.025 | 98.886 |

# APPENDIX A4 – ELECTRON MICROPROBE ANALYSES OF REDDISH BROWN, BLACK, YELLOW AND BLUE RUTILE GRAINS

**Blue**

| No. | 1 | 2 | 3 | 4 | 5 | 6 | 7 |
|---|---|---|---|---|---|---|---|
| SiO2 | 0.105 | 0.037 | 1.438 | 0.428 | 0.035 | 0.110 | 0.671 |
| TiO2 | 96.812 | 97.660 | 94.779 | 96.327 | 98.198 | 98.931 | 96.464 |
| ZrO2 | 0.110 | nd | 0.120 | 0.078 | 0.029 | 0.036 | 0.083 |
| V2O3 | nd | nd | nd | nd | nd | nd | nd |
| Nb2O5 | 0.176 | 0.447 | 0.277 | 0.243 | 0.277 | 0.337 | 0.291 |
| Al2O3 | 2.871 | nd | 1.365 | 0.686 | 0.026 | 0.015 | 0.595 |
| Cr2O3 | nd | nd | nd | 0.119 | nd | nd | 0.125 |
| FeO | 0.168 | nd | 0.057 | 0.129 | 0.052 | 0.115 | 0.149 |
| Total | 100.242 | 98.144 | 98.036 | 98.010 | 98.617 | 99.544 | 98.378 |

**Yellow**

| No. | 1 | 2 | 3 | 4 |
|---|---|---|---|---|
| SiO2 | nd | 0.038 | 0.020 | 0.045 |
| TiO2 | 97.349 | 96.556 | 97.427 | 97.920 |
| ZrO2 | nd | nd | nd | 0.055 |
| V2O3 | nd | nd | 0.236 | nd |
| Nb2O5 | 0.481 | 0.372 | 0.056 | 0.834 |
| Al2O3 | 0.093 | nd | 0.021 | nd |
| Cr2O3 | 0.042 | 0.153 | nd | nd |
| FeO | 0.359 | 0.845 | 0.240 | 0.631 |
| Total | 98.324 | 97.964 | 98.000 | 99.485 |

# APPENDIX A5

**Colour plates of reddish brown, black, yellow and blue rutile grains**

Plate 1: Reddish brown rutile grains from the Sibaya Formation (63 X Magnification).



Plate 2: Black rutile grains from the Sibaya Formation (63 X Magnification).
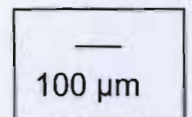
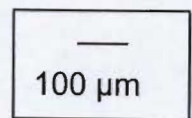Plate 3: Yellow rutile grain from the Sibaya Formation (63 X Magnification).



Plate 4: Blue rutile grains from the Sibaya Formation (63 X Magnification).